THE UNIVERSITY OF CHICAGO

MECHANISMS AND STRUCTURE REACTIVITY RELATIONSHIPS IN NITROGEN DELETION

A DISSERTATION SUBMITTED TO

THE FACULTY OF THE DIVISION OF THE PHYSICAL SCIENCES

IN CANDIDACY FOR THE DEGREE OF

DOCTOR OF PHILOSOPHY

DEPARTMENT OF CHEMISTRY

BY

JULIA LUCETTE DRISCOLL

CHICAGO, ILLINOIS

JUNE 2025

© 2025 Julia Driscoll

Abstract

Anomeric amides are a unique class of molecules that can perform a variety of functions in synthesis. To empower future discovery of anomeric amide reagents and their reactions, it is imperative to understand the existing transformations as much as possible. This thesis is based in trying to uncover and distinguish differences in reactivity of anomeric amides and their reaction partners to enhance our understanding of how these reagents can be best manipulated and put safely into practice in synthetic chemistry.

Chapter one reviews the applications of anomeric amide reagents, with a focus on modern developments within synthetic chemistry. Chapter two covers investigations of structure-reactivity relationships in *N*-(benzyloxy)-*N*-(pivaloyloxy)benzamides. These include kinetic reaction monitoring, linear free energy relationships, and DFT computed parameters to improve our knowledge of the structural features that influence the reactivity of these reagents within the context of secondary amine deletion. Chapter 3 looks instead at the impact of the amine's structure on the reaction mechanism. The discovery and scope of primary amine deletion is briefly discussed, while the chapter's focus is on the mechanistic experiments that were used to elucidate the radical-chain mechanism that accounts for the drastically different reactivity requirements observed for these substrates. Chapter 4 discusses optimization efforts and safety considerations in scaling a primary amine deletion, as these can be a useful transformation for transforming readily available amine feedstocks. The Appendix ventures away from nitrogen deletion and anomeric amides to share a story of a failed decarbonylation strategy that took on a new life within a tandem nitrene-internalization carbon-deletion reaction that transforms aryl azides into pyridines through removal of the *ipso*-carbon.

For Jeddo and Mom, for showing me the value in education despite facing unimaginable barriers in the pursuit of their own.

Table of Contents

List of Figures ix

List of Schemes xviii

List of Tables xxi

List of Equations xxvi

Acknowledgements xxvii

Chapter 1 : Anomeric Amide Reactivity and Synthetic Utility 1

1.1 General Structure and Reactivity of Anomeric Amides 1

1.2 N-Alkoxy-N-Acyloxy Amides Reactivity with Amines 1

1.2.1 Deamination of Secondary Amines and Strategic Applications 2

1.2.2 Deaminative Transformations of Alkyl Primary Amines 6

1.2.3 Deaminative Transformations of Anilines 10

1.3 N-Alkoxy-N-Acyloxy Amides Reactivity with Thiols 12

1.4 α-Reactive Anomeric Amide Reagents 13

1.5 References 14

Chapter 2 : Structure-Reactivity Relationships of Anomeric Amide Reagents 17

2.1 Introduction 17

2.1.1 Previous Optimization 17

2.1.2 Limitations of First Generation Anomeric Amide 18

2.2 Design and Synthesis of Novel Anomeric Amides 19

2.2.1 Cyclic Anomeric Amides 19

2.2.2 Benzyl Derivatives 21

2.2.3 Aryl Derivatives 27

2.2.4 Evaluation of Anomeric Amides with Enhanced Reactivity 31

2.3 Experimental 32

2.3.1 General Information 32

2.3.2 Anomeric Amide Synthesis: General Procedures and Considerations 33

2.3.3 Characterization of N-(benzyloxy)-N-(pivaloyloxy)benzamides 37

2.3.4 Characterization of N-(benzyloxy)-N-chlorobenzamides 41

2.3.5 Characterization of N-Alkoxy Amide Intermediates 45

2.3.6 Synthesis and Characterization of Synthetic Intermediates 52

2.3.7 Synthesis and Characterization of Cyclic Anomeric Amide Intermediates 54

2.3.8 Kinetics 61

2.3.9 Computational Details 65

2.4 References 69

2.5 NMR Spectra 71

2.6 Cartesian Coordinates of Select Structures 112

Chapter 3 : Mechanistic Investigations of Primary Amine Deletion 172

3.1 Introduction 172

3.1.1 Primary Amine Activation 172

3.1.2 Anomeric Amides and Secondary Amine Deletion 173

3.2 Results and Discussion 175

3.2.1 Initial Discovery and Scope 175

3.2.2 Mechanistic Investigations 177

3.3 Conclusions 182

3.4 Experimental 182

3.4.1 General Procedures 182

3.4.2 Characterization Data 185

3.4.3 Mechanistic Experiments 188

3.4.4 NMR Spectra 197

3.5 References 198

Chapter 4 : Gram Scale Application of Nitrogen Deletion to Synthesize Abietatriene 202

4.1 Introduction 202

4.2 Optimization of Reaction Conditions 204

4.2.1 Experimental Results 204

4.2.2 Conclusions: Summary of Procedural Modifications 208

4.3 Experimental 209

4.3.1 Optimized Procedure 209

4.3.2 Procedure Notes and Characterization Data 217

4.3.3 Byproduct Identification 224

4.3.4 NMR Spectra 225

4.4 References 227

Appendix 1 : Carbon Deletion as Heterocyclic Carbenes for Ring Contractions 229

A1.1 The Untold Story of Ketone Condensation-Decarbonylation 229

A1.2 Ipso-Selective Nitrene Internalization 231

A1.2.1 Background 231

A1.2.2 Reaction Development 232

A1.3 References 235

Cartesian Coordinates for All Computed Structures xyzfiles.zip

List of Figures

Figure 1.1 General structure and electronic effects of anomeric amides 1

Figure 2.1 First-generation optimization: A. fragments optimized; B. leaving group experiments, Ar = *p*-bromophenyl; C. aryl fragment Hammett plot 17

Figure 2.2 Limitations of first generation anomeric amide reagent 18

Figure 2.3 Initial attempted synthesis of a cyclic anomeric amide 19

Figure 2.4 Cyclic anomeric amide synthesis: leaving group salt screen 19

Figure 2.5 alternative cyclic scaffolds pursued 20

Figure 2.6 Synthesis of anomeric amide benzyl analogs, [a] diethyl ether used for filtration of 20 due to poor solubility in pentane 21

Figure 2.7 A. Optimized reaction conditions for kinetic data collection; B. kinetic data with model fitting; C. Reaction steps used in reaction model 22

Figure 2.8 Benzyl derivative Hammett trends 24

Figure 2.9 A. conformational descriptors used for classification; B. Boltzmann weighted conformer class distribution by derivative; C. Lowest energy conformers from classes A-C for 1i with distance between p-Ar and closest benzyl carbon labelled 25

Figure 2.10 Distribution of N-O charge transfer energy (A) and NBO O(Bn) charge (B) by conformer and derivative. “Boltz Weight” shows distribution of Boltzmann weight for the parameter across all conformer classes. Dot plots for each conformer class show unweighted distribution of values for improved visibility. 26

Figure 2.11 A. Single parameter reactivity model; B. Multi-parameter reactivity model 27

Figure 2.12 Synthetic results for electron-poor derivatives with first and second generation procedures and byproducts observed in anomeric amide synthesis, *estimated purity based on integration of using integration of benzyl methylene ^{1}H NMR peak of 1 relative to the total integration from 4.5-6.0 ppm 28

Figure 2.13 A. Conditions for same pot competition experiments, Ar = *p*-bromophenyl; B. Updated Hammett plot 29

Figure 2.14 A. impact of solvent on reaction time of 19n chlorination; B. Concentration of 19n throughout chlorination reaction in DCM 30

Figure 2.15 Optimized reaction conditions for the synthesis of 1n 30

Figure 2.16 Sample ^{1}H NMR spectra from kinetic experiment and peaks used to determine the concentration of each species 62

Figure 2.17 Titration fitting data using 1:2 association model on BindFit 64

Figure 2.18 conformational descriptor definitions; dihedrals in equations 2.5-2.7 represented by orange arcs 66

Figure 2.19 example from each conformational class for 1i 66

Figure 2.19 ^{1}H NMR spectra of 1d in $CDCl_3$ 71

Figure 2.20 ^{13}C NMR spectra of 1d in $CDCl_3$ 71

Figure 2.21 ^{19}F NMR spectra of 1d in $CDCl_3$ 72

Figure 2.22 ^{1}H NMR spectra of 1e in $CDCl_3$ 72

Figure 2.23 ^{13}C NMR spectra of 1e in $CDCl_3$ 73

Figure 2.24 ^{19}F NMR spectra of 1e in $CDCl_3$ 73

Figure 2.25 ^{1}H NMR spectra of 1g in $CDCl_3$ 74

Figure 2.26 ^{13}C NMR spectra of 1g in $CDCl_3$ 74

Figure 2.27 ^{19}F NMR spectra of 1g in $CDCl_3$ 75

Figure 2.28 ^{1}H NMR spectra of 1h in $CDCl_3$ 75

Figure 2.29 ^{13}C NMR spectra of 1h in $CDCl_3$ 76

Figure 2.30 ^{19}F NMR spectra of 1h in $CDCl_3$ 76

Figure 2.31 ^{1}H NMR spectra of 1i in $CDCl_3$ 77

Figure 2.32 ^{13}C NMR spectra of 1i in $CDCl_3$ 77

Figure 2.33 ^{19}F NMR spectra of 1i in $CDCl_3$ 78

Figure 2.34 ^{1}H NMR spectra of 1j in $CDCl_3$ 78

Figure 2.35 ^{13}C NMR spectra of 1j in $CDCl_3$ 79

Figure 2.36 ^{19}F NMR spectra of 1j in $CDCl_3$ 79

Figure 2.37 ^{1}H NMR spectra of 1k in $CDCl_3$ 80

Figure 2.38 ^{13}C NMR spectra of 1k in $CDCl_3$ 80

Figure 2.39 ^{19}F NMR spectra of 1k in $CDCl_3$ 81

Figure 2.40 ^{1}H NMR spectra of 1m in $CDCl_3$ 81

Figure 2.41 ^{13}C NMR spectra of 1m in $CDCl_3$ 82

Figure 2.42 ^{1}H NMR spectra of 1n in $CDCl_3$ 82

Figure 2.43 ^{13}C NMR spectra of 1n in $CDCl_3$ 83

Figure 2.44 ^{19}F NMR spectra of 1n in $CDCl_3$ 83

Figure 2.45 ^{1}H NMR spectra of 19d in DMSO-*d6* 84

Figure 2.46 ^{13}C NMR spectra of 19d in DMSO-*d6* 84

Figure 2.47 ^{19}F NMR spectra of 19d in DMSO-*d6* 85

Figure 2.48 ^{1}H NMR spectra of 19e in DMSO-*d6* 85

Figure 2.49 ^{13}C NMR spectra of 19e in DMSO-*d6* 86

Figure 2.50 ^{19}F NMR spectra of 19e in DMSO-*d6* 86

Figure 2.51 ^{1}H NMR spectra of 19g in CD_3OD 87

Figure 2.52 ^{13}C NMR spectra of 19g in DMSO-*d6* 87

Figure 2.53 ^{19}F NMR spectra of 19g in CD_3OD 88

Figure 2.54 ^{1}H NMR spectra of 19h in DMSO-*d6* 88

Figure 2.55 ^{13}C NMR spectra of 19h in DMSO-*d6* 89

Figure 2.56 ^{19}F NMR spectra of 19h in DMSO-*d6* 89

Figure 2.57 ^{1}H NMR spectra of 19i in CD_3OD 90

Figure 2.58 ^{13}C NMR spectra of 19i in CD_3OD 90

Figure 2.59 ^{19}F NMR spectra of 19i in CD_3OD 91

Figure 2.60 ^{1}H NMR spectra of 19j in CD_3OD 91

Figure 2.61 ^{13}C NMR spectra of 19j in CD_3OD 92

Figure 2.62 ^{19}F NMR spectra of 19j in CD_3OD 92

Figure 2.63 ^{1}H NMR spectra of 19k in CD_3OD 93

Figure 2.64 ^{13}C NMR spectra of 19k in CD_3OD 93

Figure 2.65 ^{19}F NMR spectra of 19k in CD_3OD 94

Figure 2.66 ^{1}H NMR spectra of 19l in CD_3OD 94

Figure 2.67 ^{13}C NMR spectra of 19l in DMSO-*d6* 95

Figure 2.68 ^{19}F NMR spectra of 19l in CD_3OD 95

Figure 2.69 ^{1}H NMR spectra of 19m in CD_3OD 96

Figure 2.70 ^{13}C NMR spectra of 19m in DMSO-*d6* 96

Figure 2.71 ^{1}H NMR spectra of 19n in DMSO-*d6* 97

Figure 2.72 ^{13}C NMR spectra of 19n in DMSO-*d6* 97

Figure 2.73 ^{19}F NMR spectra of 19n in DMSO-*d6* 98

Figure 2.74 ^{1}H NMR spectra of 19o in DMSO-*d6* 98

Figure 2.75 ^{13}C NMR spectra of 19o in DMSO-*d6* 99

Figure 2.76 ^{19}F NMR spectra of 19o in CD_3OD 99

Figure 2.77 ^{1}H NMR spectra of 19p in DMSO-*d6* 100

Figure 2.78 ^{13}C NMR spectra of 19p in DMSO-*d6* 100

Figure 2.79 ^{1}H NMR spectra of 20d in $CDCl_3$ 101

Figure 2.80 ^{19}F NMR spectra of 20d in $CDCl_3$ 101

Figure 2.81 ^{1}H NMR spectra of 20e in $CDCl_3$ 102

Figure 2.82 ^{19}F NMR spectra of 20e in $CDCl_3$ 102

Figure 2.83 ^{1}H NMR spectra of 20f in $CDCl_3$ 103

Figure 2.84 ^{19}F NMR spectra of 20f in $CDCl_3$ 103

Figure 2.85 ^{1}H NMR spectra of 20g in $CDCl_3$ 104

Figure 2.86 ^{19}F NMR spectra of 20g in $CDCl_3$ 104

Figure 2.87 ^{1}H NMR spectra of 20h in $CDCl_3$ 105

Figure 2.88 ^{19}F NMR spectra of 20h in $CDCl_3$ 105

Figure 2.89 ^{1}H NMR spectra of 20i in $CDCl_3$ 106

Figure 2.90 ^{19}F NMR spectra of 20i in $CDCl_3$ 106

Figure 2.91 ^{1}H NMR spectra of 20j in $CDCl_3$ 107

Figure 2.92 ^{19}F NMR spectra of 20j in $CDCl_3$ 107

Figure 2.93 ^{1}H NMR spectra of 20k in $CDCl_3$ 108

Figure 2.94 ^{19}F NMR spectra of 20k in $CDCl_3$ 108

Figure 2.95 ^{1}H NMR spectra of 20m in $CDCl_3$ 109

Figure 2.96 ^{1}H NMR spectra of 20n in $CDCl_3$ 109

Figure 2.97 ^{19}F NMR spectra of 20n in $CDCl_3$ 110

Figure 2.98 ^{1}H NMR spectra of 20o in $CDCl_3$ 110

Figure 2.99 ^{19}F NMR spectra of 20o in $CDCl_3$ 111

Figure 2.100 ^{1}H NMR spectra of 20p in $CDCl_3$ 111

Figure 3.1 a) Examples of primary amines in pharmaceuticals and (b) directing group chemistry, c) Previous methods for primary amine reduction 173

Figure 3.2 a) Precedence for isodiazene generation from secondary amines and *N*-acyloxy-*N*-alkoxyamides, b) Structure of anomeric amide reagent (1) used for secondary-amine deletion, c) General conditions and mechanism of secondary-amine deletion reaction, d) Initial mechanistic proposal for primary-amine deletion by an anomeric amide..... 174

Figure 3.3 Selected reaction scope for the deletion of primary amines. Conditions: 1.2 equiv 1, 0.08 M MeCN, 1 h. [a]NMR Yield; [b]45 °C; [c]1.5 equiv 1, 24 h; [d]5 h; [e]16 h; [f]1:1 DMSO/MeCN; [g]3 h. Personal contributions in blue. 176

Figure 3.4 a) Secondary amine radical clock results, b) Evidence for free-radical intermediates via radical clock experiments and (c) observed TEMPO adducts. 177

Figure 3.5 a) Deuterium labelling studies suggest that HAT occurs from the N-H bond, b) Anion clock experiment discounts competitive anionic mechanism. 179

Figure 3.6 a) Mechanism for initiation, and mechanistic proposals for HAT from alkoxyhydrazine (part b), isodiazene (part c), and diazenyl radical (part d), e) N-centered radical clock experiment and computational values for rate constants Results discount mechanism where alkoxyhydrazine intermediate acts as an H-atom donor. 180

Figure 3.7 Chiral GC traces of 2,2-dimethyl4-phenyl-1,3-dioxane from racemic 3e (left) vs 3e from deamination of enantiopure 2e..... 186

Figure 3.8 ^{1}H NMR of the crude reaction of 2u with 1, 1,3,5-trimethoxybenzene added as internal standard in CD_3CN 188

Figure 3.9 ^{1}H NMR of the crude reaction of 2v with 1, 1,3,5-trimethoxybenzene added as internal standard in $CDCl_3$ 189

Figure 3.10 ^{1}H NMR of the crude reaction of 2x with 1, 1,3,5-trimethoxybenzene added as internal standard in CD_3CN 190

Figure 3.11 products from the trapping of radicals generated from amines 2a and 2c..... 191

Figure 3.12 ^{1}H NMR of the crude reaction of 2a and 1 with 1.2 equiv of TEMPO in CD_3CN 191

Figure 3.13 ^{1}H NMR of the crude reaction of 2c and 1 with 1.2 equiv of TEMPO in CD_3CN..... 192

Figure 3.14 products from the trapping of radicals generated from amines 2a and 2c..... 193

Figure 3.15 ^{1}H NMR of 2d-H_2 in CD_3CN, NH_2 peak highlighted in gold..... 194

Figure 3.16^{1}H NMR of 2d-D_2 in CD_3CN, disappearance of NH_2 peak highlighted in gold 195

Figure 3.17^{1}H NMR after the deamination of 2d-D_2 in CD_3CN, peaks used for assessing deuterium incorporation highlighted..... 195

Figure 3.18^{1}H NMR of the crude reaction of 3w and 1 with 1,3,5-trimethoxybenzene as an internal standard in CD_3CN 196

Figure 3.19 ^{1}H NMR of 6d in $CDCl_3$ 197

Figure 3.20 ^{13}C NMR of 6d in $CDCl_3$ 197

Figure 4.1 Compounds synthesized from abietatriene 202

Figure 4.2 Byproducts identified during scale-up 206

Figure 4.3 A) leelamine, B) leelamine dissolved in toluene, C) reaction setup, D) reaction after acetic acid addition, photos taken by author 209

Figure 4.4 Slurry throughout procedure: A) initial slurry formation, B) after 30 min at 35 °C, C) at 26 °C, D) cooling in ice water bath, E) final slurry (5 °C), photos taken by author 210

Figure 4.5 First filtration: A) vacuum filtration setup, B) slurry in funnel, C) filtered slurry and mother liquor, D) mother liquor with material remaining in reaction flask, E) filter cake immediately before washes, F, G) filter cake after washes, photos taken by author 210

Figure 4.6 Recrystallization: A) filtered solids in flask, B) suspension in toluene, C) solution at 65 °C, D) start of crystallization (49 °C), E, F) slurry progression at 49 °C, G) at 30 °C, H) cooling in ice water bath, I, J) final slurry (5 °C), photos taken by author 211

Figure 4.7 Second filtration: A) slurry in funnel, B) mother liquor, C) filter cake immediately before rinses, D, E) dried filter cake, F) solids broken up, G, H) dried solids, photos taken by author 212

Figure 4.8 A) reaction setup, B) leelamine acetate in MeCN, C) 4 in flask, photos taken by author 213

Figure 4.9 A) reaction immediately after removing ice water bath, B) reaction after 1 hour at room temperature, photos taken by author 214

Figure 4.10 A) liquid-liquid extraction, B) funnel with cotton plug in round bottom flask, C) crude reaction oil, photos taken by author 215
Figure 4.11 Purified product: A) oil, B, C) crystallized, photos taken by author 216
Figure 4.12 TLC of completed reaction (20% EA/hexanes) A) under UV(active spots circled w/ pencil), B) ninhydrin stain, C) back of stained plate (inverted for consistency) , photos taken by author 221
Figure 4.13 TLC of column fractions A) under UV, B) with PAA stain, photos taken by author . 222
Figure 4.14 TLC of column fractions from replicate reaction with PAA stain, photos taken by author 222
Figure 4.15 Comparison of byproduct spectra with N-(benzyloxy)-4-(trifluoromethyl)benzamide 224
Figure 4.16 Overlayed ^{1}H NMR spectra of non-polar byproducts with product 3 224
Figure 4.17 ^{1}H NMR spectra of 16 in $CDCl_3$ 225
Figure 4.18 ^{13}C NMR spectra of 16 in $CDCl_3$ 225
Figure 4.19 ^{1}H NMR spectra of 3 in $CDCl_3$ 226
Figure 4.20 ^{13}C NMR spectra of 3 in $CDCl_3$ 226
Figure A1.1 Proposed carbon deletion strategy and literature precedent examples 229

List of Schemes

Scheme 1.1 Reaction and proposed mechanism of methyl aniline with N-acetoxy-N-butoxybenzamide 2

Scheme 1.2 Reaction and proposed mechanism of bibenzyl amines with (N-(Benzyloxy)-N-(pivaloyloxy)-4-(trifluoromethyl)-benzamide) 3

Scheme 1.3 deaminative strategy to synthesize rotaxanes 4

Scheme 1.4 deaminative strategy to synthesize BCPs 5

Scheme 1.5 partial stereo-retention observed in the deamination of tetrahydroisoquinolines 5

Scheme 1.6 reaction of tetrahydroisoquinolines with(N-(Benzyloxy)-N-(pivaloyloxy)-4-(trifluoromethyl)-benzamide) 5

Scheme 1.7 Intercepting diene intermediate with a dienophile to synthesize tetralins 6

Scheme 1.8 Primary amine directed C-H arylation followed by deamination 7

Scheme 1.9 [2+2] cyclization followed by deamination to remove amine used to impart diastereoselectivity 7

Scheme 1.10 [4+3] cycloaddition using a 2-aminoallyl cation intermediate followed by imine reduction and nitrogen deletion 7

Scheme 1.11 mechanism of deaminative bromination 8

Scheme 1.12 deaminative hydroxylation of aliphatic amines 9

Scheme 1.13 deaminative trifluoromethylation of aliphatic amines 10

Scheme 1.14 example deaminative thiolation of aniline 11

Scheme 1.15 example deaminative phosphonylation 11

Scheme 1.16 reaction of glutathione with *N*-acyloxy-*N*-butoxybenzamide 12

Scheme 1.17 proposed mechanism based on kinetic studies and observed products 12

Scheme 2.1 Synthesis of *N*-(benzyloxy)benzamides 33

Scheme 2.2 *In situ* benzoyl chloride formation from benzoic acid 34

Scheme 2.3 formation of O-benzyl hydroxylamine in solution from N-benzyloxyphthalimide .. 34

Scheme 2.4 Chlorination of *N*-(benzyloxy)benzamides 35

Scheme 2.5 Chlorination of *N*-(benzyloxy)benzamides 36

Scheme 2.6 Synthesis of 1H-benzo[d][1,2]oxazin-4(3H)-one (12) 56

Scheme 2.7 Synthesis of intermediate 36 (1H,3H-benzo[de]isochromen-1-one) 57

Scheme 2.8 Synthesis of intermediate 39 from 37 58

Scheme 2.9 Synthesis of 1H-naphtho[1,8-de][1,2]oxazepin-4(3H)-one (13) from 40 60

Scheme 2.10 Nitrogen deletion conditions for kinetics experiments 61

Scheme 3.1 Reaction of radical clock 2u with 1 188

Scheme 3.2 Reaction of radical clock 2v with 1 189

Scheme 3.3 Reaction of nitrogen-centered radical clock 2x with 1 190

Scheme 3.4 Reaction of anion probe 2w with 1 196

Scheme 4.1 A) synthetic routes to 3 proceeding through an aldehyde or alcohol intermediate 203

Scheme 4.2, A) alternative synthetic routes to 3 from leelamine, B) fragment pairs for the synthesis of 3 via ring construction strategies 204

Scheme 4.3 reaction of *leelamine acetate* with anomeric amide 205

Scheme A1.1 attempted spirocyclization and carbon extrusion conditions 230

Scheme A1.2 condensation of DMEDA (2d) onto tropone 231

Scheme A1.3 Carbon-nitrogen atom swap strategy and literature precedent of related transformations *figure adapted from *Science*. 2023, *381*, 1474 – 1479. 232
Scheme A1.4 initial hit for pyridine formation through *ipso*-C deletion 232
Scheme A1.5 nitrene insertion and decarbonylation of 6b using 2e and observed reaction intermediates 233

List of Tables

Table 1.1 Selection of reaction scope for the deamination of benzylic amines with an anomeric amide; [a]2 equivalents anomeric amide, [b]2 equiv triethylamine added, [c]deamination product formed stereospecifically 3

Table 1.2 Selected scope of primary amine deletion 6

Table 1.3 Deaminative halogenation of primary aliphatic amines 9

Table 1.4 hydrodeamination of anilines 10

Table 1.5 deaminative halogenation of an aniline substrate 11

Table 1.6 select scope of anomeric amide mediated disulfide formation 12

Table 1.7 selected examples of C-H halogenation using anomeric halogenating reagents 13

Table 1.8 comparison of novel anomeric nitrating reagent from Baran and coworkers with existing reagents 13

Table 2.1 Screening amines with new anomeric amides, qNMR yields reported..... 31

Table 2.2 rate data from kinetic experiments used for each derivative 63

Conformational descriptors were determined using the definitions in equations 1.5-7, where DH_{wxyz} represents the dihedral angle of the four atoms listed. The percent representation from each conformer class in Figure 2.9B were determined by the sum of the Boltzmann weights for all structures within that class. This stacked bar chart and the distribution of parameter values across derivatives and conformational classes, as shown in Figure 2.10, were visualized using ggplot2.[24]Table 2.3 Definition of conformational descriptor terms 65

Table 2.4 reactivity model coefficients, variables, and fit statistics..... 67

Table 2.5 Boltzmann average and normalized values for parameters used in models 68

Table 2.6 Example computed structure of an A conformer of 1k (1) 112

Table 2.7 Example computed structure of a B conformer of 1k (37) 113

Table 2.8 Example computed structure of an E conformer of 1k (49) 114

Table 2.9 Example computed structure of a C conformer of 1k (50) 115

Table 2.10 Example computed structure of a G conformer of 1k (63) 116

Table 2.11 Example computed structure of an F conformer of 1k (65) 117

Table 2.12 Example computed structure of an H conformer of 1k (71) 118

Table 2.13 Example computed structure of a D conformer of 1k (92) 119

Table 2.14 Example computed structure of a B conformer of 1j (11) 120

Table 2.15 Example computed structure of an E conformer of 1j (12) 121

Table 2.16 Example computed structure of a C conformer of 1j (15) 122

Table 2.17 Example computed structure of an H conformer of 1j (34) 123

Table 2.18 Example computed structure of an F conformer of 1j (44) 124

Table 2.19 Example computed structure of a D conformer of 1j (51) 125

Table 2.20 Example computed structure of a G conformer of 1j (56) 126

Table 2.21 Example computed structure of an A conformer of 1j (63) 127

Table 2.22 Example computed structure of an F conformer of 1i (100) 128

Table 2.23 Example computed structure of an A conformer of 1i (11) 129

Table 2.24 Example computed structure of a B conformer of 1i (31) 130

Table 2.25 Example computed structure of an E conformer of 1i (39) 131

Table 2.26 Example computed structure of an H conformer of 1i (42) 132

Table 2.27 Example computed structure of a G conformer of 1i (71) 133

Table 2.28 Example computed structure of a D conformer of 1i (85) 134

Table 2.29 Example computed structure of a C conformer of 1i (9) 135

Table 2.30 Example computed structure of an A conformer of 1f (1) 136

Table 2.31 Example computed structure of an F conformer of 1f (45) 137

Table 2.32 Example computed structure of a D conformer of 1f (52) 138

Table 2.33 Example computed structure of a B conformer of 1f (62) 139

Table 2.34 Example computed structure of an E conformer of 1f (7) 140

Table 2.35 Example computed structure of a B conformer of 1g (11) 141

Table 2.36 Example computed structure of an H conformer of 1g (16) 142

Table 2.37 Example computed structure of an F conformer of 1g (44) 143

Table 2.38 Example computed structure of a D conformer of 1g (53) 144

Table 2.39 Example computed structure of a C conformer of 1g (63) 145

Table 2.40 Example computed structure of an A conformer of 1g (6) 146

Table 2.41 Example computed structure of an E conformer of 1g (8) 147

Table 2.42 Example computed structure of a B conformer of 1e (15) 148

Table 2.43 Example computed structure of an F conformer of 1e (35) 149

Table 2.44 Example computed structure of a D conformer of 1e (39) 150

Table 2.45 Example computed structure of a C conformer of 1e (42) 151

Table 2.46 Example computed structure of an A conformer of 1e (4) 152

Table 2.47 Example computed structure of an H conformer of 1e (76) 153

Table 2.48 Example computed structure of a B conformer of 1d (11) 154

Table 2.49 Example computed structure of an E conformer of 1d (13) 155

Table 2.50 Example computed structure of an A conformer of 1d (1) 156

Table 2.51 Example computed structure of an H conformer of 1d (51) 157

Table 2.52 Example computed structure of an A conformer of 1a (10) 158

Table 2.53 Example computed structure of a B conformer of 1a (12) 159

Table 2.54 Example computed structure of an H conformer of 1a (17) 160

Table 2.55 Example computed structure of an F conformer of 1a (21) 161

Table 2.56 Example computed structure of a D conformer of 1a (22) 162

Table 2.57 Example computed structure of an E conformer of 1a (58) 163

Table 2.58 Example computed structure of a C conformer of 1a (61) 164

Table 2.59 Example computed structure of a B conformer of 1h (17) 165

Table 2.60 Example computed structure of an E conformer of 1h (30) 166

Table 2.61 Example computed structure of an H conformer of 1h (36) 167

Table 2.62 Example computed structure of an A conformer of 1h (3) 168

Table 2.63 Example computed structure of an F conformer of 1h (43) 169

Table 2.64 Example computed structure of a G conformer of 1h (46) 170

Table 2.65 Example computed structure of a C conformer of 1h (47) 171

Table 4.1 Optimization for the crystallization of 16 207

Table 4.2 published general conditions for primary amine deletion[17] vs. these conditions 208

Table A1.1 (A) Scope of the reaction. Standard conditions: (i) 0.3 mmol aryl azide, 0.3 mmol ethylaminoethanol, 3 ml MeCN, and 427-nm light-emitting diode (LED); (ii) 0.3 mmol DBU, 3 ml dioxane heated to 80°C, and 0.6 mmol N-bromocaprolactam added dropwise

at 80°C. Isolated yield of pyridine from aryl azide (black). Proton NMR (1H NMR) yield of photolysis (blue) and interpolated yield of pyridine based on azepine yield (orange), shown in parentheses. Asterisk indicates NMR yield. (B) Demonstration that nonsymmetric substrates form only one pyridine isomer. *figure adapted from *Science*. 2023, *381*, 1474 – 1479. 234

List of Equations

Parametric function rate model	2.1	63
$K_{1:1} = \frac{k_{1:1a}}{k_{1:1d}} = \frac{89.39}{1}$	2.2	63
$S_X = \frac{\sigma_X}{\sqrt{n}}$	2.3	63
$S_{final} = \frac{1}{\ln(10)} * \sqrt{\left(\frac{S_X}{k_{Xavg}}\right)^2 + \left(\frac{S_H}{k_{Havg}}\right)^2}$	2.4	63
$DH_{(Bn)CONO(Piv)} + DH_{(Bn)CONC(Amide)}$	2.5	65
$DH_{(Piv)CONO(Bn)} + DH_{(Piv)CONC(Amide)}$	2.6	65
$DH_{(Amide)OCNO(Piv)}$	2.7	65
$X_n = (X - \mu)/\sigma$	2.8	67
$\log\left(\frac{k_X}{k_H}\right)_{pred} = b + m * X_{n\,p} + n * X_{n\,q}$	2.9	67

Acknowledgements

I truly cannot express how lucky I feel to be surrounded by everyone who has helped this thesis come to fruition. To Professor Mark Levin, I am constantly in awe of your unwavering enthusiasm and unmatched email response time. Thank you for your constant support, understanding, and encouragement. You have had such a large influence on my approach to both doing science and sharing science and I am so grateful for your mentorship. Thank you to Professors John Anderson and Anna Wuttig for taking the time to serve on my committee, and particularly to John for being willing to step-in at a moment's notice. I am so inspired by your enthusiasm and commitment to the science and people within the department.

To everyone in the Levin Group, it has been the greatest honor working with all of you. I have learned so much from each and every one of you and feel extremely lucky to have worked alongside such a creative and supportive group of scientists. Dr. Balu Dherange, Dr. Kate Berger and Dr. Patrick Kelly, it is no small task to manage a lab during a pandemic, and I am so appreciative for all that you did for us as first year students. Patrick and Kate, you truly laid the foundation for graduate students in the group, and I cannot thank you enough for all that you did to create a supportive environment and ensure that we all thrived. Kate, thank you additionally for bringing me onto the primary amine deletion project, I learned and grew so much from working with you. Patrick, thank you for teaching me the practical aspects of running computations, so much of the work in chapter 2 would not have been possible without all of your help. Carys Obertone and Dr. Cecile Elgindy, thank you for all of the thoughtful and entertaining conversations over the years, both scientific and not. I have learned so much from both of you and there was truly never a dull moment. Rubén and Liao, thank you so much for all of your

contributions to these projects, they would not be what they are without your help. Dr. Tyler Pearson, I have learned so much from you and I'm so grateful for your friendship and support over the years. Thank you for bringing heterocyclic carbene deletion to life, it will always be one of my favorite reactions. Colin, I cannot imagine going through graduate school without you. You have been my constant support and comic relief, both in and outside of lab and I will forever be grateful for your friendship. Finally, to Megan Morales, I feel so lucky to have mentored you. Beyond all of your efforts and contributions in lab that are included in this work, your passion and enthusiasm for science is truly inspirational and reminds me of why I entered the field.

Thank you also to the wonderful facilities support that enabled all of the work in this thesis to take place. Dr. Josh Kurutz, thank you for your thoughtful maintenance of the NMR facilities and for all of your helpful discussions. I would also like to thank Dr. Yong Han, Dr. Jin Qin, and Dr. Guangchang Zhou for maintenance of the mass spectrometry facilities. Laura Luburich and Michael Reedy, thank you so much for your promptness and dedication to keeping Searle running smoothly.

Aside from the work presented in this thesis, I was also lucky enough to spend a summer learning process chemistry from Dr. Greg Beutner and Dr. Nic Webb at Bristol-Myers Squibb. You have both taught me so much about process chemistry and working in an industrial setting, I am so appreciative of the thoughtful mentorship and support that I received from you. I would also like to thank Dr. Hester Dang for all of her help and support within the lab while I was at BMS. I'm so grateful for all of our conversations and your commitment to creating a welcoming environment.

To everyone I worked with in the Koide Group at the University of Pittsburgh, thank you so much for fostering my growth and providing me with a strong foundation in organic synthesis. Professor Kaz Koide, thank you for taking a chance on a first-year undergraduate and allowing me to begin my training so early. To Dr. Rob Bressin and Dr. Ivanna Pohorilets, you have truly taught me everything I know in the lab, and I can never thank you enough. I'm so grateful for the mentorship and support I received from all three of you and it has had an immense impact on the scientist that I am today.

Beyond lab mentorship, there have been so many educators that have helped me to reach this point. To Dr. Josh Cannon, at the University of Pittsburgh Honors College thank you for all of your support and guidance in putting together application materials. I attribute much of my success to everything that I learned from you, and they're lessons that I will carry with me for life. To Mr. Daniel Long, the teacher that introduced me to organic chemistry, I am so grateful to have had your class in high school, it genuinely changed the course of my life. Thank you for recognizing my abilities and encouraging me to pursue the field further.

Thank you to my family, without whom I would not have had any of the educational opportunities that I have experienced. Tati, I cannot imagine half of what you and Jeddo endured, and I'm so grateful for all that you have done to take care of the family. I have learned so much from you and would not have the life that I do without you. To Nana, your love of learning and the constant love and support from you and Grandad has been so influential in my life. Danny and Thalia, I have learned so much from the different ways that you both approach life. Thank you for providing a source of competition growing up that pushed me to be the best I can be. To my parents for always encouraging me to pursue my interests and for their constant support in

all aspects of my life. You have both had such an immense influence on me, Mom through your perseverance, creativity, and constant support for the people around you, and Dad through your quick wit, creative problem solving, and commitment to showing up for the people you love. Thank you both for instilling in me a strong value for education and for providing me with all of the opportunities that have allowed me to be here today.

I also would not have been able to make it through this PhD without the love and support of my friends. Jamie Smith and Adelyne Bejjani, our lengthy friendships have shaped me into the person that I am today. Jesse Pak, it's so special to have a friend that can understand the ups and downs of a PhD and I'm so thankful for all of your support. Hannah Reiling and Meera Sakthivel, I am so lucky to have you both in Chicago with me and spending time with both of you has provided me with more sanity than you realize. All of you have provided me with so much joy, comfort, and support and I'm so grateful for your friendship.

This material is based upon work supported by the National Science Foundation Graduate Research Fellowship Program under Grant No 2140001. Any opinions, findings, and conclusions or recommendations expressed in this material are those of the author(s) and do not necessarily reflect the views of the National Science Foundation.

Chapter 1 : Anomeric Amide Reactivity and Synthetic Utility

Note: Portions of this work have been published in an alternate format in Driscoll, J.L. and Levin, M.D. (2025). *N*-(Benzyloxy)-*N*-(pivaloyloxy)-4-(trifluoromethyl)-benzamide. In Encyclopedia of Reagents for Organic Synthesis. https://doi.org/10.1002/047084289X.rn02565

1.1 General Structure and Reactivity of Anomeric Amides

Anomeric amides are a class of compounds in which the nitrogen-atom of an amide is bound to two electronegative heteroatoms.[1] This results in an anomeric effect, much like observed in carbohydrates, where one heteroatom's lone-pair (n_X) can donate into the anti-bonding orbital of the other nitrogen-heteroatom bond ($\sigma^*_{N\text{-}Y}$) (Figure 1.1). These effects increase the electrophilicity of the nitrogen atom, while also weakening the N-Y bond. As such, nucleophilic attack can occur at both the amide nitrogen and the position α to the nitrogen (Y) depending on the identity of X and Y, and the nucleophilic species.

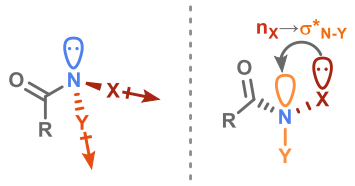
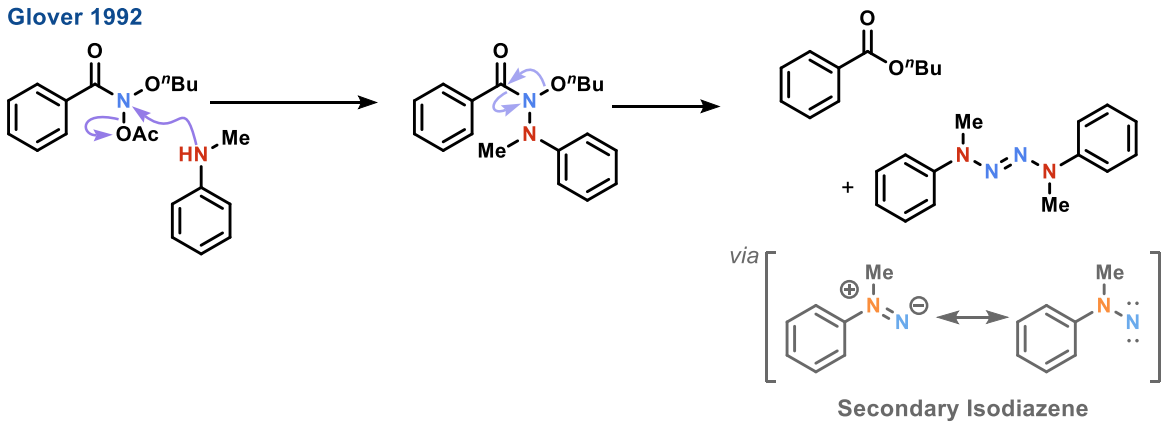


Figure 1.1 General structure and electronic effects of anomeric amides

1.2 N-Alkoxy-N-Acyloxy Amides Reactivity with Amines

One of the most explored classes of anomeric amides is *N*-alkoxy-*N*-acyloxy amides, which have been studied for both their mutagenic properties[2–7] and their synthetic utility.[8–12] They consist of an alkoxide and carboxylate bound to the amide nitrogen and typically react with nucleophiles through substitution at the amide nitrogen, generating a new anomeric amide species with varying downstream reactivity.

The reactivity of *N*-alkoxy-*N*-acyloxy amides with amines was first reported by Glover and coworkers using methyl aniline with N-acetoxy-N-butoxybenzamide (Scheme 1.1).[8] They



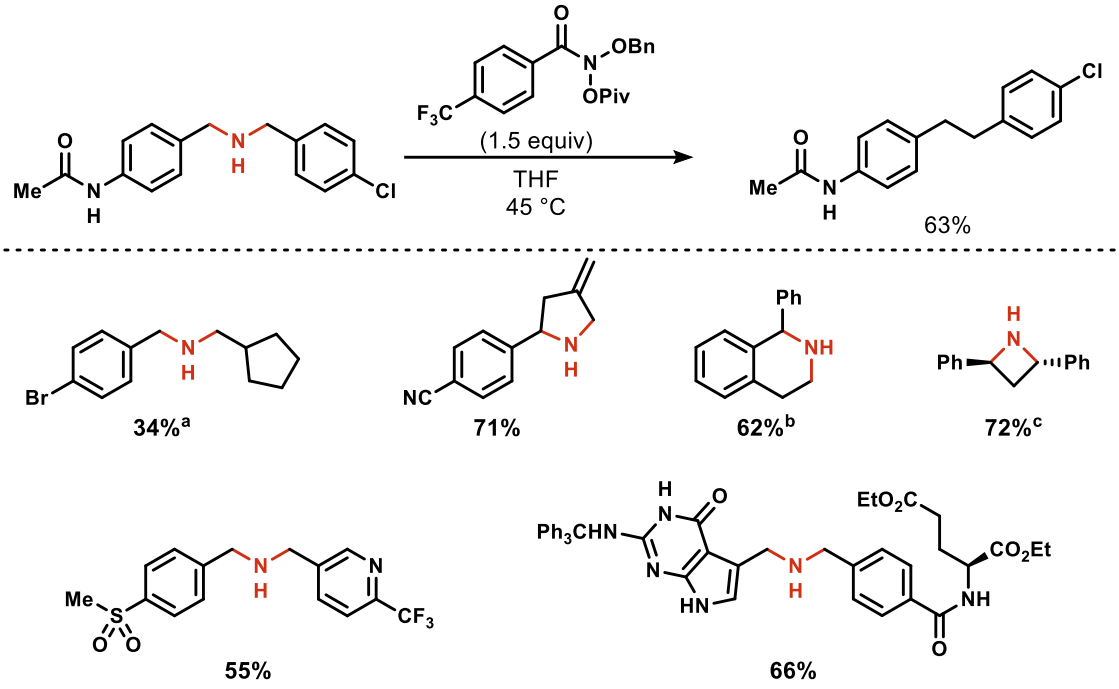
Scheme 1.1 Reaction and proposed mechanism of methyl aniline with N-acetoxy-N-butoxybenzamide

found that this resulted in the formation of a tetrazene and ester, providing evidence for the intermediacy of an isodiazene formed from displacement of the acetoxy group and subsequent reductive elimination. This reductive elimination was also coined as a HeteroAtom Rearrangement On Nitrogen, or HERON reaction.[13] Further reactivity studies of amines by Glover's group focused on understanding the factors that influence its reactivity with guanine and adenine, as this is proposed to be related to its mutagenicity.[14]

1.2.1 Deamination of Secondary Amines and Strategic Applications

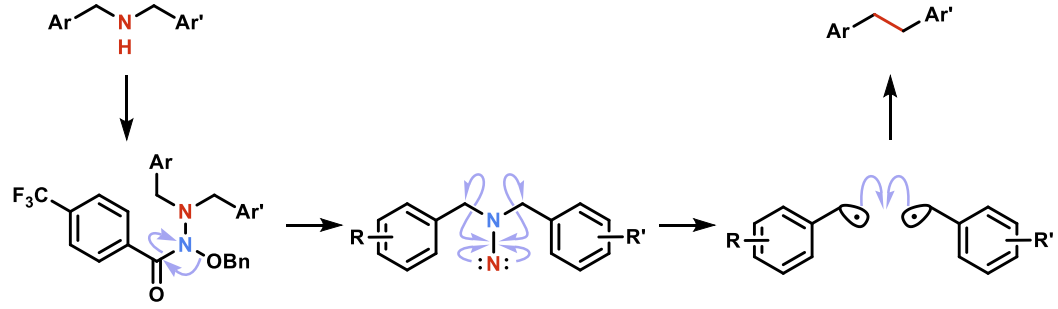
Within our own group, we have primarily studied the reactivity of (N-(Benzyloxy)-N-(pivaloyloxy)-4-(trifluoromethyl)-benzamide) as a deaminating reagent. When added to benzylic secondary amines, this reagent enables the extrusion of the amine nitrogen atom, forming a C-C bond in its place.[12] This method has demonstrated success with acyclic secondary amines that contain at least one benzylic fragment and cyclic secondary amines that possess two radical-stabilizing groups alpha to the amine nitrogen atom (Table **1.1**). Broad functional group tolerance has been observed under these conditions and compatible substrates can be

Table 1.1 Selection of reaction scope for the deamination of benzylic amines with an anomeric amide; [a]2 equivalents anomeric amide, [b]2 equiv triethylamine added, [c]deamination product formed stereospecifically



readily accessed through reductive amination. These factors coupled with the simplicity of the procedure enable the use of this method for the synthesis of diverse compound libraries.[15,16]

This reaction initially proceeds through the same mechanism as methyl aniline, with substitution at the anomeric nitrogen atom of the reagent, displacing the pivalate group to form a nitrogen-nitrogen bond with the amine and undergoing reductive elimination, to afford an isodiazene intermediate. The isodiazene then fragments, extruding nitrogen gas, and the resulting alkyl radicals recombine within the primary solvent cage to form a C-C bond (Scheme



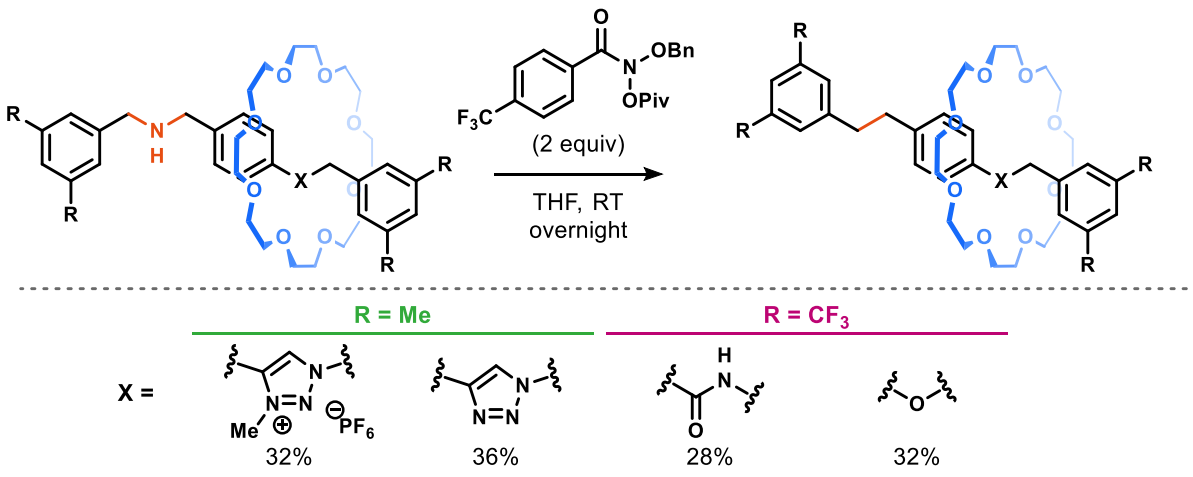
Scheme 1.2 Reaction and proposed mechanism of bibenzyl amines with (N-(Benzyloxy)-N-(pivaloyloxy)-4-(trifluoromethyl)-benzamide)

1.2). The predominantly in-cage recombination in this reaction ensures that the intramolecular product is formed in acyclic, asymmetric substrates.

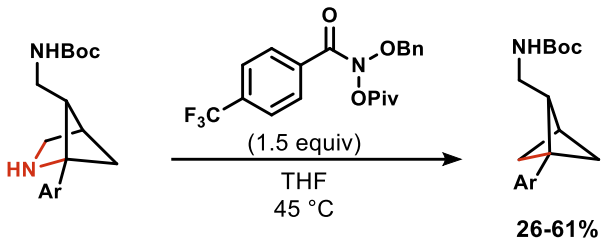
While this method is tolerant of most functionalities, the anomeric amide can oxidize compounds bearing thiols and electron rich arenes, typically precluding their use. Additionally, α-tertiary and most acyclic α-secondary amines are unreactive towards the anomeric amide due to the steric requirements of the substitution step. Certain motifs have also been observed to show alternative reactivity due to either rearrangement of the isodiazene intermediate or radical fragmentation.

1.2.1.1 Synthesis of Rotaxanes

This reagent has also been used to modify rotaxanes.[19] This strategy takes advantage of the nucleophilicity of amines to create a bond through the crown ether followed by nitrogen-deletion to form a stable C-C bond. The in-cage recombination of the radicals also prevents the captured crown ether from dethreading after scission of the C-N bonds. This method has helped to expand the structural diversity of rotaxanes.



Scheme 1.3 deaminative strategy to synthesize rotaxanes



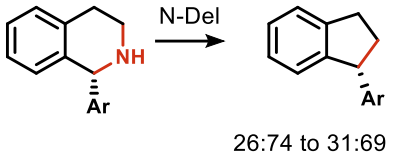
Scheme 1.4 deaminative strategy to synthesize BCPs

1.2.1.2 Synthesis of BCPs

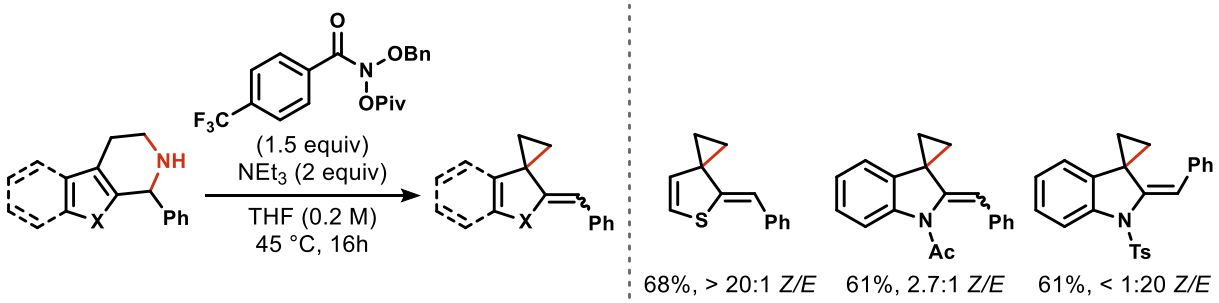
This reactivity has been demonstrated as a method to synthesize bicyclo[1.1.1]pentanes (BCPs) (eq 6).[17,18] These strained polycycles are prevalent within medicinal chemistry as bio-isosteres for aromatic moieties.

1.2.1.3 Radical Rearrangements and Downstream Chemistry

Certain amine substrates can also undergo unique reactions due to the reactivity of their radical intermediates. One example of this is tetrahydroisoquinolines, which undergo a spirocyclization process. This spirocyclization is dynamically controlled, with implications for the enantiospecificity of the deamination reaction (Scheme 1.5). In some instances, this results in isolable, dearomatized spirocyclic products (Scheme 1.6).[21]

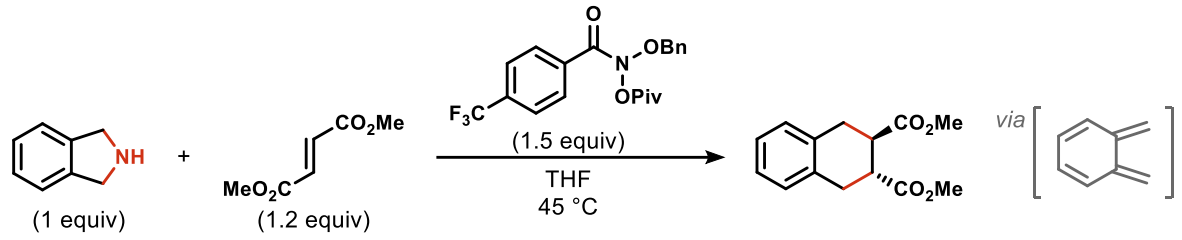


Scheme 1.5 partial stereo-retention observed in the deamination of tetrahydroisoquinolines



Scheme 1.6 reaction of tetrahydroisoquinolines with(N-(Benzyloxy)-N-(pivaloyloxy)-4-(trifluoromethyl)-benzamide)

Another example of this is isoindolines, which rearrange to orthoquinodimethanes. This can be intercepted by dienophiles to undergo a Diels-Alder reaction, forming substituted tetralin products (Scheme 1.7).[20]



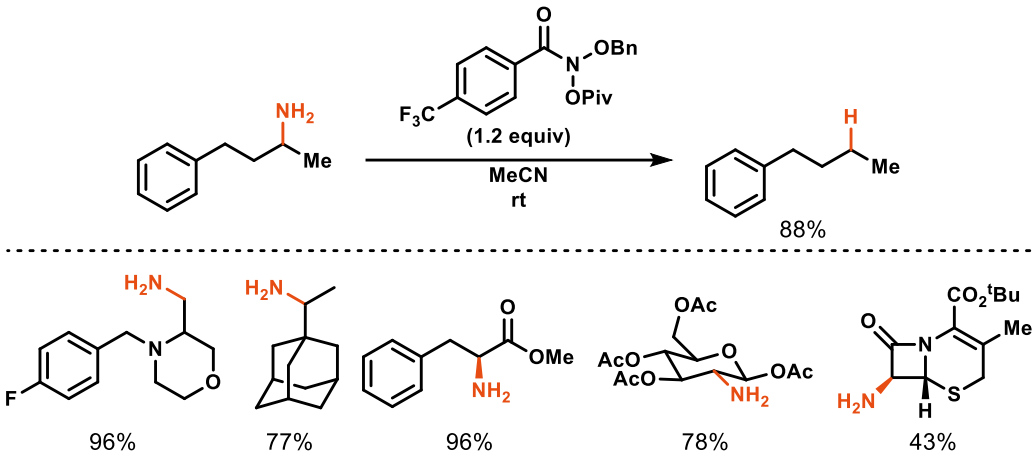
Scheme 1.7 Intercepting diene intermediate with a dienophile to synthesize tetralins

1.2.2 Deaminative Transformations of Alkyl Primary Amines

1.2.2.1 Deamination/Reduction

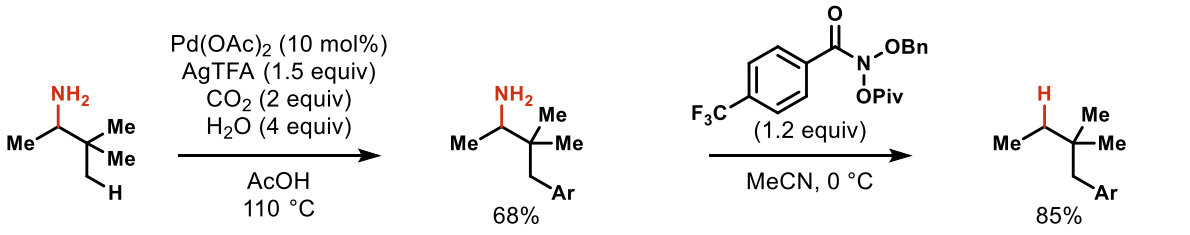
The title reagent can also be used for the deamination of primary amines. The mechanism and scope of this transformation is covered in greater depth in Chapter 3.[22] This reactivity applies to α-primary and α-secondary primary amines, cleaving the C-N bond and forming a C-H bond in its place (Table 1.2).

Table 1.2 Selected scope of primary amine deletion

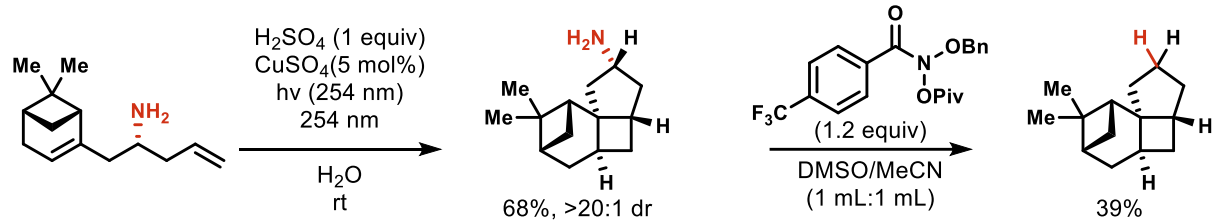


1.2.2.2 Strategic Deamination Applications

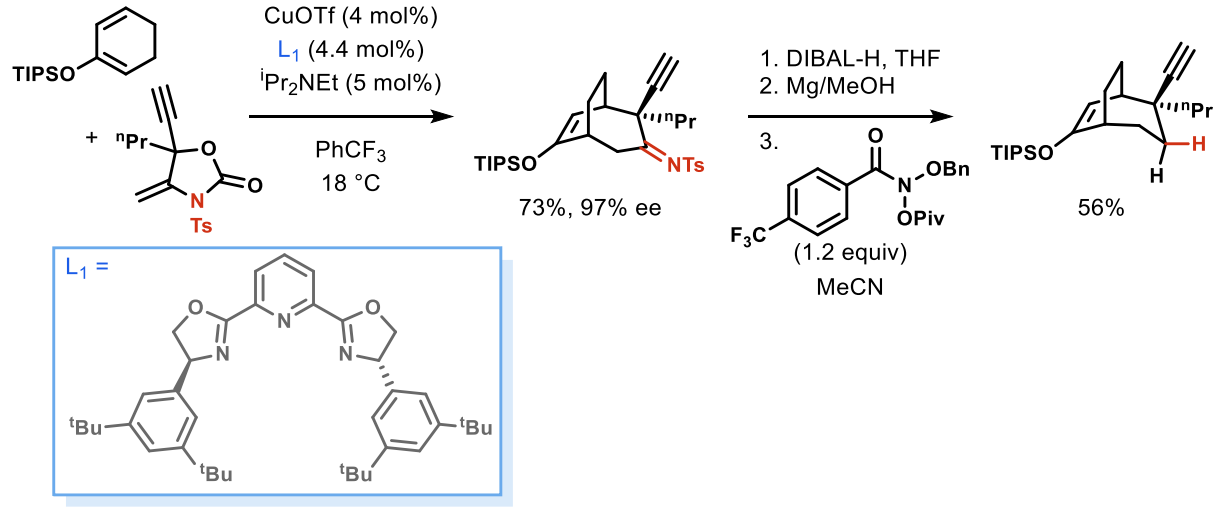
An important application of this reactivity is the removal of amines after they serve a functional purpose in a synthetic pathway. This enables the use of amine-based chemistries to access targets regardless of whether an amino-group is present on the target molecule. This has been demonstrated with primary amine-directed C-H arylation (Scheme 1.8),[22,23] diastereoselective [2+2] cycloaddition (Scheme 1.9),[24] and a [4+3] cycloaddition proceeding through a 2-aminoallyl cation intermediate (Scheme 1.10).[25]



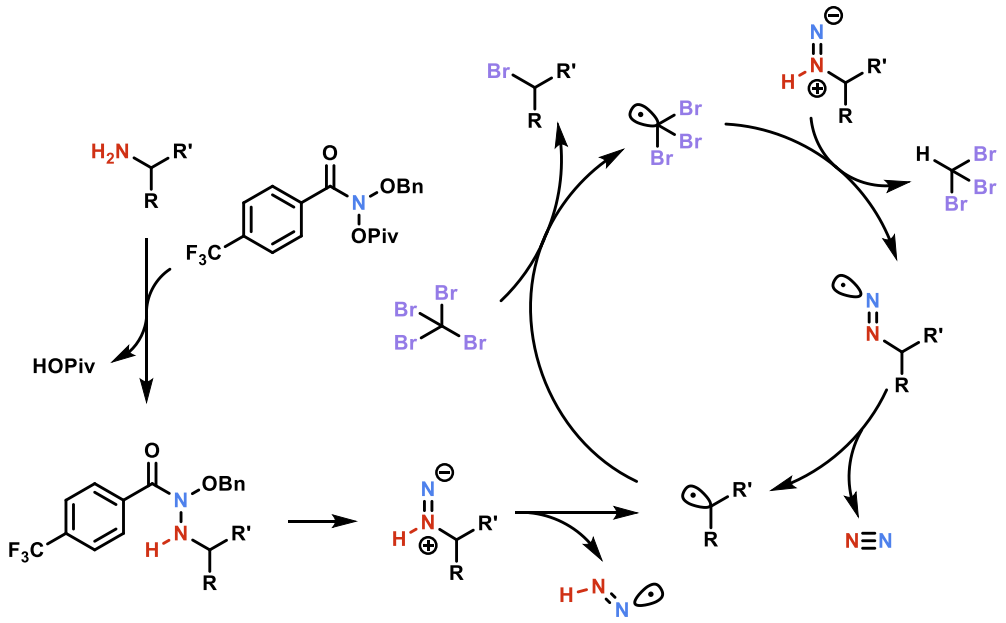
Scheme 1.8 Primary amine directed C-H arylation followed by deamination



Scheme 1.9 [2+2] cyclization followed by deamination to remove amine used to impart diastereoselectivity



Scheme 1.10 [4+3] cycloaddition using a 2-aminoallyl cation intermediate followed by imine reduction and nitrogen deletion



Scheme 1.11 mechanism of deaminative bromination

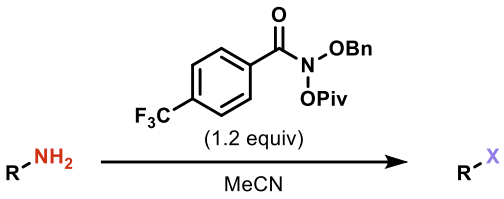
1.2.2.3 Deaminative functionalization

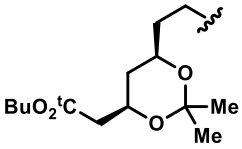
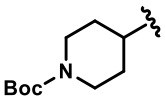
In addition to protio-deamination, the C-N bond cleavage enabled by the title reagent can be utilized to convert primary amines into a variety of other functionalities, which are covered individually in more detail below. Generally, this strategy involves trapping of the free-alkyl radical intermediate formed (mechanistic details in Chapter 3). Given the chain-nature of the reaction mechanism, compatible trapping agents must produce a radical with comparable or better H-atom accepting properties than the parent alkyl radical in order to outcompete hydro-deamination and insert into the radical chain (Scheme 1.11).[26]

1.2.2.4 Halogenation

Primary amines can be converted into alkyl halides using various halogenated reagents in conjunction with the title reagent.[26] Both α-primary and α-secondary amines can be converted to alkyl bromides or iodides with the inclusion of carbon tetrabromide or isopropyl iodide, respectively (Table 1.3). The deaminative bromination was also found to be compatible

Table 1.3 Deaminative halogenation of primary aliphatic amines

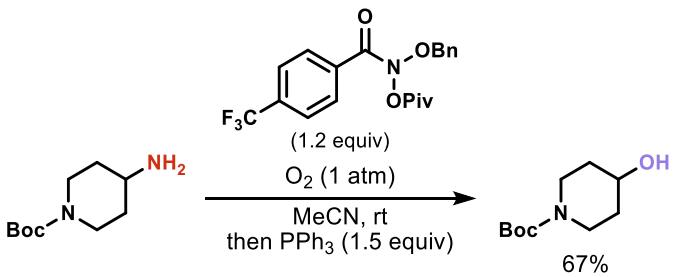


R	X	additive	equiv	yield (%)
	Cl	CCl_4	5	<5
	Br	CBr_4	2	64
	I	^{i}Pr-I	5	39
	Cl	CCl_4	5	66
	Br	CBr_4	2	63
	I	^{i}Pr-I	5	64

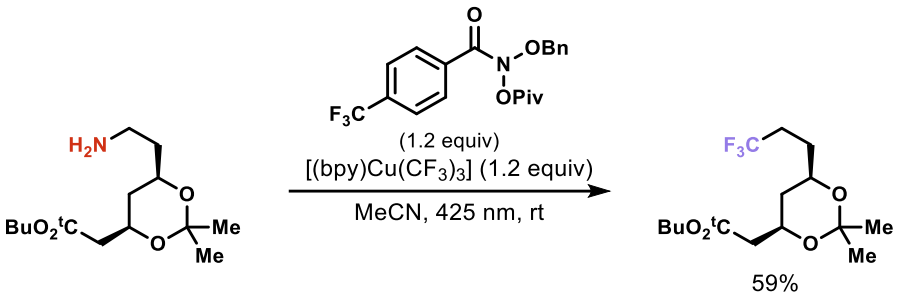
with benzylic amines, contrary to the amine-deletion conditions. Additionally, α-secondary amines could be converted to alkyl-chlorides with the inclusion of carbon tetrachloride. This was unsuccessful starting from α-primary amines, as hydrogen-atom transfer outcompeted chlorination of the radical intermediate.

1.2.2.5 Hydroxylation

Both α-primary and α-secondary amines can be converted to alcohols (Scheme 1.12).[26] To achieve this, a solution of the title reagent is saturated with oxygen by sparging, and a solution of the amine is added with active oxygen sparging. This forms a peroxide, which is reduced to the alcohol upon treatment with triphenylphosphine.



Scheme 1.12 deaminative hydroxylation of aliphatic amines



Scheme 1.13 deaminative trifluoromethylation of aliphatic amines

1.2.2.6 Trifluoromethylation

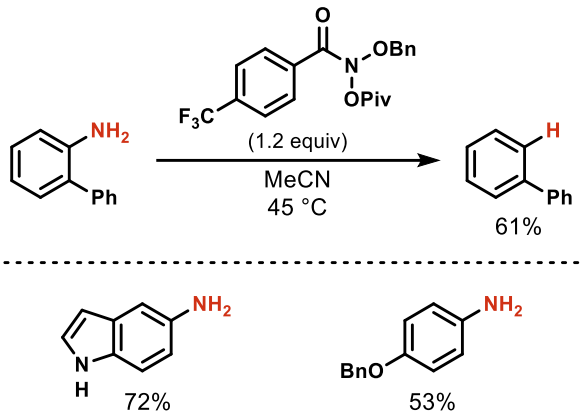
Conditions to for deaminative trifluoromethylation using the title reagent have also been disclosed (Scheme 1.13).[27] This is accomplished through adding the amine to a solution containing [(bpy)Cu(CF_3)$_3$] and the title reagent under 425 nm irradiation.

1.2.3 Deaminative Transformations of Anilines

1.2.3.1 Deamination/Reduction

Anilines can also be deaminated using the title reagent, though some substrates require a slightly elevated temperature (Table 1.4).[22] This proceeds via an analogous mechanism as aliphatic primary amines and works well for electron rich anilines.

Table 1.4 hydrodeamination of anilines

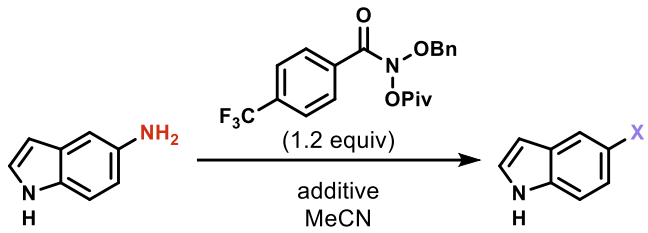


1.2.3.2 Halogenation

Similar to primary amines, deaminating in the presence of carbon tetrabromide or isopropyl iodide forms the aryl bromide or iodide respectively (Table 1.5).[26] Chlorination using the title reagent and carbon tetrachloride was unsuccessful on the model aniline substrate.

Notably, expanded scope is observed for deaminative bromination in comparison with the hydro-deamination reaction. Deaminative bromination of anilines is typically successful at room temperature and works well with both electron-rich and electron-neutral substrates.

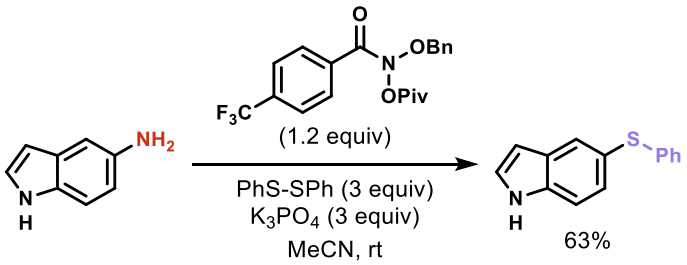
Table 1.5 deaminative halogenation of an aniline substrate



X	additive	equiv	yield (%)
Cl	CCl_4	5	<5
Br	CBr_4	2	67
I	^{i}Pr-I	5	68

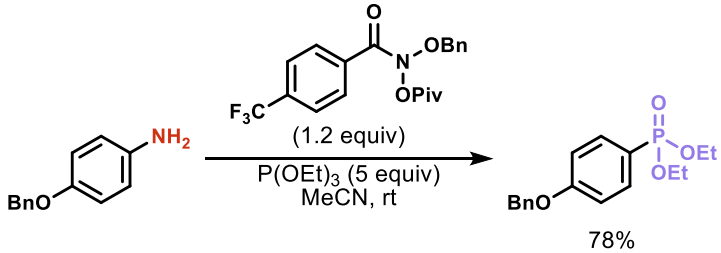
1.2.3.3 Thiolation and Phosphonylation

Deaminative thiolation (Scheme 1.14) and phosphonylation (Scheme 1.15) can also be achieved with aniline substrates. Thiolation can be achieved by adding the aniline substrate to a solution of the title reagent, an aryl disulfide, and an inorganic base (e.g. K_3PO_4).

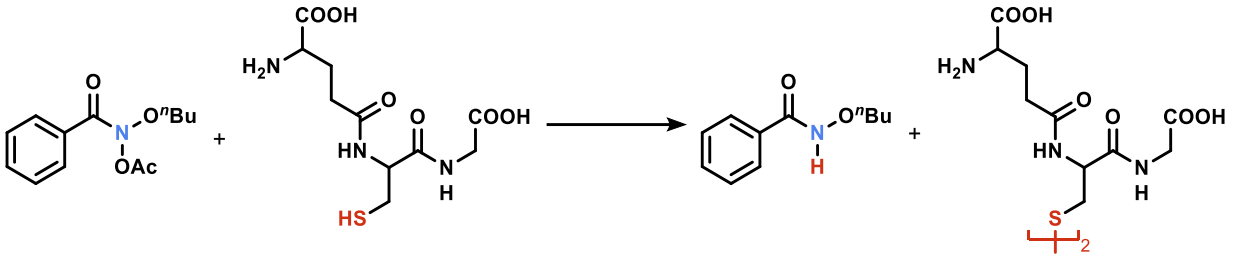


Scheme 1.14 example deaminative thiolation of aniline

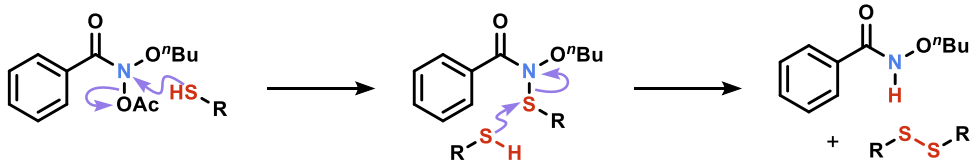
For phosphonylation, the aniline is added to a solution of the title reagent and triethyl phosphite. Electron-rich substrates tend to be the most successful for both thiolation and phosphonylation, and neither protocol was applicable to aliphatic primary amines.



Scheme 1.15 example deaminative phosphonylation



Scheme 1.16 reaction of glutathione with *N*-acyloxy-*N*-butoxybenzamide

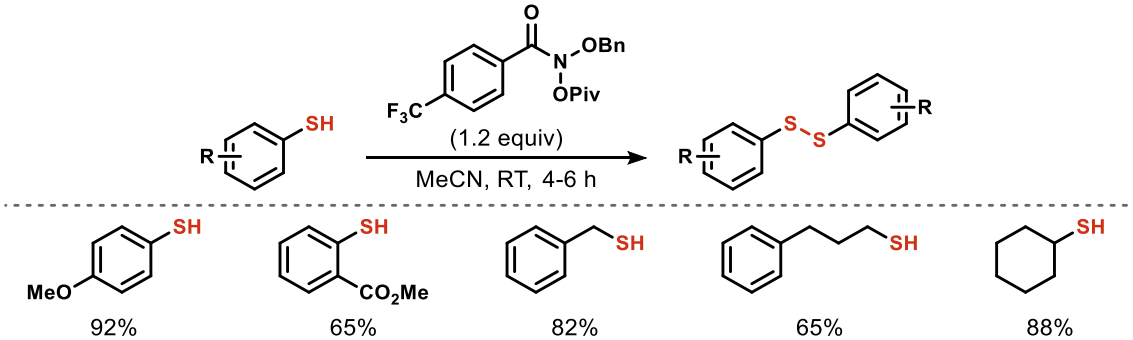


Scheme 1.17 proposed mechanism based on kinetic studies and observed products

1.3 N-Alkoxy-N-Acyloxy Amides Reactivity with Thiols

These anomeric amides can also react with thiols to form disulfide bonds.[10,28] The first report of this is by Glover and Adams, detailing the reaction of glutathione with *N*-acyloxy-*N*-butoxybenzamide (Scheme 1.16). They observed the formation of the disulfide dimer in addition to *N*-butoxybenzamide, formed through the reduction of the anomeric amide. Kinetic data showed that glutathione was consumed at twice the rate of the anomeric amide, suggesting that the thiol first attacks at the anomeric nitrogen atom, forming a thio-anomeric amide, followed by attack from another thiol molecule at the sulfur atom to form the disulfide bond (Scheme 1.17). A similar transformation was also recently reported using the reagent developed in our group, likely through the same mechanism as above (Table 1.6).

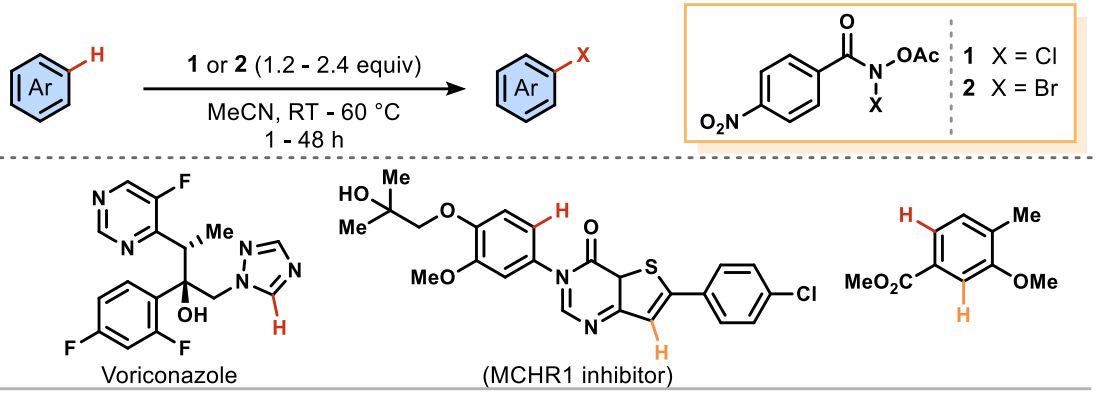
Table 1.6 select scope of anomeric amide mediated disulfide formation



1.4 α-Reactive Anomeric Amide Reagents

Recently, the Baran lab has also developed *N*-halo-*N*-acetoxybenzamide regents. Aryl substrates react with these reagents through attack at the electrophilic halogen atom, enabling halogenation of aryl C-H bonds. These compounds show improved reactivity, and enhanced selectivity in some cases, over alternative reagents (Table 1.7).[29]

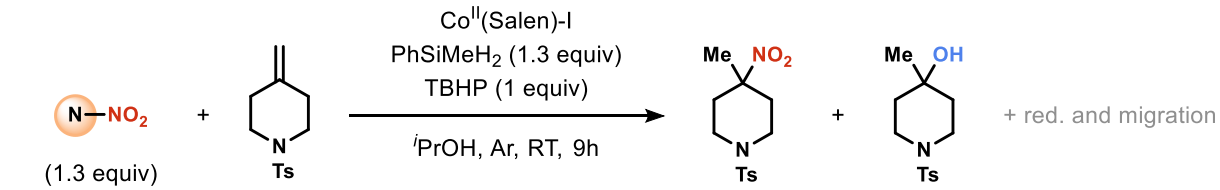
Table 1.7 selected examples of C-H halogenation using anomeric halogenating reagents

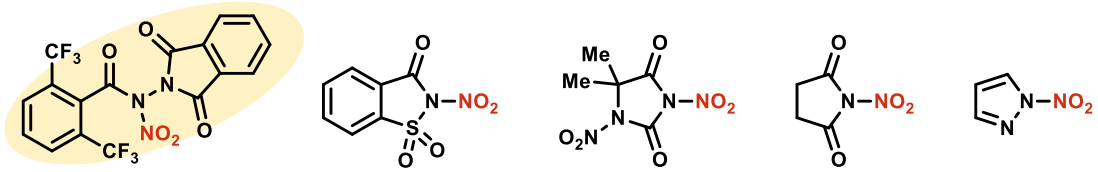


	Voriconazole	(MCHR1 inhibitor)	
X = Cl	**1**: 52% TCICA, TfOH, HFIP: 27%		**1**: 86% (8.2:1) Palau'chlor: 17% (8:1)
X = Br	**2**: 79% NBS, AcOH: 36%	**2**: 54% (4.4:1) NBS: 7% (1.5:1)	**2**: 91% (>50:1) NBS: 81% (4:1)

The same lab has also developed an anomeric amide nitrating reagent,[30] shown in Table 1.8. They have demonstrated that this reagent shows enhanced selectivity under their conditions relative to commonly used nitrating reagents, highlighting the utility of anomeric amides in a variety of transformations.

Table 1.8 comparison of novel anomeric nitrating reagent from Baran and coworkers with existing reagents





53% (5%) 17% (14%) 4% (50%) 3% (56%) 4% (20%)

1.5 References

(1) Glover, S. A. Anomeric Amides — Structure, Properties and Reactivity. *Tetrahedron* **1998**, *54* (26), 7229–7271. https://doi.org/10.1016/S0040-4020(98)00197-5.

(2) Gerdes, R. G.; Glover, S. A.; ten Have, J. F.; Rowbottom, C. A. N-Acetoxy-N-Alkoxyamides - a New Class of Nitrenium Ion Precursors Which Are Mutagenic. *Tetrahedron Letters* **1989**, *30* (20), 2649–2652. https://doi.org/10.1016/S0040-4039(00)99089-0.

(3) J. Campbell, J.; A. Glover, S. Bimolecular Reactions of Mutagenic N-Acyloxy-N-Alkoxybenzamides with Aromatic Amines. *J. Chem. Res. (S)* **1999**, No. 8, 474–475. https://doi.org/10.1039/A903555I.

(4) Andrews, L. E.; Banks, T. M.; Bonin, A. M.; Clay, S. F.; Gillson, A.-M. E.; Glover, S. A. Mutagenic N-Acyloxy-N-Alkoxyamides: Probes for Drug–DNA Interactions. *Aust. J. Chem.* **2004**, *57* (4), 377–381. https://doi.org/10.1071/ch03276.

(5) Glover, S. A.; Schumacher, R. R.; Bonin, A. M.; Fransson, L. E. Steric Effects on the Direct Mutagenicity of N-Acyloxy-N-Alkoxyamides—Probes for Drug–DNA Interactions. *Mutation Research/Genetic Toxicology and Environmental Mutagenesis* **2011**, *722* (1), 32–38. https://doi.org/10.1016/j.mrgentox.2011.02.007.

(6) Glover, S. A.; Hammond, G. P.; Bonin, A. M. A Comparison of the Reactivity and Mutagenicity of N-(Benzoyloxy)-N-(Benzyloxy)Benzamides. *J. Org. Chem.* **1998**, *63* (26), 9684–9689. https://doi.org/10.1021/jo980863z.

(7) Andrews, L. E.; Bonin, A. M.; Fransson, L. E.; Gillson, A.-M. E.; Glover, S. A. The Role of Steric Effects in the Direct Mutagenicity of N-Acyloxy-N-Alkoxyamides. *Mutation Research/Genetic Toxicology and Environmental Mutagenesis* **2006**, *605* (1), 51–62. https://doi.org/10.1016/j.mrgentox.2006.02.003.

(8) Campbell, J. J.; Glover, S. A. Bimolecular Reactions of Mutagenic N-Acetoxy-N-Alkoxybenzamides and N-Methylaniline. *J. Chem. Soc., Perkin Trans. 2* **1992**, No. 10, 1661–1663. https://doi.org/10.1039/P29920001661.

(9) Glover, S. A.; Mo, G. Hindered Ester Formation by SN2 Azidation of N-Acetoxy-N-Alkoxyamides and N-Alkoxy-N-Chloroamides—Novel Application of HERON Rearrangements. *J. Chem. Soc., Perkin Trans. 2* **2002**, No. 10, 1728–1739. https://doi.org/10.1039/B111250N.

(10) Glover, S. A.; Adams, M. Reaction of N-Acyloxy-N-Alkoxyamides with Biological Thiol Groups †. *Aust. J. Chem.* **2011**, *64* (4), 443–453. https://doi.org/10.1071/CH10470.

(11) Cavanagh, K. L.; Glover, S. A.; Price, H. L.; Schumacher, R. R. SN2 Substitution Reactions at the Amide Nitrogen in the Anomeric Mutagens, N-Acyloxy-N-Alkoxyamides. *Aust. J. Chem.* **2009**, *62* (7), 700–710. https://doi.org/10.1071/CH09166.

(12) Kennedy, S. H.; Dherange, B. D.; Berger, K. J.; Levin, M. D. Skeletal Editing through Direct Nitrogen Deletion of Secondary Amines. *Nature (London, U. K.)* **2021**, *593* (7858), 223–227. https://doi.org/10.1038/s41586-021-03448-9.

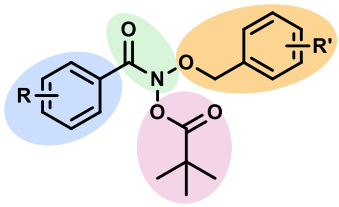
(13) Glover, S. A. The HERON Reaction — Origin, Theoretical Background, and Prevalence. *Can. J. Chem.* **2005**, *83*. https://doi.org/10.1139/v05-150.

(14) Banks, T. M.; Bonin, A. M.; Glover, S. A.; Prakash, A. S. Mutagenicity and DNA Damage Studies of N-Acyloxy-N-Alkoxyamides — the Role of Electrophilic Nitrogen. *Org. Biomol. Chem.* **2003**, *1* (13), 2238–2246. https://doi.org/10.1039/B301618H.

(15) Holovach, S.; Melnykov, K. P.; Poroshyn, I.; Iminov, R. T.; Dudenko, D.; Kondratov, I.; Levin, M.; Grygorenko, O. O. C-C Coupling through Nitrogen Deletion: Application to Library Synthesis. *Chem. - Eur. J.* **2023**, *29* (4), e202203470. https://doi.org/10.1002/chem.202203470.
(16) Holovach, S. M.; Melnykov, K. P.; Poluektova, M. S.; Rozhenko, O. B.; Grygorenko, O. O. Incorporation of Gem-Difluorocycloalkyl Substituents into Heterocycles via the Levin's "Nitrogen Deletion" Strategy. *J. Org. Pharm.* **2023**, *21* (3), 11–16. https://doi.org/10.24959/ophcj.23.278321.
(17) Wright, B. A.; Matviitsuk, A.; Black, M. J.; García-Reynaga, P.; Hanna, L. E.; Herrmann, A. T.; Ameriks, M. K.; Sarpong, R.; Lebold, T. P. Skeletal Editing Approach to Bridge-Functionalized Bicyclo[1.1.1]Pentanes from Azabicyclo[2.1.1]Hexanes. *J. Am. Chem. Soc.* **2023**, *145* (20), 10960–10966. https://doi.org/10.1021/jacs.3c02616.
(18) Tian, D.; Pan, Y.; Zhao, X.; Yin, Y.; Jiang, Z. Chiral Lewis Acid-Catalyzed Intramolecular [2 + 2] Photocycloaddition: Enantioselective Synthesis of Azaarene-Functionalized Azabicyclo[2.1.1]Hexanes and Bicyclo[1.1.1]Pentanes. *J. Am. Chem. Soc.* **2025**. https://doi.org/10.1021/jacs.5c03542.
(19) Gauthier, M.; Whittingham, J. B. M.; Hasija, A.; Tetlow, D. J.; Leigh, D. A. Skeletal Editing of Mechanically Interlocked Molecules: Nitrogen Atom Deletion from Crown Ether-Dibenzylammonium Rotaxanes. *J. Am. Chem. Soc.* **2024**, *146* (43), 29496–29502. https://doi.org/10.1021/jacs.4c09066.
(20) Zang, Z.; Ye, W.; Cheng, K.; Wang, X.; Jin, X. Synthesis of Substituted Tetralins via Nitrogen Deletion/Diels–Alder Cascade Reaction. *J. Org. Chem.* **2024**, *89* (23), 17338–17345. https://doi.org/10.1021/acs.joc.4c01959.
(21) Masson-Makdissi, J.; Lalisse, R. F.; Yuan, M.; Dherange, B. D.; Gutierrez, O.; Levin, M. D. Evidence for Dearomatizing Spirocyclization and Dynamic Effects in the Quasi-Stereospecific Nitrogen Deletion of Tetrahydroisoquinolines. *J. Am. Chem. Soc.* **2024**, *146* (26), 17719–17727. https://doi.org/10.1021/jacs.4c02491.
(22) Berger, K. J.; Driscoll, J. L.; Yuan, M.; Dherange, B. D.; Gutierrez, O.; Levin, M. D. Direct Deamination of Primary Amines via Isodiazene Intermediates. *J. Am. Chem. Soc.* **2021**, *143* (42), 17366–17373. https://doi.org/10.1021/jacs.1c09779.
(23) Kapoor, M.; Liu, D.; Young, M. C. Carbon Dioxide-Mediated C(Sp3)–H Arylation of Amine Substrates. *J. Am. Chem. Soc.* **2018**, *140* (22), 6818–6822. https://doi.org/10.1021/jacs.8b05061.
(24) Mansson, C. M. F.; Burns, N. Z. Aqueous Amine-Tolerant [2+2] Photocycloadditions of Unactivated Olefins. *J. Am. Chem. Soc.* **2022**, *144* (43), 19689–19694. https://doi.org/10.1021/jacs.2c08778.
(25) Shen, L.; Lin, Z.; Guo, B.; Zi, W. Synthesis of Cycloheptanoids through Catalytic Enantioselective (4 + 3)-Cycloadditions of 2-Aminoallyl Cations with Dienol Silyl Ethers. *Nature Synthesis* **2022**, *1* (11), 883–891. https://doi.org/10.1038/s44160-022-00150-0.
(26) Dherange, B. D.; Yuan, M.; Kelly, C. B.; Reiher, C. A.; Grosanu, C.; Berger, K. J.; Gutierrez, O.; Levin, M. D. Direct Deaminative Functionalization. *J. Am. Chem. Soc.* **2023**, *145* (1), 17–24. https://doi.org/10.1021/jacs.2c11453.

(27) Xue, J.-H.; Li, Y.; Liu, Y.; Li, Q.; Wang, H. Site-Specific Deaminative Trifluoromethylation of Aliphatic Primary Amines. *Angewandte Chemie International Edition* **2024**, *63* (8), e202319030. https://doi.org/10.1002/anie.202319030.
(28) Xu, X.; Yan, L.; Huang, W.; Wang, Y.; Wang, M.; Feng, L.; Wang, P.; Wang, S. Facile and Efficient Transformation of Thiols to Disulfides via a Radical Pathway with N-Anomeric Amide. *RSC Adv.* **2024**, *14* (25), 17780–17784. https://doi.org/10.1039/D4RA03545C.
(29) Wang, Y.; Bi, C.; Kawamata, Y.; Grant, L. N.; Samp, L.; Richardson, P. F.; Zhang, S.; Harper, K. C.; Palkowitz, M. D.; Vasilopoulos, A.; Collins, M. R.; Oderinde, M. S.; Tyrol, C. C.; Chen, D.; LaChapelle, E. A.; Bailey, J. B.; Qiao, J. X.; Baran, P. S. Discovery of N–X Anomeric Amides as Electrophilic Halogenation Reagents. *Nat. Chem.* **2024**, *16* (9), 1539–1545. https://doi.org/10.1038/s41557-024-01539-4.
(30) Wang, Y.; Bogner, M.; Bailey, J.; Grant, L.; Gembicky, M.; Richardson, P.; Baran, P. Anomeric Nitroamide Enabled, Cobalt Catalyzed Alkene Hydronitration. ChemRxiv September 24, 2024. https://doi.org/10.26434/chemrxiv-2024-s1mhh.

Chapter 2 : Structure-Reactivity Relationships of Anomeric Amide Reagents



2.1 Introduction

2.1.1 Previous Optimization

The structure of the first generation anomeric amide (**1a**) was established through optimizing the aryl fragment and leaving group of anomeric amide **1b** (Figure 2.1A).[1] When deaminating amine **2d** with **1b**, **4b** was observed, from a competitive transacylation process. To combat this, the acetate was replaced with a bulky pivalate group (anomeric amide **1c**), which resulted in much more effective nitrogen deletion (Figure 2.1B). The reagent was improved further by modifying the electronics of the aryl fragment. A Hammett study revealed that electron-withdrawing groups accelerated the reaction (Figure 2.1C), leading to **1a**, featuring a 4-trifluoromethyl substituent, as the optimized reagent.

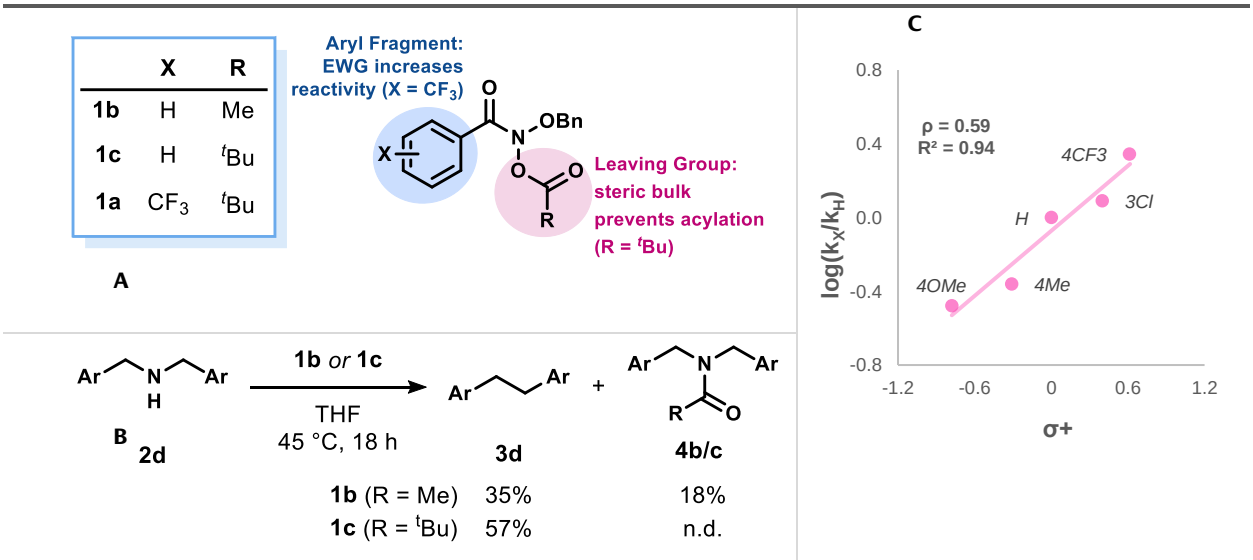


Figure 2.1 First-generation optimization: A. fragments optimized; B. leaving group experiments, Ar = *p*-bromophenyl; C. aryl fragment Hammett plot

2.1.2 Limitations of First Generation Anomeric Amide

During the development of our secondary amine deletion reaction, a few key limitations were identified, some of which are related to the reactivity of anomeric amide **1a**. For example, sterically-hindered amines (**2a-b**) showed little to no reactivity towards **1a** and substrates containing highly electron-rich aromatic rings (**2c**) underwent oxidation more rapidly than nitrogen-deletion (Figure 2.2). Because these limitations specifically relate to the reactivity of the anomeric amide reagent, we sought to design a reagent that could overcome these.

In addition to addressing these limitations, designing a reagent that could react with secondary amines more rapidly would improve the utility of this reaction for high-throughput or combinatorial synthesis applications. While its use in these contexts has already been demonstrated,[2,3] a more reactive reagent could enable these to occur at room temperature or in a shorter timeframe, empowering this strategy further.

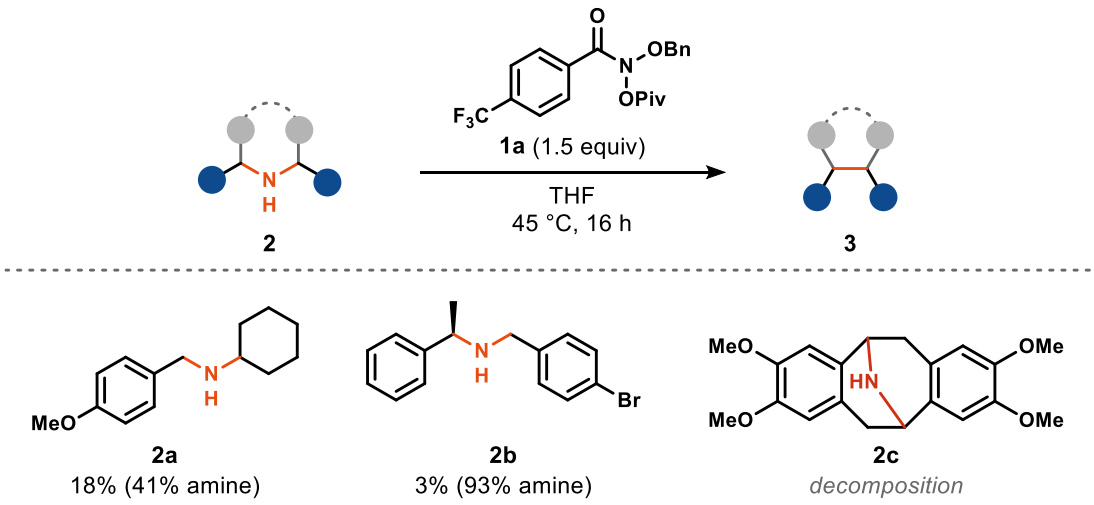


Figure 2.2 Limitations of first generation anomeric amide reagent

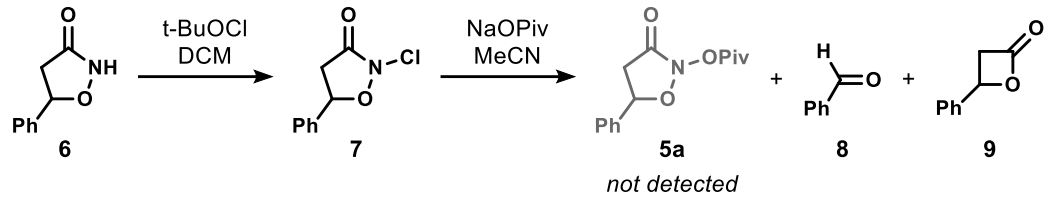


Figure 2.3 Initial attempted synthesis of a cyclic anomeric amide

2.2 Design and Synthesis of Novel Anomeric Amides

2.2.1 Cyclic Anomeric Amides

To circumvent the steric limitations of the reaction, we initially thought to use an anomeric amide with a cyclic skeleton, in order to reduce steric bulk around the amide nitrogen. With computational assistance from A. Kaan Tarhan, isoxazolidinone-based anomeric amide **5a** was designed and selected for its favorable predicted reaction barrier and synthetic accessibility. While attempting to synthesize **5a**, I found that the intermediate isoxazolidinone (**6**) successfully underwent chlorination using tert-butyl hypochlorite to form **7**, but the subsequent pivaloylation led to decomposition, with considerable formation of benzaldehyde (**8**) and 4-phenyloxetan-2-one (**9**) observed (Figure 2.3).

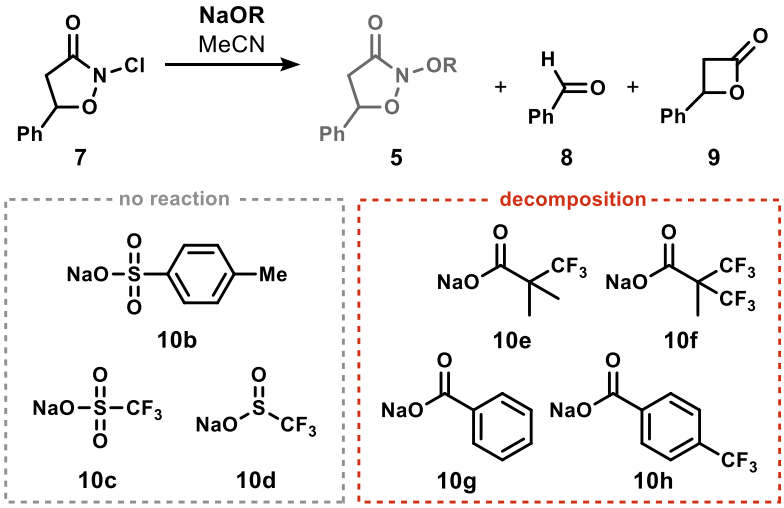


Figure 2.4 Cyclic anomeric amide synthesis: leaving group salt screen

I hypothesized that this may be due to the electron-richness of the pivalate group and attempted to synthesize derivatives with more electron-poor leaving groups (Figure 2.4). Sulfonate (**10b-c**) and sulfinate (**10d**) salts were found to be unreactive under these conditions, while the carboxylate salts screened (**10e-h**) reacted similarly to sodium pivalate, forming complex mixtures containing varying amounts of **8** and **9**. Based on these results, this scaffold was not pursued further.

Additional cyclic scaffolds were later pursued by Bumsu Park (Figure 2.5). While benzoxazinone **12** and naphthoxazepinone **13** both underwent successful N-chlorination with trichloroisocyanuric acid (TCICA), the N-chloride intermediates (**14-15**) were unreactive towards sodium pivalate and anomeric amides **16-17** were not observed. Chloro-benzoxazinone **14** reacted unproductively with silver pivalate, instead forming dimer **18**, while the chloro- naphthoxazepinone (**15**) was mostly unreactive towards silver pivalate.

While cyclic anomeric amides were a promising design for overcoming steric limitations, our efforts to synthesize derivatives of various ring sizes were largely unsuccessful. The reactivity of these derivatives and their intermediates also varied greatly from our acyclic

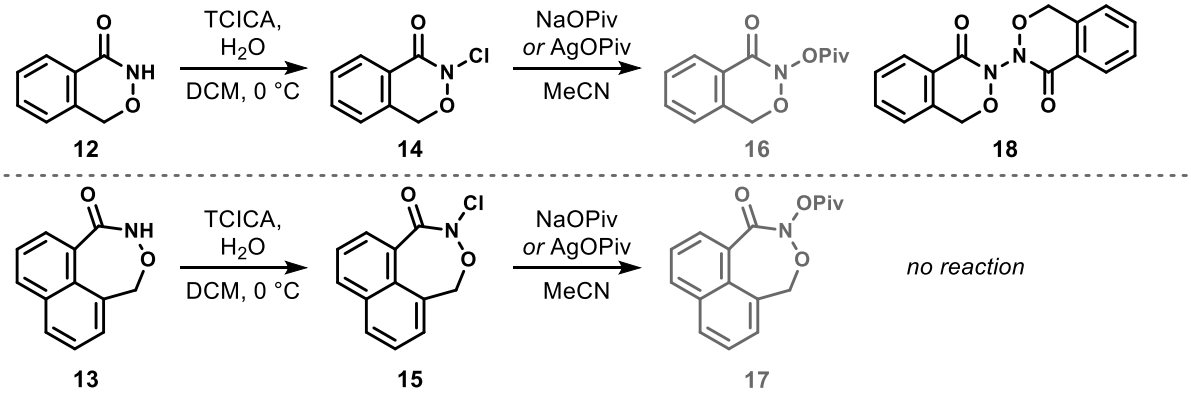


Figure 2.5 alternative cyclic scaffolds pursued

derivatives, revealing gaps in our understanding of the structure-reactivity relationship of these reagents in the context of nitrogen deletion.

2.2.2 Benzyl Derivatives

To explore the structure-reactivity relationships of this class of compounds further, I decided to turn my attention towards understanding the electronic effects on acyclic anomeric amide reactivity. Since the electronic effects of the "aryl fragment" had been elucidated in the initial optimization of the reagent,[1] I wanted to see if modification of the "benzyl fragment" could increase the reactivity further. This would additionally provide structure-reactivity data orthogonal to that of the aryl fragment, which could aid in establishing general structural trends in anomeric amide reactivity and provide a framework for future development.

Towards this goal, Megan Morales and I synthesized a library of "benzyl derivatives" to examine the effects of electron donating (**1d-e**) and withdrawing (**1f-g**) groups, as well as groups with larger π systems (**1h**) or steric bulk (**1i-k**) to probe conformational effects (Figure

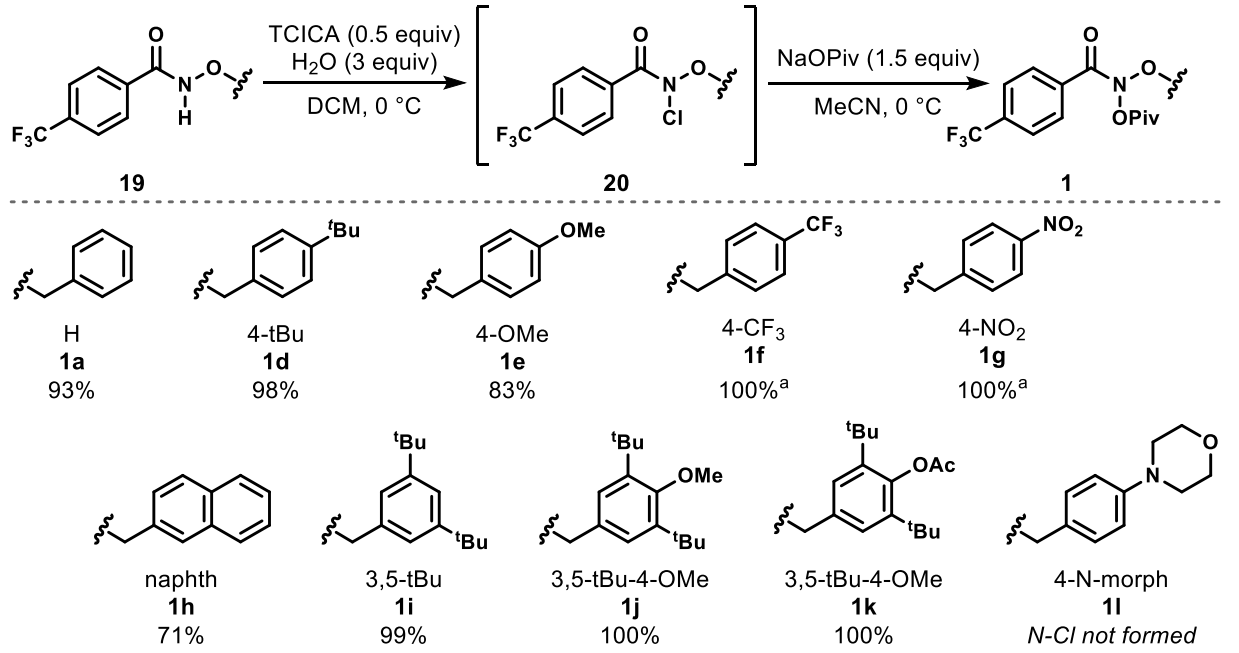


Figure 2.6 Synthesis of anomeric amide benzyl analogs, [a] diethyl ether used for filtration of **20** due to poor solubility in pentane

2.6). While most of these could be synthesized using our typical chlorination and pivaloylation procedures, the morpholino derivative (**19i**) failed to undergo chlorination at the amide nitrogen, likely due to competitive chlorination of the morpholino nitrogen.

The relative reactivity of these compounds was assessed using reaction progress kinetic analysis,[4] which involves fitting a mechanistic model to concentration data collected throughout the course of a reaction. In addition to establishing the relative rates, the mechanistic insight provided by this method can help contextualize reactivity trends. With the help of Megan Morales, we were able to establish conditions for reaction monitoring via ^{1}H NMR (Figure 2.7A). Model substrate **2e** was found to be ideal for the accurate quantification of

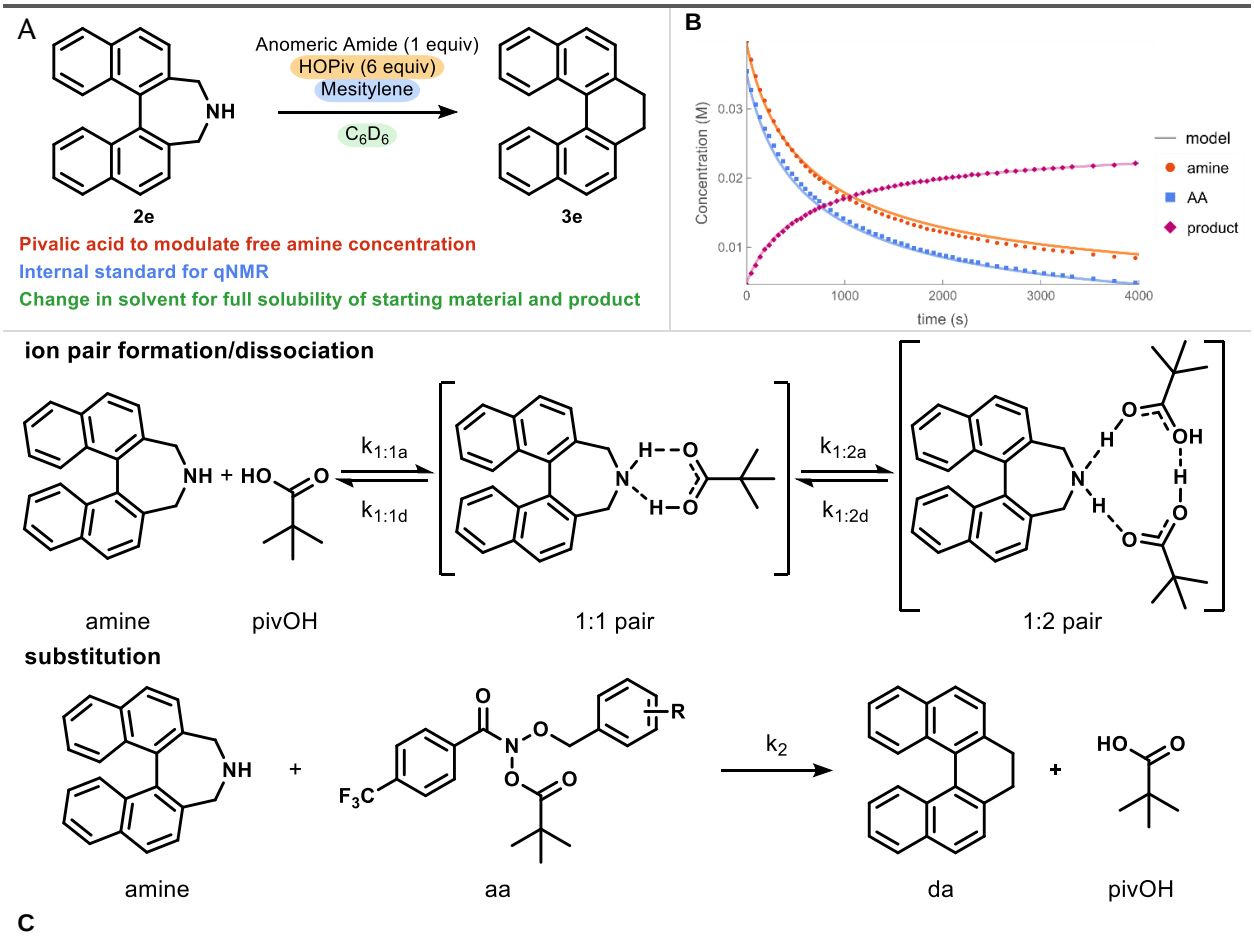


Figure 2.7 A. Optimized reaction conditions for kinetic data collection; B. kinetic data with model fitting; C. Reaction steps used in reaction model

each species in the reaction, as the symmetry, change in ring-size, and overall electronics resulted in distinct, well-isolated peaks. To ensure complete dissolution of **2e**, benzene-d_6 was selected as the solvent, with mesitylene as an internal standard due to its favorable ^{1}H NMR shifts and lack of reactivity towards anomeric amides. The reaction of **2e** toward the anomeric amides was found to be very rapid, preventing the collection of early rate data. However, the rate rapidly dropped throughout the course of the reaction, suggesting that pivalic acid, which forms as a stoichiometric byproduct in the reaction, may have an inhibitory effect. This was confirmed by the inclusion of 6 equivalents of pivalic acid in the reaction, which reduces the overall rate, enabling the collection of early rate data. This also prevents rapid shifts in the pivalic acid concentration throughout the reaction, allowing for more accurate quantification.

In order to determine the reaction rates, we then needed to fit a mathematic model of the rate law for our proposed mechanism to our concentration data. This is complicated by the inhibitory coordination of pivalic acid with the amine – an equilibrium driven process involving two species whose concentrations are shifting in opposite directions throughout the reaction. This precludes the use of standard integrated rate laws, instead requiring a model that can account for these dynamic effects over time. To accomplish this, we built a model based on a parametric function describing the general mechanism outlined in Figure 2.7C. We were able to establish that the pivalic acid coordinated with the amine in a 2:1 fashion, as well as the equilibrium constants for the coordination through a ^{1}H NMR titration (see section 2.3.8.3). This allows the free amine concentration to be accurately modeled throughout the reaction. Overall, we found that this equilibrium paired with a rate-limiting substitution step provided a model that fit very well to our experimental data Figure 2.7B.

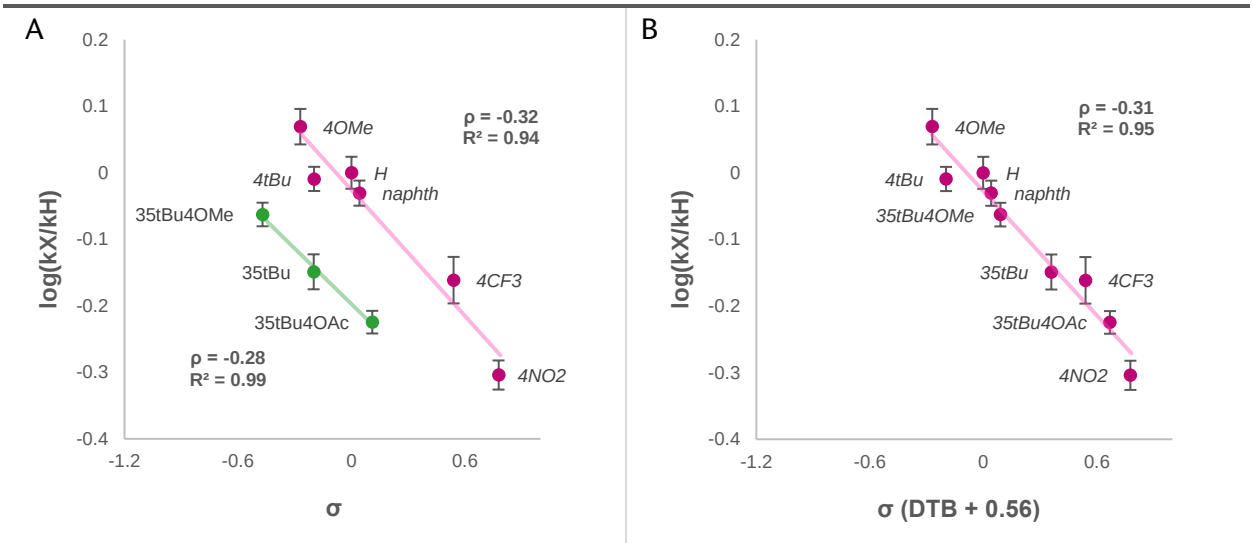


Figure 2.8 Benzyl derivative Hammett trends

The relative rate data revealed several structure-reactivity relationships. The electronic derivatives (**1a-g**) and naphthyl derivative (**1h**) revealed a slightly negative Hammett σ correlation (ρ = -0.32), with the 4-OMe derivative (**1e**) as the first example to outcompete our first generation reagent. This trend was echoed by the 3,5-di-tert-butyl (DTB) derivatives (**1i-k**, ρ = -0.26), though each of these reacted around 65% slower than predicted by their Hammett σ value, relative to the other derivatives (Figure 2.8A). This dissonance can be rectified by applying a correction factor of 0.56 to the DTB derivatives (Figure 2.8B), demonstrating the profound effect of steric bulk at this position. Given the distance of these bulky groups from the reactive center of the molecule, conformational effects were deemed a likely culprit for the observed reactivity difference.

To understand the stereo-electronic effects of the two tert-butyl groups, I used DFT to predict the properties of each derivative using a conformational ensemble. The conformers were then sorted based on the orientation of the benzyl and pivaloyl C-O bonds relative to the nitrogen lone pair and the orientation of the amide C=O bond to the benzyl and pivaloyl groups

(Figure 2.9A). This leads to a total of eight conformational classes, five of which account for >97% of the Boltzmann weight of each derivative (Figure 2.9B).

Notably, the majority of the derivatives primarily preferred classes A, B, and D, while the DTB derivatives demonstrated a unique preference for class C, alongside A. The major structural difference for this class is the position of the benzyl ring, which points away from the nitrogen lone pair, towards the concave side of the molecule. With this configuration, the distance between the aryl rings in pi-stacked conformers is increased, reducing steric clash between the aromatic substituents (Figure 2.9C). Conformers in this class also exhibit a unique $n_N \rightarrow \sigma^*_{OC(Bn)}$ interaction (Figure 2.10A), due to the anti-periplanar relationship of the nitrogen lone pair and benzyl O-C bond. This interaction reduces the electron density on the nitrogen atom, which

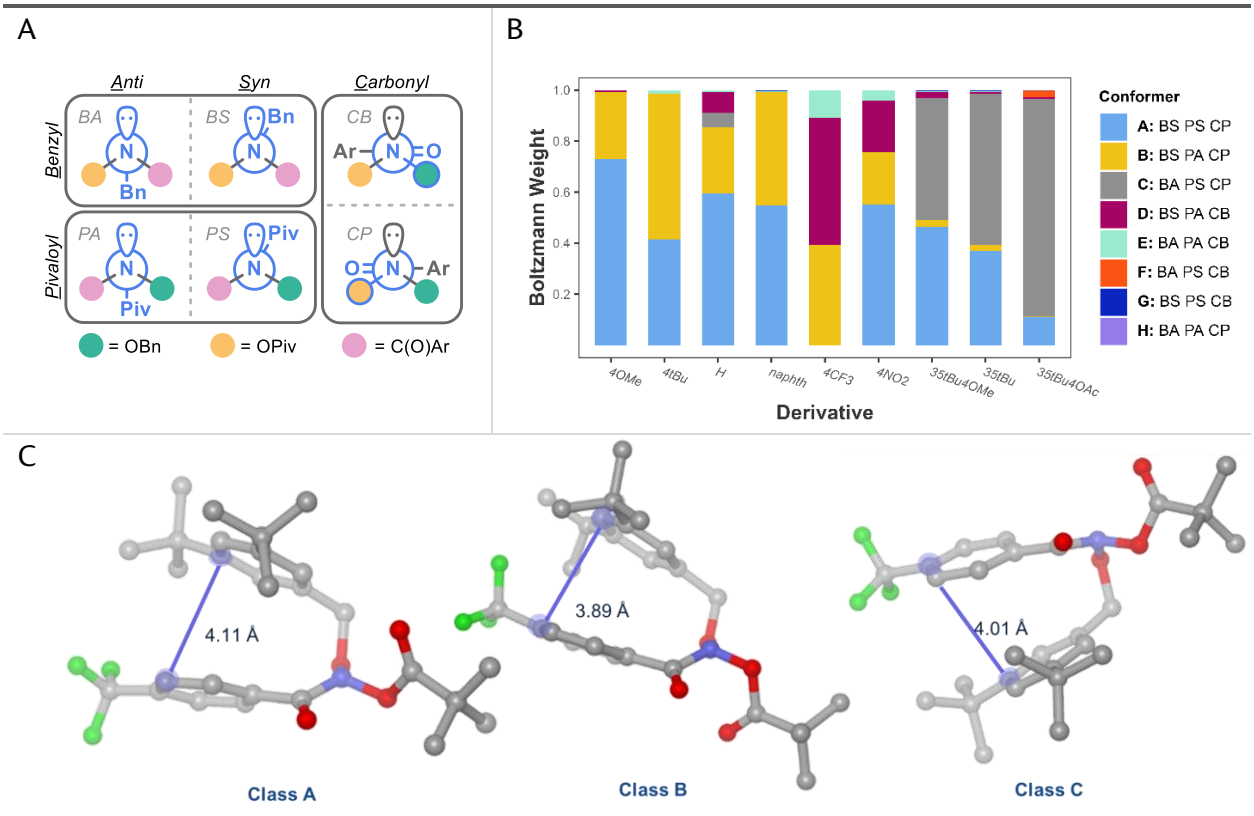


Figure 2.9 A. conformational descriptors used for classification; B. Boltzmann weighted conformer class distribution by derivative; C. Lowest energy conformers from classes A-C for 1i with distance between p-Ar and closest benzyl carbon labelled

could counteract the electron-donating effect of the benzyl ring and slow down the rate of substitution.

Linear free-energy relationships (LFER) can also provide useful insights for understanding conformational influences and remote steric effects.[5,6] The best fit univariate LFER came from the NBO charge of the benzylic oxygen atom (Figure 2.11A). This value correlates fairly well with Hammet σ for most of the derivatives but is less negative than expected for the DTB derivatives. It also had strong conformational ties, with more negative values for conformers in classes A and B compared to classes C, D, and E (Figure 2.10B), possibly due to the $n_N \rightarrow \sigma^*_{OC(Bn)}$ interaction altering the polarity of the C-O bond. Of the multivariate LFER models, a the NBO charge of the aryl C-1 carbon of the benzyl group with the $n_N \rightarrow \sigma^*_{OC(Bn)}$

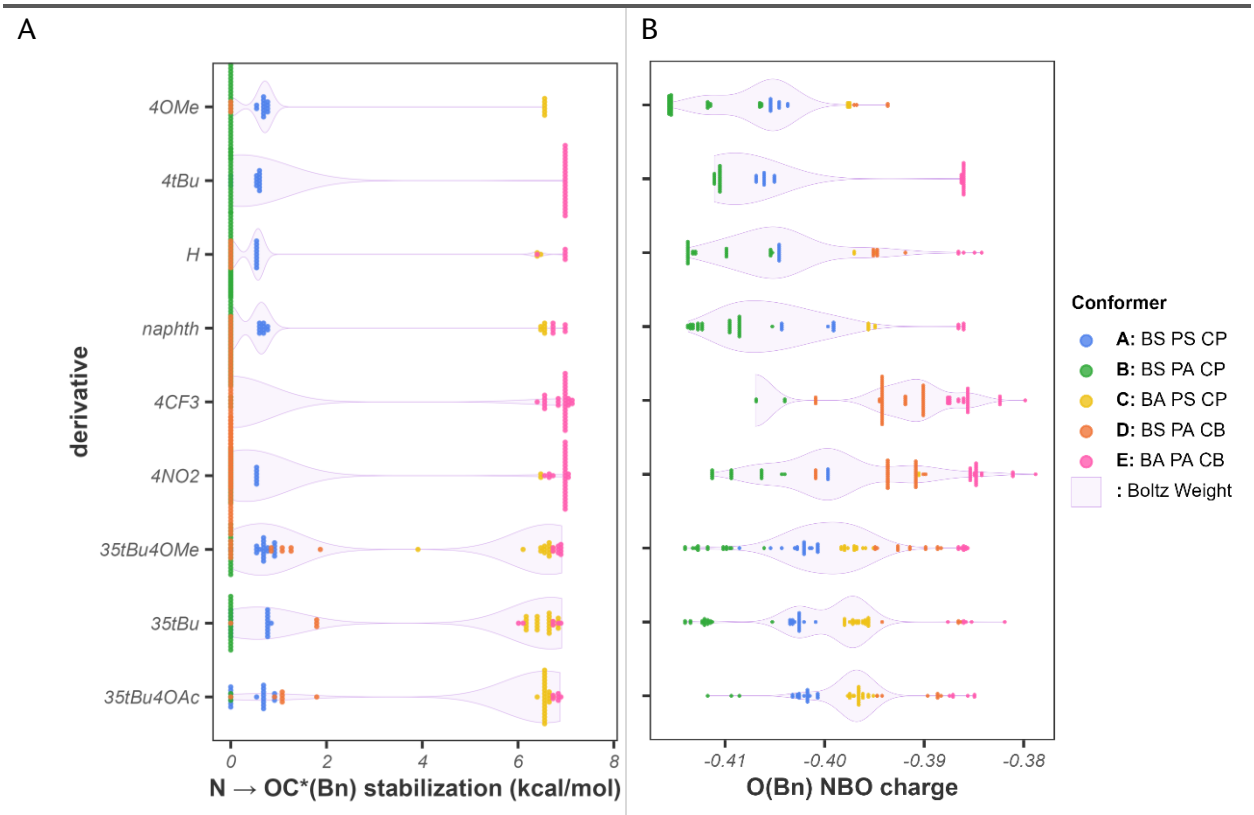


Figure 2.10 Distribution of N-O charge transfer energy (A) and NBO O(Bn) charge (B) by conformer and derivative. "Boltz Weight" shows distribution of Boltzmann weight for the parameter across all conformer classes. Dot plots for each conformer class show unweighted distribution of values for improved visibility.

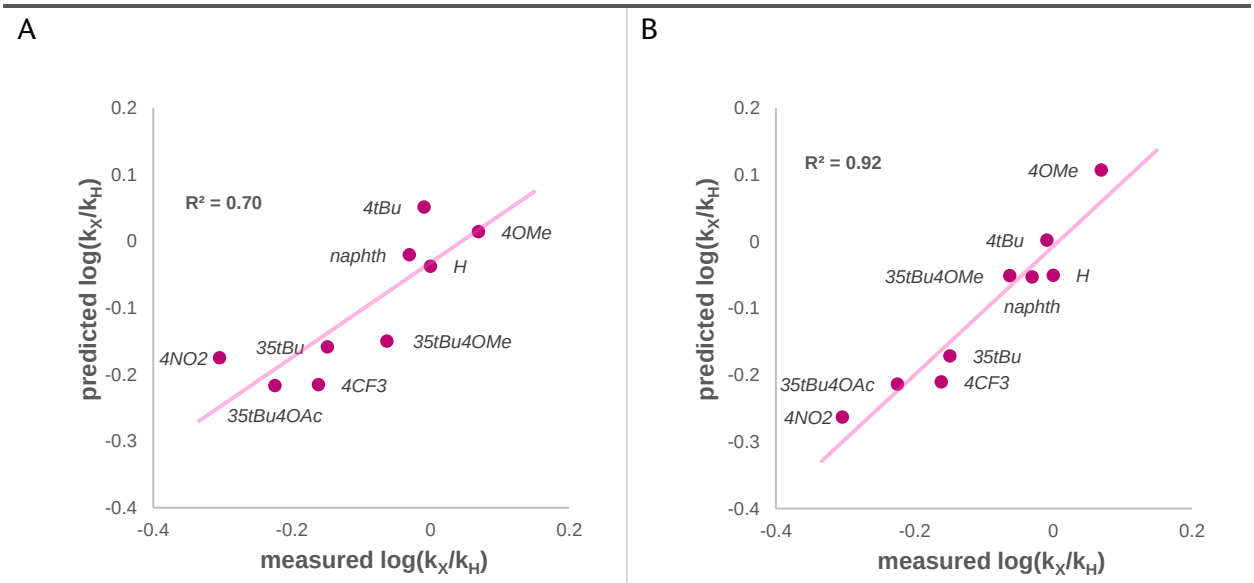


Figure 2.11 A. Single parameter reactivity model; B. Multi-parameter reactivity model

charge transfer energy results in a well-fitting model (Figure 2.11B). The NBO charge of this carbon atom provides a computed value that mirrors the Hammett parameters, accounting for the beneficial electron-donor effect, while the charge transfer energy encapsulates the opposing influence from the $n_N \rightarrow \sigma^*_{OC(Bn)}$ interaction. As such, the strong correlation of this model with the experimental data lends credence to the aforementioned theories.

As a whole, the benzyl derivatives provided interesting structure-reactivity information related to conformational effects but were only able to provide a modest increase in reactivity. Based on this, I decided to turn my attention to optimizing reactivity using the aryl fragment, which had a much stronger influence on reactivity based on our initial optimization data.

2.2.3 Aryl Derivatives

During the original reagent optimization within our group, modifying the electronics of this group was found to have a strong impact on the reactivity of the reagent.[1] However, the extent of this optimization was limited synthetically, as more electron-poor derivatives (**m-n**)

were observed to degrade either completely or partially throughout the course of the synthesis (Figure 2.12, cond. A).

Since the initial development of **1a**, I worked on a team led by Dr. Kate Berger and Dr. Balu Dherange to improve the synthesis of the reagent for publication in *Organic Syntheses*.[7] The chlorination step was improved through the use of trichloroisocyanuric acid (TCICA) in place of tert-butyl hypochlorite (tBuOCl), the addition of 3 equivalents of water, and conducting the reaction at 0 °C. The substitution step was improved through slowing the addition of the chloride intermediate to sodium pivalate and cooling to 0 °C to mitigate the exotherm of the reaction, and careful exclusion of water and air from the reaction. These improvements enabled the synthesis of **1a** in 98% purity on a 5 g scale, compared to 83% using the original procedure (Figure 2.12, cond. B).

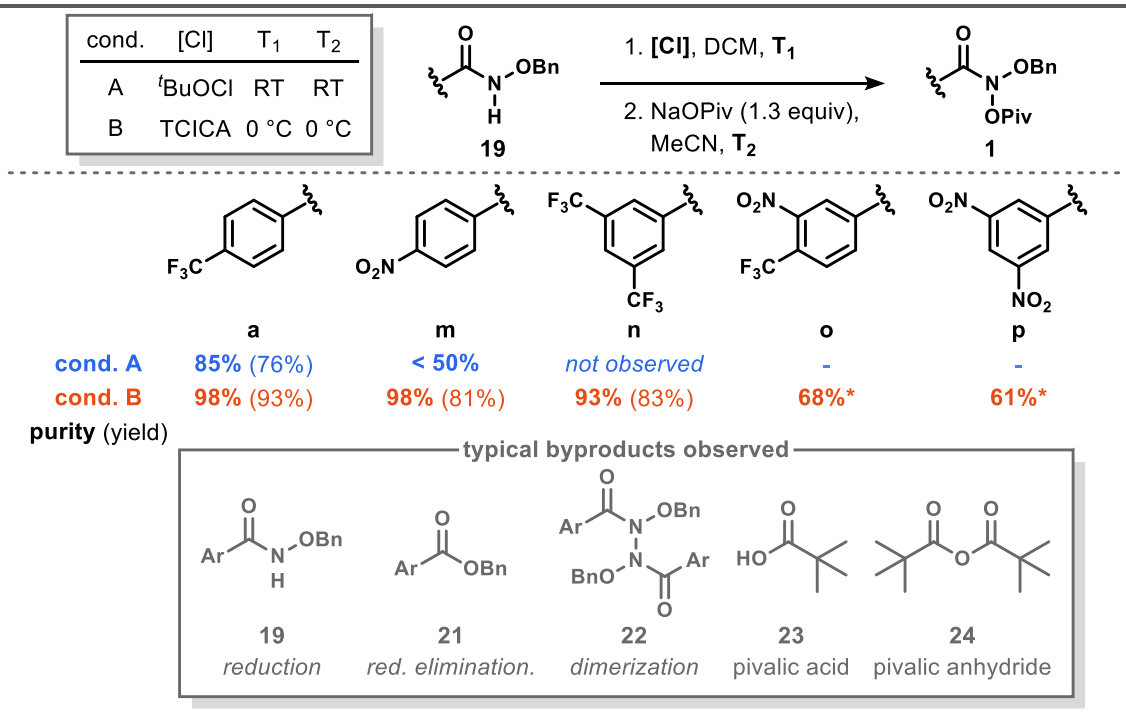


Figure 2.12 Synthetic results for electron-poor derivatives with first and second generation procedures and byproducts observed in anomeric amide synthesis, *estimated purity based on integration of using integration of benzyl methylene ^{1}H NMR peak of 1 relative to the total integration from 4.5-6.0 ppm

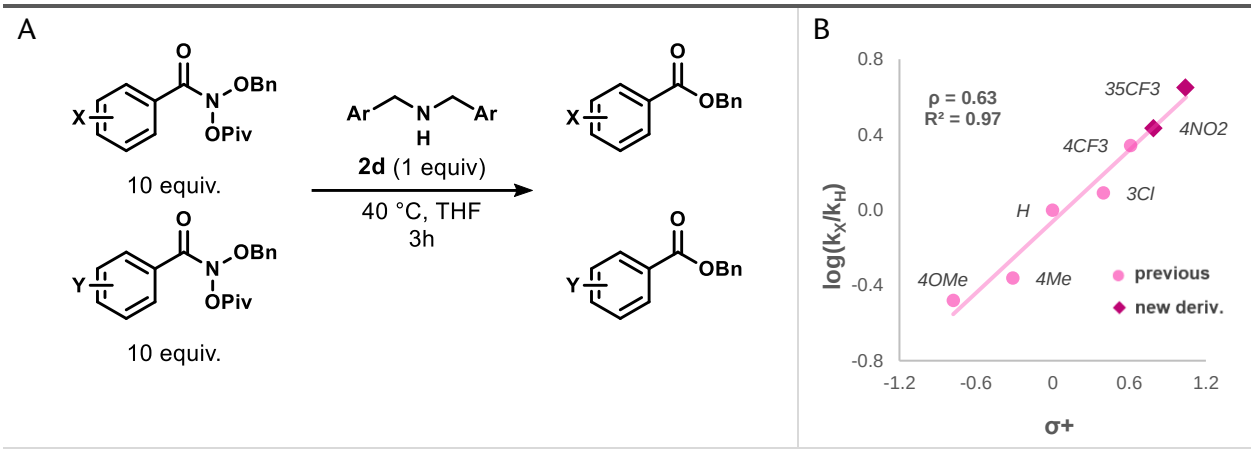


Figure 2.13 A. Conditions for same pot competition experiments, Ar = *p*-bromophenyl; B. Updated Hammett plot

Given the improved purity of **1a** I hypothesized that we should be able to synthesize more reactive derivatives under these conditions or with further optimization efforts. In my initial attempt, I was able to synthesize 4-nitro aryl derivative (**1m**) in 98% purity and 81% yield, and the 3,5-bis(trifluoromethyl) aryl derivative (**1n**) in 93% purity and 83% yield using the *Org. Synth.* conditions. Derivatives **1o** and **1p**, however, proved to be too electron-poor and formed as a mixture with their degradation byproducts (**19, 21-22**), pivalic acid (**23**) and pivalic anhydride (**24**) (Figure 2.12). The reactivity of derivatives **1m** and **1n** was established using same-pot competition experiments with a limiting quantity of amine **2d** (Figure 2.13A), the same method used to establish the previous trend. The results of these experiments aligned well with the previous data, showing enhanced reactivity relative to our first-generation reagent (**1a**) (Figure 2.13B).

While this was a very exciting result, synthesis of the 3,5-bis(trifluoromethyl) aryl derivative (**1n**) was found to lack reproducibility, prompting further optimization efforts. The chlorination step in particular suffered from highly variable reaction times, which could result in partial degradation of the chlorination product and impact the success of the subsequent

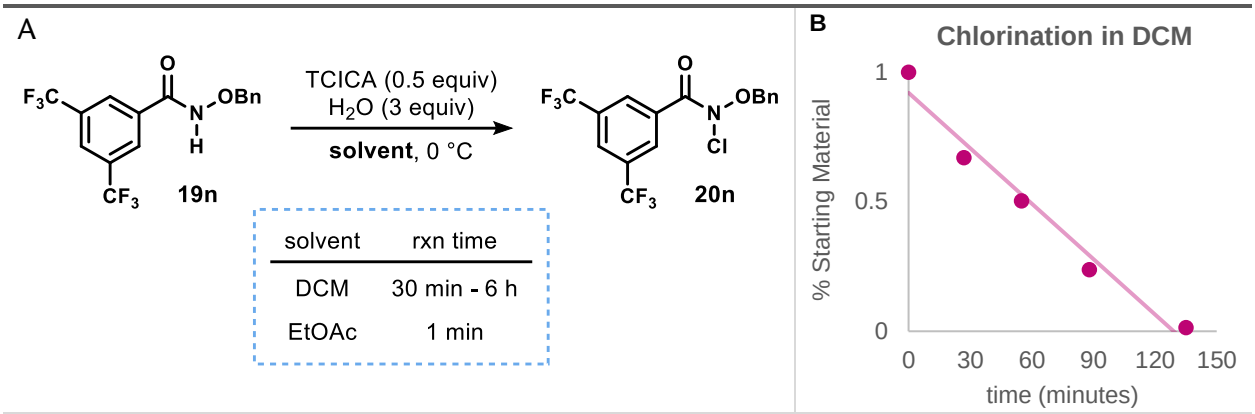


Figure 2.14 A. impact of solvent on reaction time of 19n chlorination; B. Concentration of 19n throughout chlorination reaction in DCM

step. The rate of the reaction was studied with Carys Obertone, who characterized aliquots by ^{1}H NMR throughout the reaction. This data showed apparent zeroth-order consumption of starting material, suggesting that poor solubility of **19n** in H_2O or TCICA in DCM could be limiting. As such, when EtOAc was used in place of DCM, complete consumption of **19n** was observed by TLC immediately following TCICA addition, with high purity maintained.

With rapid and reliable chlorination conditions in hand, I turned my attention to the subsequent pivaloylation step. I suspected that the more reactive derivatives had a larger exotherm, or were at least more sensitive to the exotherm, and that and the presence of water may increase the solubility of sodium pivalate in the solution, leading to increased amounts of pivalic acid and pivalic anhydride. Indeed, I found that, the use of freshly dried acetonitrile and lowering of the reaction temperature to -15 °C provided a reliable method for the isolation of **1n** in 90% purity and 96% yield.

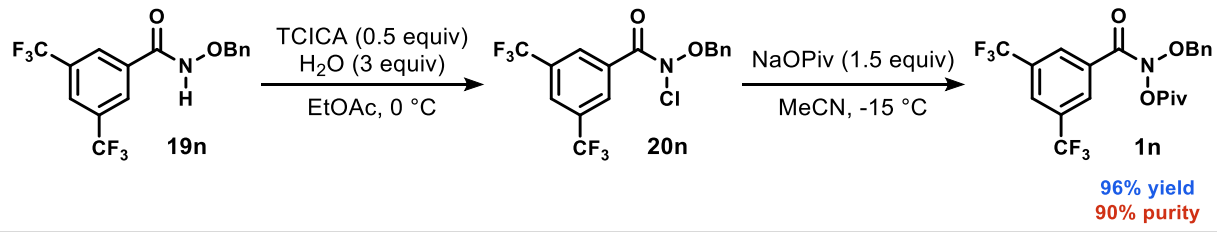


Figure 2.15 Optimized reaction conditions for the synthesis of **1n**

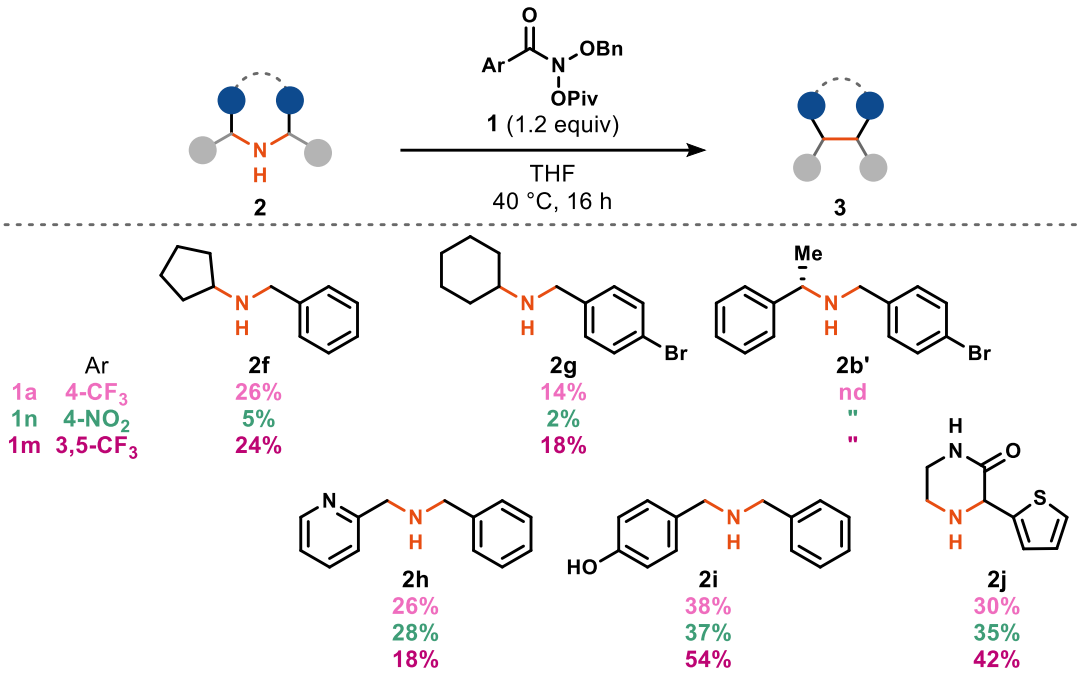


Table 2.1 Screening amines with new anomeric amides, qNMR yields reported

2.2.4 Evaluation of Anomeric Amides with Enhanced Reactivity

Working in collaboration with Rubén Miguélez Moreno, anomeric amides **1n** and **1m** were screened against **1a** with a variety of amines (Table 2.1). With α-cycloalkyl amines (**2g-f**) **1m** showed similar reactivity to **1a** while **1n** had diminished yields with increased amounts of byproducts observed. Amine **2b'** proved to be too sterically hindered to react with any of the anomeric amides and no product formation was able to be observed by ^{1}H NMR. Pyridinyl amine **2h** reacted similarly with **1a** and **1n**, with a slightly lower yield with **1m**, possibly due to increased reactivity towards the pyridine. The phenolic and thiophenyl amines (**2i**-**2j**) showed slightly more promising results, with yields increasing by 12-16% with **1m** compared to **1a**.

Overall, the promiscuous reactivity of the nitro-moiety may limit the utility of **1n**, but **1m** afforded improved yields with some oxidatively sensitive amines. The increased reactivity of **1m** could possibly improve reaction outcomes with amines that are prone to thermal degradation or require longer reaction times, which will be the focus of future work.

2.3 Experimental

2.3.1 General Information

High resolution mass spectra were recorded on an Agilent 6224 TOF High Resolution Accurate MS with electrospray ionization. All mass spectra were processed with an Agilent MassHunter Operating System. Nuclear magnetic resonance spectra (^{1}H NMR, ^{13}C NMR and ^{19}F NMR) were recorded with Bruker spectrometers operating at 400, 500 or 600 MHz for 1H. For kinetic data collection a time delay of 37 seconds was used for all ^{1}H NMR experiments. Chemical shifts are reported in parts per million (ppm, δ), downfield from tetramethylsilane (TMS, δ=0.00 ppm) and are referenced to residual solvent.[8] Coupling constants were reported in Hertz (Hz). Data for ^{1}H NMR spectra were reported as follows: chemical shift (ppm, s = singlet, d = doublet, t = triplet, q = quartet, quin = quintet, dd = doublet of doublets, td = triplet of doublets, ddd = doublet of doublet of doublets, m = multiplet, coupling constant (Hz), and integration).

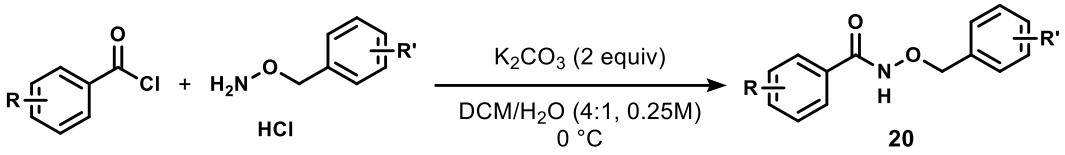
Unless otherwise noted, all reagents were used as received. (S)-N-(4-bromobenzyl)-1-phenylethan-1-amine (**2b'**), bis(4-bromobenzyl)amine (**2d**), N-benzylcyclopentanamine (**2f**), N-(4-bromobenzyl)cyclohexanamine (**2g**), N-benzyl-1-(pyridin-2-yl)methanamine (**2h**), and 4-((benzylamino)methyl)phenol (**2i**) were all synthesized according to the literature procedure.[1] 4,5-dihydro-3H-dinaphtho[2,1-c:1',2'-e]azepine (**2e**) was synthesized according to the literature procedure.[9] 3-(thiophen-2-yl)piperazin-2-one (**2j**) was purchased from Enamine and used without further purification.

Relative rate data for **1m** and **1n** were obtained using a same-pot competition experiment, following the published procedure used to establish the rest of the Hammett plot.[1]

2.3.2 Anomeric Amide Synthesis: General Procedures and Considerations

Procedures adapted from the *Organic Syntheses* procedure for *N*-(benzyloxy)-*N*-(pivaloyloxy)-4-(trifluoromethyl)benzamide.[7]

General Procedure A for the synthesis of *N*-(benzyloxy)benzamides

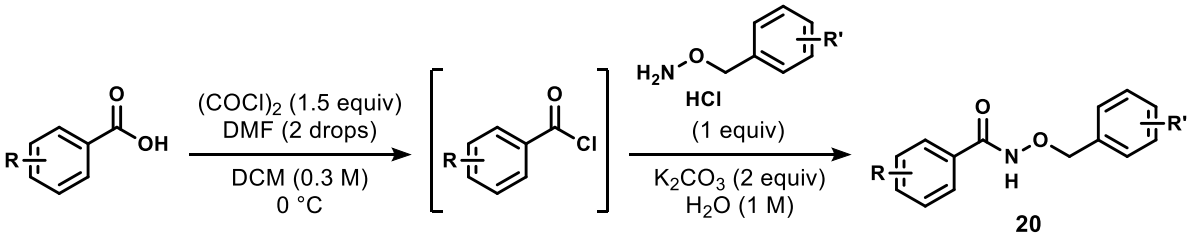


Scheme 2.1 Synthesis of *N*-(benzyloxy)benzamides

Under air, the *O*-benzyl hydroxylamine hydrochloride (1 equiv) and K_2CO_3 (2 equiv) were added to a round bottom flask with a stir bar. Water (1.25 M) was added followed by DCM (CH_2Cl_2) (0.3 M) and the mixture was stirred at room temperature to dissolve the solids. The mixture was then cooled to 0 °C and the benzoyl chloride was added dropwise. The reaction was then warmed to room temperature. After stirring for 1 h the DCM was removed by rotary evaporation and replaced with Et_2O. The solids were then collected on a glass fritted filter and rinsed with H_2O followed by Et_2O. After drying on the filter, the solids were transferred to a glass vial and dried in a vacuum oven at 65 °C overnight.

Notes: If **20** was soluble in Et_2O, hexanes was added until the product began to crystallize or crash out of solution and could be filtered. The *N*-(benzyloxy)benzamides are also stable to silica gel and could be purified by column chromatography if filtration was not feasible.

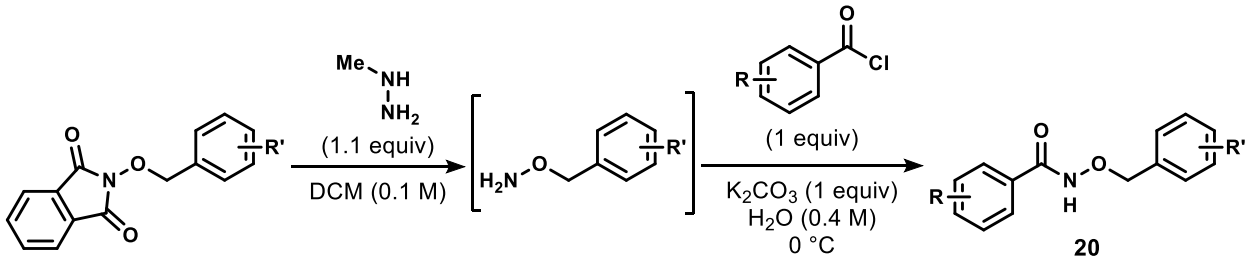
Modification 1: *In situ* benzoyl chloride formation from benzoic acid



Scheme 2.2 *In situ* benzoyl chloride formation from benzoic acid

Under air, the benzoic acid was dissolved in DCM (0.3 M) and two drops of dry DMF were added before cooling to 0 °C. After 5 minutes, oxalyl chloride (1.5 equiv, 2 M solution in DCM) was added over 4 minutes. The reaction was stirred for 30 minutes, then warmed to room temperature before sequentially adding K_2CO_3 (2 equiv), the *O*-benzyl hydroxylamine hydrochloride (1 equiv), and H_2O (1 M). After 1 hour, the reaction was worked up as written in the general procedure.

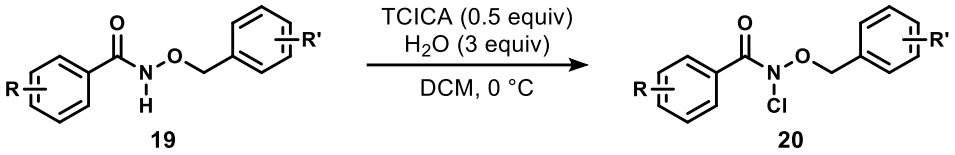
Modification 2: formation of *O*-benzyl hydroxylamine solution from *N*-benzyloxyphthalimide



Scheme 2.3 formation of O-benzyl hydroxylamine in solution from N-benzyloxyphthalimide

Under air, the *N*-benzyloxyphthalimide was dissolved in DCM (0.1 M), then methyl hydrazine (1.1 equiv) was added. After 30 minutes, the solution was filtered through a fritted funnel into a round bottom flask. A stir bar was added, and the solution was cooled to 0 °C for 5 minutes, then K_2CO_3 (1 equiv) and H_2O (0.4 M) were added. Then, the general procedure was followed as written above from the addition of the benzoyl chloride.

General Procedure B for the synthesis of *N*-(benzyloxy)-*N*-chlorobenzamides from *N*-(benzyloxy)benzamides

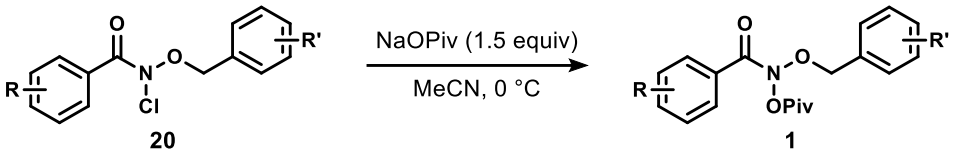


Scheme 2.4 Chlorination of *N*-(benzyloxy)benzamides

Under air, *N*-(benzyloxy)benzamide **19** (1 equiv) was added to a round bottom flask with a stir bar. DCM (CH_2Cl_2) was added (0.25 M) followed by DI H_2O (3 equiv). The flask was topped with a yellow plastic stopper, covered in foil, and cooled to 0 °C in an ice water bath while stirring. After cooling for 5 minutes, TCICA (0.5 equiv) was added in 1 portion. Upon consumption of starting material by TLC (typically 30 min – 3 h), the DCM was removed by rotary evaporation (bath temperature <30 °C) and replaced with pentane (0.25M) and stirred for 2 min at room temperature before filtering the suspension through a pad of celite into an oven-dried flask. Pentane was removed from the filtrate by rotary evaporation followed by further drying under high vacuum to yield the corresponding *N*-(benzyloxy)-*N*-chlorobenzamide **20**, which was immediately carried forward to the following reaction.

Notes: Some N-chlorobenzamides (**20**) were found to have poor solubility in pentane. In these cases, ether or DCM could be used in the filtration without any notable effects on the subsequent reaction. In other cases, the reaction proceeded extremely slowly. The best remedy for this was to use EtOAc as the reaction solvent in place of DCM, though the addition of a small amount of 1M aq HCl was also found to help accelerate the reaction in DCM.

General Procedure C for the synthesis of *N*-(benzyloxy)-*N*-(pivaloyloxy)benzamides from *N*-(benzyloxy)-*N*-chlorobenzamides



20 1

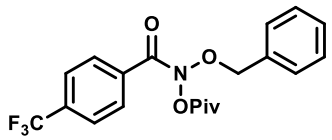
Scheme 2.5 Chlorination of *N*-(benzyloxy)benzamides

NaOPiv (1.5 equiv), dried in a vacuum oven, was added to an oven-dried Schlenk flask. The flask was sealed with a rubber septum and connected to a Schlenk line via its hose adapter before evacuating the flask and purging with N_2 gas (x3). Dry, degassed MeCN (6 mL/mmol) was added, the flask was covered in foil, and vigorously stirred in an ice water bath for 10 minutes. The *N*-(benzyloxy)-*N*-chlorobenzamide **20** (in a dry flask, 1 equiv) was capped with a rubber septum and evacuated and purged with N_2 gas (x3), then dissolved in dry, degassed MeCN (3.2 mL/mmol). This solution was added to the sodium pivalate suspension down the side of the flask by syringe pump over 10-30 min, covering the syringe with foil (see note). After the addition, additional MeCN (0.8 mL/mmol) was used to rinse the *N*-chlorobenzamide flask then added slowly to the reaction mixture. The reaction was stirred at 0 °C until consumption of the *N*-chlorobenzamide by TLC (typically 2-5 h). Et_2O (0.1 M) was then added and the mixture was filtered through a silica plug and rinsed with additional Et_2O. The solvents were removed by rotary evaporation to yield the corresponding *N*-(benzyloxy)-*N*-(pivaloyloxy)benzamide **1**.

Notes: The total acetonitrile concentration should be around 0.1 M, but some derivatives were found to have poor solubility in MeCN, forming a thick slurry. In these cases it was beneficial to add additional MeCN and/or to sonicate the mixture if the reaction stalls. The addition time was determined by the scale of the reaction and the reactivity of the derivative, with longer addition

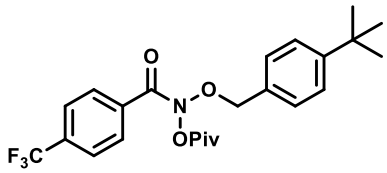
times for highly reactive derivatives or large scale syntheses. For more reactive derivatives, colder reaction temperatures were essential to attaining high purity and the reaction was typically done within 1.5 h. For less reactive derivatives (remaining SM after 5h), it was beneficial to warm the reaction to room temperature to expedite the reaction and prevent product degradation.

2.3.3 Characterization of N-(benzyloxy)-N-(pivaloyloxy)benzamides



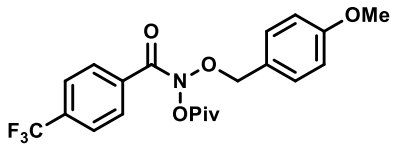
1a

N-(benzyloxy)-N-(pivaloyloxy)-4-(trifluoromethyl)benzamide (**1a**) was synthesized from **20a** (16.9 mmol) according to general procedure C, to afford the title compound (6.6 g, 98% yield, 93% purity) as a clear oil that turned to a white solid after storing at -20 °C. ^{1}H NMR (400 MHz, $CDCl_3$): δ 7.76 (d, J = 9.1 Hz, 2 H), 7.64 (d, J = 7.4 Hz, 2 H), 7.40 – 7.33 (m, 5 H), 5.14 (s, 2 H), 1.10 (s, 9 H).



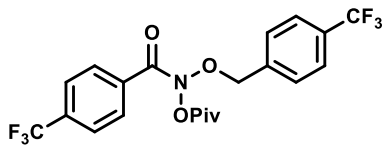
1d

N-((4-(tert-butyl)benzyl)oxy)-N-(pivaloyloxy)-4-(trifluoromethyl)benzamide (**1d**) was synthesized from **20d** (2.0 mmol) according to general procedure C, to afford the title compound (868.9 mg, 98% yield, 98% purity) as a white solid. ^{1}H NMR (400 MHz, $CDCl_3$) δ 7.76 (d, J = 8.1 Hz, 2H), 7.63 (d, J = 8.1 Hz, 2H), 7.37 (d, J = 8.4 Hz, 2H), 7.29 (d, J = 8.4 Hz, 2H), 5.09 (s, 2H), 1.31 (s, 9H), 1.09 (s, 9H). ^{13}C NMR (151 MHz, $CDCl_3$) δ 175.33,173.30, 152.16, 135.66, 133.89 (q, J = 32.9 Hz), 131.82, 129.40, 129.35, 125.63, 125.22 (q, J = 3.8 Hz),124.54 (q, J = 272.4 Hz), 77.84, 38.52, 34.79, 31.42, 26.74. ^{19}F NMR (376 MHz, $CDCl_3$) δ -63.15. HRMS (ESI) calculated 451.197 for $C_{24}H_{28}F_3NO_4$, found 451.1963.



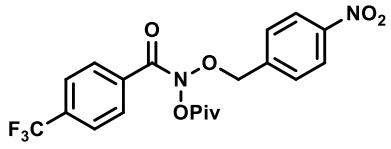
1e

N-((4-methoxybenzyl)oxy)-N-(pivaloyloxy)-4-(trifluoromethyl)benzamide (**1e**) was synthesized from **20e** (3.0 mmol) according to general procedure C, to afford the title compound (1.1 g, 83% yield, 91% purity) as a white solid after triturating with pentane. ^{1}H NMR (400 MHz, $CDCl_3$) δ 7.74 (d, *J* = 8.2 Hz, 2H), 7.63 (d, *J* = 8.2 Hz, 2H), 7.30 (d, *J* = 8.6 Hz, 2H), 6.87 (d, *J* = 8.6 Hz, 2H), 5.05 (s, 2H), 3.80 (s, 3H), 1.12 (s, 9H). ^{13}C NMR (151 MHz, $CDCl_3$) δ 175.41, 173.34, 160.28, 135.67, 133.88 (q, J = 32.6 Hz), 131.26, 129.38, 126.90, 125.20 (q, J = 3.8 Hz), 123.64 (q, J = 272.8 Hz), 114.04, 77.62, 55.43, 38.53, 26.78. ^{19}F NMR (376 MHz, $CDCl_3$) δ -63.15. HRMS (ESI) calculated 425.145 for $C_{21}H_{22}F_3NO_5$, found 425.144.



1f

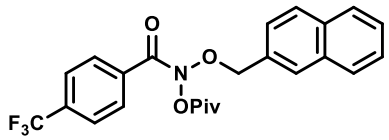
N-(pivaloyloxy)-4-(trifluoromethyl)-N-((4-(trifluoromethyl)benzyl)oxy)benzamide (**1f**) was synthesized from **20f** (1.4 mmol) according to general procedure C, to afford the title compound (637.8 mg, 100% yield, 95% purity) as a yellow solid. ^{1}H NMR (600 MHz, $CDCl_3$) δ 7.76 (d, J = 8.1 Hz, 2H), 7.65 (d, J = 8.1 Hz, 2H), 7.62 (d, J = 7.9 Hz, 2H), 7.53 (d, J = 8.0 Hz, 2H), 5.20 (s, 2H), 1.06 (s, 9H). ^{13}C NMR (151 MHz, $CDCl_3$) δ 175.44, 173.47, 139.07, 135.39, 134.19 (q, *J* = 32.9 Hz), 131.05 (q, *J* = 32.1 Hz), 129.32 (d, *J* = 3.1 Hz), 125.63 (q, *J* = 3.8 Hz), 125.34 (q, *J* = 3.7 Hz), 124.72 (d, *J* = 80.3 Hz), 122.92 (d, *J* = 80.9 Hz), 76.99, 38.48, 26.66. ^{19}F NMR (376 MHz, $CDCl_3$): δ -62.74, -63.21. HRMS (ESI) calculated 463.1218 for $C_{21}H_{19}F_6NO_4$, found 463.1202. Spectroscopic data is in agreement with the literature.[10]



1g

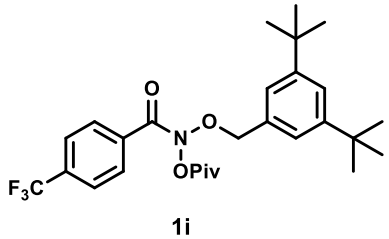
N-((4-nitrobenzyl)oxy)-N-(pivaloyloxy)-4-(trifluoromethyl)benzamide (**1g**) was synthesized from **20g** (2.5 mmol) according to general procedure C, warming to

room temperature after 3h, to afford the title compound (1.1 g, 100% yield, 95% purity) as a light yellow crystaline ish solid. ^{1}H NMR (500 MHz, $CDCl_3$) δ 8.22 (d, J = 8.7 Hz, 2H), 7.76 (d, J = 8.1 Hz, 2H), 7.66 (d, J = 8.2 Hz, 2H), 7.61 (d, J = 8.7 Hz, 2H), 5.27 (s, 2H), 1.06 (s, 9H). ^{13}C NMR (151 MHz, $CDCl_3$) δ 175.39, 173.41, 148.04, 142.34, 135.13, 134.13 (q, J = 32.8 Hz), 129.44, 129.25, 125.28 (q, J = 3.7 Hz), 123.68, 123.43 (q, J = 272.7 Hz), 76.26, 38.34, 26.48. ^{19}F NMR (470 MHz, CCl3) δ -63.22. HRMS (ESI) calculated 440.1195 for $C_{20}H_{19}F_3N_2O_6$, found 440.1169.



1h

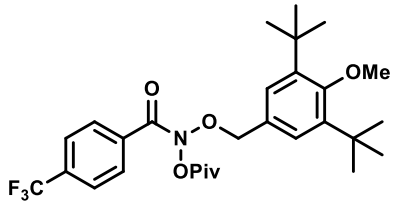
N-(naphthalen-2-ylmethoxy)-N-(pivaloyloxy)-4-(trifluoromethyl)benzamide (**1h**) was synthesized from **20h** (1.0 mmol) according to general procedure C, to afford the title compound (302.1 mg, 71% yield, 89% purity) as a yellow solid. ^{1}H NMR (600 MHz, $CDCl_3$) δ 7.85 – 7.80 (m, 4H), 7.75 (d, J = 8.1 Hz, 2H), 7.60 (d, J = 8.1 Hz, 2H), 7.52 – 7.48 (m, 2H), 7.47 (dd, J = 8.4, 1.7 Hz, 1H), 5.30 (s, 2H), 1.08 (s, 7H). ^{13}C NMR (151 MHz, $CDCl_3$) δ 175.41, 173.41, 135.53, 133.85 (q, J = 32.8 Hz), 133.48, 133.18, 132.28, 129.31, 128.76, 128.42, 128.16, 127.79, 126.67, 126.62, 126.45, 125.17 (q, J = 3.7 Hz), 123.58 (q, J = 272.6 Hz), 78.10, 38.45, 26.65. ^{19}F NMR (565 MHz, $CDCl_3$) δ -63.16. HRMS (ESI) calculated 445.1501 for $C_{24}H_{22}F_3NO_4$, found 445.1508.



1i

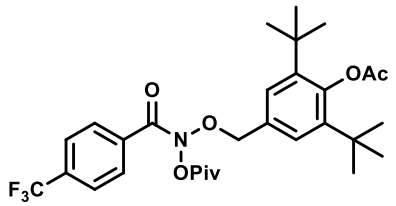
N-((3,5-di-tert-butylbenzyl)oxy)-N-(pivaloyloxy)-4-(trifluoromethyl)benzamide (**1i**) was synthesized from **20i** (0.8 mmol) according to general procedure C, warming to room temperature after 3h, to afford the title compound (377.6 mg, 99% yield, 98% purity) as a clear resin. ^{1}H NMR (600 MHz, $CDCl_3$) δ 7.83 (d, *J* =

8.1 Hz, 2H), 7.68 (d, *J* = 8.1 Hz, 2H), 7.44 (t, *J* = 1.9 Hz, 1H), 7.22 (d, *J* = 1.8 Hz, 2H), 5.16 (s, 2H), 1.33 (s, 18H), 1.15 (s, 9H). ^{13}C NMR (151 MHz, $CDCl_3$) δ 175.24, 173.25, 151.21, 135.79, 133.89 (q, J = 32.8 Hz), 133.77, 129.40, 125.22 (q, J = 3.7 Hz), 123.72, 123.62 (q, J = 272.7 Hz), 123.07, 78.78, 38.51, 34.91, 31.51, 26.75. ^{19}F NMR (376 MHz, $CDCl_3$) δ -63.17. HRMS (ESI) calculated 507.2596 for $C_{28}H_{36}F_3NO_4$, found 507.2596.



1j

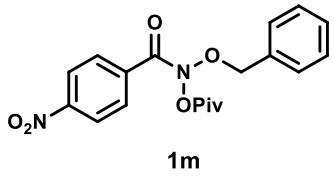
N-((3,5-di-tert-butyl-4-methoxybenzyl)oxy)-N-(pivaloyloxy)-4-(trifluoromethyl)benzamide (**1j**) was synthesized from **20j** (1.1 mmol) according to general procedure C, to afford the title compound (603.4 mg, 100% yield, 95% purity) as a yellow resin. ^{1}H NMR (400 MHz, $CDCl_3$) δ 7.81 (d, J = 8.1 Hz, 2H), 7.66 (d, J = 8.2 Hz, 2H), 7.21 (s, 2H), 5.05 (s, 2H), 3.66 (s, 3H), 1.39 (s, 18H), 1.13 (s, 9H). ^{13}C NMR (151 MHz, $CDCl_3$) δ 175.28, 173.23, 160.30, 144.05, 135.78, 133.92 (q, J = 32.8 Hz), 129.40, 128.60, 128.12, 125.24 (q, J = 3.7 Hz), 123.61 (q, J = 272.7 Hz), 78.52, 64.39, 38.53, 35.84, 32.09, 26.79. ^{19}F NMR (376 MHz, $CDCl_3$) δ -63.17. HRMS (ESI) calculated 537.2702 for $C_{29}H_{38}F_3NO_5$, found 537.2703.



1k

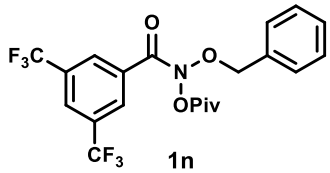
2,6-di-tert-butyl-4-(((N-(pivaloyloxy)-4-(trifluoromethyl)benzamido)oxy)methyl)phenyl acetate (**1k**) was synthesized from **20k** (1.8 mmol) according to general procedure C, warming to room temperature after 3h, to afford the title compound (1.0 g, 100% yield, 87% purity) as a sticky white foam. ^{1}H NMR (400 MHz, $CDCl_3$) δ 7.80 – 7.73 (m, 2H), 7.66 (d, *J* = 8.3 Hz, 2H), 7.30 (s, 2H), 5.07 (s, 2H), 2.34 (s, 3H), 1.32 (s, 18H), 1.13 (s, 9H). ^{13}C NMR (151 MHz, $CDCl_3$) δ 175.29, 173.33, 171.00,

148.61, 142.91, 135.69, 133.87 (q, J = 32.8 Hz), 131.49, 129.31, 127.64, 125.27 (q, J = 3.7 Hz), 123.60 (q, J = 272.6 Hz), 78.01, 38.50, 35.49, 31.44, 26.75, 22.70. ^{19}F NMR (376 MHz, $CDCl_3$) δ -63.17. HRMS (ESI) calculated 565.2651 for $C_{30}H_{38}F_3NO_6$, found 565.2631.



1m

N-(benzyloxy)-4-nitro-N-(pivaloyloxy)benzamide (**1m**) was synthesized from **20m** (1.0 mmol) according to general procedure C, to afford the title compound (365.3 mg, 98% yield, 81% purity) as a yellow to white solid. ^{1}H NMR (600 MHz, $CDCl_3$) δ 8.21 (d, J = 8.6 Hz, 2H), 7.78 (d, J = 8.7 Hz, 2H), 7.40 – 7.33 (m, 5H), 5.12 (s, 2H), 1.12 (s, 9H). ^{13}C NMR (151 MHz, $CDCl_3$) δ 175.37, 172.63, 149.87, 137.98, 134.64, 130.02, 129.56, 129.13, 128.74, 123.38, 78.09, 38.52, 26.75. HRMS (ESI) calculated 372.1321 for $C_{19}H_{20}N_2O_6$, found 372.1307.

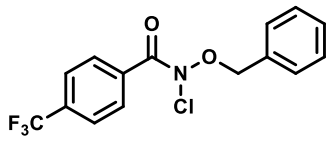


1n

N-(benzyloxy)-N-(pivaloyloxy)-3,5-bis(trifluoromethyl)benzamide (**1n**) was synthesized from **20n** (5.0 mmol) according to general procedure C, cooling the reaction to - 15 °C in a salt and ice bath, to afford the title compound (2.2 g, 93% yield, 83% purity) as a clear oil. ^{1}H NMR (600 MHz, $CDCl_3$) δ 8.12 (s, 2H), 7.99 (s, 1H), 7.40 – 7.31 (m, 5H), 5.13 (s, 2H), 1.14 (s, 9H). ^{13}C NMR (151 MHz, $CDCl_3$) δ 175.29, 171.34, 134.30, 134.07, 131.97 (q, J = 34.1 Hz), 129.56, 129.33 (q, J = 3.9 Hz), 129.22, 128.77, 125.76, 122.85 (q, J = 273.0 Hz), 78.20, 38.56, 26.71. ^{19}F NMR (565 MHz, $CDCl_3$) δ -62.98. HRMS (ESI) calculated 463.1218 for $C_{21}H_{19}F_6NO_4$, found 463.1113.

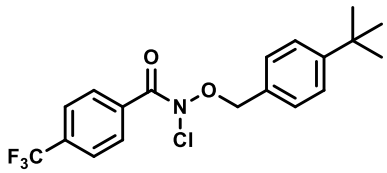
2.3.4 Characterization of N-(benzyloxy)-N-chlorobenzamides

Due to thermal and photochemical instability, these species were characterized by ^{1}H and ^{19}F NMR (where applicable) and carried forward immediately.



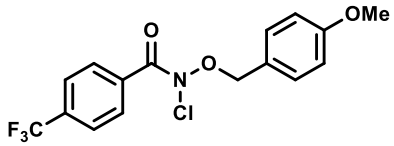
20a

N-(benzyloxy)-N-chloro-4-(trifluoromethyl)benzamide (**20a**) was synthesized from **19a** (5.0 g, 16.9 mmol) according to general procedure B, to afford the title compound as a pale yellow solid. ^{1}H NMR (400 MHz, $CDCl_3$) δ 7.69 (d, J = 9.0 Hz, 2H), 7.63 (d, J = 8.3 Hz, 2H), 7.38 – 7.29 (m, 3H), 7.24 (dd, J = 7.9, 1.7 Hz, 2H), 5.07 (s, 2H). ^{19}F NMR (376 MHz, chloroform-d) δ: -63.2.



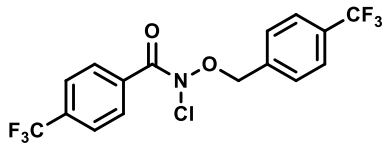
20d

N-((4-(tert-butyl)benzyl)oxy)-N-chloro-4-(trifluoromethyl)benzamide (**20d**) was synthesized from **19d** (690.0 mg, 2.0 mmol) according to general procedure B, using EtOAc as the reaction solvent and hexanes in place of pentane, to afford the title compound as a yellow oil. ^{1}H NMR (400 MHz, $CDCl_3$) δ 7.67 (d, J = 8.3 Hz, 2H), 7.62 (d, J = 8.3 Hz, 2H), 7.37 – 7.29 (m, 2H), 7.18 – 7.10 (m, 2H), 5.03 (s, 2H), 1.30 (s, 9H). ^{19}F NMR (376 MHz, $CDCl_3$) δ -63.18.



20e

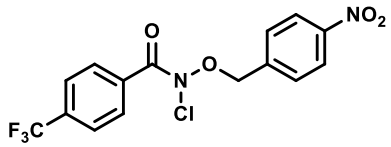
N-chloro-N-((4-methoxybenzyl)oxy)-4-(trifluoromethyl)benzamide (**20e**) was synthesized from **19e** (975.9 mg, 3.0 mmol) according to general procedure B, to afford the title compound as a yellow oil. ^{1}H NMR (500 MHz, $CDCl_3$) δ 7.68 (d, J = 8.2 Hz, 2H), 7.63 (d, J = 8.3 Hz, 2H), 7.17 – 7.12 (m, 2H), 6.88 – 6.78 (m, 2H), 4.99 (s, 2H), 3.80 (s, 3H). ^{19}F NMR (471 MHz, $CDCl_3$) δ -63.17.



20f

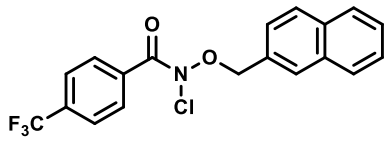
N-chloro-4-(trifluoromethyl)-N-((4-(trifluoromethyl)benzyl)oxy)benzamide (**20f**) was synthesized from **19f** (500.0 mg, 1.4 mmol) according to general procedure B, using ether in the place of pentane, to afford the title compound as a

white solid. ^{1}H NMR (600 MHz, $CDCl_3$) δ 8.21 (d, *J* = 8.7 Hz, 2H), 7.80 (d, *J* = 8.1 Hz, 2H), 7.70 (d, *J* = 8.3 Hz, 2H), 7.48 (d, *J* = 8.7 Hz, 2H), 5.21 (s, 2H). ^{19}F NMR (565 MHz, $CDCl_3$) δ -63.25.



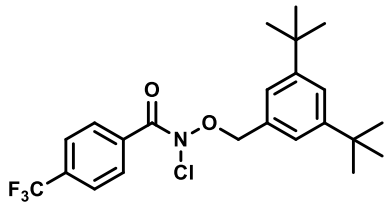
20g

N-chloro-N-((4-nitrobenzyl)oxy)-4-(trifluoromethyl)benzamide (**20g**) was synthesized from **19g** (851.6 mg, 2.5 mmol) according to general procedure B, using ether in the place of pentane, to afford the title compound as a white solid. ^{1}H NMR (600 MHz, $CDCl_3$) δ 8.21 (d, J = 8.7 Hz, 2H), 7.80 (d, J = 8.1 Hz, 2H), 7.70 (d, J = 8.3 Hz, 2H), 7.48 (d, J = 8.7 Hz, 2H), 5.21 (s, 2H). ^{19}F NMR (565 MHz, $CDCl_3$) δ -63.25.



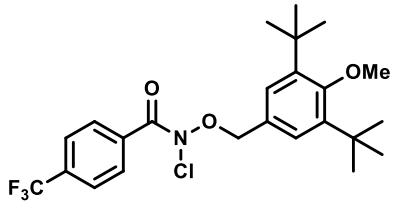
20h

N-chloro-N-(naphthalen-2-ylmethoxy)-4-(trifluoromethyl)benzamide (**20h**) was synthesized from **19h** (329.9 mg, 1.0 mmol) according to general procedure B, filtering the DCM mixture directly rather than replacing with pentane, to afford the title compound as a white solid. ^{1}H NMR (400 MHz, $CDCl_3$) δ 7.87 – 7.81 (m, 1H), 7.78 (t, J = 8.0 Hz, 2H), 7.73 – 7.69 (m, 1H), 7.64 (d, J = 8.2 Hz, 2H), 7.56 (d, J = 8.3 Hz, 2H), 7.54 – 7.47 (m, 2H), 7.33 – 7.27 (m, 1H), 5.22 (s, 2H). ^{19}F NMR (565 MHz, $CDCl_3$) δ -63.19.



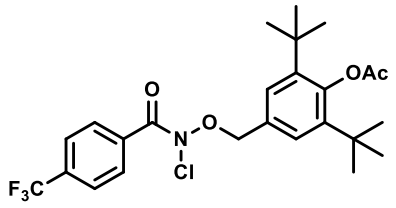
20i

N-chloro-N-((3,5-di-tert-butylbenzyl)oxy)-4-(trifluoromethyl)benzamide (**20i**) was synthesized from **19i** (306.2 mg, 0.8 mmol) according to general procedure B, to afford the title compound as a yellow oil. ^{1}H NMR (600 MHz, $CDCl_3$) δ 7.76 (d, J = 8.1 Hz, 2H), 7.66 (d, J = 8.1 Hz, 2H), 7.40 (d, J = 1.7 Hz, 1H), 7.01 (d, J = 1.7 Hz, 2H), 5.06 (s, 2H), 1.26 (s, 18H). ^{19}F NMR (565 MHz, $CDCl_3$) δ -63.21.



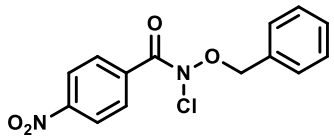
20j

N-chloro-N-((3,5-di-tert-butyl-4-methoxybenzyl)oxy)-4-(trifluoromethyl)benzamide (**20j**) was synthesized from **19j** (491.0 mg, 1.1 mmol) according to general procedure B, to afford the title compound as a yellow oil. ^{1}H NMR (400 MHz, $CDCl_3$) δ 7.77 (d, J = 8.1 Hz, 2H), 7.67 (d, J = 8.2 Hz, 2H), 7.05 (s, 2H), 4.99 (s, 2H), 3.66 (s, 3H), 1.35 (s, 18H). ^{19}F NMR (376 MHz, $CDCl_3$) δ -63.21.



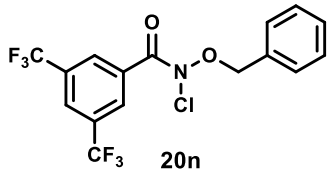
20k

2,6-di-tert-butyl-4-(((N-chloro-4-(trifluoromethyl)benzamido)oxy)methyl)phenyl acetate (**20k**) was synthesized from **19k** (828.9 mg, 1.8 mmol) according to general procedure B, using EtOAc as the reaction solvent and ether in place of pentane, to afford the title compound as a white solid. ^{1}H NMR (400 MHz, $CDCl_3$) δ 7.73 – 7.60 (m, 4H), 7.13 (s, 2H), 5.01 (s, 2H), 2.34 (s, 3H), 1.28 (s, 18H). ^{19}F NMR (376 MHz, $CDCl_3$) δ -63.20.



20m

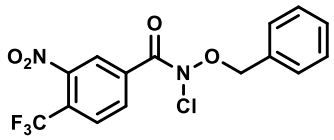
N-(benzyloxy)-N-chloro-4-nitrobenzamide (**20m**) was synthesized from **19m** (272.5 mg, 1.0 mmol) according to general procedure B, filtering the DCM mixture directly rather than replacing with pentane, to afford the title compound as a white solid. ^{1}H NMR (400 MHz, $CDCl_3$) δ 8.20 (d, J = 8.6 Hz, 2H), 7.68 (d, J = 8.7 Hz, 2H), 7.35 (dt, J = 14.2, 6.9 Hz, 3H), 7.24 (d, J = 7.1 Hz, 2H), 5.06 (s, 2H).



20n

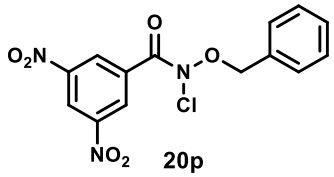
N-(benzyloxy)-N-chloro-3,5-bis(trifluoromethyl)benzamide (**20n**) was synthesized from **19n** (1.8 g, 5.0 mmol) according to general procedure B, using EtOAc as the reaction solvent, to afford the title

compound as a yellow oil. ^{1}H NMR (400 MHz, $CDCl_3$) δ 8.00 (s, 2H), 7.98 (s, 1H), 7.39 – 7.25 (m, 3H), 7.25 – 7.17 (m, 2H), 5.08 (s, 2H). ^{19}F NMR (376 MHz, $CDCl_3$) δ -62.96.



20o

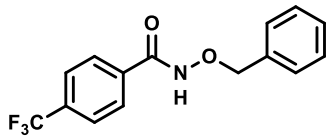
N-(benzyloxy)-N-chloro-3-nitro-4-(trifluoromethyl)benzamide (**20o**) was synthesized from **19o** (297.4 mg, 0.9 mmol) according to general procedure B, using ether in the place of pentane, to afford the title compound as a white solid. ^{1}H NMR (600 MHz, $CDCl_3$) δ 7.84 (d, J = 1.4 Hz, 1H), 7.81 – 7.77 (m, 2H), 7.41 – 7.35 (m, 1H), 7.34 – 7.28 (m, 2H), 7.25 – 7.20 (m, 2H), 5.06 (s, 2H). ^{19}F NMR (565 MHz, $CDCl_3$) δ -60.31.



20p

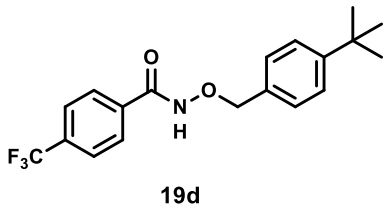
N-(benzyloxy)-N-chloro-3,5-dinitrobenzamide (**20p**) was synthesized from **19p** (443.1 mg, 1.4 mmol) according to general procedure B, filtering the DCM mixture directly rather than replacing with pentane, to afford the title compound as a white solid. ^{1}H NMR (600 MHz, $CDCl_3$) δ 9.09 (d, J = 1.8 Hz, 1H), 8.59 (t, J = 1.6 Hz, 2H), 7.34 (t, J = 7.4 Hz, 1H), 7.28 (t, J = 7.2 Hz, 2H), 7.22 (d, J = 7.6 Hz, 2H), 5.11 (s, 2H).

2.3.5 Characterization of N-Alkoxy Amide Intermediates



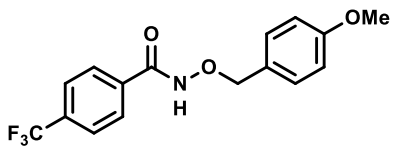
19a

N-(benzyloxy)-4-(trifluoromethyl)benzamide (**19a**) was synthesized from 4-(trifluoromethyl)benzoyl chloride (7.4 mL, 50.1 mmol) and O-benzyl hydroxylamine hydrochloride (8.0 g, 50.1 mmol) according to general procedure A to afford the title compound (13.5 g, 91%) as a white solid. ^{1}H NMR (400 MHz, DMSO) δ 12.00 (s, 1H), 7.94 (d, J = 8.2 Hz, 2H), 7.86 (d, J = 8.3 Hz, 2H), 7.50 – 7.32 (m, 5H), 4.95 (s, 2H).



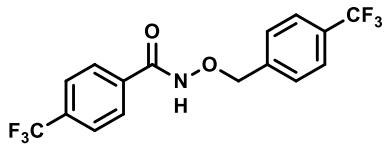
19d

N-((4-(tert-butyl)benzyl)oxy)-4-(trifluoromethyl)benzamide (**19d**) was synthesized from 4-(trifluoromethyl)benzoyl chloride (750.0 µL, 5.0 mmol) and 2-((4-(tert-butyl)benzyl)oxy)isoindoline-1,3-dione (919.0 µL, 5.0 mmol) according to general procedure A, with modification 2, to afford the title compound (0.8 g, 44%) as a white solid. ^{1}H NMR (500 MHz, DMSO) δ 12.00 (s, 1H), 7.96 (d, J = 8.0 Hz, 2H), 7.84 (d, J = 8.1 Hz, 2H), 7.40 (q, J = 8.1 Hz, 4H), 4.92 (s, 2H), 1.28 (s, 9H). ^{13}C NMR (126 MHz, DMSO) δ 162.63, 150.84, 136.19, 132.93, 131.38 (q, J = 31.9 Hz), 128.85, 128.00, 125.43 (q, J = 4.1 Hz), 125.08, 123.86 (q, J = 272.4 Hz), 76.77, 34.30, 31.08. ^{19}F NMR (470 MHz, DMSO) δ -61.48. HRMS (ESI) calculated 351.1446 for $C_{19}H_{20}F_3NO_2$, found 351.14336.



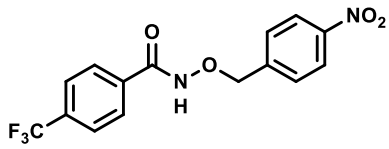
19e

N-((4-methoxybenzyl)oxy)-4-(trifluoromethyl)benzamide (**19e**) was synthesized from 4-(trifluoromethyl)benzoyl chloride (2.3 ml, 15.8 mmol) and O-(4-methoxybenzyl)hydroxylamine hydrochloride (3.0 g, 15.8 mmol) according to general procedure A to afford the title compound (4.3 g, 84%) as a white solid. ^{1}H NMR (600 MHz, DMSO) δ 11.99 (s, 1H), 7.97 (d, J = 7.9 Hz, 2H), 7.83 (d, J = 7.9 Hz, 2H), 7.40 (d, J = 8.0 Hz, 2H), 6.95 (d, J = 8.1 Hz, 2H), 4.90 (s, 2H), 3.76 (s, 3H). ^{13}C NMR (151 MHz, DMSO) δ 163.09, 159.50, 136.28, 131.54 (q, J = 32.0 Hz), 130.84, 128.09, 127.75, 125.43 (q, J = 3.8 Hz), 123.88 (q, J = 272.5 Hz), 113.72, 76.79, 55.05. ^{19}F NMR (565 MHz, DMSO) δ -61.61. HRMS (ESI) calculated 325.0926 for $C_{16}H_{14}F_3NO_3$, found 325.0913.



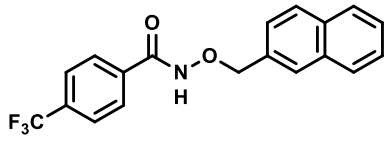
19f

4-(trifluoromethyl)-N-((4-(trifluoromethyl)benzyl)oxy)benzamide (**19f**) was synthesized from 4-(trifluoromethyl)benzoyl chloride (703.0 µL, 4.7 mmol) and O-(4-trifluoromethylbenzyl)hydroxylamine hydrochloride (1.1 g, 4.7 mmol) according to general procedure A to afford the title compound (1.7 g, 97%) as a white solid. ^{1}H NMR (400 MHz, MeOD) δ 7.89 (d, J = 8.2 Hz, 2H), 7.76 (d, J = 8.2 Hz, 2H), 7.69 (s, 4H), 5.09 (s, 2H). ^{19}F NMR (376 MHz, MeOD) δ -64.13, -64.55. Spectrascopic data in agreement with the literature values.[10]



19g

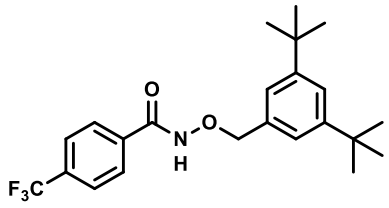
N-((4-nitrobenzyl)oxy)-4-(trifluoromethyl)benzamide (**19g**) was synthesized from 4-(trifluoromethyl)benzoyl chloride (847.0 µL, 5.7 mmol) and O-(4-nitrobenzyl)hydroxylamine hydrochloride (1.2 g, 5.7 mmol) according to general procedure A to afford the title compound (1.7 g, 88%) as a pale yellow solid. ^{1}H NMR (400 MHz, MeOD) δ 8.27 (d, J = 8.7 Hz, 2H), 7.90 (d, J = 8.2 Hz, 2H), 7.76 (dd, J = 11.2, 8.3 Hz, 4H), 5.13 (s, 2H). ^{13}C NMR (151 MHz, DMSO) δ 163.39, 147.35, 143.69, 135.90, 131.69 (q, J = 32.1 Hz), 129.54, 128.14, 125.44 (q, J = 3.8 Hz), 123.83 (q, J = 272.6 Hz), 123.41, 75.87. ^{19}F NMR (376 MHz, MeOD) δ -64.58. HRMS (ESI) calculated 340.0671 for $C_{15}H_{11}F_3N_2O_4$, found 340.0673.



19h

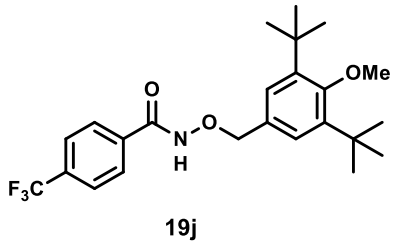
N-(naphthalen-2-ylmethoxy)-4-(trifluoromethyl)benzamide (**19h**) was synthesized according to the literature procedure[10,11] from N-hydroxy-4-(trifluoromethyl)benzamide (**#,** 923.1 mg, 4.5 mmol) and 2-(bromomethyl)naphthalene (669.1 mg, 3.0 mmol) to afford the title compound (382.9 mg, 46% yield) as a yellow solid. ^{1}H NMR* (600 MHz, DMSO) δ

12.06 (s, 1H), 8.16 – 7.40 (m, 11H), 5.14 (s, 2H). ^{13}C NMR* (151 MHz, DMSO) δ 165.48, 163.20, 162.12, 154.67, 142.95, 136.16, 133.41, 132.82, 132.72, 131.95, 131.50 (q, J = 30.3 Hz), 129.20, 128.87, 128.60, 128.08, 127.91, 127.58, 126.81, 126.32, 126.28, 125.48 (d, J = 3.9 Hz), 123.85 (q, J = 272.5 Hz), 123.53, 120.99, 120.11, 77.19. ^{19}F NMR* (565 MHz, DMSO) δ -60.31, -61.45. *Additional peaks in NMR spectra due to suspected rotamers as a result of poor solubility. HRMS (ESI) calculated 345.0977 for $C_{19}H_{14}F_3NO_2$, found 345.0932.



19i

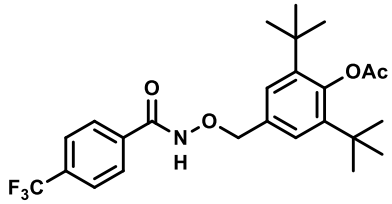
N-((3,5-di-tert-butylbenzyl)oxy)-4-(trifluoromethyl)benzamide (**19i**) was synthesized from 4-(trifluoromethyl)benzoyl chloride (1.1 mL, 7.5 mmol) and 2-((3,5-di-tert-butylbenzyl)oxy)isoindoline-1,3-dione (2.1 g, 7.5 mmol) according to general procedure A, with modification 2, to afford the title compound (2.0 g, 66%) as a white solid after purification by column chromatography. ^{1}H NMR (500 MHz, MeOD) δ 7.88 (d, J = 8.0 Hz, 2H), 7.76 (d, J = 8.0 Hz, 2H), 7.46 (t, J = 1.9 Hz, 1H), 7.34 (s, 2H), 4.99 (s, 2H), 1.33 (s, 18H). ^{13}C NMR (151 MHz, DMSO) δ 163.00, 150.28, 136.22, 134.81, 131.47 (q, J = 32.4 Hz), 128.05, 125.48 (q, J = 3.4 Hz), 123.86 (q, J = 272.5 Hz), 123.14, 122.00, 77.72, 34.48, 31.23. ^{19}F NMR (470 MHz, MeOD) δ -64.55. HRMS (ESI) calculated 407.2072 for $C_{23}H_{28}F_3NO_2$, found 407.2091.



19j

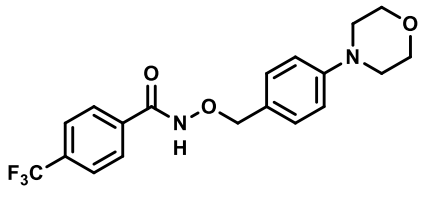
N-((3,5-di-tert-butyl-4-methoxybenzyl)oxy)-4-(trifluoromethyl)benzamide (**19j**) was synthesized from 4-(trifluoromethyl)benzoyl chloride (691.0 µL, 4.7 mmol) and 2-((3,5-di-tert-butyl-4-methoxybenzyl)oxy)isoindoline-1,3-dione (1.7 g, 4.2 mmol) according to general procedure A, with modification 2. Rather than

filtration, the crude reaction was extracted into hexanes, concentrated, and purified by column chromatography to afford the title compound (1.2 g, 60%) as a white, foamy solid. ^{1}H NMR (500 MHz, MeOD) δ 7.88 (d, J = 8.0 Hz, 2H), 7.76 (d, J = 8.0 Hz, 2H), 7.38 (s, 2H), 4.92 (s, 2H), 3.66 (s, 3H), 1.42 (s, 18H). ^{13}C NMR (126 MHz, MeOD) δ 166.33, 161.31, 144.77, 137.16, 134.42 (d, *J* = 35.3 Hz), 130.74, 129.47, 129.04, 126.61 (d, *J* = 4.1 Hz), 125.20 (q, *J* = 271.7 Hz), 79.50, 65.01, 36.63, 32.54. ^{19}F NMR (470 MHz, MeOD) δ -64.50. HRMS (ESI) calculated 437.2178 for $C_{24}H_{30}F_3NO_3$, found 437.2152.



19k

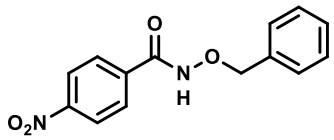
2,6-di-tert-butyl-4-(((4-(trifluoromethyl)benzamido)oxy)methyl)phenyl acetate (**19k**) was synthesized from 4-(trifluoromethyl)benzoyl chloride (913.0 µL, 6.1 mmol) and 2,6-di-tert-butyl-4-(((1,3-dioxoisoindolin-2-yl)oxy)methyl)phenyl acetate (2.4 g, 5.6 mmol) according to general procedure A, with modification 2, to afford the title compound (1.9 g, 74%) as a white solid. ^{1}H NMR (500 MHz, MeOD) δ 7.86 (d, *J* = 8.0 Hz, 2H), 7.75 (d, *J* = 8.1 Hz, 2H), 7.46 (s, 2H), 4.97 (s, 2H), 2.36 (s, 3H), 1.34 (s, 18H). ^{13}C NMR (151 MHz, MeOD) δ 173.00, 166.34, 149.72, 143.90, 137.10, 134.38 (d, J = 31.3 Hz), 133.68, 129.06, 126.59 (d, J = 4.0 Hz), 125.17 (q, J = 271.8 Hz), 79.04, 36.31, 31.85, 22.75. ^{19}F NMR (565 MHz, MeOD) δ -64.55. HRMS (ESI) calculated 465.2127 for $C_{25}H_{30}F_3NO_4$, found 465.2136.



19l

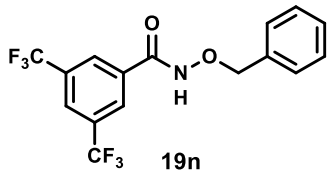
N-((4-morpholinobenzyl)oxy)-4-(trifluoromethyl)benzamide (**19l**) was synthesized from 4-(trifluoromethyl)benzoyl chloride (304.0 µL, 2.0 mmol) and O-(4-morpholinobenzyl)hydroxylamine hydrochloride

(500.1 mg, 2.0 mmol) according to general procedure A to afford the title compound (0.6 g, 72%) as a white solid. ^{1}H NMR (400 MHz, MeOD) δ 7.88 (d, J = 8.1 Hz, 2H), 7.76 (d, J = 8.2 Hz, 2H), 7.38 (d, J = 8.2 Hz, 2H), 6.98 (d, J = 8.3 Hz, 2H), 4.90 (s, 2H), 3.86 – 3.79 (m, 4H), 3.19 – 3.13 (m, 4H). ^{13}C NMR (151 MHz, DMSO) δ 162.41, 151.10, 136.97, 131.03 (q, J = 32.0 Hz), 130.27, 127.97, 126.45, 125.28 (q, J = 3.8 Hz), 123.96 (q, J = 272.4 Hz), 114.59, 76.59, 66.09, 48.26. ^{19}F NMR (376 MHz, MeOD) δ -66.05. HRMS (ESI) calculated 380.1348 for $C_{19}H_{19}F_3N_2O_3$, found 380.1347.



19m

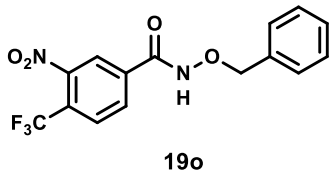
N-(benzyloxy)-4-nitrobenzamide (**19m**) was synthesized from 4-nitrobenzoyl chloride (1.1 g, 5.7 mmol) and O-benzyl hydroxylamine hydrochloride (0.9 g, 5.7 mmol) according to general procedure A to afford the title compound (1.3 g, 80%) as a white solid. ^{1}H NMR (500 MHz, MeOD) δ 8.30 (d, *J* = 8.4 Hz, 2H), 7.92 (d, *J* = 8.4 Hz, 2H), 7.49 (d, *J* = 7.1 Hz, 2H), 7.42 – 7.32 (m, 3H), 5.01 (s, 2H). ^{13}C NMR (151 MHz, DMSO) δ 162.60, 149.23, 138.01, 135.70, 129.01, 128.67, 128.42, 128.36, 123.65, 77.15. HRMS (ESI) calculated 272.0797 for $C_{14}H_{12}N_2O_4$, found 272.0796.



19n

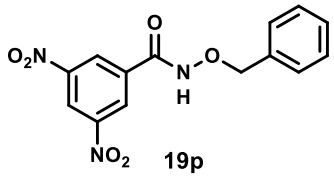
N-(benzyloxy)-3,5-bis(trifluoromethyl)benzamide (**19n**) was synthesized from 3,5-bis(trifluoromethyl)benzoyl chloride (2.3 g, 8.4 mmol) and O-benzyl hydroxylamine hydrochloride (1.3 g, 8.4 mmol) according to general procedure A to afford the title compound (2.7 g, 89%) as a white solid. ^{1}H NMR (600 MHz, DMSO) δ 12.29 (s, 1H), 8.40 (s, 2H), 8.25 (s, 1H), 7.47 (d, J = 7.2 Hz, 2H), 7.43 – 7.30 (m, 3H), 5.00 (s, 2H). ^{13}C NMR (151 MHz, DMSO) δ 160.80, 135.81, 134.67, 130.63 (q, J = 33.4 Hz), 129.03, 128.39, 128.34, 127.86, 124.94, 123.03 (q, J = 272.9 Hz),

77.20. ^{19}F NMR (565 MHz, DMSO) δ -61.75. HRMS (ESI) calculated 363.0694 for $C_{16}H_{11}F_6NO_2$, found 363.0671.



19o

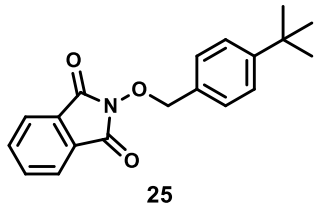
N-(benzyloxy)-3-nitro-4-(trifluoromethyl)benzamide (**19o**) was synthesized from 3-nitro-4-(trifluoromethyl)benzoic acid (1.1 g, 4.3 mmol) and O-benzyl hydroxylamine hydrochloride (0.7 g, 4.7 mmol) according to general procedure A, with modification 1, to afford the title compound (1.1 g, 70%) as a white solid. ^{1}H NMR (600 MHz, DMSO) δ 12.30 (s, 1H), 8.45 (s, 1H), 8.24 (d, J = 8.2 Hz, 1H), 8.16 (d, J = 8.2 Hz, 1H), 7.47 (d, J = 7.3 Hz, 2H), 7.42 – 7.33 (m, 3H), 4.99 (s, 2H). ^{13}C NMR (151 MHz, DMSO) δ 160.16, 147.34, 137.69, 135.78, 131.74, 128.98, 128.83 (q, J = 5.0 Hz), 128.41, 128.36, 123.93, 123.43 (q, J = 33.8 Hz), 121.85 (q, J = 273.3 Hz), 77.12. ^{19}F NMR (470 MHz, MeOD) δ -61.71. HRMS (ESI) calculated 340.0671 for $C_{15}H_{11}F_3N_2O_4$, found 340.0688.



19p

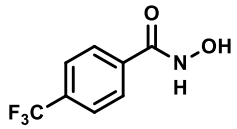
N-(benzyloxy)-3,5-dinitrobenzamide (**19p**) was synthesized from 3,5-dinitrobenzoyl chloride (1.9 g, 8.3 mmol) and O-benzyl hydroxylamine hydrochloride (1.3 g, 8.3 mmol) according to general procedure A to afford the title compound (0.5 g, 20%) as a yellow solid. ^{1}H NMR (600 MHz, MeOD) δ 9.12 (s, 1H), 8.93 (s, 2H), 7.50 (d, J = 7.2 Hz, 2H), 7.39 (dt, J = 12.2, 7.2 Hz, 3H), 5.05 (s, 2H). ^{13}C NMR (151 MHz, DMSO) δ 160.03, 148.17, 135.66, 134.82, 129.02, 128.47, 128.40, 127.30, 121.10, 77.21. HRMS (ESI) calculated 317.0648 for $C_{14}H_{11}N_3O_6$, found 317.0767.

2.3.6 Synthesis and Characterization of Synthetic Intermediates



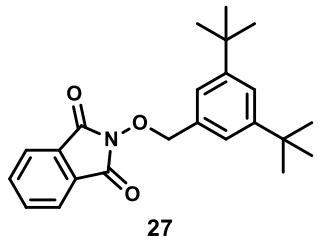
25

2-((4-(tert-butyl)benzyl)oxy)isoindoline-1,3-dione (**25**) was synthesized from 1-(bromomethyl)-4-(tert-butyl)benzene (919 µL, 5 mmol) and *N*-hydroxyphthalimide (0.82 g, 5 mmol) according to the literature procedure[12] to obtain the title compound as a white solid (1.4 g, 92% yield), which was used in the next step without further purification. ^{1}H NMR (500 MHz, $CDCl_3$) δ 7.82 (dd, J = 5.4, 3.1 Hz, 2H), 7.73 (dd, J = 5.5, 3.0 Hz, 2H), 7.48 (d, J = 8.3 Hz, 2H), 7.41 (d, J = 8.3 Hz, 2H), 5.19 (s, 2H), 1.31 (s, 9H). ^{13}C NMR (126 MHz, $CDCl_3$) δ 163.65, 152.60, 134.53, 130.82, 129.80, 129.11, 125.66, 123.60, 79.94, 34.84, 31.40.



26

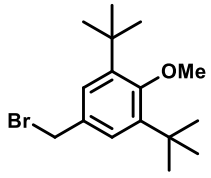
N-hydroxy-4-(trifluoromethyl)benzamide (**26**) was synthesized from 4-(trifluoromethyl)benzoyl chloride (4.47 mL, 30 mmol) and hydroxylamine hydrochloride (2.1 g, 30 mmol) according to general procedure A, using Et_2O as the reaction solvent to obtain the title compound as a white solid (4.5 g, 73% yield). ^{1}H NMR (400 MHz, DMSO) δ 11.45 (s, 1H), 9.22 (s, 1H), 7.95 (d, J = 8.1 Hz, 2H), 7.84 (d, J = 8.2 Hz, 2H).



27

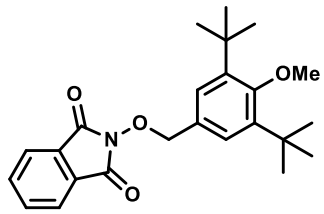
2-((3,5-di-tert-butylbenzyl)oxy)isoindoline-1,3-dione (**27**) was synthesized from 1-(bromomethyl)-3,5-di-tert-butylbenzene (2.1 g, 7.5 mmol) and *N*-hydroxyphthalimide (1.2 g, 7.5 mmol) according to the literature procedure[12] to obtain the title compound as a shiny white solid (2.8 g, 100% yield), which was used in the next step without further purification. ^{1}H NMR (400 MHz, $CDCl_3$) δ 7.83 – 7.76 (m, 2H), 7.76 – 7.68 (m, 2H), 7.41 (t, J = 1.9 Hz, 1H), 7.34 (d, J = 1.8 Hz, 2H), 5.22 (s, 2H), 1.29 (s, 18H). ^{13}C NMR (151 MHz,

$CDCl_3$) δ 163.61, 151.21, 134.48, 132.79, 129.09, 124.44, 123.50, 123.48, 80.69, 34.96, 31.50.



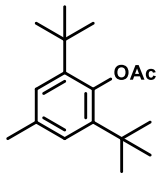
28

5-(bromomethyl)-1,3-di-tert-butyl-2-methoxybenzene (**28**) was synthesized according to the literature procedure[13] from 2,6-di-tert-butyl-4-methylphenol (2.0 g, 9.1 mmol) to afford the title compound as a colorless oil (1.3 g, 50% yield). ^{1}H NMR (500 MHz, $CDCl_3$) δ 7.26 (s, 2H), 4.48 (s, 2H), 3.69 (s, 3H), 1.42 (s, 18H).



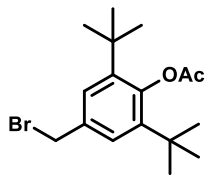
29

2-((3,5-di-tert-butyl-4-methoxybenzyl)oxy)isoindoline-1,3-dione (**29**) was synthesized from **28** (1.3 g, 4.2 mmol) and *N*-hydroxyphthalimide (0.69 g, 4.2 mmol) according to the literature procedure,[12] then extracted into hexanes before concentrating to obtain the title compound as an orange, gummy mixture that was used in the next step without further purification. ^{1}H NMR (400 MHz, $CDCl_3$) δ 7.79 (dd, *J* = 5.5, 3.1 Hz, 2H), 7.72 (dd, *J* = 5.5, 3.1 Hz, 2H), 7.36 (s, 2H), 5.16 (s, 2H), 3.62 (s, 3H), 1.38 (s, 18H).



30

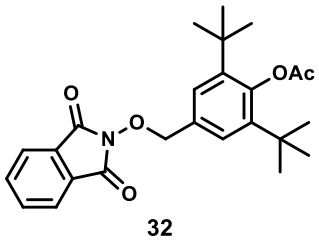
2,6-di-tert-butyl-4-methylphenyl acetate (**30**) was synthesized according to the literature procedure[14] from 2,6-di-tert-butyl-4-methylphenol (2.1 g, 9.5 mmol) to afford the title compound as a white solid (2.5 g, 99% yield). ^{1}H NMR (400 MHz, $CDCl_3$) δ 7.11 (s, 2H), 2.33 (s, 3H), 2.31 (s, 3H), 1.33 (s, 18H).



31

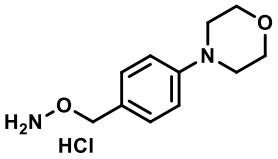
4-(bromomethyl)-2,6-di-tert-butylphenyl acetate (**31**) was synthesized from **30** (2.5 g, 9.5 mmol), following the literature procedure used for **28**,[13] using 1.2 equiv of *N*-bromosuccinimide, to afford the title compound as a mixture, presumably with the dibrominated byproduct, which was carried forward without

further purification. **31**: ^{1}H NMR (600 MHz, $CDCl_3$) δ 7.37 (s, 2H), 4.49 (s, 2H), 2.36 (s, 3H), 1.37 (s, 18H). Byproduct: ^{1}H NMR (400 MHz, $CDCl_3$) δ 7.52 (s, 2H), 6.64 (s, 1H), 2.35 (s, 3H), 1.36 (s, 18H).



32

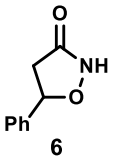
2,6-di-tert-butyl-4-(((1,3-dioxoisoindolin-2-yl)oxy)methyl)phenyl acetate (**32**) was synthesized from **31** (1.3 g, 4.2 mmol) and *N*-hydroxyphthalimide (0.69 g, 4.2 mmol) according to the literature procedure,[12] then extracted into DCM and purified by silica gel chromatography to afford the title compound as a white foamy solid (2.4 g, 59% yield over 2 steps). ^{1}H NMR (500 MHz, $CDCl_3$) δ 7.80 (dd, J = 5.5, 3.1 Hz, 2H), 7.72 (dd, J = 5.5, 3.1 Hz, 2H), 7.48 (s, 2H), 5.18 (s, 2H), 2.33 (s, 3H), 1.32 (s, 18H). ^{13}C NMR (126 MHz, $CDCl_3$) δ 170.97, 163.59, 148.90, 142.92, 134.53, 130.57, 129.04, 128.30, 123.54, 80.19, 35.55, 31.45, 22.76. HRMS (ESI) calculated 423.2105 for $C_{25}H_{29}NO_5$, found 423.2046.



33

O-(4-morpholinobenzyl)hydroxylamine hydrochloride (**33**) was synthesized from (4-morpholinophenyl)methanol (2 g, 10.3 mmol) and *N*-hydroxyphthalimide (1.7 g, 10.3 mmol) according to the literature procedure[12] to afford the title compound as a pink solid (0.97 g, 68% yield). ^{1}H NMR (400 MHz, MeOD) δ 7.46 – 7.39 (m, 2H), 7.23 (d, *J* = 8.3 Hz, 2H), 4.98 (s, 2H), 3.95 – 3.89 (m, 4H), 3.37 – 3.30 (m, 6H), 2.78 (s, 1H).

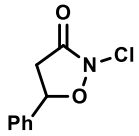
2.3.7 Synthesis and Characterization of Cyclic Anomeric Amide Intermediates



6

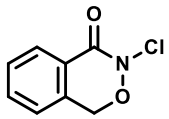
5-phenylisoxazolidin-3-one (**6**) was prepared in 2 steps from 1,1-dibromoformaldoxime (1 g, 5 mmol) and styrene (570 μL) according to the literature procedures[15–17] in 59% yield (1 g). ^{1}H NMR (400 MHz, $CDCl_3$): δ 7.34 –

7.26 (m, 5H), 5.58 (dd, *J* = 10.3, 7.3 Hz, 1H), 3.06 (dd, *J* = 16.6, 7.8 Hz, 1H), 2.92 (dd, *J* = 16.6, 10.4 Hz, 1H). Spectroscopic data are in agreement with those in the literature.[15]



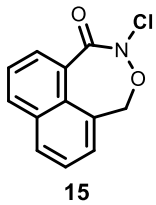
7

2-chloro-5-phenylisoxazolidin-3-one (**7**) was synthesized from **6** and *tert*-butyl hypochlorite adapted from the literature procedure.[1] ^{1}H NMR (500 MHz, $CDCl_3$) δ 7.42 (tdd, *J* = 6.9, 5.4, 2.0 Hz, 5H), 5.81 (dd, *J* = 10.8, 5.8 Hz, 1H), 3.22 (dd, *J* = 17.8, 5.8 Hz, 1H), 3.03 (dd, *J* = 17.8, 10.8 Hz, 1H).



14

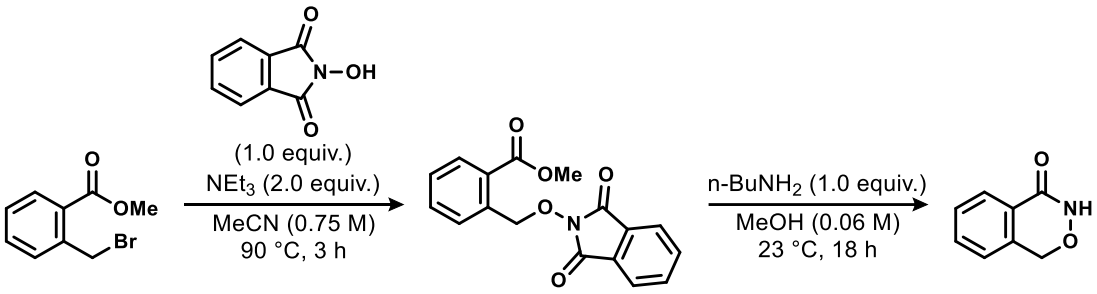
3-chloro-1H-benzo[d][1,2]oxazin-4(3H)-one (**14**): Synthesized according to general procedure B from 1H,3H-benzo[de]isochromen-1-one (used 50 mL round-bottom flask, reaction time 5 h) (596 mg, 4.0 mmol); The title compound was obtained in 98% yield (723 mg, 3.93 mmol) as a white powder. ^{1}H NMR (600 MHz, $CDCl_3$) δ 8.14 (dd, *J* = 7.8, 1.3 Hz, 1H), 7.61 (td, *J* = 7.6, 1.3 Hz, 1H), 7.49 (td, *J* = 7.7, 1.1 Hz, 1H), 7.25 – 7.21 (m, 1H), 5.27 (s, 2H). ^{13}C NMR (151 MHz, $CDCl_3$) δ 169.9, 138.3, 134.4, 129.4, 128.7, 125.0, 123.8, 72.3. HRMS (APCI-TOF) *m/z* calculated 184.0160 for $C_8H_7ClNO_2$ $[M+H]^+$, found 184.0158.



15

3-chloro-1H-naphtho[1,8-de][1,2]oxazepin-4(3H)-one (**15**): Synthesized according to general procedure B from 1H-naphtho[1,8-de][1,2]oxazepin-4(3H)-one, reaction time 2 h (39.8 mg, 0.20 mmol); The title compound was obtained in 100% yield (47.0 mg, 0.20 mmol) as a white powder. ^{1}H NMR (500 MHz, $CDCl_3$) δ 8.25 (dd, *J* = 7.4, 1.4 Hz, 1H), 8.14 (dd, *J* = 8.2, 1.4 Hz, 1H), 7.94 (dd, *J* = 8.3, 1.3 Hz, 1H), 7.66 (t, *J* = 7.8 Hz, 1H), 7.51 (dd, *J* = 8.2, 7.0 Hz, 1H), 7.42 (dd, *J* = 7.0, 1.3 Hz, 1H), 5.49 (s, 2H). ^{13}C NMR (126 MHz, $CDCl_3$) δ 174.2, 134.8, 133.92, 133.85, 132.1, 130.5, 128.5, 127.5,

127.3, 126.0, 125.6, 80.4. HRMS (APCI-TOF) *m/z* calculated 234.0316 for $C_{12}H_9ClNO_2$ $[M+H]^+$, found 234.0316.

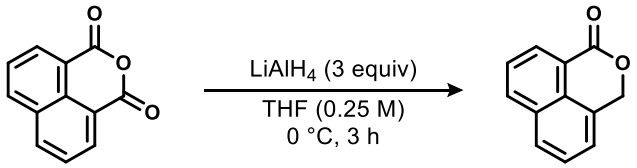


Scheme 2.6 Synthesis of 1H-benzo[d][1,2]oxazin-4(3H)-one (**12**)

Step 1. To a 100 mL round-bottomed flask equipped with a stir bar was added methyl 2-(bromomethyl)benzoate (2.30 g, 10.0 mmol), 2-hydroxyisoindoline-1,3-dione (1.63 g, 10.0 mmol, 1.0 equiv.) and anhydrous acetonitrile (14 mL). To the reaction mixture was added triethylamine (2.8 mL, 20.0 mmol, 2.0 equiv.) and stirred for 3 h at 90 °C. After reaction completion, the crude reaction mixture was concentrated under reduced pressure. The crude mixture was then diluted with dichloromethane (100 mL), washed with water (3 × 50 mL) and brine (50 mL), dried over Na_2SO_4, filtered, and concentrated under reduced pressure. The crude product was used directly for the next step.

Step 2. To a 500 mL round-bottomed flask equipped with a stir bar was added crude product and methanol (167 mL). To the reaction mixture was added *n*-butylamine (0.99 mL, 10.0 mmol, 1.0 equiv.), and stirred for 18 h at 23 °C. After the reaction completion, the crude reaction mixture was concentrated under reduced pressure. The crude product was then subjected to flash column chromatography over silica gel (0 to 30% EtOAc in hexanes), affording the title compound as a white powder (1.13 g, 7.5 mmol, 75% for two steps). 1H-benzo[d][1,2]oxazin-4(3H)-one (12): ^{1}H NMR (600 MHz, $CDCl_3$) δ 8.80 (s, 1H), 8.10 (dd, *J* = 7.7,

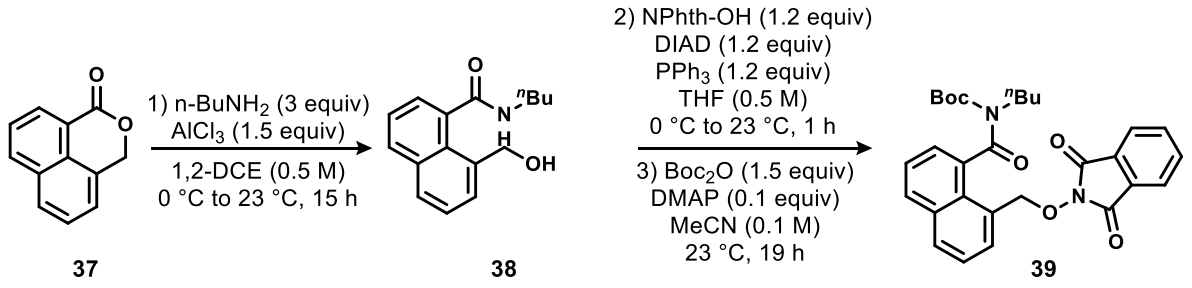
1.3 Hz, 1H), 7.56 (td, *J* = 7.5, 1.4 Hz, 1H), 7.47 (td, *J* = 7.6, 1.1 Hz, 1H), 7.20 (d, *J* = 7.5 Hz, 1H), 5.11 (s, 2H). ^{13}C NMR (151 MHz, $CDCl_3$) δ 167.2, 137.6, 133.4, 128.5, 127.6, 125.8, 123.7, 71.3. HRMS (APCI-TOF) *m/z* calculated 150.0550 for $C_8H_8NO_2$ $[M+H]^+$, found 150.0550.



36

Scheme 2.7 Synthesis of intermediate **36** (1H,3H-benzo[de]isochromen-1-one)

This procedure was adapted from the literature.[18] To a 250 mL round-bottomed flask equipped with a stir bar was added lithium aluminum hydride (1.70 g, 45.0 mmol, 3.0 equiv.) and anhydrous THF (60 mL). To the reaction mixture was added 1,8-naphthalic anhydride (3.00 g, 15.0 mmol) portion-wise and stirred for 3 h at 0 °C. After reaction completion, the crude reaction mixture was quenched with water (50 mL) and 1 M HCl (50 mL). The reaction mixture was extracted with ethyl acetate (3 × 100 mL), and the combined organic layer was washed with brine (100 mL), dried over Na_2SO_4, filtered, and concentrated under reduced pressure. The crude product was diluted with dichloromethane (150 mL), filtered, and concentrated under reduced pressure to remove over-reduced side product. The crude product was then subjected to flash column chromatography over silica gel (0 to 50% DCM in hexanes), affording the title compound as a pale yellow powder (1.75 g, 9.5 mmol, 63%). 1H,3H-benzo[de]isochromen-1-one: ^{1}H NMR (600 MHz, $CDCl_3$) δ 8.41 (dd, *J* = 7.2, 1.1 Hz, 1H), 8.12 (dd, *J* = 8.3, 1.1 Hz, 1H), 7.87 (dd, *J* = 8.3, 1.1 Hz, 1H), 7.67 (dd, *J* = 8.2, 7.2 Hz, 1H), 7.57 (dd, *J* = 8.2, 7.1 Hz, 1H), 7.39 (dd, *J* = 7.1, 1.3 Hz, 1H), 5.85 (s, 2H). Spectroscopic data are in agreement with those in the literature.[19]



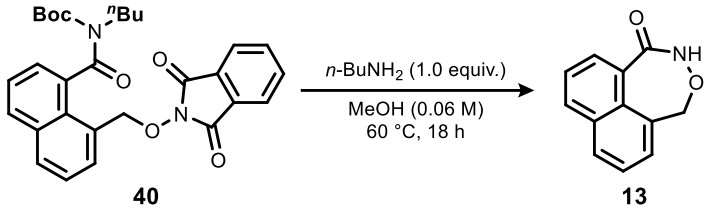
Scheme 2.8 Synthesis of intermediate **39** from **37**

Step 1. To an oven-dried 50 mL round-bottomed flask equipped with a stir bar was added aluminum chloride (1.00 g, 7.5 mmol, 1.5 equiv.), backfilled with N_2 three times. To the reaction mixture was added 1,2-dichloroethane (10 mL) and *n*-butylamine (1.5 mL, 15.0 mmol, 3.0 equiv.) at 0 °C. The reaction mixture was stirred for 5 minutes, then lactone (921 mg, 5.0 mmol) was added at 0 °C. The solution was stirred at 23 °C for 15 h. Then, the reaction mixture was quenched with water (50 mL) and extracted with diethyl ether (3 × 50 mL). The combined organic layer was dried over Na_2SO_4, filtered through a short plug of silica, and concentrated under reduced pressure. The crude product was used directly for the next step. *Note*: this intermediate is unstable toward reformation of the lactone and should not be stored for more than 1 hour.

Step 2. To a 50 mL round-bottomed flask equipped with a stir bar was added crude product, 2-hydroxyisoindoline-1,3-dione (979 mg, 6.0 mmol, 1.2 equiv.), triphenylphosphine (1.57 g, 6.0 mmol, 1.2 equiv.) and anhydrous THF (10 mL). The reaction mixture was cooled to 0 °C and diisopropyl azodicarboxylate (1.2 mL, 6.0 mmol, 1.2 equiv.) was added. The solution was stirred at room temperature for 1 h. After reaction completion, water (50 mL) was added and extracted with diethyl ether (3 × 100 mL). The combined layer was dried over Na_2SO_4, filtered, and concentrated under reduced pressure. The crude product was then subjected to flash column chromatography over silica gel (0 to 10% MeOH in DCM), affording a mixture of

the title compound and diisopropyl hydrazine-1,2-dicarboxylate as a white powder (1.88 g, 3.3mmol of product and 2.7 mmol of hydrazine mixture). This inseparable mixture was used directly for the next step.

Step 3. To a 250 mL round-bottomed flask equipped with a stir bar was added the above mixture (1H from the desired intermediate and 2H from the contaminating hydrazine: 3.3+2.7+2.7 = 8.7 mmol considered as 1.0 equiv.), 4-dimethylaminopyridine (106 mg, 0.87 mmol, 0.10 equiv.) and anhydrous acetonitrile (87 mL). To the reaction mixture was added di-*tert*-butyl dicarbonate (2.83 g, 13.0 mmol, 1.5 equiv.), and the mixture was stirred for 19 h at 23 °C. After reaction completion, the crude reaction mixture was concentrated under reduced pressure. The crude mixture was then diluted with ethyl acetate (150 mL), washed with 1M HCl (50 mL), saturated $NaHCO_3$ (50 mL), and brine (50 mL), dried over Na_2SO_4, filtered, and concentrated under reduced pressure. The crude product was then subjected to flash column chromatography over silica gel (0 to 15% EtOAc in hexanes), affording the title compound as a white powder (1.37 g, 2.7 mmol, 55% over three steps). *tert*-butyl butyl(8-(((1,3-dioxoisoindolin-2-yl)oxy)methyl)-1-naphthoyl)carbamate: ^{1}H NMR (600 MHz, $CDCl_3$) δ 8.22 (dd, *J* = 7.3, 1.2 Hz, 1H), 7.92 (dd, *J* = 8.2, 1.3 Hz, 1H), 7.87 (dd, *J* = 8.3, 1.2 Hz, 1H), 7.86 – 7.82 (m, 2H), 7.77 – 7.73 (m, 2H), 7.62 (t, *J* = 7.7 Hz, 1H), 7.42 (dd, *J* = 8.2, 7.0 Hz, 1H), 7.27 (dd, *J* = 7.1, 1.3 Hz, 1H), 5.68 (d, *J* = 11.8 Hz, 1H), 5.42 (d, *J* = 11.8 Hz, 1H), 3.99 – 3.80 (m, 2H), 1.77 – 1.57 (m, 2H), 1.38 – 1.31 (m, 2H), 0.90 (s, 9H), 0.80 (t, *J* = 7.4 Hz, 3H). ^{13}C NMR (151 MHz, $CDCl_3$) δ 173.5, 163.3, 153.2, 136.0, 134.6, 134.5, 130.9, 130.7, 129.3, 129.2, 127.062, 127.056, 126.3, 124.2, 123.7, 123.7, 84.0, 78.1, 44.9, 30.5, 27.2, 20.3, 13.9. HRMS (APCI-TOF) *m/z* calculated 503.2177 for $C_{29}H_{31}N_2O_6$ $[M+H]^+$, found 503.2180.

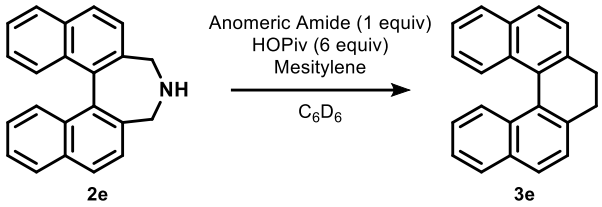


Scheme 2.9 Synthesis of 1H-naphtho[1,8-de][1,2]oxazepin-4(3H)-one (**13**) from **40**

To a 4-dram screw cap vial equipped with a stir bar was added *tert*-butyl butyl(8-(((1,3-dioxoisoindolin-2-yl)oxy)methyl)-1-naphthoyl)carbamate (251.3 mg, 0.5 mmol) and methanol (8 mL). To the reaction mixture was added *n*-butylamine (0.05 mL, 0.5 mmol, 1.0 equiv.), heated to 60 °C and stirred for 18 h. After the reaction completion, the crude reaction mixture was concentrated under reduced pressure. The crude product was then subjected to flash column chromatography over silica gel (0 to 40% EtOAc in hexanes), affording the title compound as a white powder (87.2 mg, 0.44 mmol, 88%). 1H-naphtho[1,8-de][1,2]oxazepin-4(3H)-one: ^{1}H NMR (600 MHz, $CDCl_3$) δ 9.57 (s, 1H), 8.56 – 8.52 (m, 1H), 8.10 (dd, *J* = 8.2, 2.5 Hz, 1H), 7.89 (d, *J* = 8.2 Hz, 1H), 7.68 – 7.63 (m, 1H), 7.50 – 7.43 (m, 1H), 7.32 (d, *J* = 6.9 Hz, 1H), 5.50 (s, 2H). ^{13}C NMR (151 MHz, $CDCl_3$) δ 171.9, 135.0, 134.7, 134.6, 133.5, 130.0, 128.8, 128.2, 126.3, 125.7, 125.2, 83.2. HRMS (APCI-TOF) *m/z* calculated 200.0706 for $C_{12}H_{10}NO_2$ $[M+H]^+$, found 200.0708.

2.3.8 Kinetics

2.3.8.1 Reaction Procedure and 1H NMR parameters



Scheme 2.10 Nitrogen deletion conditions for kinetics experiments

Stock solution preparation

Benzene-d_6 (36.0 g) was added to an oven-dried 100 mL Teflon-valved storage flask with 4 Å molecular sieves. Mesitylene was added (70.0 mg, 2.5 mg/g solvent) and the solution was degassed using freeze-pump-thaw (x3). The exact concentration of mesitylene in the degassed solution was established to be 19.5 mM through quantitative ^{1}H NMR with 1,3,5-trimethoxybenzene as an internal standard. This solution was then used to create separate stock solutions of **2e** (154 mM) and pivalic acid (**23**, 924 mM), which were stored in oven-dried Schlenk tubes with Teflon stoppers in the glovebox.

General Procedure for Kinetic Data Collection

The anomeric amide (**1**, 50 μmol) was added to an oven dried 5 mL conical reaction vial, sealed with a rubber septum, and evacuated and purged with N_2 gas (x3). The mesitylene stock was added (350 μL) then the solution was sonicated. In the glove box, the amine (**2e**) and pivalic acid (**23**) stock solutions (325 μL each) were combined in a dry NMR tube, sealed with a septum cap. This was vigorously shaken and fully inverted 3 times, to ensure homogeneity. After collecting an initial NMR spectrum of the solution containing **2e** and **23**, the solution of **1** was added via syringe and the tube was shaken vigorously and inverted at least three times before returning the tube to the instrument for data collection.

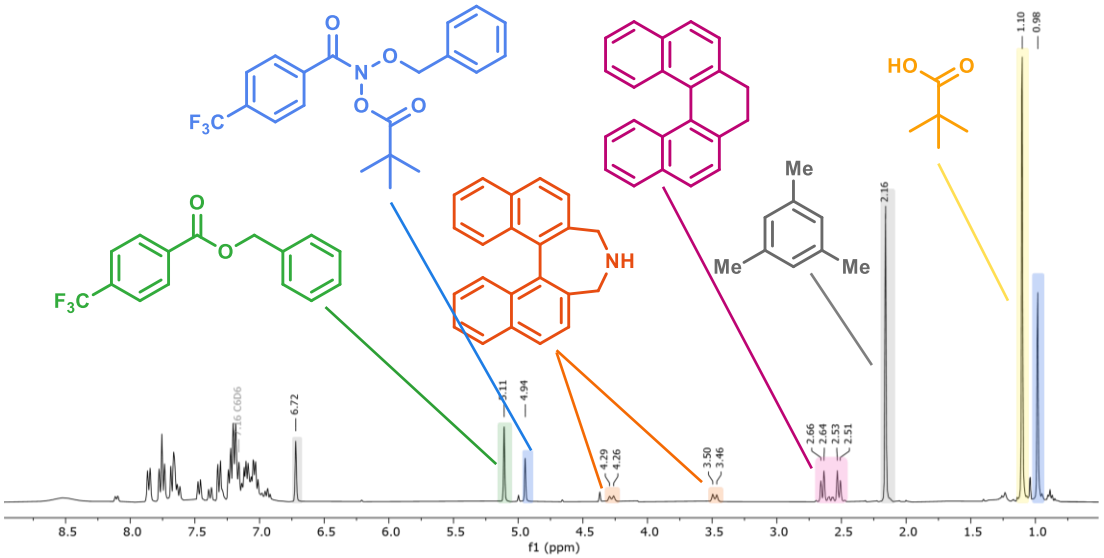


Figure 2.16 Sample ^{1}H NMR spectra from kinetic experiment and peaks used to determine the concentration of each species

2.3.8.2 Rate Model

Rate constants for the kinetic data (k_{sub}) were obtained using a multi nonlinear model fitting function in Mathematica, with parametric function 2.1 as the modeled equation and the concentrations of the first data point used for the analysis as the initial concentrations of each species. The non-variable k values ($k_{1:nx}$) were encoded based on the equilibrium constants determined in the ^{1}H NMR titration experiment and equation 2.2.

Each reaction was performed n times (Table 2.2 column 7) and the mean of the k_{sub} values were used to calculate $\log\left(\frac{k_X}{k_H}\right)$ for the Hammett plot. Standard error for each derivative was calculated using equation 2.3 where σ_X is the standard deviation of the experimental values for that derivative, and n is the number of experiments performed. This was propagated for the final $\log\left(\frac{k_X}{k_H}\right)$ value using equation 2.4. X=3-ClAr refers to *N*-(benzyloxy)-3-chloro-*N*-(pivaloyloxy)benzamide, which was used to validate the relative rate data obtained using RPKA. This result correlated well with the value from the same-pot competition experiment,[1] suggesting that the relative rates obtained using each of these methods are comparable.

$$
\begin{aligned}
\text{eqs}\,(k_{sub}, \text{yield}) = \{ & \\
\text{da}'(t) &= k_{sub} * \text{yield} * \text{aa}(t) * \text{amine}(t), \\
\text{amine}'(t) &= -k_{sub} * \text{aa}(t) * \text{amine}(t) \\
&\quad - k_{1:1a} * \text{amine}(t) * \text{pivOH}(t) + k_{1:1d} * \text{iona}(t), \\
\text{aminetot}'(t) &= -k_{sub}\ \text{aa}(t)\ \ \text{amine}(t), \\
\text{aa}'(t) &= -k_{sub} * \text{aa}(t) * \text{amine}(t), \\
\text{pivOH}'(t) &= k_{sub} * \text{aa}(t) * \text{amine}(t) \\
&\quad - k_{1:1a} * \text{amine}(t) * \text{pivOH}(t) + k_{1:1d} * \text{iona}(t) \\
&\quad - k_{1:2a} * \text{iona}(t) * \text{pivOH}(t) + k_{1:2d} * \text{ionb}(t), \\
\text{iona}'(t) &= k_{1:1a} * \text{amine}(t) * \text{pivOH}(t) - k_{1:1d} * \text{iona}(t) \\
&\quad - k_{1:2a} * \text{iona}(t) * \text{pivOH}(t) + k_{1:2d} * \text{ionb}(t), \\
\text{ionb}'(t) &= k_{1:2a} * \text{iona}(t) * \text{pivOH}(t) - k_{1:2d} * \text{ionb}(t), \\
\text{pivOHtot}'(t) &= k_{sub} * \text{aa}(t) * \text{amine}(t) \\
& \};
\end{aligned}
\tag{2.1}
$$

$$K_{1:1} = \frac{k_{1:1a}}{k_{1:1d}} = \frac{89.39}{1} \tag{2.2}$$

$$S_X = \frac{\sigma_X}{\sqrt{n}} \tag{2.3}$$

$$S_{final} = \frac{1}{\ln(10)} * \sqrt{\left(\frac{S_X}{k_{Xavg}}\right)^2 + \left(\frac{S_H}{k_{Havg}}\right)^2} \tag{2.4}$$

Table 2.2 rate data from kinetic experiments used for each derivative

X	sigma	ksub	std error	log(kx/kh)	Prop. error	n
H	0	6.29	0.25	0.000	0.024	4
4-OMe	-0.27	7.38	0.35	0.069	0.027	4
4-NO2	0.778	3.12	0.10	-0.304	0.022	3
4-CF3	0.54	4.34	0.30	-0.161	0.035	3
35-tBu	-0.2	4.46	0.21	-0.149	0.026	3
naphth	0.042	5.86	0.11	-0.031	0.019	3
35-tBu-4-OMe	-0.47	5.44	0.06	-0.063	0.018	4
35-tBu-4-OAc	0.11	3.75	0.06	-0.225	0.018	3
4-tBu	-0.197	6.16	0.07	-0.009	0.018	3
3-ClAr	0.373	4.34	0.03	-0.161	0.017	3

2.3.8.3 1H NMR Titration of Model Amine and Pivalic Acid

Procedure: Amine **2e** (28 mg) was dissolved in a solution of mesitylene in benzene-d_6 (1.7 mL, 25 mM). 650 µL of this solution was transferred to an NMR tube, and 1 mL of the solution was added to a vial containing pivalic acid (159 mg). After an initial NMR spectrum was taken, the pivalic acid solution was added to the tube incrementally between spectra, shaking and inverting the NMR tube each time.

Equilibrium constants were determined using the BindFit webapp.[20] The 1:2 association model using an L-BFGS-B fit method provided the best fit and a non-cooperative association was assumed to prevent over-fitting. Based on this model, $K_{1:1}$ was determined to be 89.39 and 22.35 M^{-1} respectively.

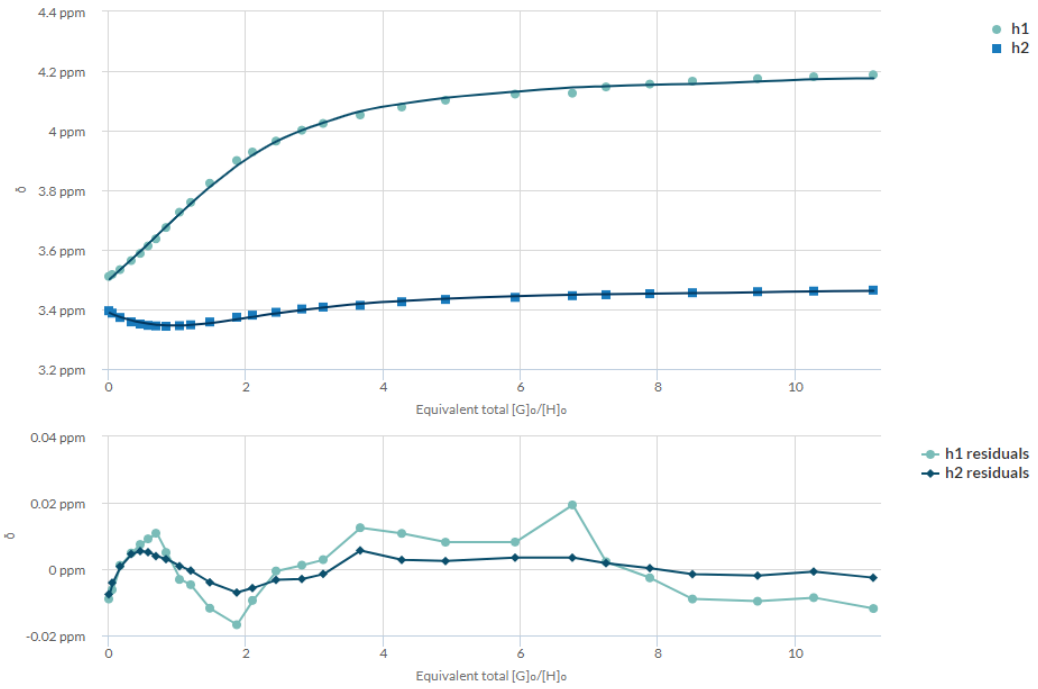


Figure 2.17 Titration fitting data using 1:2 association model on BindFit

Fitting information for this experiment can be viewed at:

http://app.supramolecular.org/bindfit/view/c45f093f-672e-40a7-b2b4-c0bafa41d200

2.3.9 Computational Details

Conformational searches were conducted for all ground states using CREST as implemented in the XTB python package.[21] Structures within 6 kcal/mol of the minimum were sorted within CREST to afford an ensemble of up to 100 representative conformers of each derivative that were used as starting coordinates for geometry optimization, with frequency calculations conducted using density functional theory (DFT) in Gaussian16 (Revision A.03)[22] with NBO analysis.[23] Each structure was optimized using the polarizable continuum model (PCM) in benzene (C_6D_6) at the B3LYP-GD3BJ/6-31g(d) level of theory. Frequency calculations were conducted at the same level to check whether each optimized structure is an energy minimum or transition state.

2.3.9.1 Conformational Sorting

Conformational descriptors were determined using the definitions in equations 1.5-7, where DH_{wxyz} represents the dihedral angle of the four atoms listed. The percent representation from each conformer class in Figure 2.9B were determined by the sum of the Boltzmann weights for all structures within that class. This stacked bar chart and the distribution of parameter values across derivatives and conformational classes, as shown in Figure 2.10, were visualized using ggplot2.[24]

Table 2.3 Definition of conformational descriptor terms

Category	Defining features	Classification (Figure 2.18)	
Benzyl	$DH_{(Bn)CONO(Piv)} + DH_{(Bn)CONC(Amide)}$	$< 180° \rightarrow$ Anti (BA) $> 180° \rightarrow$ Syn (BS)	**2.5**
Pivaloyl	$DH_{(Piv)CONO(Bn)} + DH_{(Piv)CONC(Amide)}$	$< 180° \rightarrow$ Anti (BA) $> 180° \rightarrow$ Syn (BS)	**2.6**
Carbonyl	$DH_{(Amide)OCNO(Piv)}$	$< 90° \rightarrow$ Piv (CP) $> 90° \rightarrow$ Bn (CB)	**2.7**

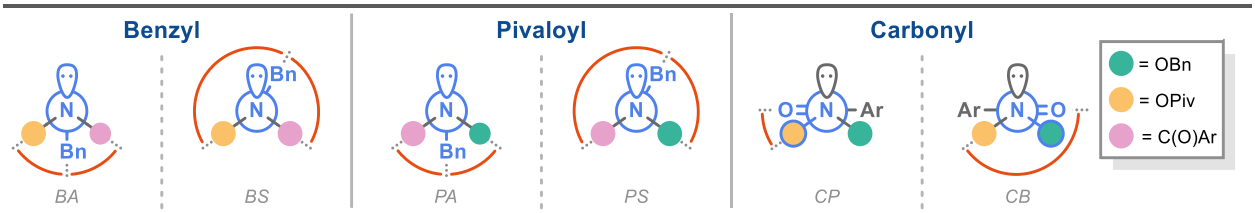
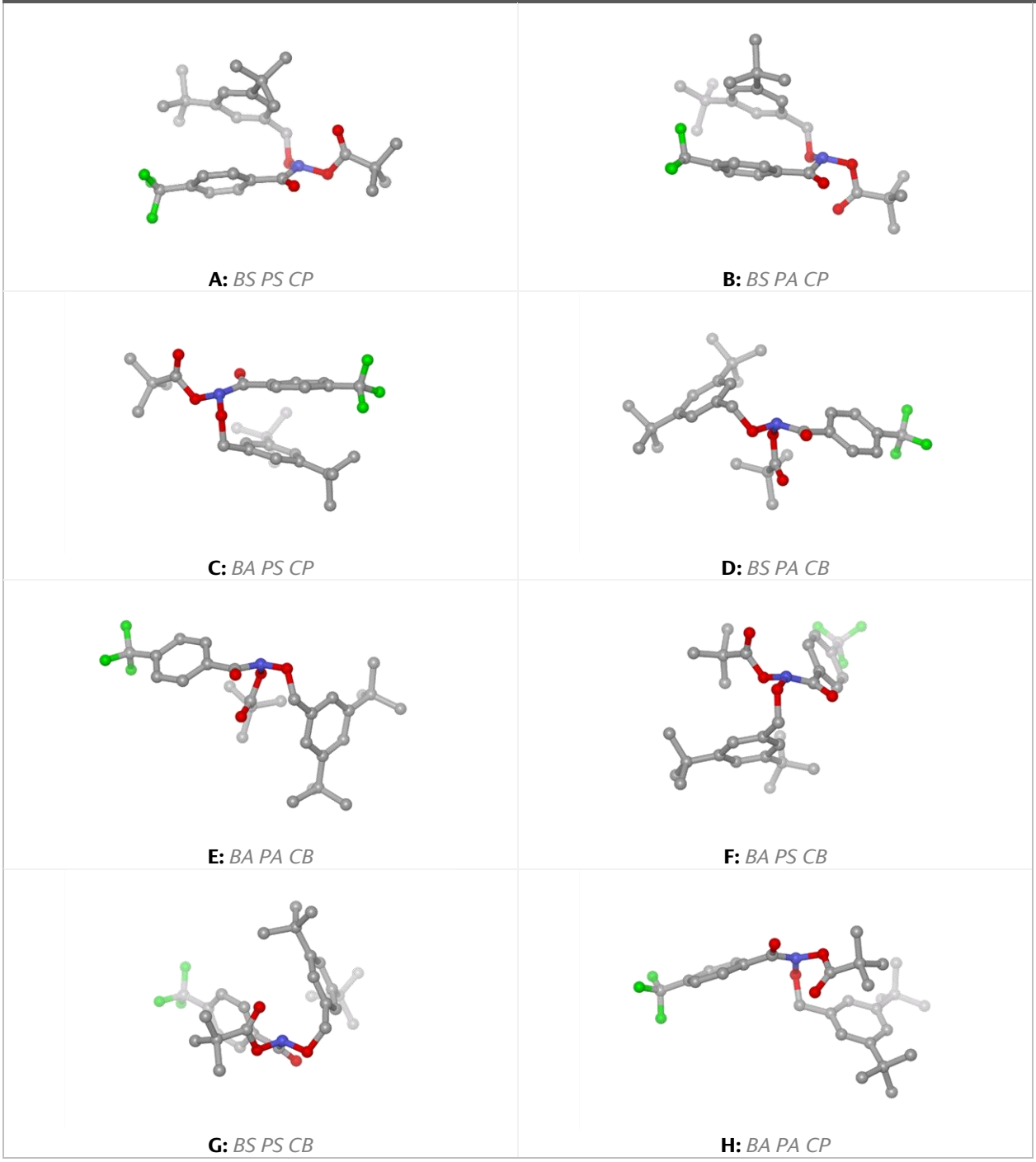


Figure 2.18 conformational descriptor definitions; dihedrals in equations **2.5**-**2.7** represented by orange arcs



A: *BS PS CP*

B: *BS PA CP*

C: *BA PS CP*

D: *BS PA CB*

E: *BA PA CB*

F: *BA PS CB*

G: *BS PS CB*

H: *BA PA CP*

Figure 2.19 example from each conformational class for **1i**

2.3.9.2 Mathematical Modeling

Molecular descriptors capturing electronic descriptors were extracted as Boltzmann averages for each derivative from DFT optimized conformers. The values were normalized according to equation 2.8, where X is the Boltzmann-averaged parameter value, μ is the mean of the averaged values for all derivatives, and σ is the standard deviation of those values. Statistical models of $\log\left(\frac{k_X}{k_H}\right)$ using the normalized parameters were selected using forward stepwise linear regression with previously reported algorithms.[25] Models with parameters that closely correlated with each other ($R^2 > 0.3$). The regression results for the best fit one and two parameter models are included below, as well as the values of the corresponding parameters. Models follow the formula in equation 2.9.

$$X_n = (X - \mu)/\sigma \quad \textbf{2.8}$$

$$\log\left(\frac{k_X}{k_H}\right)_{pred} = b + m * X_{n\,p} + n * X_{n\,q} \quad \textbf{2.9}$$

Table 2.4 reactivity model coefficients, variables, and fit statistics

b	m	p	n	q	R^2	Q^2	k-fold
-0.097	-0.064	NBO BnC1	0.066	NBO BnCH2	0.95	0.89	0.88
-0.097	-0.124	NBO BnC1	0.063	NBO Amide C	0.91	0.81	0.80
-0.097	-0.099	NBO BnC1	-0.056	CTE Bn Pi-CH2O*	0.92	0.77	0.73
-0.097	-0.100	NBO BnC1	-0.056	CTE N-OBn*	0.92	0.77	0.76
-0.097	-0.103	NBO BnC1	0.057	NBO OBn LP1	0.92	0.76	0.75
-0.097	-0.115	NBO BnC1	0.055	CTE OPiv-NOBn*	0.88	0.76	0.74
-0.097	-0.094	NBO OBn			0.68	0.53	0.51
-0.097	-0.095	NBO BnC1			0.70	0.50	0.50
-0.097	0.095	NBO BnCH2			0.70	0.45	0.42

Table 2.5 Boltzmann average and normalized values for parameters used in models

		NBO chg BnC1		NBO chg OBn		NBO chg BnCH2		NBO occ. OBn LP1	
Compound	Bn	X	X_n	X	X_n	X	X_n	X	X_n
1k	35tBu4OAc	-0.09	0.01	-0.40	1.13	-0.049	-1.87	1.97	-1.80
1i	35tBu	-0.09	0.05	-0.40	0.56	-0.045	-0.64	1.97	-1.16
1j	35tBu4OMe	-0.12	-0.85	-0.40	0.48	-0.043	-0.25	1.97	-0.94
1f	4CF3	-0.06	1.26	-0.40	1.11	-0.043	-0.17	1.98	0.57
1a	H	-0.10	-0.16	-0.40	-0.62	-0.040	0.60	1.98	0.59
1g	4NO2	-0.05	1.77	-0.40	0.72	-0.045	-0.71	1.98	0.69
1e	4OMe	-0.13	-1.51	-0.41	-1.12	-0.038	1.01	1.98	0.61
1h	naphth	-0.09	-0.05	-0.41	-0.78	-0.039	0.83	1.98	0.74
1d	4tBu	-0.11	-0.53	-0.41	-1.48	-0.037	1.20	1.98	0.69

		CTE N-OBn*		NBO chg Amide C		CTE Bn Pi-CH2O*		CTE OPiv-NOBn*	
Compound	Bn	X	X_n	X	X_n	X	X_n	X	X_n
1k	35tBu4OAc	5.86	1.92	0.66	-1.12	18.80	1.59	6.47	-0.91
1i	35tBu	4.18	1.11	0.66	-1.16	18.04	1.17	5.88	-1.40
1j	35tBu4OMe	3.52	0.79	0.66	-1.41	18.06	1.18	5.84	-1.44
1f	4CF3	0.77	-0.53	0.67	1.35	15.20	-0.39	9.08	1.25
1a	H	0.74	-0.55	0.67	0.41	14.65	-0.69	8.01	0.36
1g	4NO2	0.59	-0.62	0.67	0.82	14.47	-0.79	8.35	0.64
1e	4OMe	0.53	-0.65	0.67	-0.07	14.81	-0.60	7.75	0.14
1h	naphth	0.39	-0.72	0.67	0.45	14.69	-0.67	8.13	0.46
1d	4tBu	0.33	-0.75	0.67	0.74	14.46	-0.79	8.64	0.89

2.4 References

(1) Kennedy, S. H.; Dherange, B. D.; Berger, K. J.; Levin, M. D. Skeletal Editing through Direct Nitrogen Deletion of Secondary Amines. *Nature (London, U. K.)* **2021**, *593* (7858), 223–227. https://doi.org/10.1038/s41586-021-03448-9.

(2) Holovach, S.; Melnykov, K. P.; Poroshyn, I.; Iminov, R. T.; Dudenko, D.; Kondratov, I.; Levin, M.; Grygorenko, O. O. C-C Coupling through Nitrogen Deletion: Application to Library Synthesis. *Chem. - Eur. J.* **2023**, *29* (4), e202203470. https://doi.org/10.1002/chem.202203470.

(3) Holovach, S. M.; Melnykov, K. P.; Poluektova, M. S.; Rozhenko, O. B.; Grygorenko, O. O. Incorporation of Gem-Difluorocycloalkyl Substituents into Heterocycles via the Levin's "Nitrogen Deletion" Strategy. *J. Org. Pharm.* **2023**, *21* (3), 11–16. https://doi.org/10.24959/ophcj.23.278321.

(4) Blackmond, D. G. Reaction Progress Kinetic Analysis: A Powerful Methodology for Mechanistic Studies of Complex Catalytic Reactions. *Angewandte Chemie International Edition* **2005**, *44* (28), 4302–4320. https://doi.org/10.1002/anie.200462544.

(5) Santiago, C. B.; Milo, A.; Sigman, M. S. Developing a Modern Approach To Account for Steric Effects in Hammett-Type Correlations. *J. Am. Chem. Soc.* **2016**, *138* (40), 13424–13430. https://doi.org/10.1021/jacs.6b08799.

(6) Haas, B. C.; Kalyani, D.; Sigman, M. S. Applying Statistical Modeling Strategies to Sparse Datasets in Synthetic Chemistry. *Science Advances* **2025**, *11* (1), eadt3013. https://doi.org/10.1126/sciadv.adt3013.

(7) Berger, K. J.; Dherange, B. D.; Morales, M.; Driscoll, J. L.; Tarhan, A. K.; Levin, M. D. N-(Benzyloxy)-N-(Pivaloyloxy)-4-(Trifluoromethyl)-Benzamide. *Org. Synth.* **2023**, *100*, 113–135. https://doi.org/10.15227/orgsyn.100.0113.

(8) Fulmer, G. R.; Miller, A. J. M.; Sherden, N. H.; Gottlieb, H. E.; Nudelman, A.; Stoltz, B. M.; Bercaw, J. E.; Goldberg, K. I. NMR Chemical Shifts of Trace Impurities: Common Laboratory Solvents, Organics, and Gases in Deuterated Solvents Relevant to the Organometallic Chemist. *Organometallics* **2010**, *29* (9), 2176–2179. https://doi.org/10.1021/om100106e.

(9) Ooi, T.; Kameda, M.; Maruoka, K. Design of N-Spiro C2-Symmetric Chiral Quaternary Ammonium Bromides as Novel Chiral Phase-Transfer Catalysts: Synthesis and Application to Practical Asymmetric Synthesis of α-Amino Acids. *J. Am. Chem. Soc.* **2003**, *125* (17), 5139–5151. https://doi.org/10.1021/ja021244h.

(10) Berger, K. J. C-N and C-H Bond Activation via New Reactive Intermediates and Hydrogen Atom Transfer Processes, The University of Chicago. https://doi.org/10.6082/uchicago.3933.

(11) Mamalis, P.; Green, J.; Mchale, D. 45. Amino-Oxy-Derivatives. Part II. Some Derivatives of N-Hydroxydiguanide. *J. Chem. Soc.* **1960**, No. 0, 229–238. https://doi.org/10.1039/JR9600000229.

(12) Fensholdt, J.; Thorhauge, J.; Noerremark, B. Novel Hydroxamic Acid Esters and Pharmaceutical Use Thereof. WO2005054179A2, June 16, 2005.

(13) Power, M. J.; Morris, D. T. J.; Vitorica-Yrezabal, I. J.; Leigh, D. A. Compact Rotaxane Superbases. *J. Am. Chem. Soc.* **2023**, *145* (15), 8593–8599. https://doi.org/10.1021/jacs.3c01202.
(14) Ishihara, K.; Kubota, M.; Kurihara, H.; Yamamoto, H. Scandium Trifluoromethanesulfonate as an Extremely Active Acylation Catalyst. *J. Am. Chem. Soc.* **1995**, *117* (15), 4413–4414. https://doi.org/10.1021/ja00120a030.
(15) Bruno, S.; Pinto, A.; Paredi, G.; Tamborini, L.; De Micheli, C.; La Pietra, V.; Marinelli, L.; Novellino, E.; Conti, P.; Mozzarelli, A. Discovery of Covalent Inhibitors of Glyceraldehyde-3-Phosphate Dehydrogenase, A Target for the Treatment of Malaria. *J. Med. Chem.* **2014**, *57* (17), 7465–7471. https://doi.org/10.1021/jm500747h.
(16) Pinto, A.; Conti, P.; De Amici, M.; Tamborini, L.; Grazioso, G.; Colleoni, S.; Mennini, T.; Gobbi, M.; De Micheli, C. Synthesis of Enantiomerically Pure HIP-A and HIP-B and Investigation of Their Activity as Inhibitors of Excitatory Amino Acid Transporters. *Tetrahedron: Asymmetry* **2008**, *19* (7), 867–875. https://doi.org/10.1016/j.tetasy.2008.03.001.
(17) Tarhan, A. K. *Computationally Guided Design & Synthesis of Anomeric Amides for Nitrogen Deletion*. Knowledge UChicago. https://doi.org/10.6082/uchicago.3915.
(18) Reza, A. I.; Iwai, K.; Nishiwaki, N. A Study of the Correlation between the Bulkiness of Peri-Substituents and the Distortion of a Naphthalene Ring. *Molecules* **2023**, *28* (14), 5343. https://doi.org/10.3390/molecules28145343.
(19) Luo, H.; Zeng, Q.; Liu, Z.; Wei, Y.; Li, B.; Wang, F. Mild and Efficient Synthesis of 1,8-Naphthalide and 1,8-Naphthalenedimethanol. *Synthetic Communications* **2004**. https://doi.org/10.1081/SCC-120038510.
(20) *Supramolecular.org - Binding Constant Calculators | Supramolecular*. http://supramolecular.org/ (accessed 2025-02-15).
(21) Pracht, P.; Bohle, F.; Grimme, S. Automated Exploration of the Low-Energy Chemical Space with Fast Quantum Chemical Methods. *Phys. Chem. Chem. Phys.* **2020**, *22* (14), 7169–7192. https://doi.org/10.1039/C9CP06869D.
(22) Frisch, M. J.; Trucks, G. W.; Schlegel, H. B.; Scuseria, G. E.; Robb, M. A.; Cheeseman, J. R.; Scalmani, G.; Barone, V.; Petersson, G. A.; Nakatsuji, H.; Li, X.; Caricato, M.; Marenich, A. V.; Bloino, J.; Janesko, B. G.; Gomperts, R.; Mennucci, B.; Hratchian, H. P.; Ortiz, J. V.; Izmaylov, A. F.; Sonnenberg, J. L.; Williams; Ding, F.; Lipparini, F.; Egidi, F.; Goings, J.; Peng, B.; Petrone, A.; Henderson, T.; Ranasinghe, D.; Zakrzewski, V. G.; Gao, J.; Rega, N.; Zheng, G.; Liang, W.; Hada, M.; Ehara, M.; Toyota, K.; Fukuda, R.; Hasegawa, J.; Ishida, M.; Nakajima, T.; Honda, Y.; Kitao, O.; Nakai, H.; Vreven, T.; Throssell, K.; Montgomery Jr., J. A.; Peralta, J. E.; Ogliaro, F.; Bearpark, M. J.; Heyd, J. J.; Brothers, E. N.; Kudin, K. N.; Staroverov, V. N.; Keith, T. A.; Kobayashi, R.; Normand, J.; Raghavachari, K.; Rendell, A. P.; Burant, J. C.; Iyengar, S. S.; Tomasi, J.; Cossi, M.; Millam, J. M.; Klene, M.; Adamo, C.; Cammi, R.; Ochterski, J. W.; Martin, R. L.; Morokuma, K.; Farkas, O.; Foresman, J. B.; Fox, D. J. Gaussian 16 Rev. C.01, 2016.
(23) Glendening, E. D.; Reed, A. E.; Carpenter, J. E.; Weinhold, F. NBO Version 3.1.
(24) Wickham, H. *Ggplot2: Elegant Graphics for Data Analysis*; Springer-Verlag New York, 2016.
(25) Guo, J.-Y.; Minko, Y.; Santiago, C. B.; Sigman, M. S. Developing Comprehensive Computational Parameter Sets To Describe the Performance of Pyridine-Oxazoline and Related Ligands. *ACS Catal.* **2017**, *7* (6), 4144–4151. https://doi.org/10.1021/acscatal.7b00739.

2.5 NMR Spectra

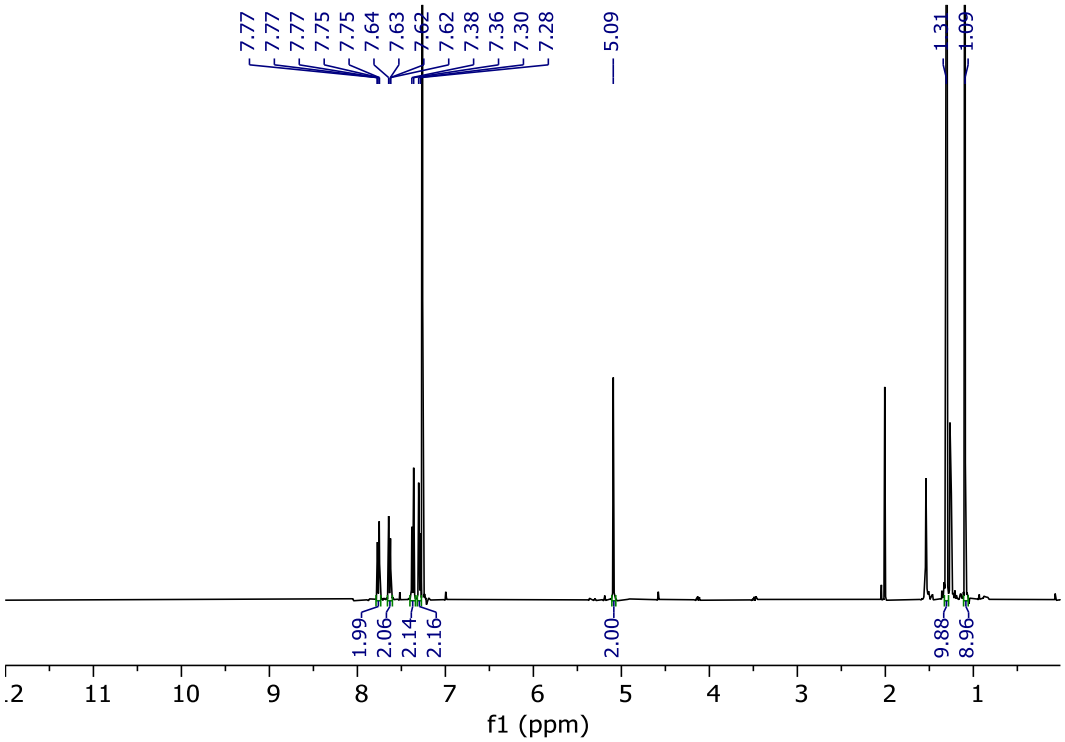


Figure 2.20 ^{1}H NMR spectra of **1d** in $CDCl_3$

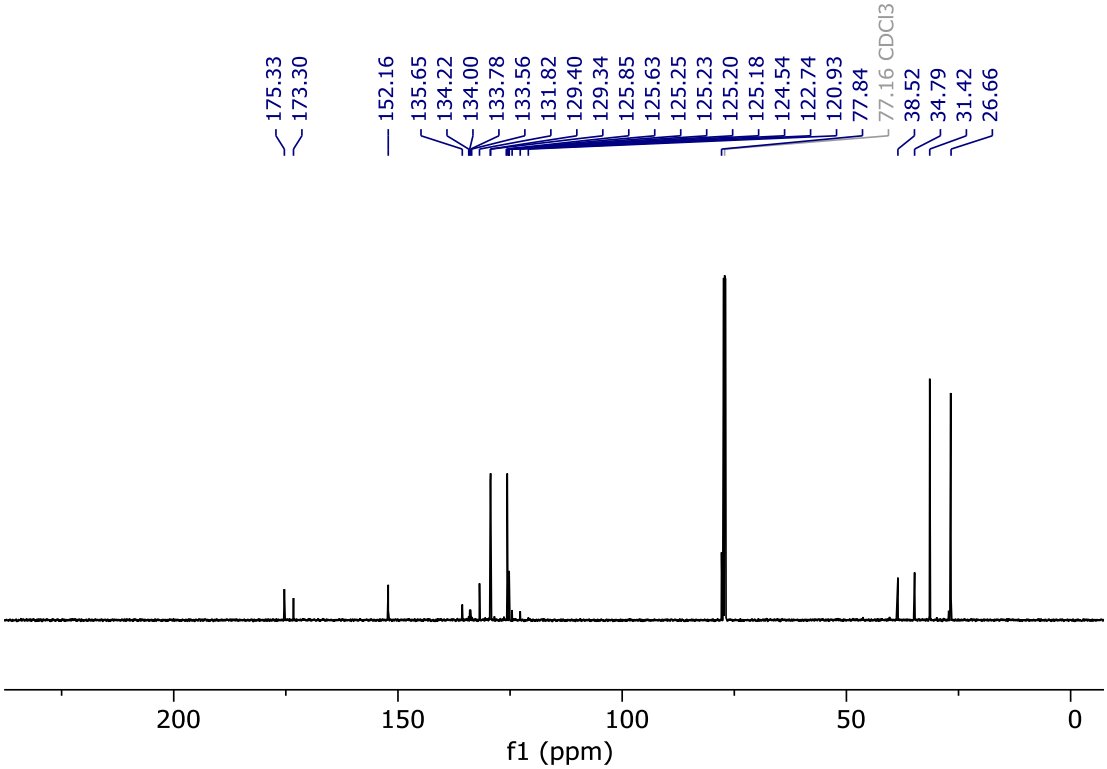


Figure 2.21 ^{13}C NMR spectra of **1d** in $CDCl_3$

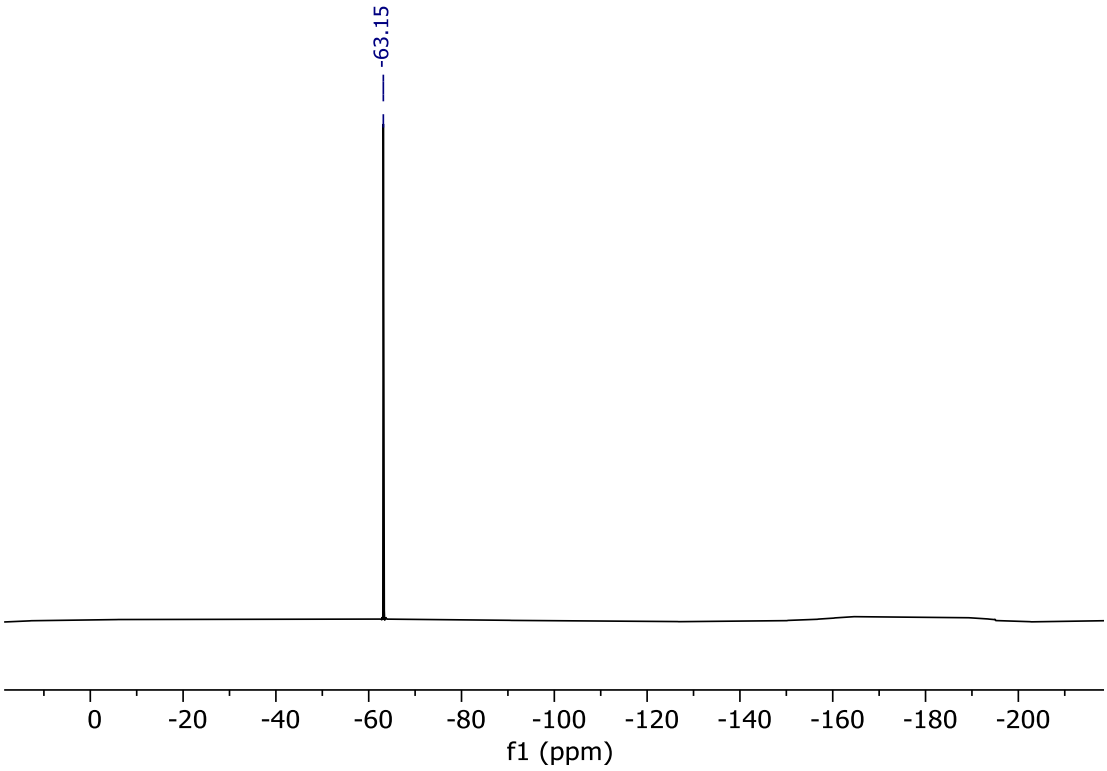


Figure 2.22 ^{19}F NMR spectra of **1d** in $CDCl_3$

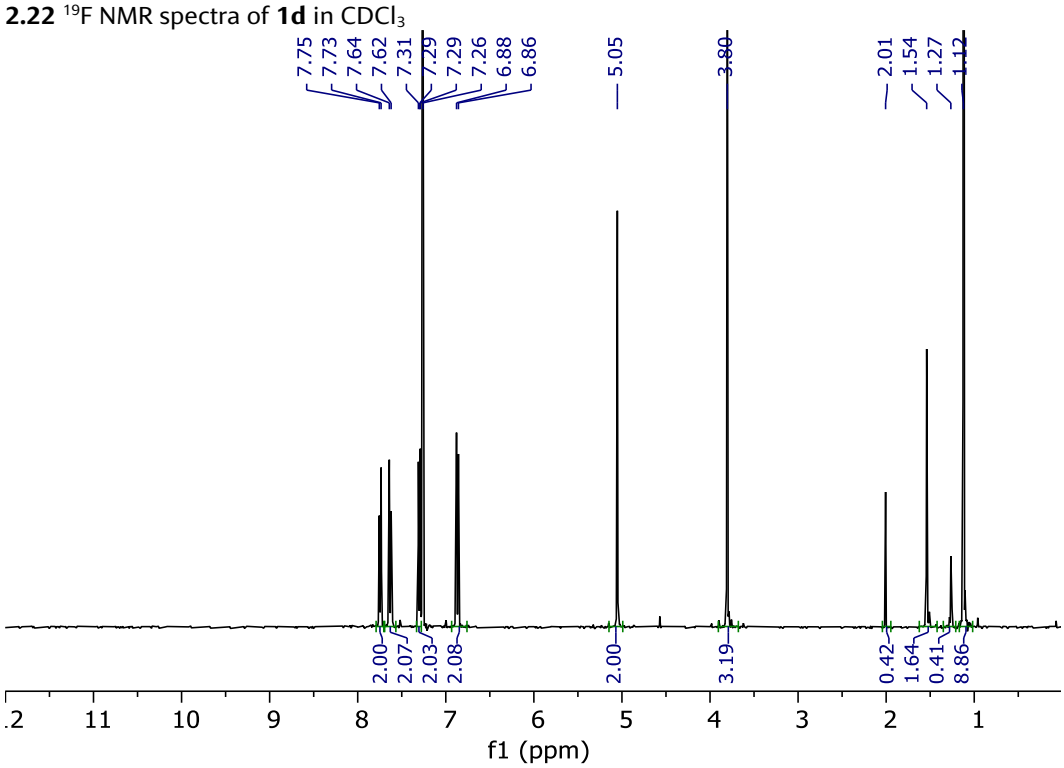


Figure 2.23 ^{1}H NMR spectra of **1e** in $CDCl_3$

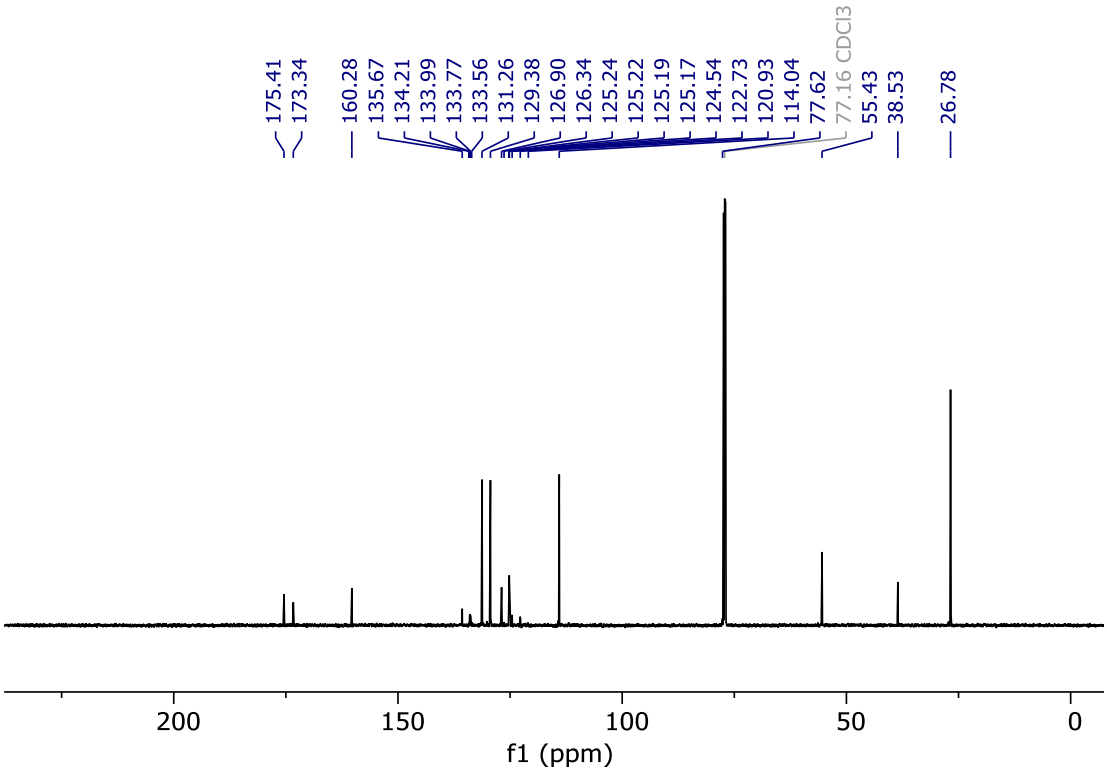


Figure 2.24 ^{13}C NMR spectra of **1e** in $CDCl_3$

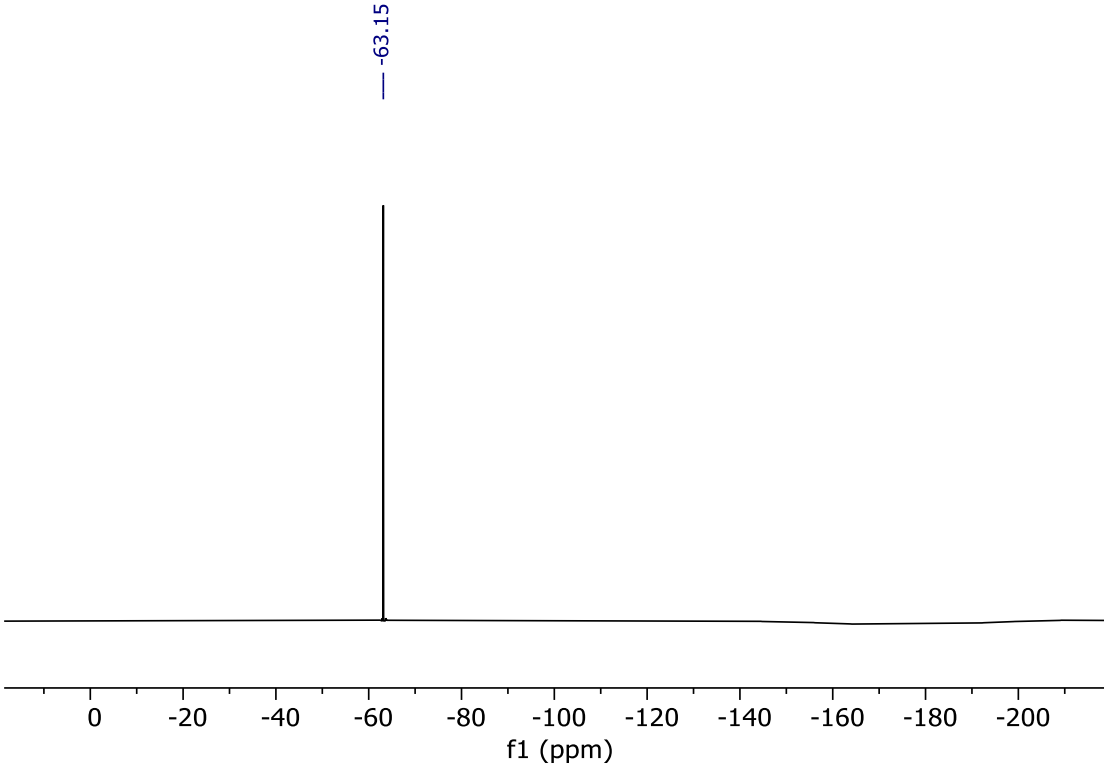


Figure 2.25 ^{19}F NMR spectra of **1e** in $CDCl_3$

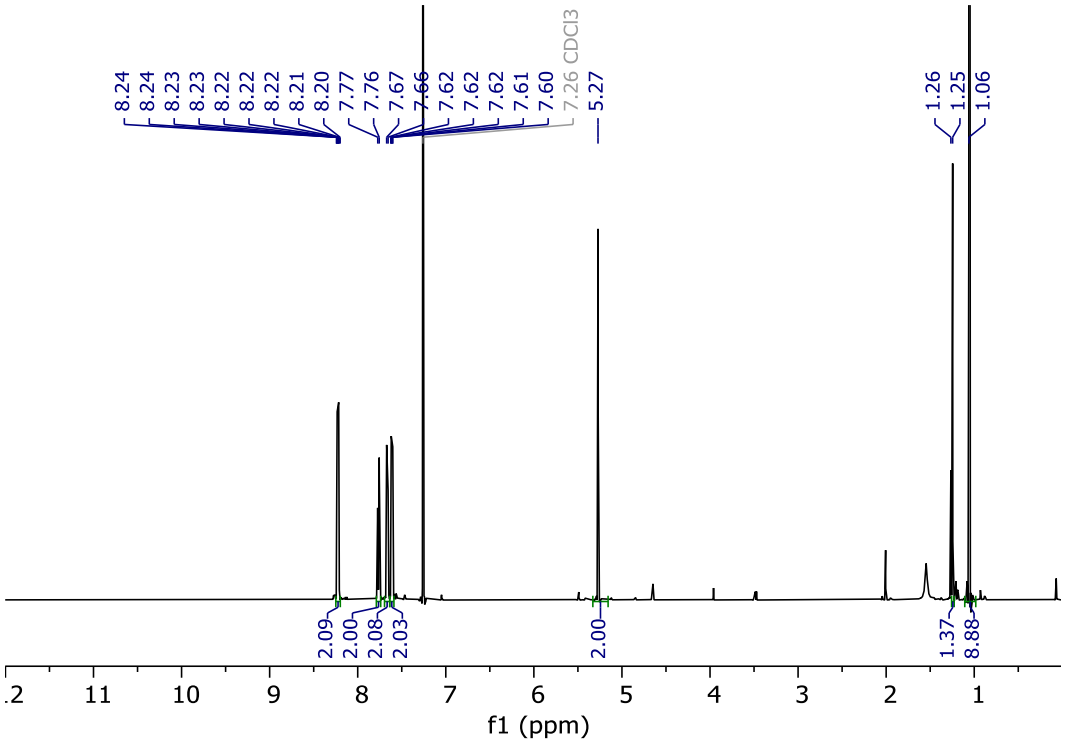


Figure 2.26 ^{1}H NMR spectra of **1g** in $CDCl_3$

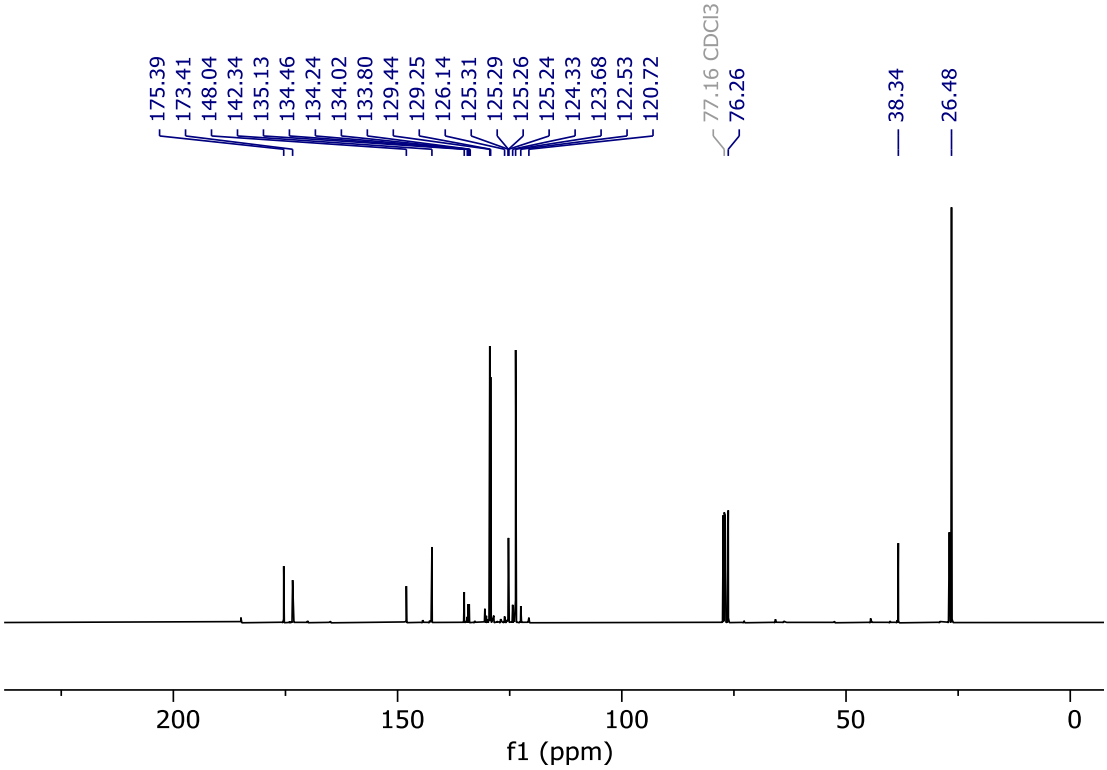


Figure 2.27 ^{13}C NMR spectra of **1g** in $CDCl_3$

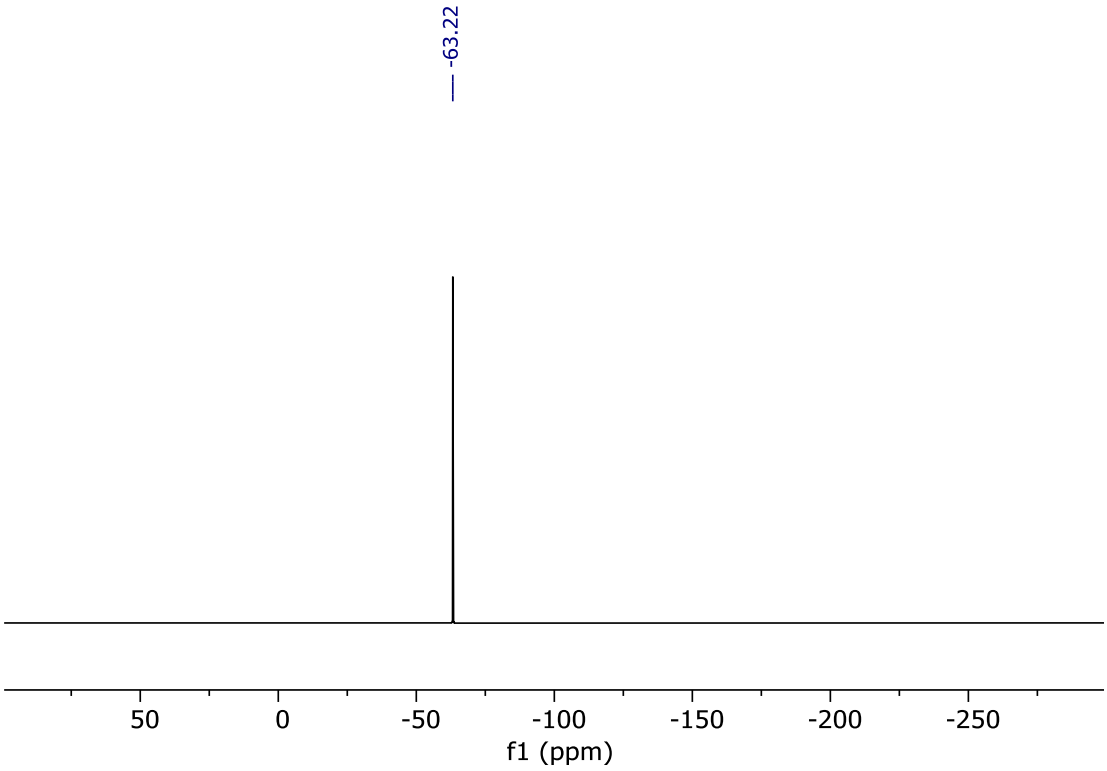


Figure 2.28 ^{19}F NMR spectra of **1g** in $CDCl_3$

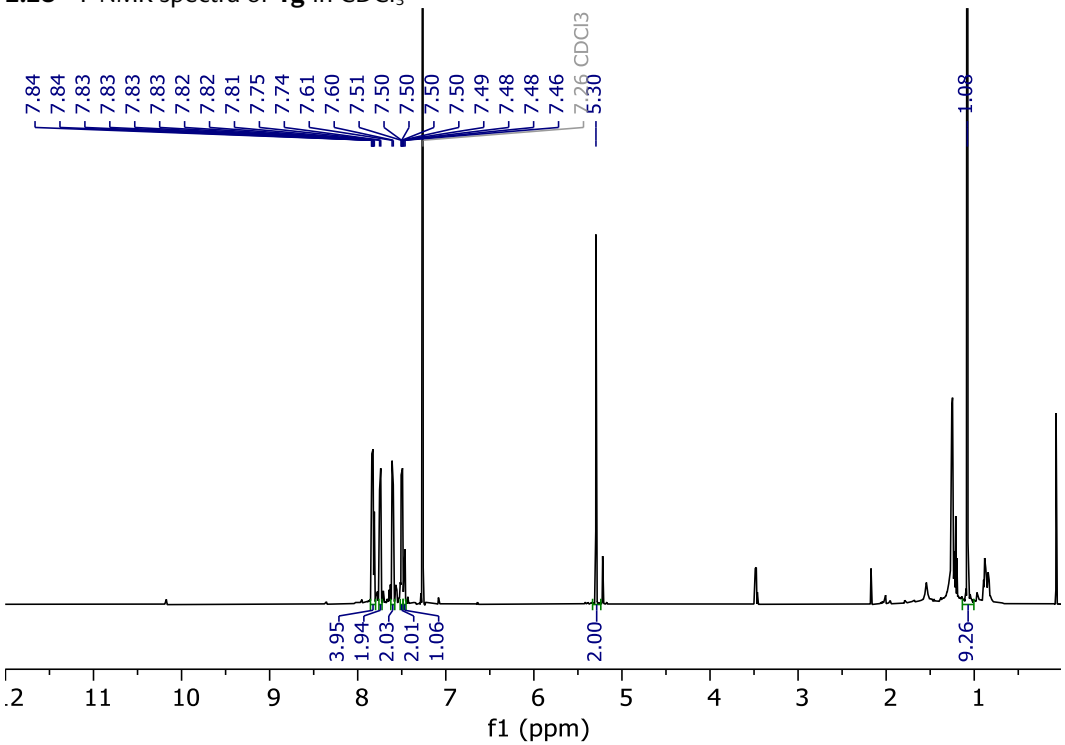


Figure 2.29 ^{1}H NMR spectra of **1h** in $CDCl_3$

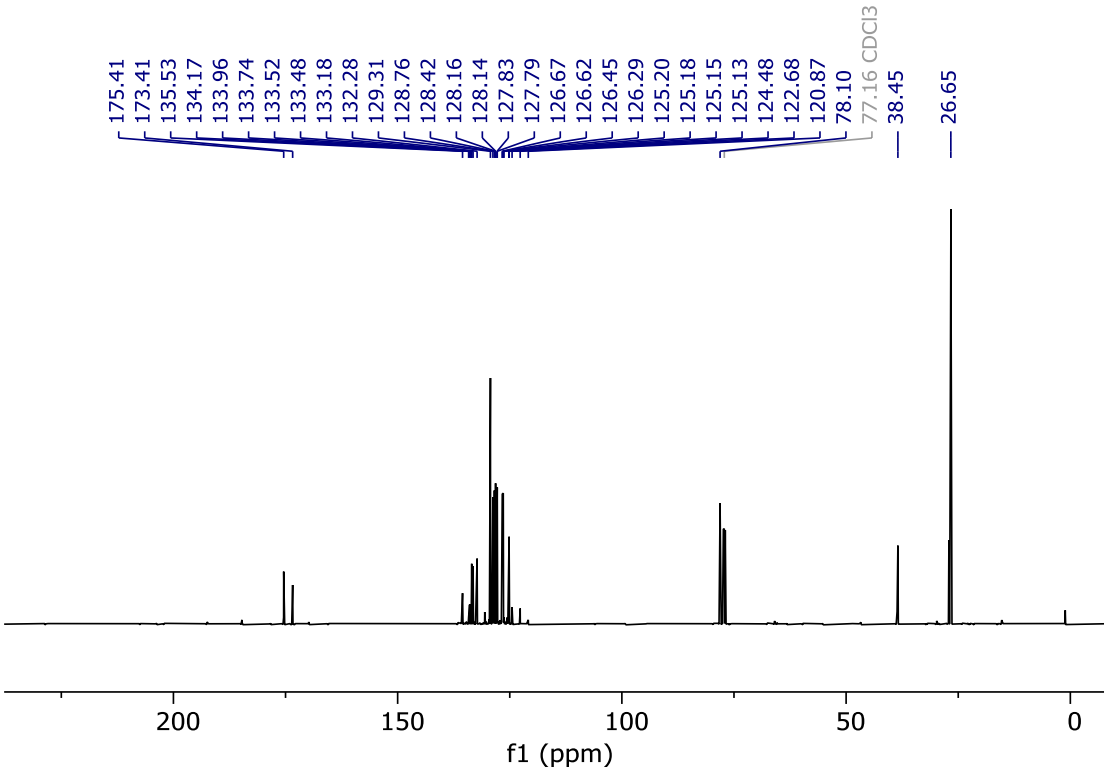


Figure 2.30 ^{13}C NMR spectra of **1h** in $CDCl_3$

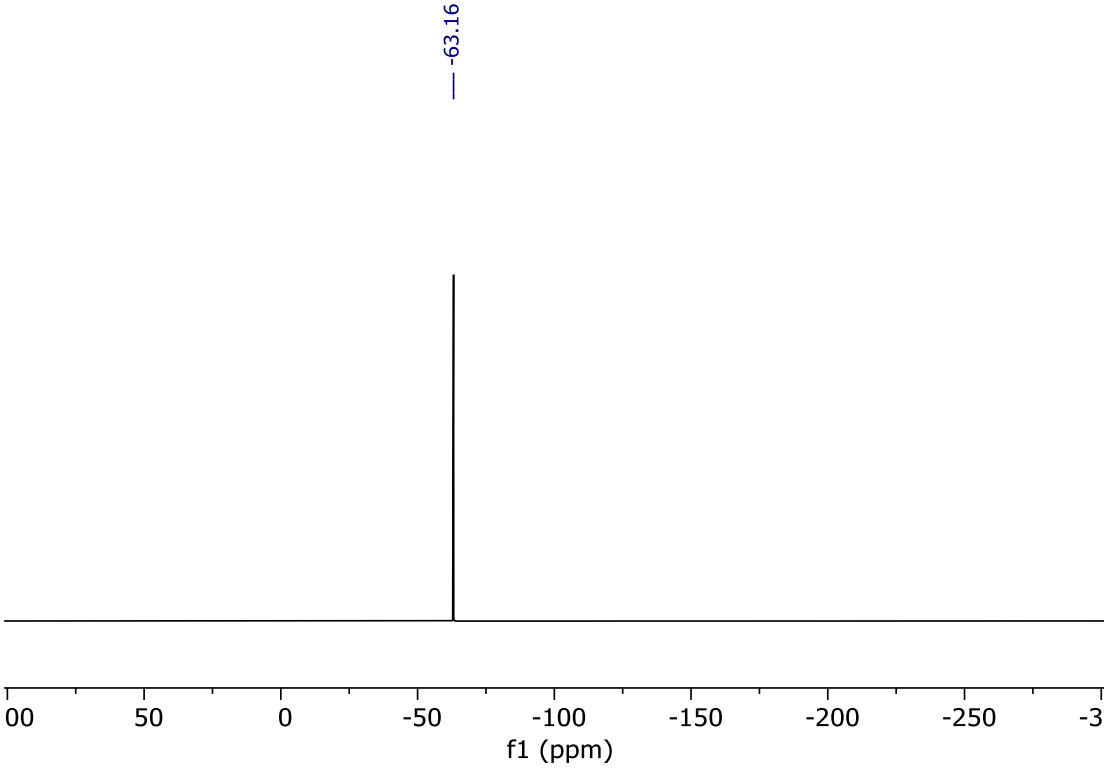


Figure 2.31 ^{19}F NMR spectra of **1h** in $CDCl_3$

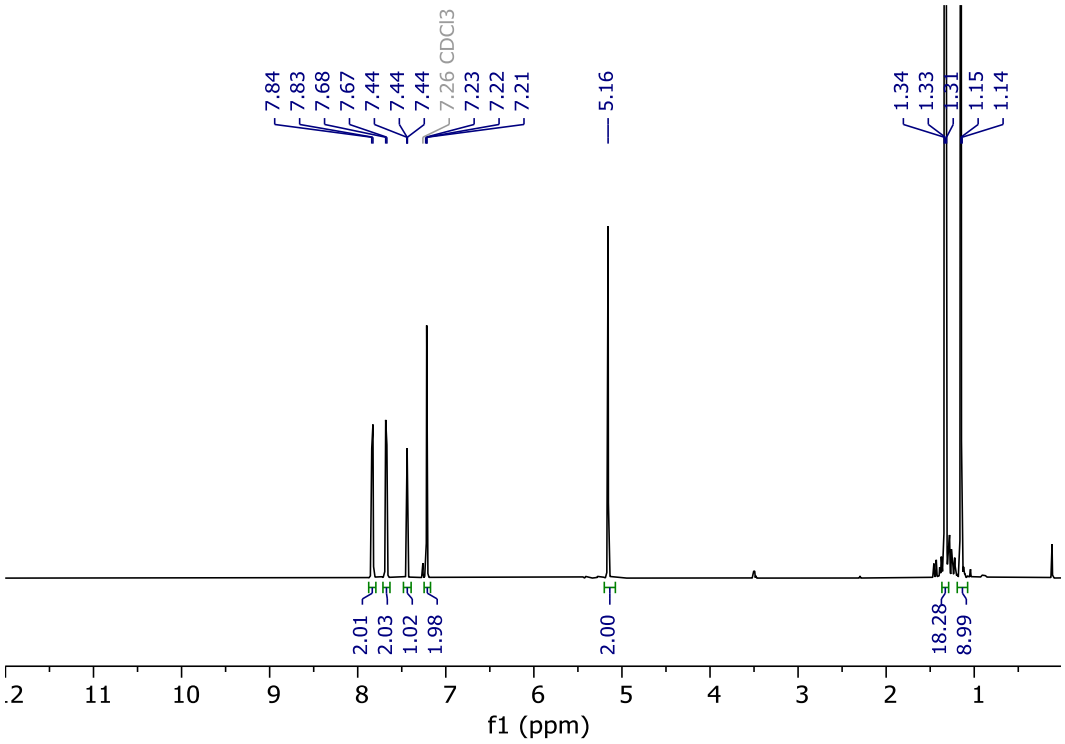


Figure 2.32 ^{1}H NMR spectra of **1i** in $CDCl_3$

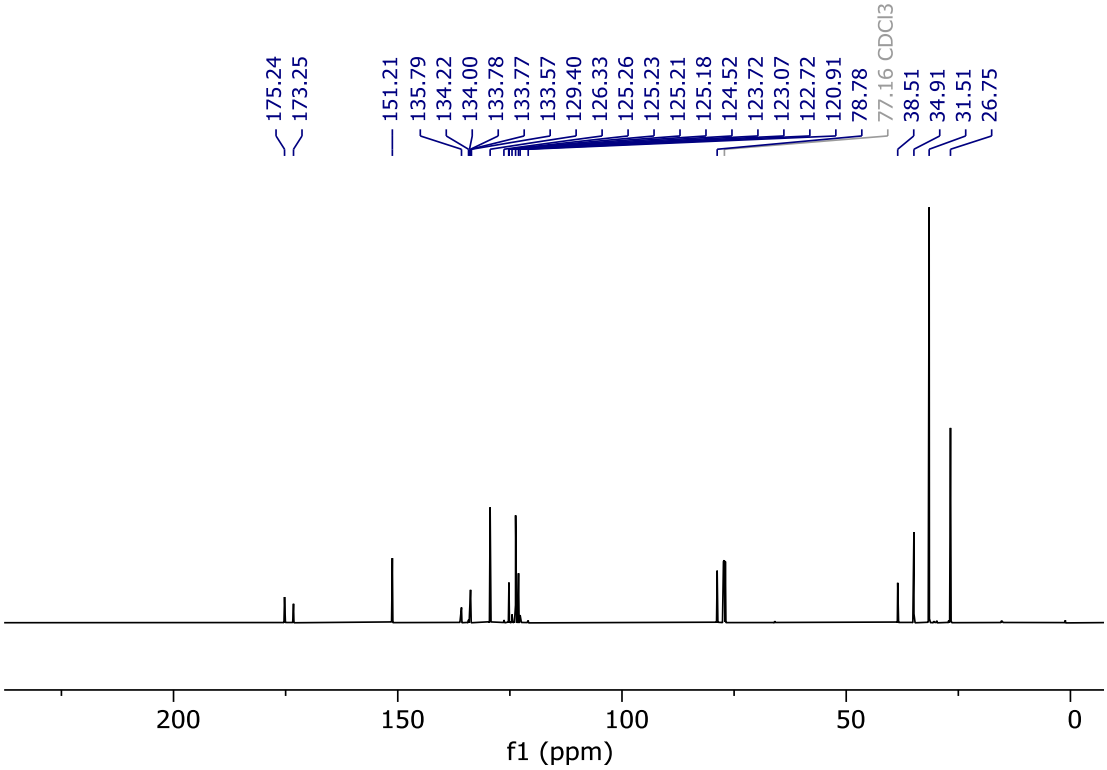


Figure 2.33 ^{13}C NMR spectra of **1i** in $CDCl_3$

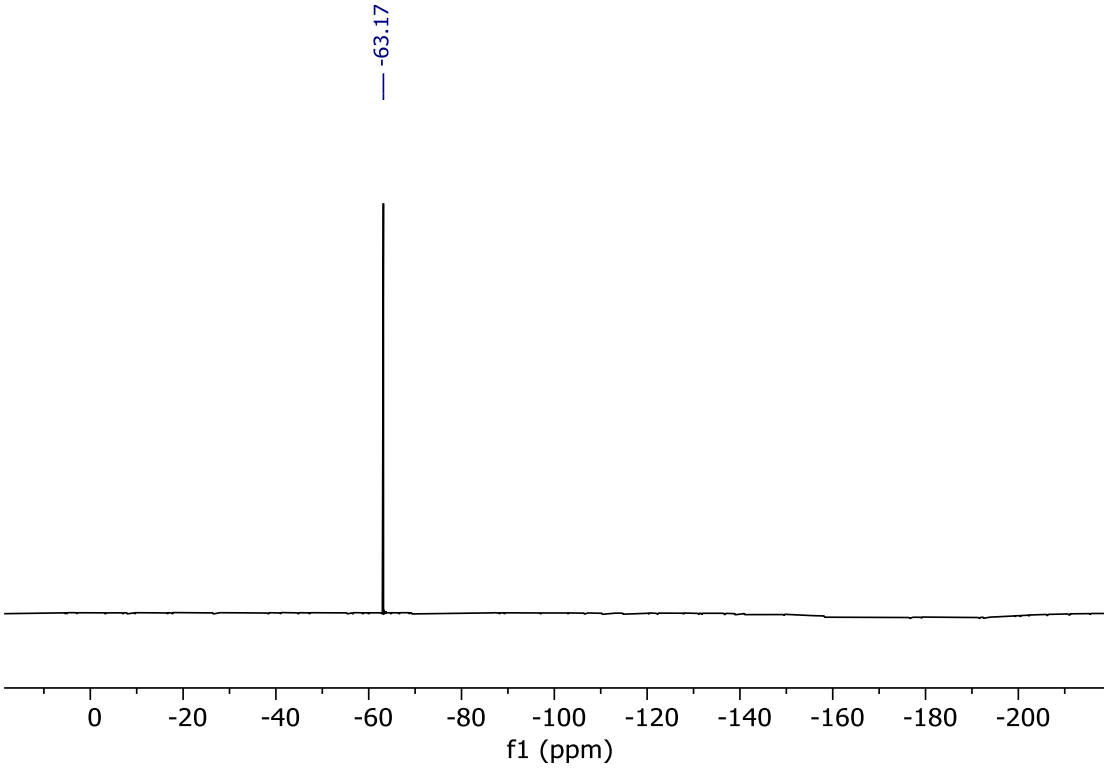


Figure 2.34 ^{19}F NMR spectra of **1i** in $CDCl_3$

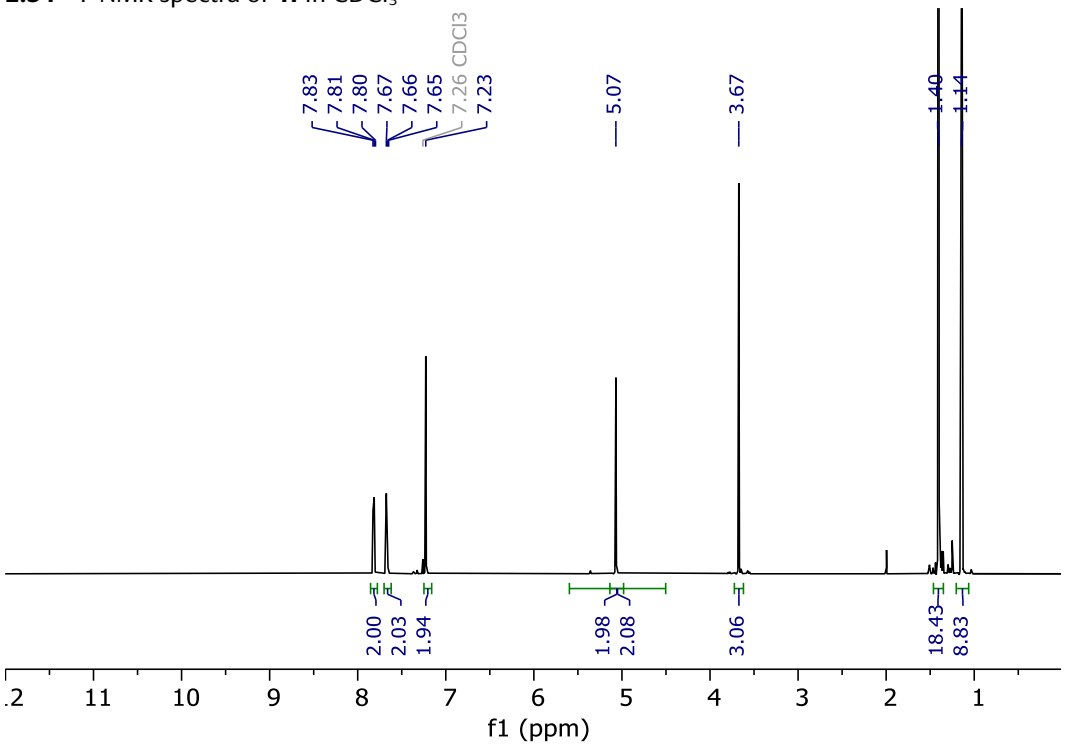


Figure 2.35 ^{1}H NMR spectra of **1j** in $CDCl_3$

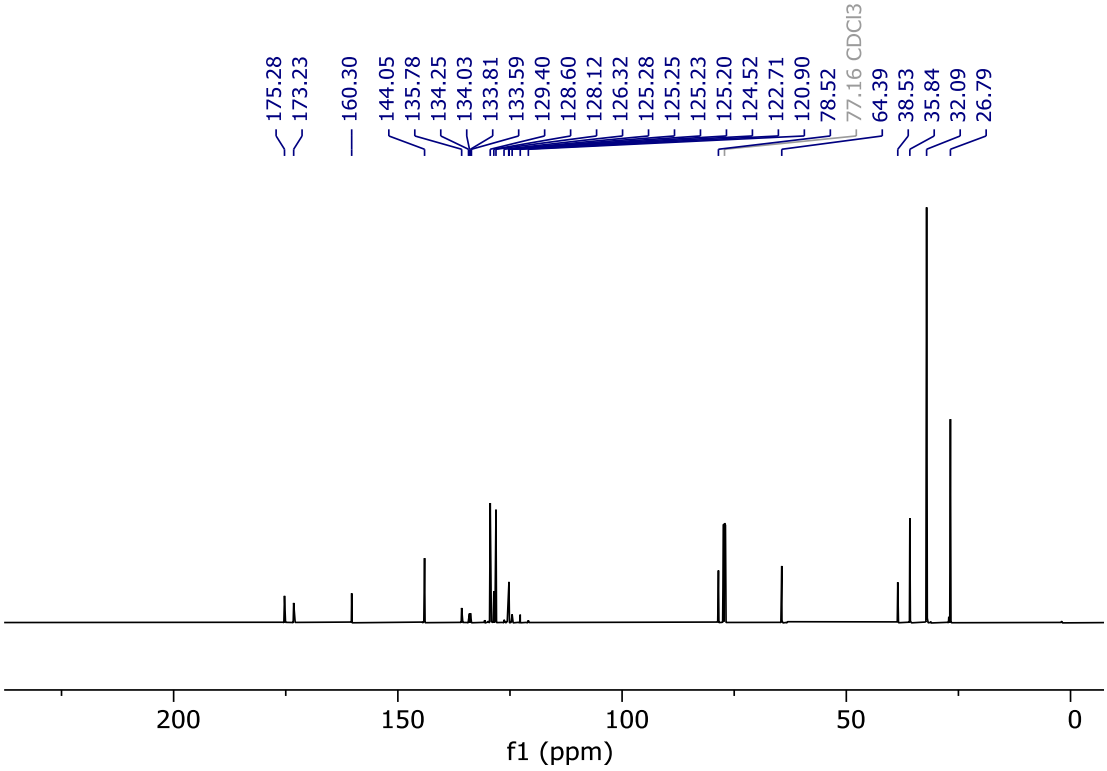


Figure 2.36 ^{13}C NMR spectra of **1j** in $CDCl_3$

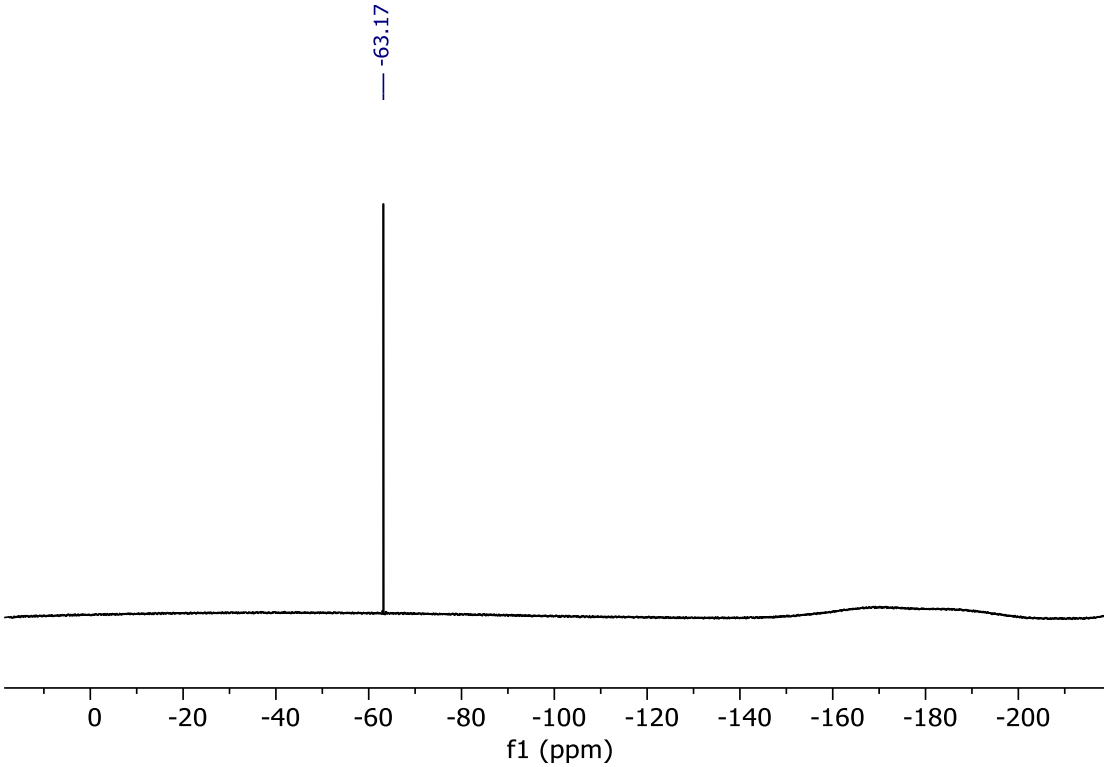


Figure 2.37 ^{19}F NMR spectra of **1j** in $CDCl_3$

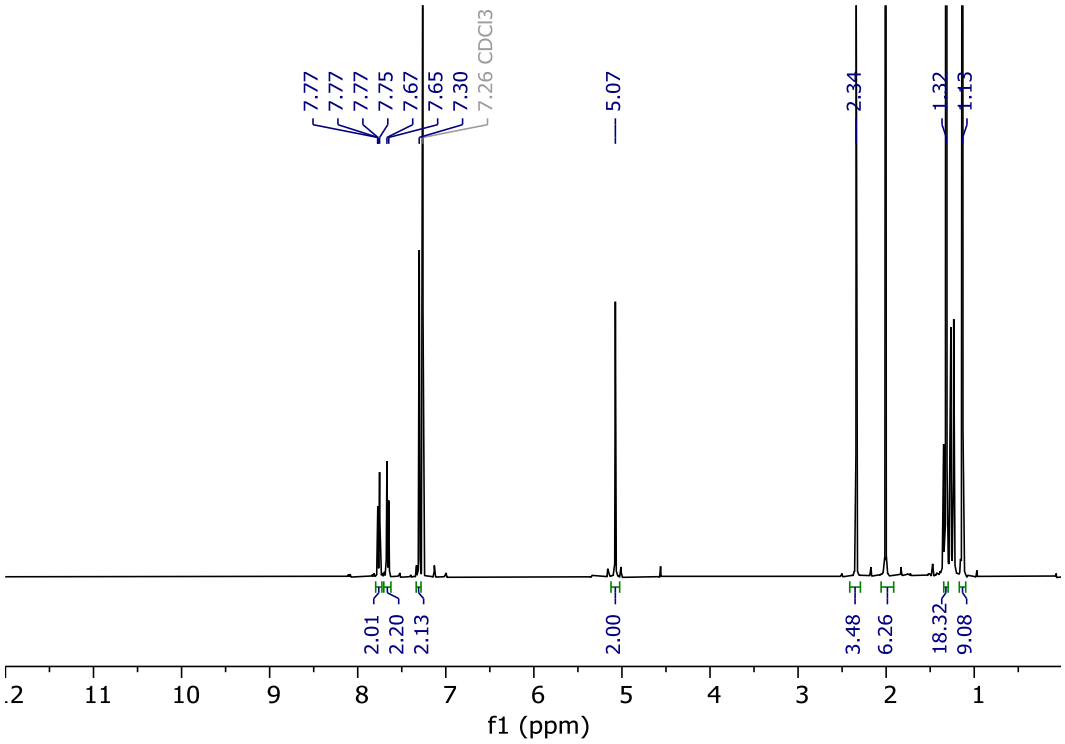


Figure 2.38 ^{1}H NMR spectra of **1k** in $CDCl_3$

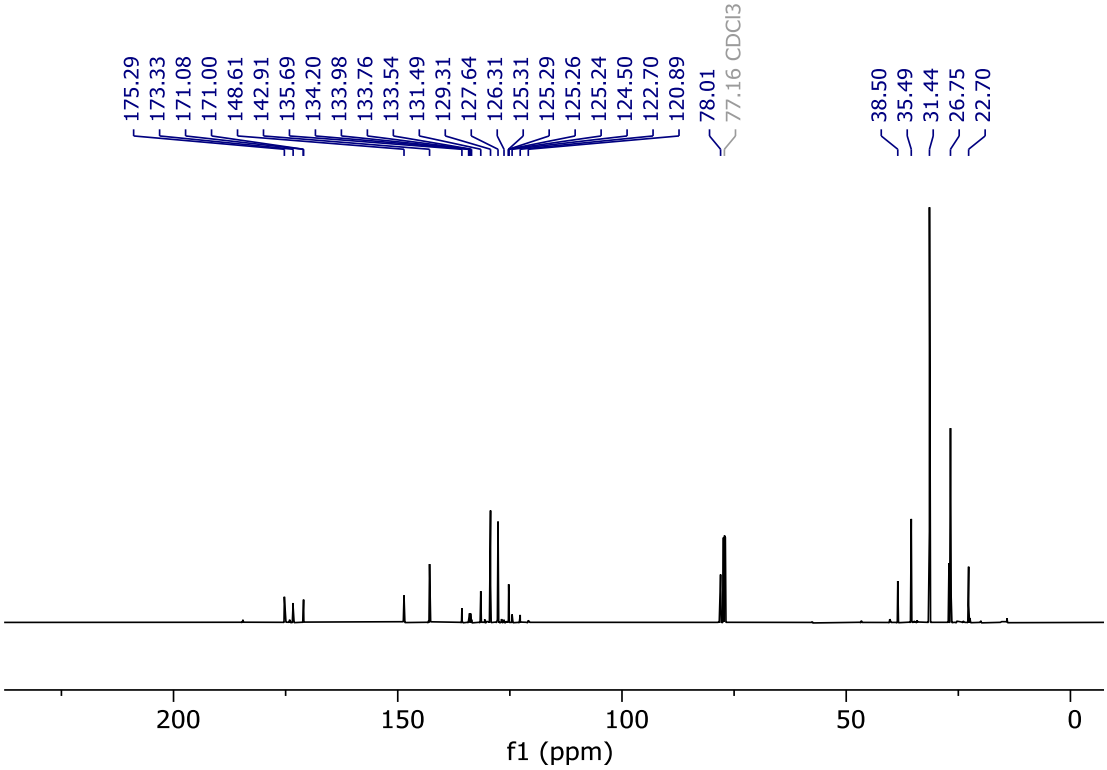


Figure 2.39 ^{13}C NMR spectra of **1k** in $CDCl_3$

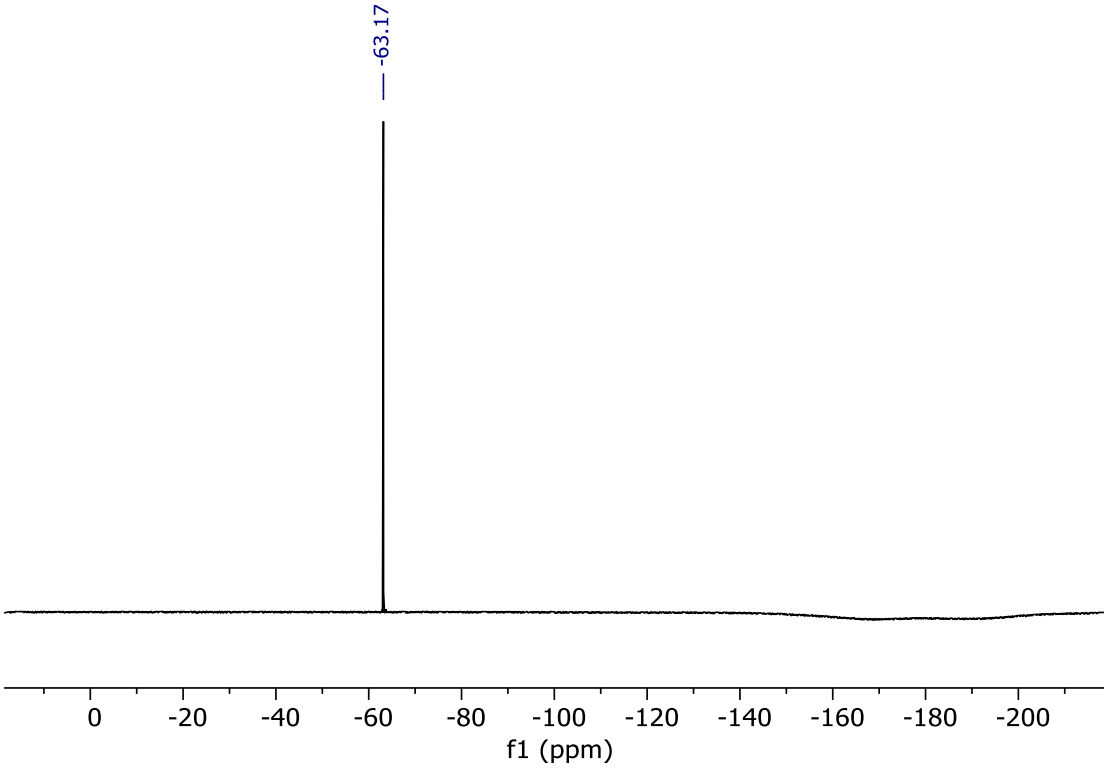


Figure 2.40 ^{19}F NMR spectra of **1k** in $CDCl_3$

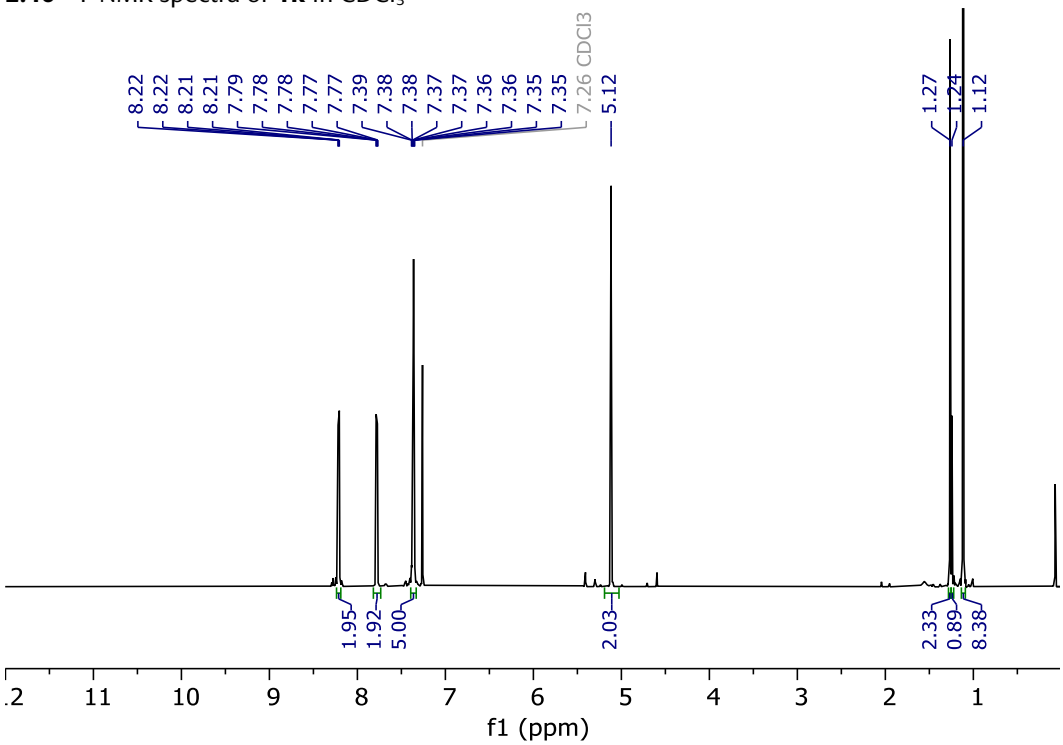


Figure 2.41 ^{1}H NMR spectra of **1m** in $CDCl_3$

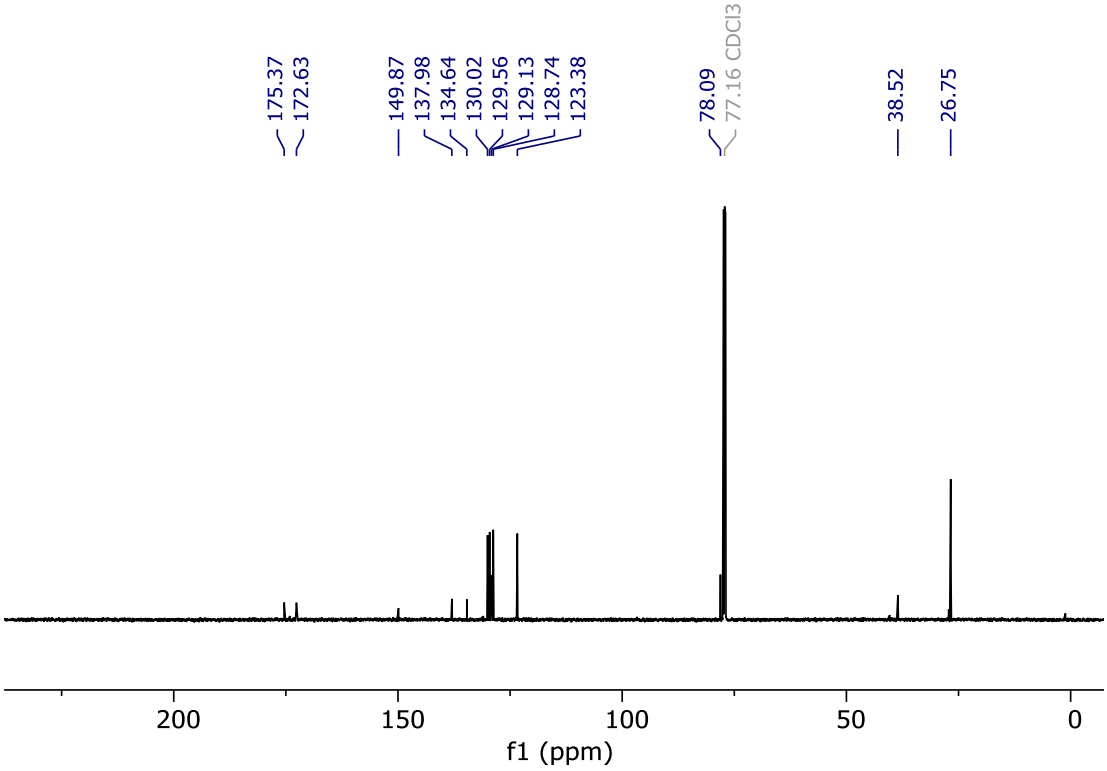


Figure 2.42 ^{13}C NMR spectra of **1m** in $CDCl_3$

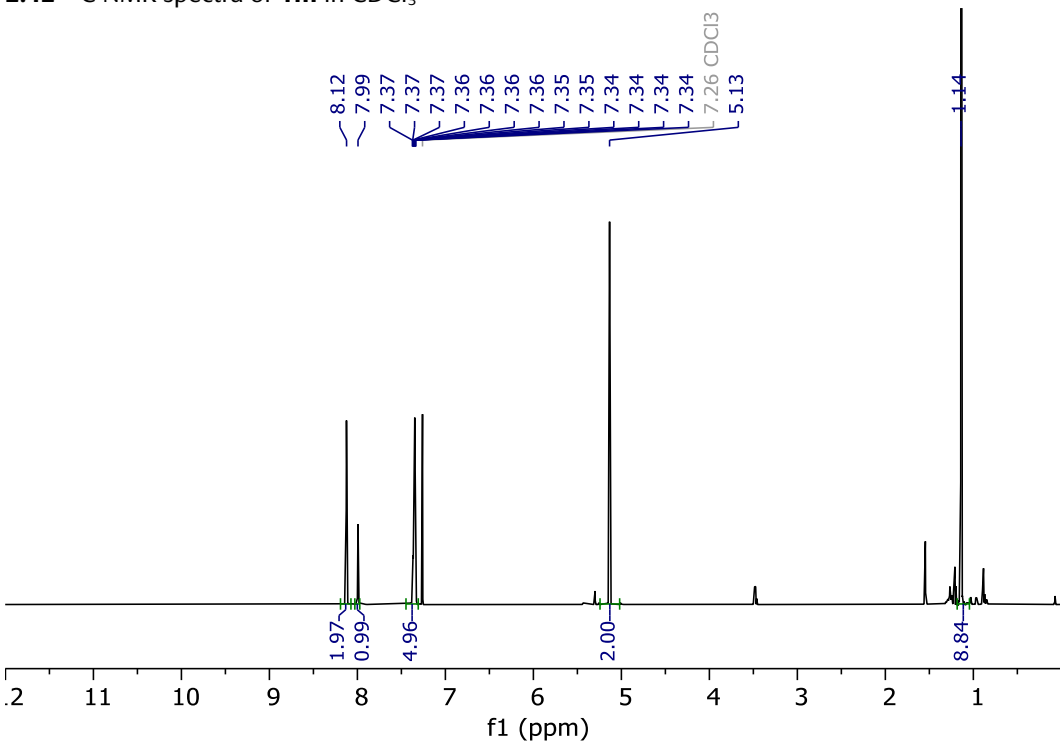


Figure 2.43 ^{1}H NMR spectra of **1n** in $CDCl_3$

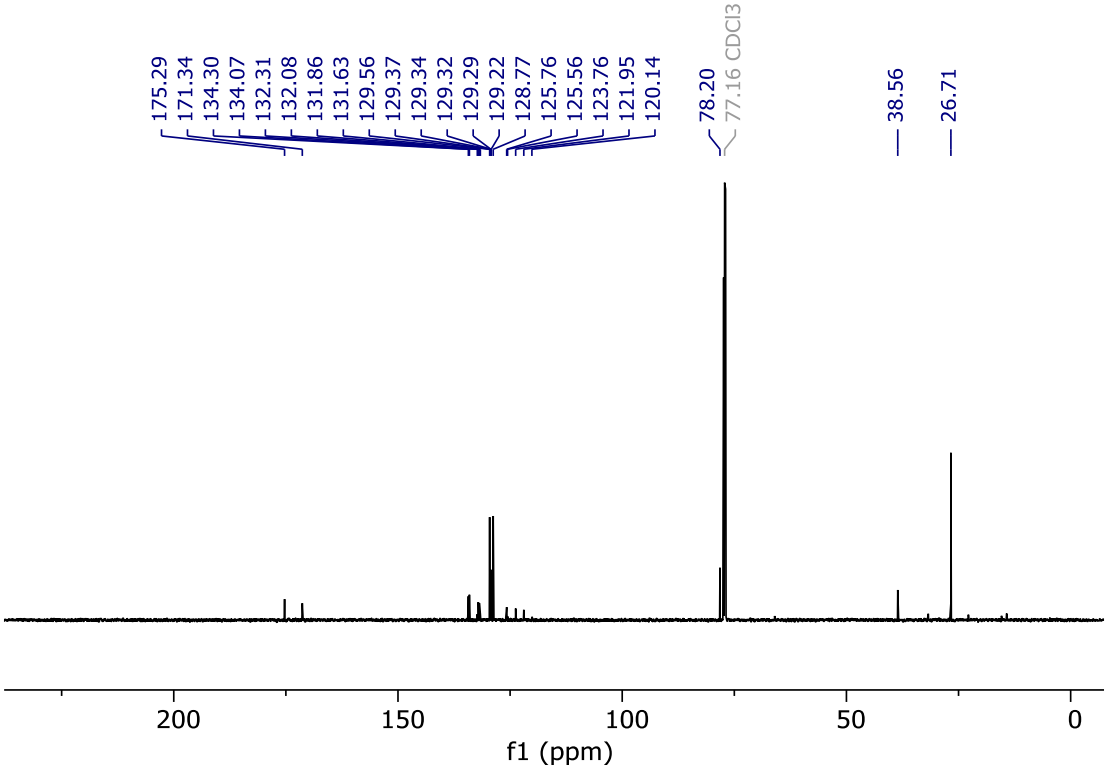


Figure 2.44 ^{13}C NMR spectra of **1n** in $CDCl_3$

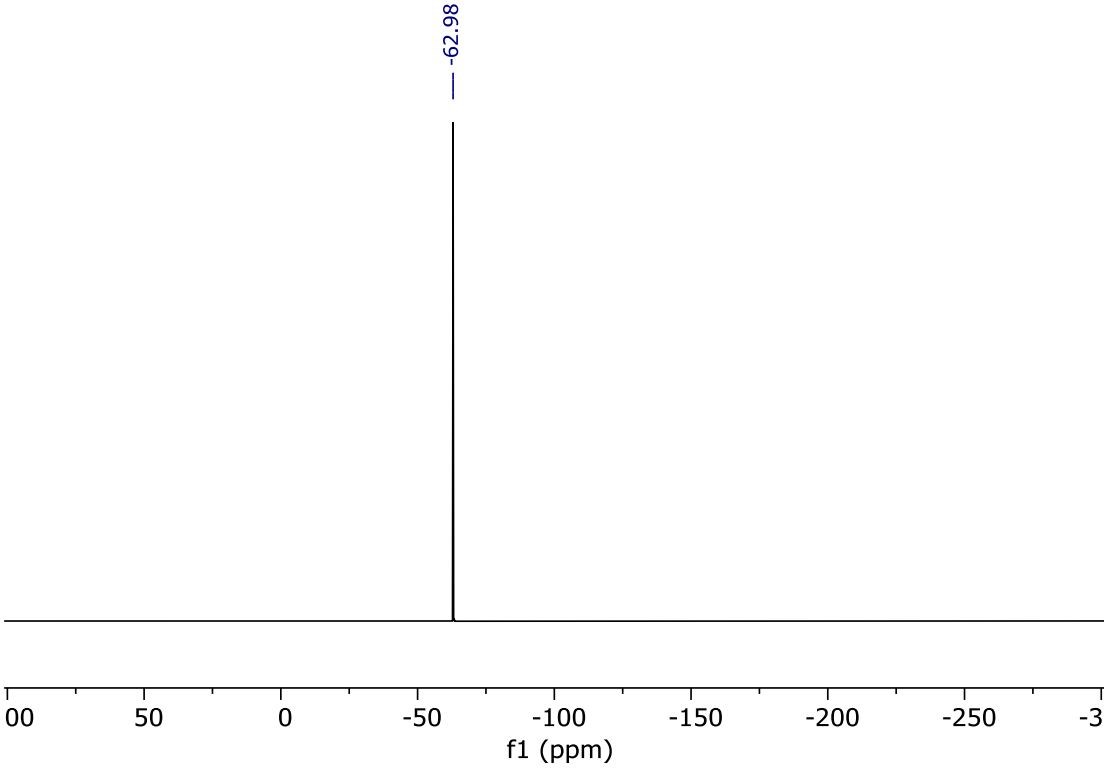


Figure 2.45 ^{19}F NMR spectra of **1n** in $CDCl_3$

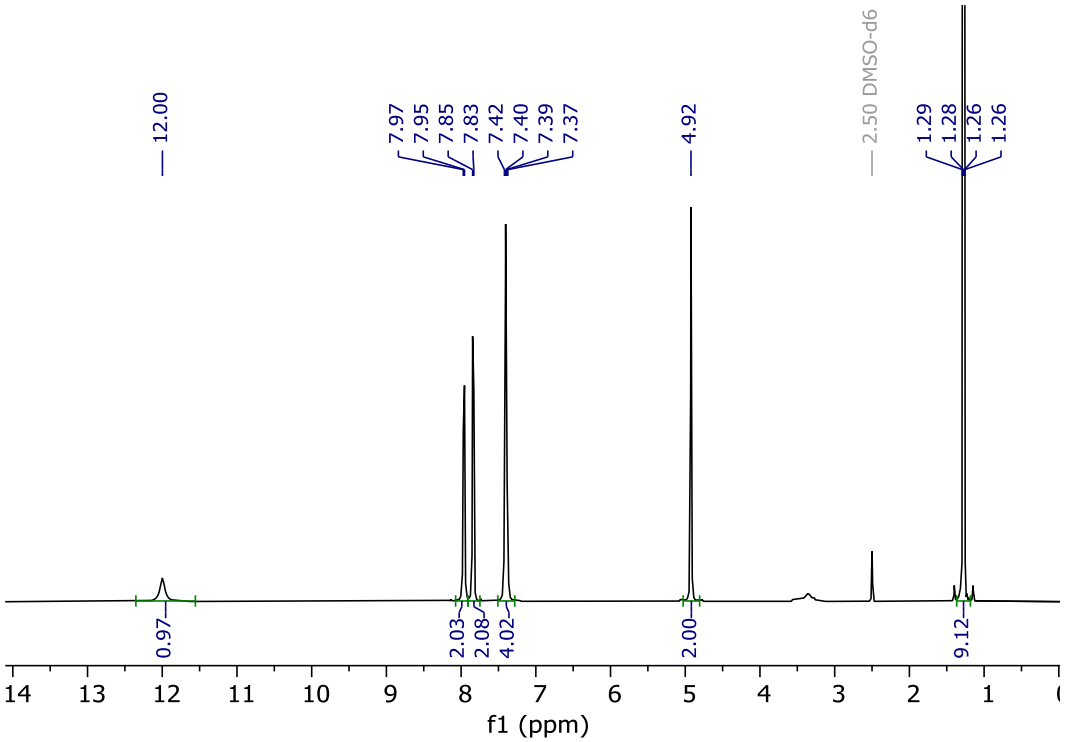


Figure 2.46 ^{1}H NMR spectra of **19d** in DMSO-*d6*

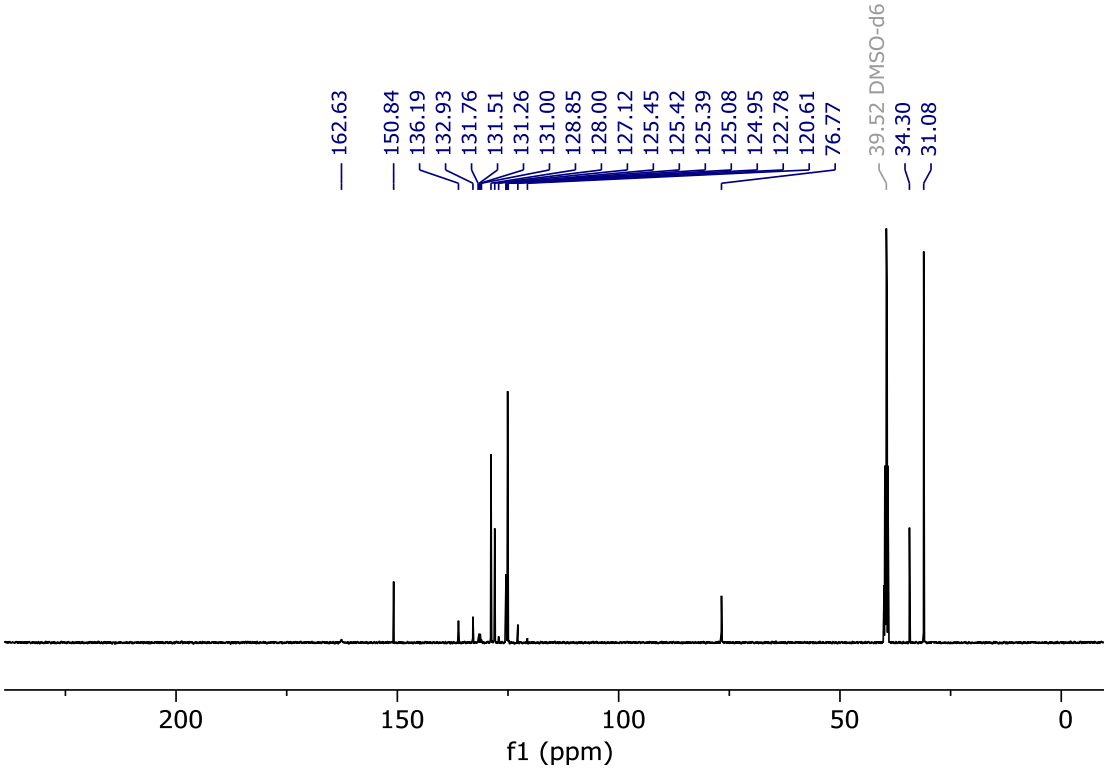


Figure 2.47 ^{13}C NMR spectra of **19d** in DMSO-*d6*

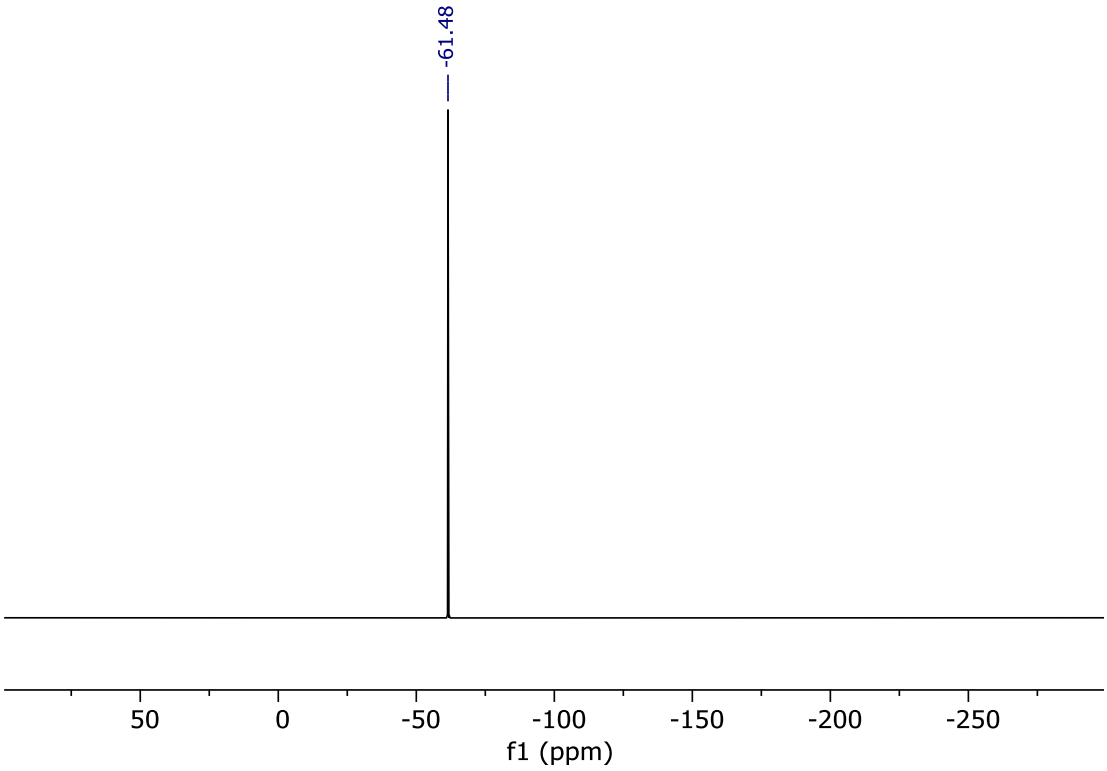


Figure 2.48 ^{19}F NMR spectra of **19d** in DMSO-*d6*

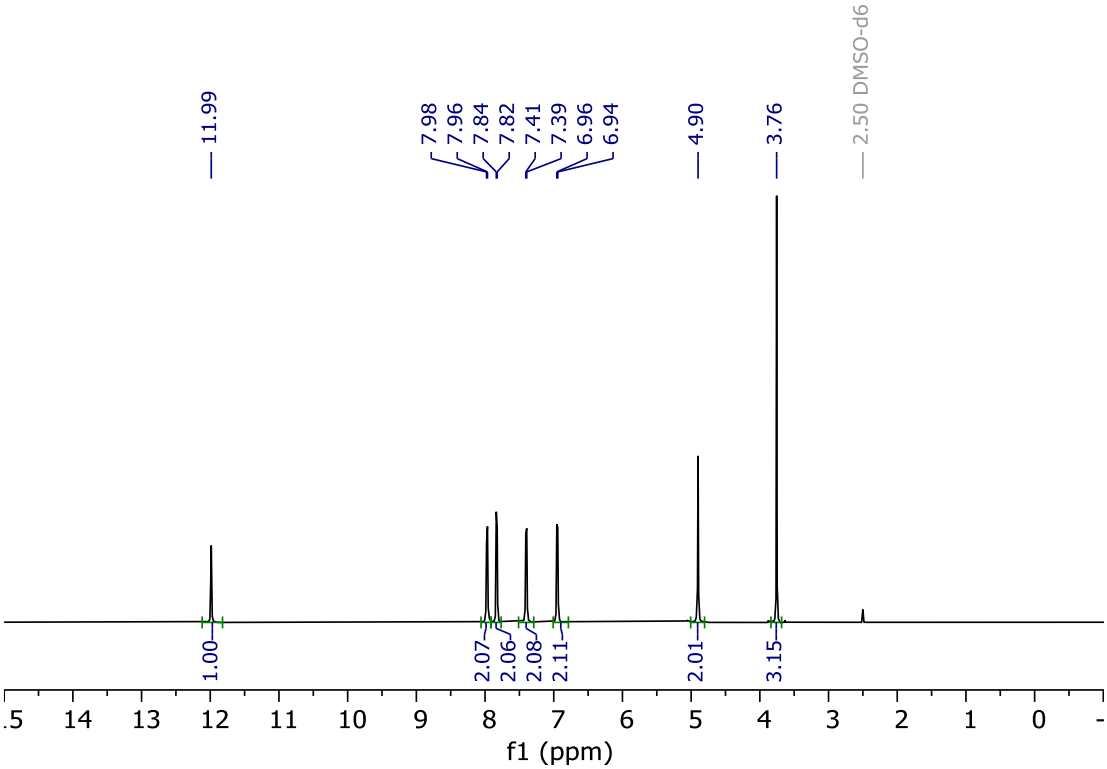


Figure 2.49 ^{1}H NMR spectra of **19e** in DMSO-*d6*

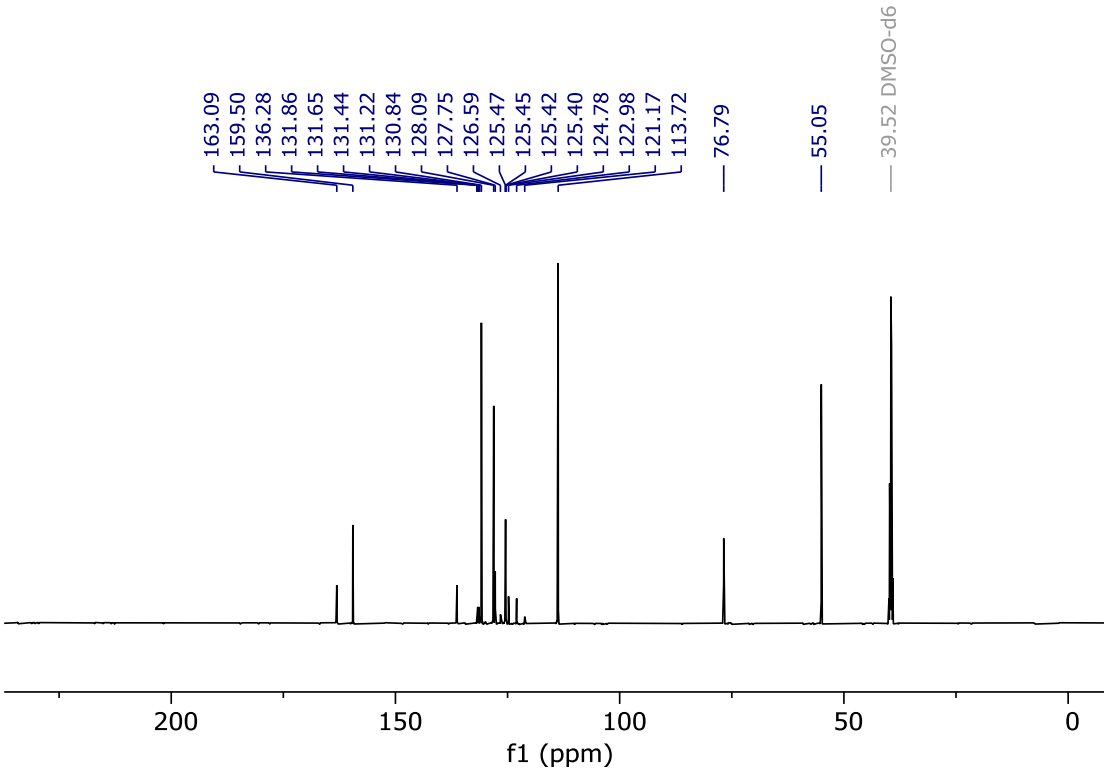


Figure 2.50 ^{13}C NMR spectra of **19e** in DMSO-*d6*

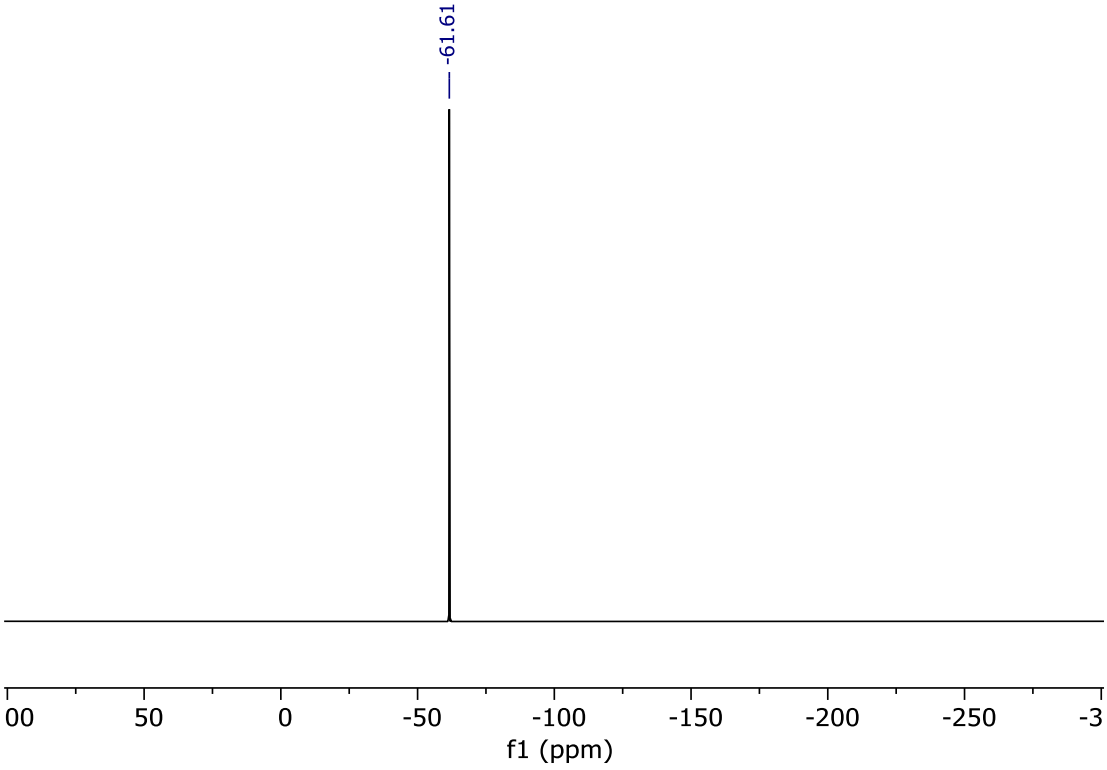


Figure 2.51 ^{19}F NMR spectra of **19e** in DMSO-*d6*

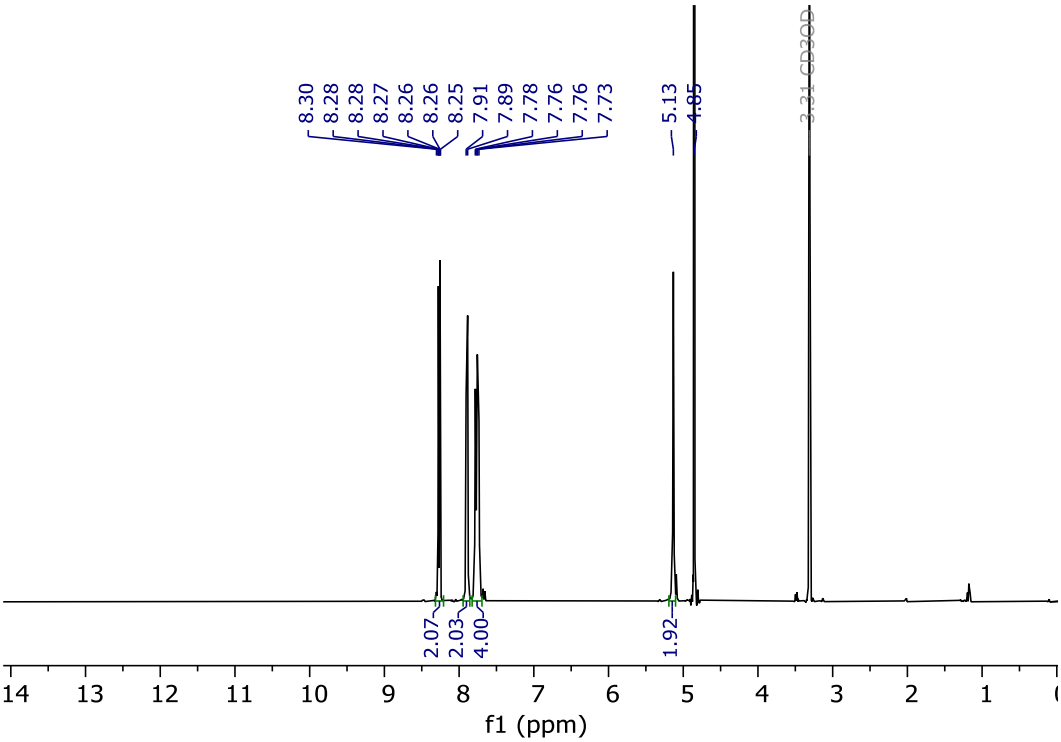


Figure 2.52 ^{1}H NMR spectra of **19g** in CD_3OD

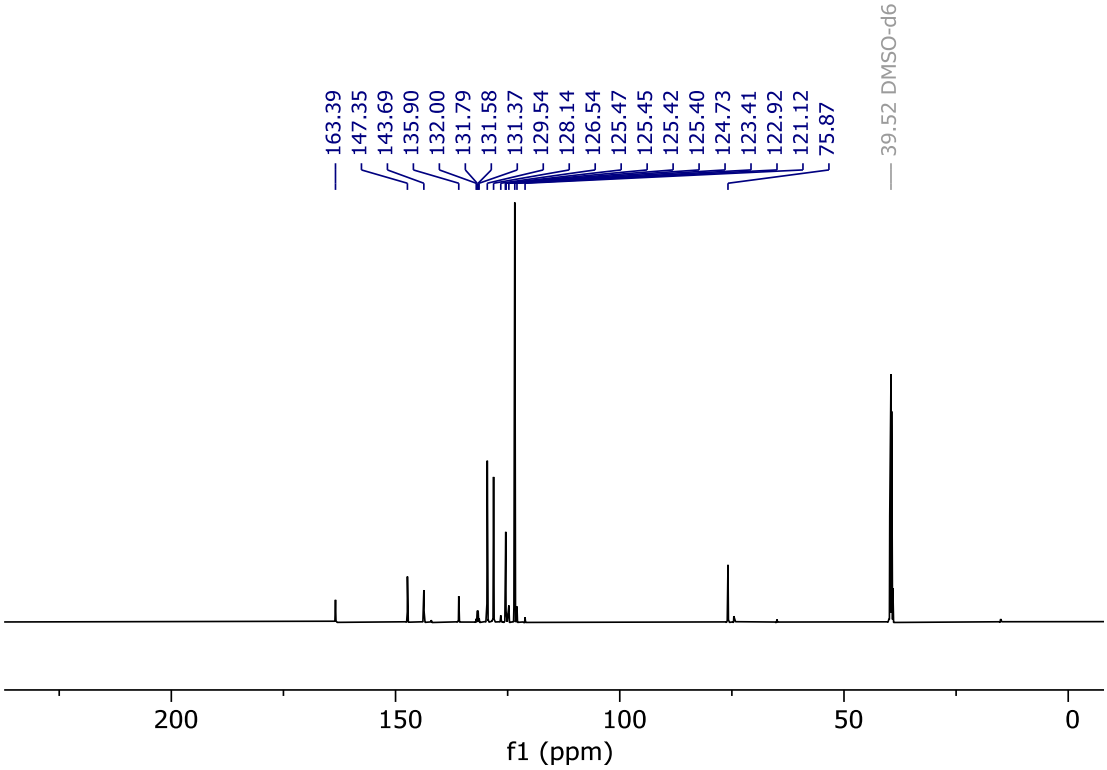


Figure 2.53 ^{13}C NMR spectra of **19g** in DMSO-*d6*

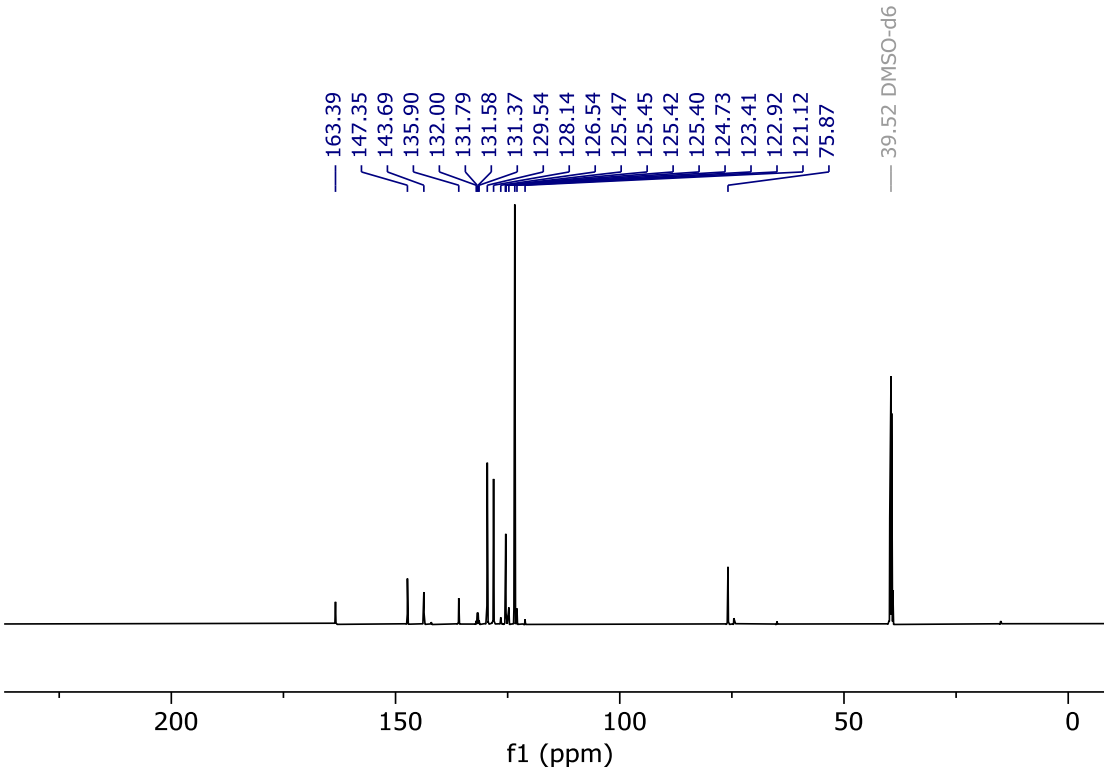


Figure 2.54 ^{19}F NMR spectra of **19g** in CD_3OD

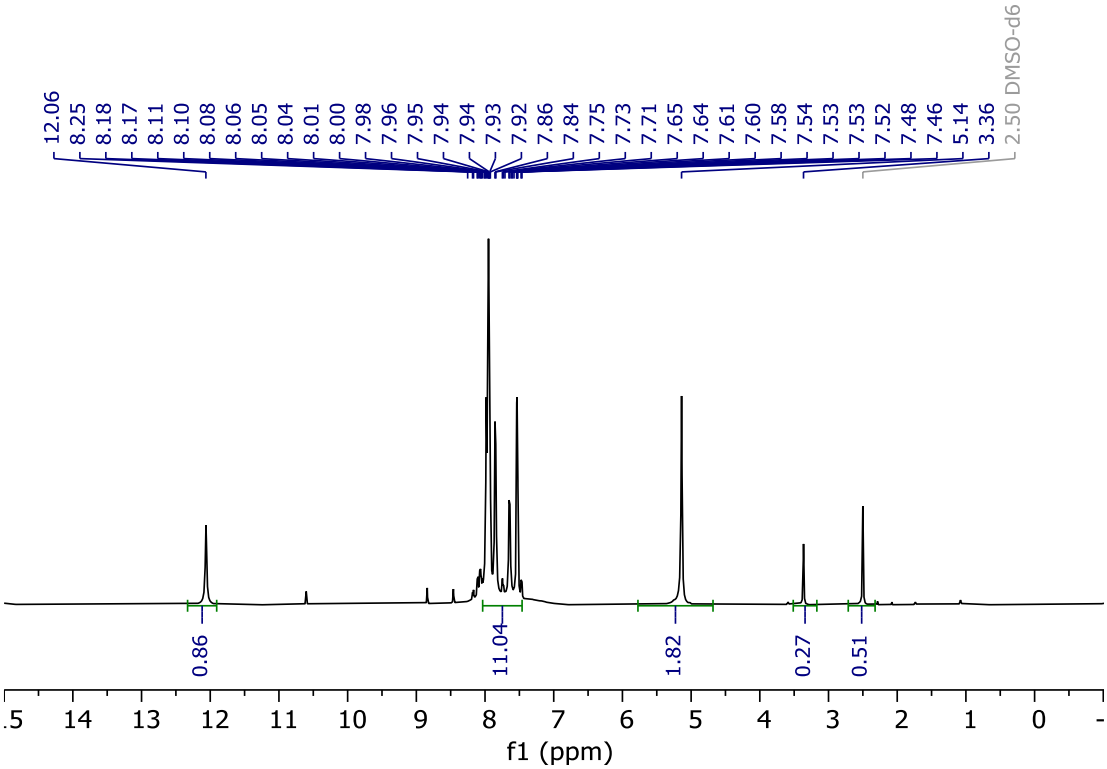


Figure 2.55 ^{1}H NMR spectra of **19h** in DMSO-*d6*

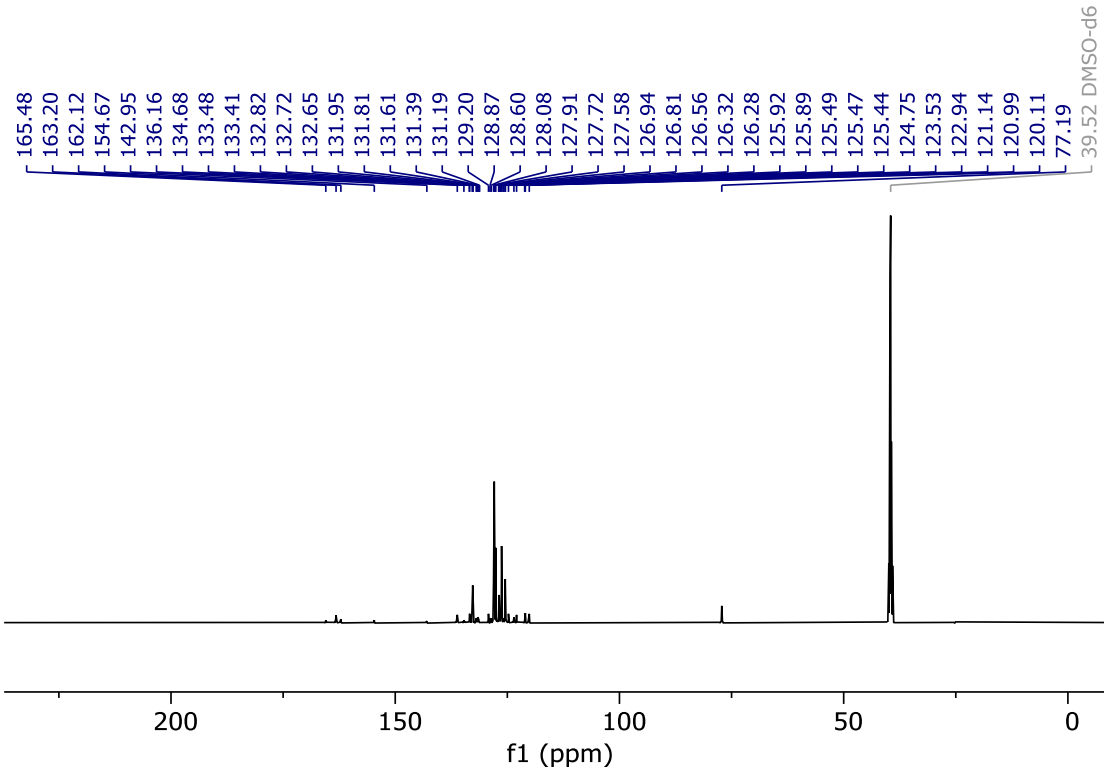


Figure 2.56 ^{13}C NMR spectra of **19h** in DMSO-*d6*

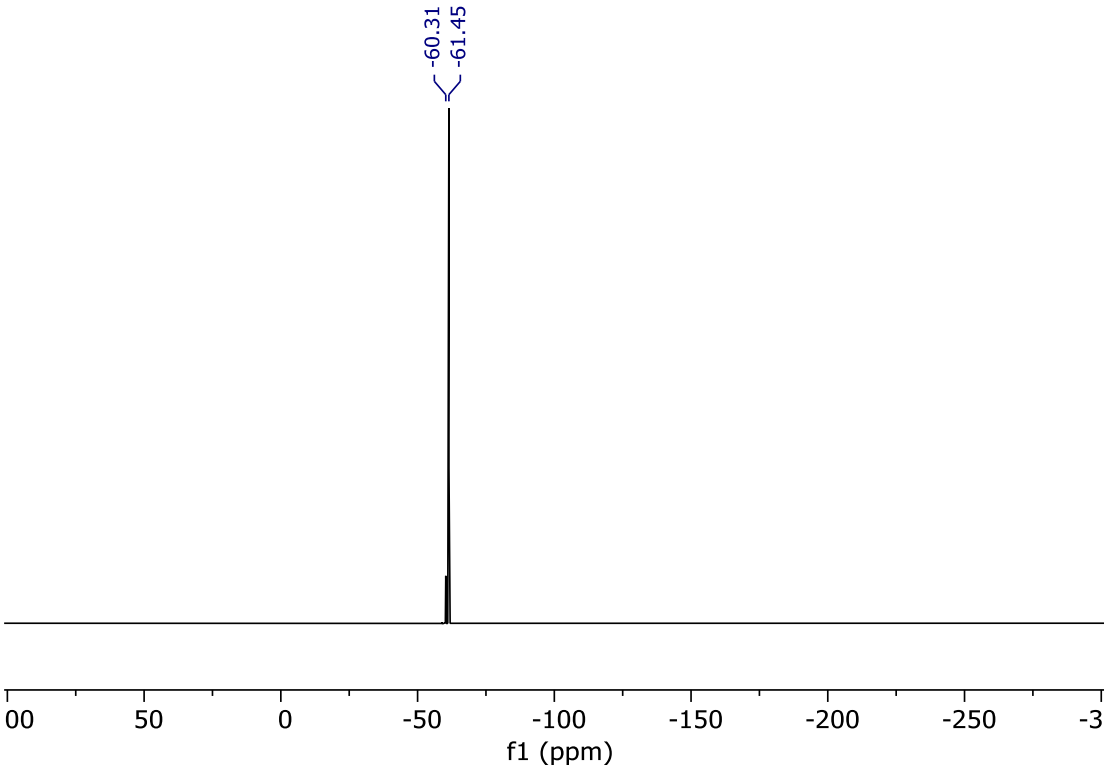


Figure 2.57 ^{19}F NMR spectra of **19h** in DMSO-*d6*

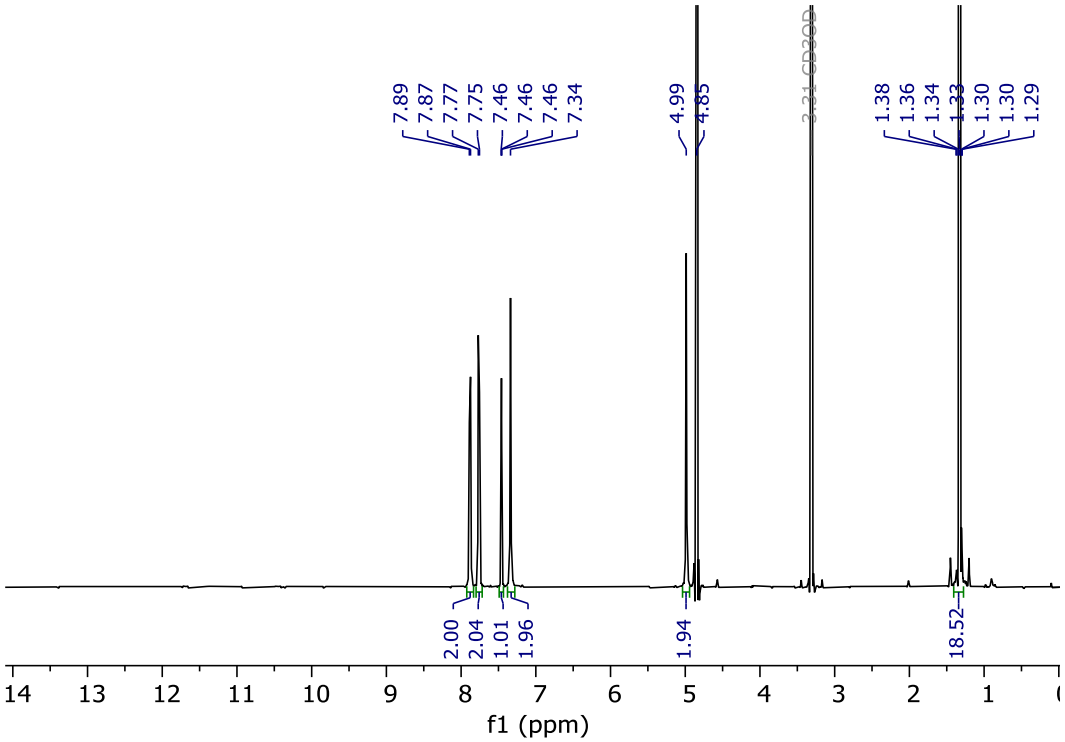


Figure 2.58 ^{1}H NMR spectra of **19i** in CD_3OD

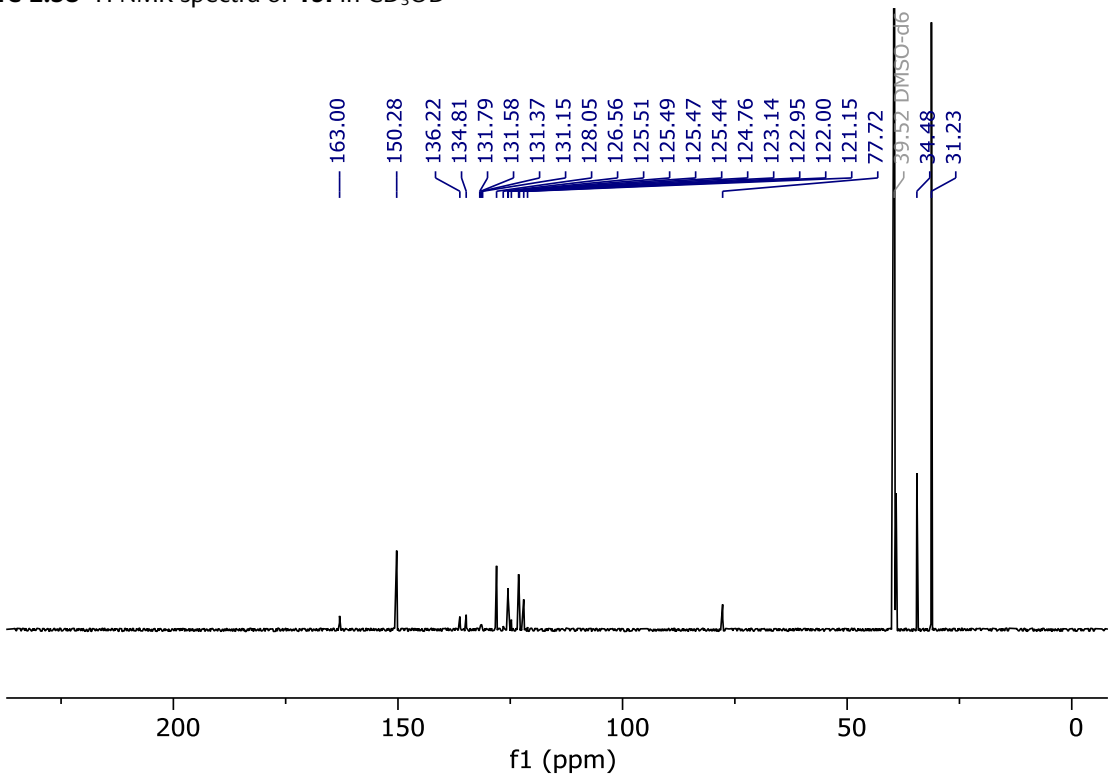


Figure 2.59 ^{13}C NMR spectra of **19i** in CD_3OD

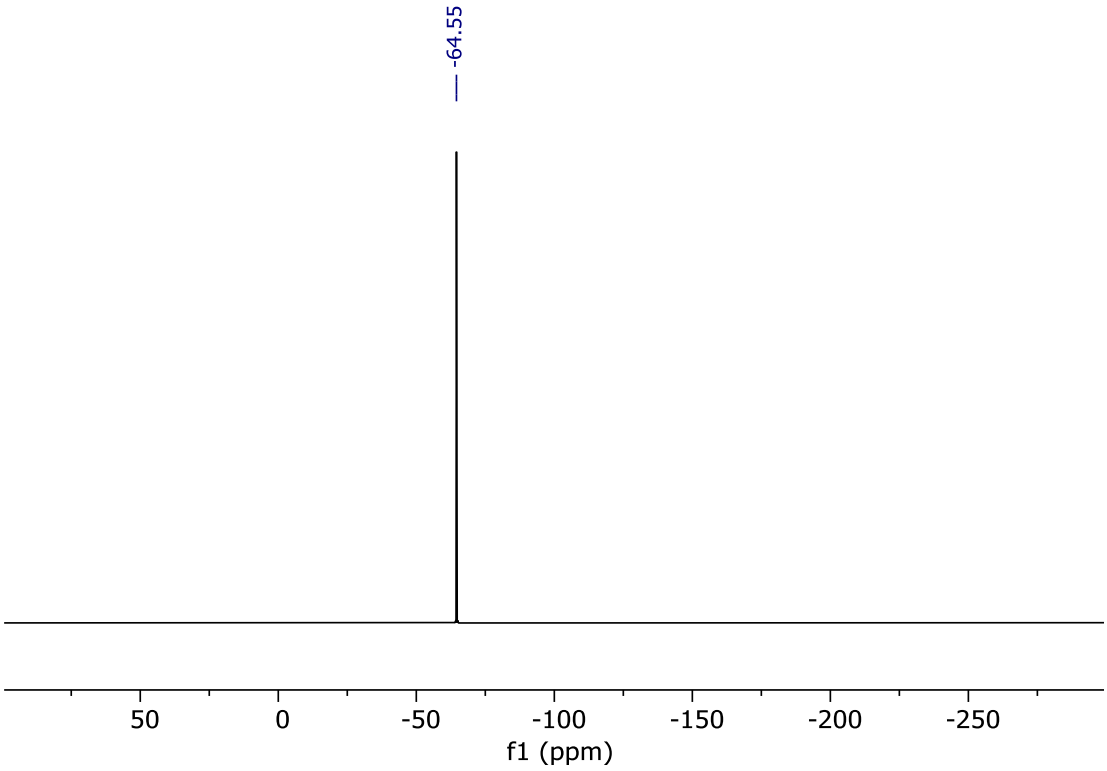


Figure 2.60 ^{19}F NMR spectra of **19i** in CD_3OD

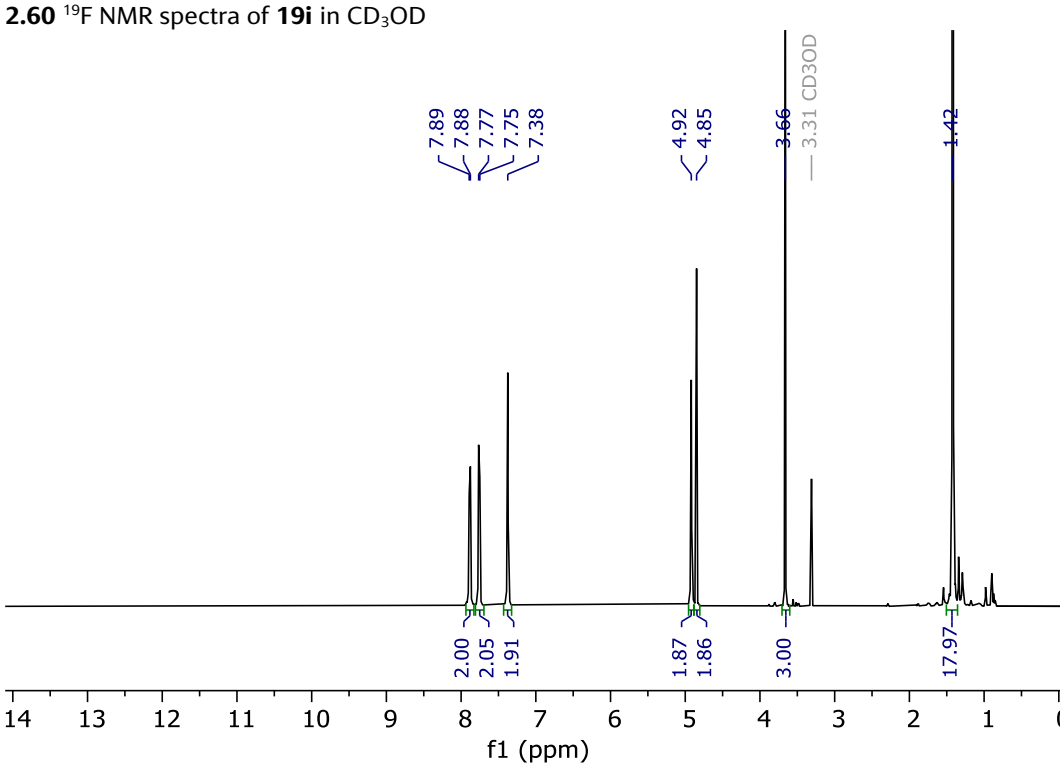


Figure 2.61 ^{1}H NMR spectra of **19j** in CD_3OD

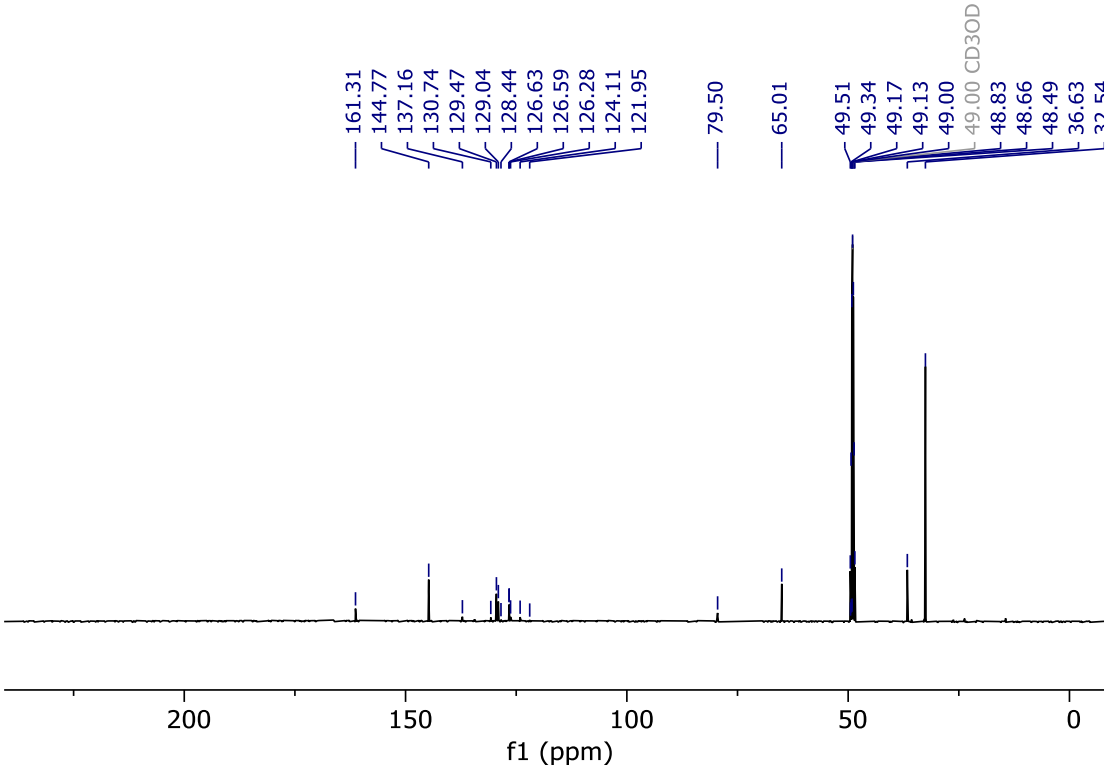


Figure 2.62 ^{13}C NMR spectra of **19j** in CD_3OD

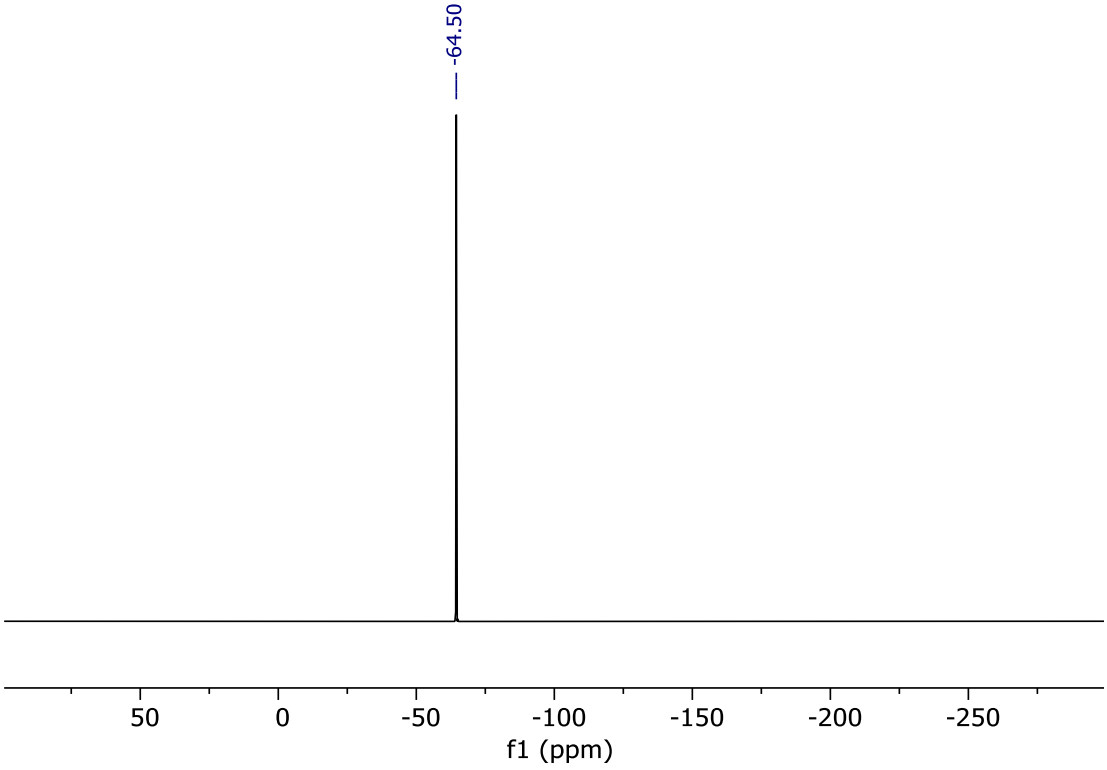


Figure 2.63 ^{19}F NMR spectra of **19j** in CD_3OD

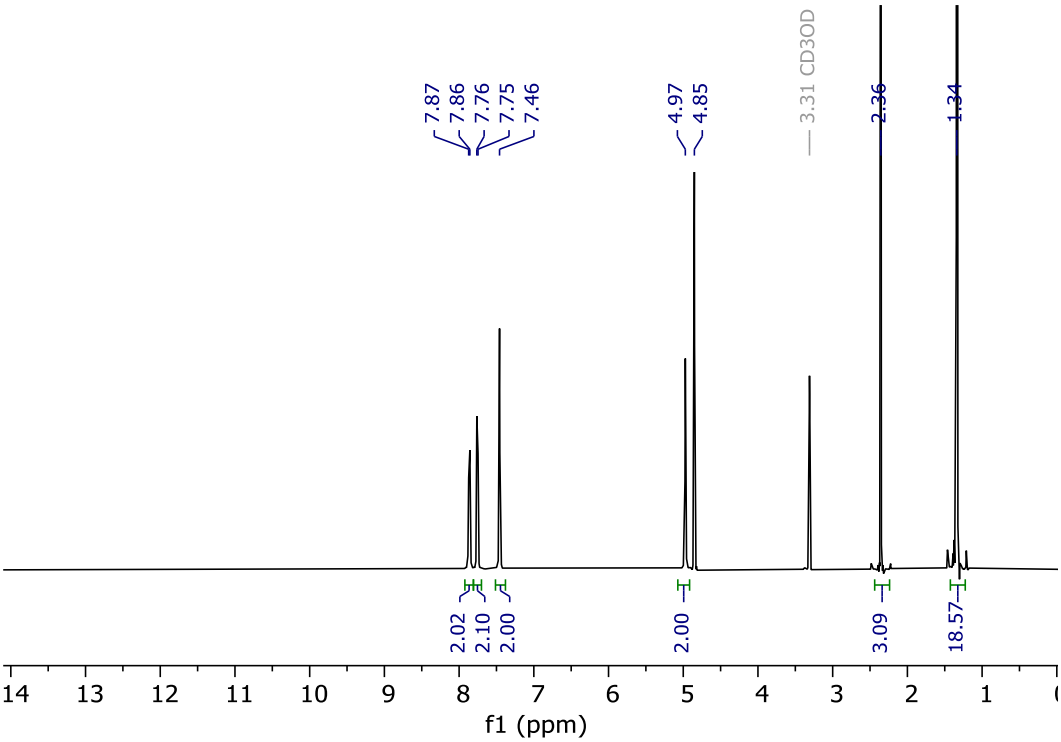


Figure 2.64 ^{1}H NMR spectra of **19k** in CD_3OD

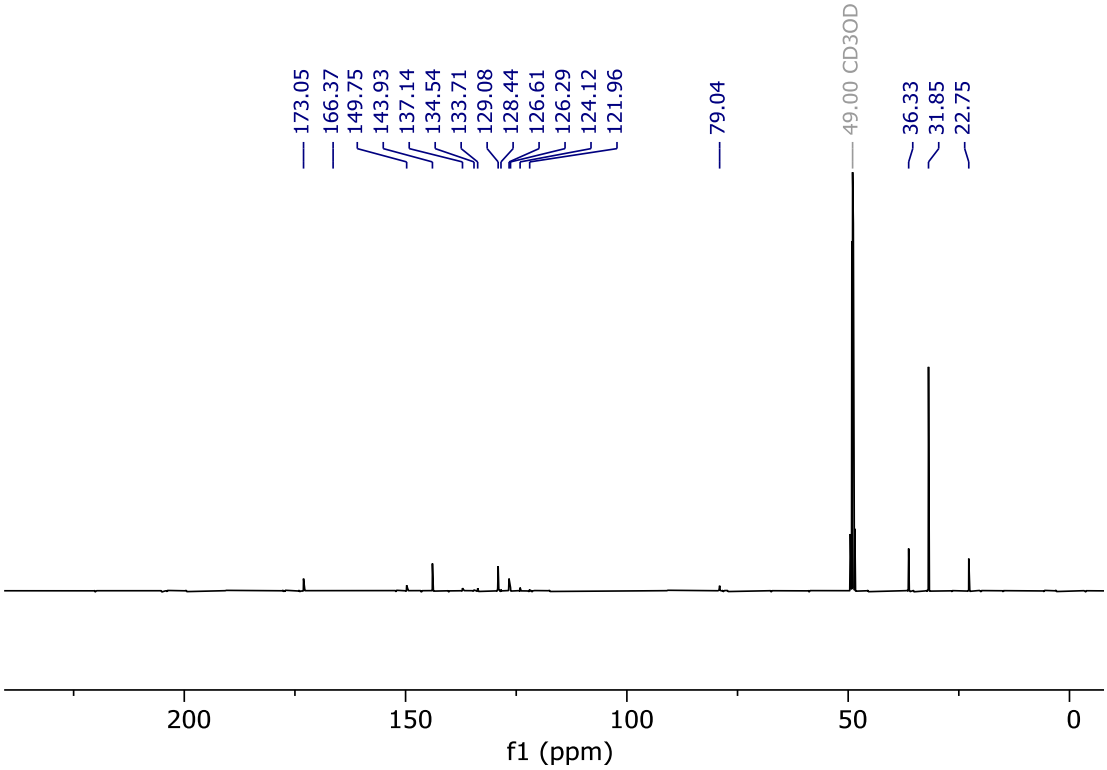


Figure 2.65 ^{13}C NMR spectra of **19k** in CD_3OD

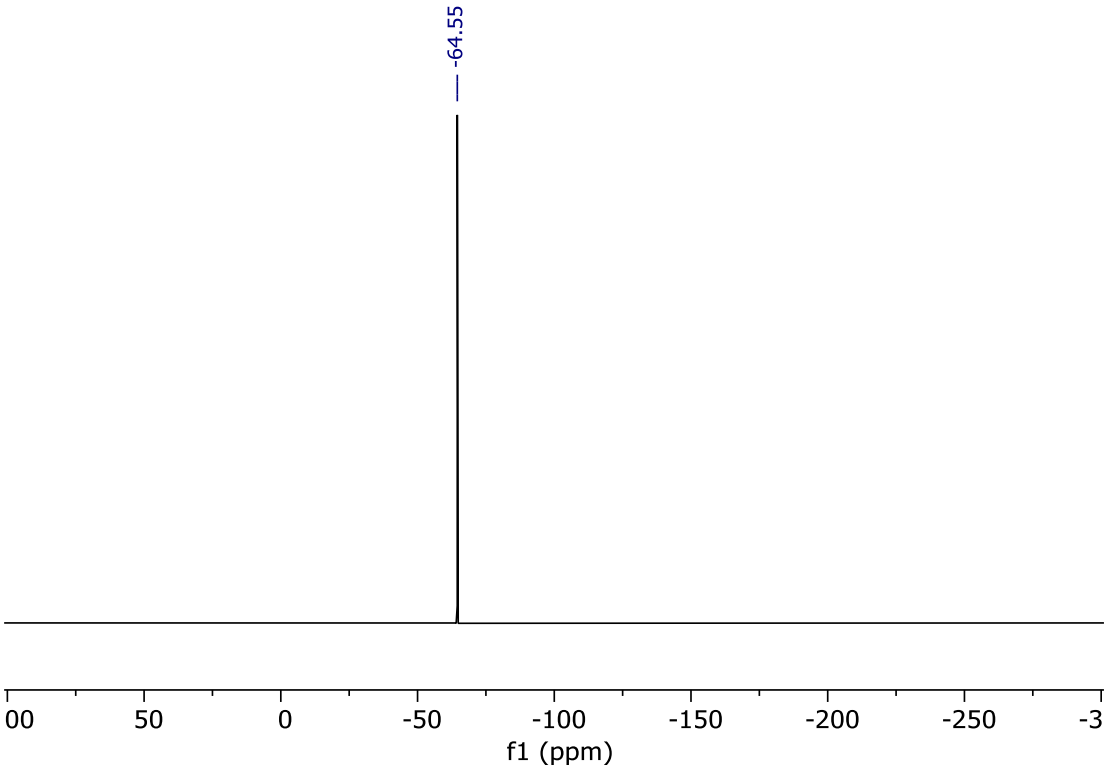


Figure 2.66 ^{19}F NMR spectra of **19k** in CD_3OD

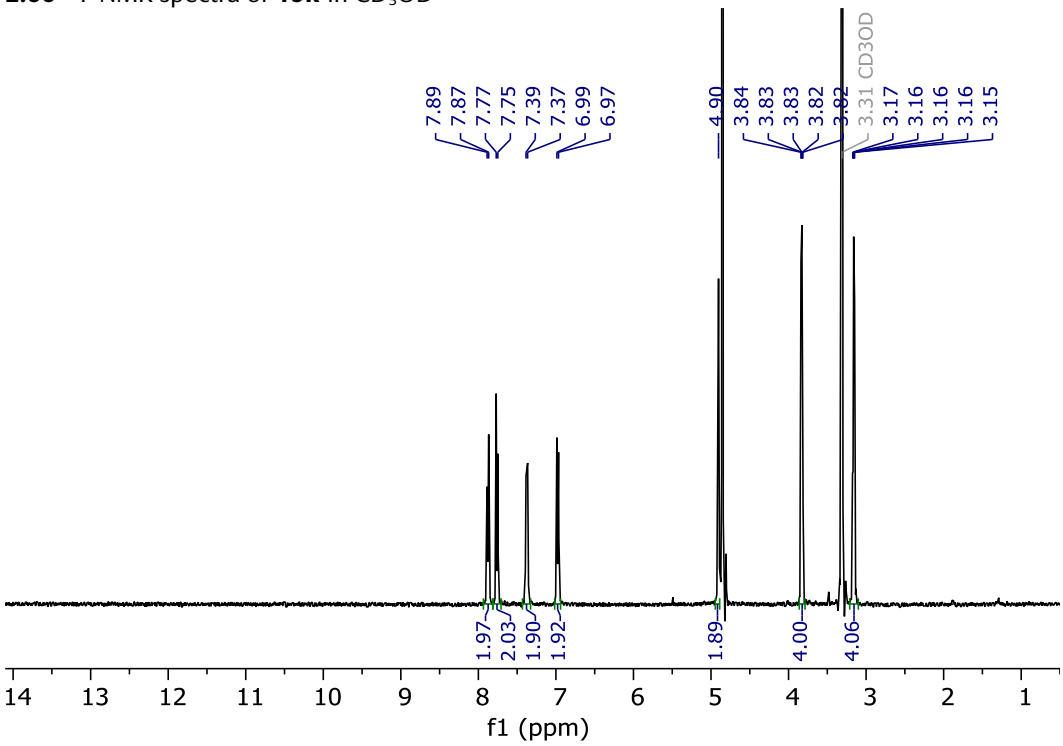


Figure 2.67 ^{1}H NMR spectra of **19l** in CD_3OD

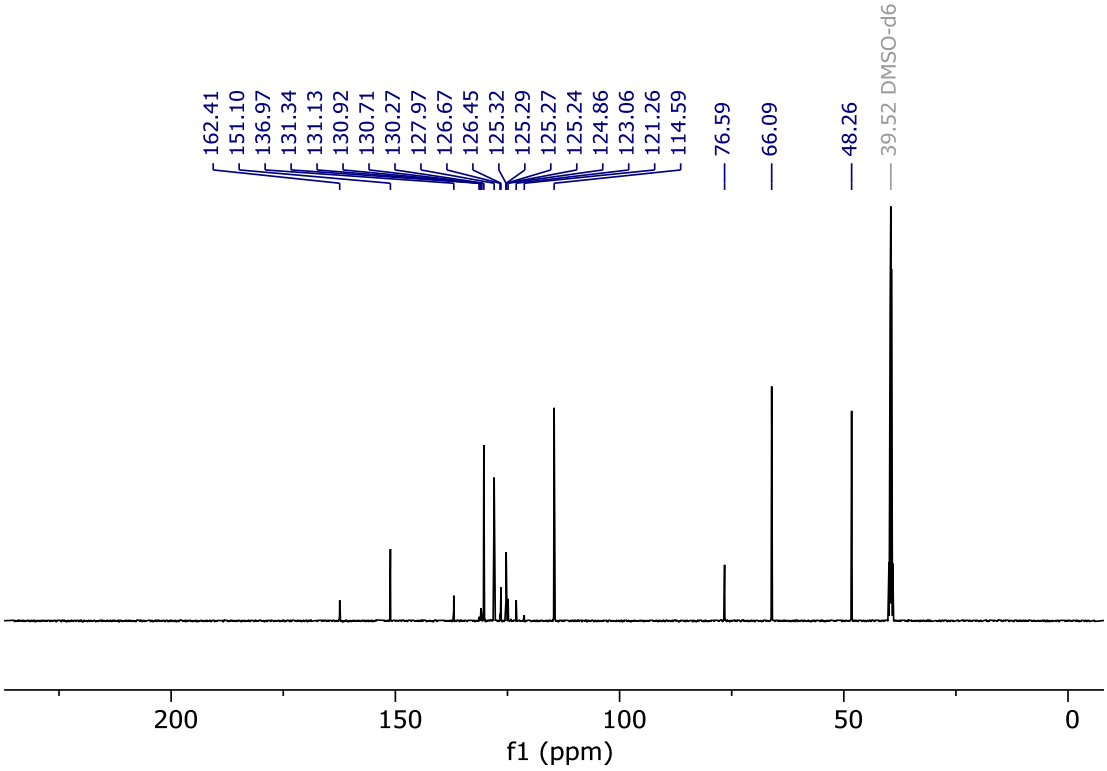


Figure 2.68 ^{13}C NMR spectra of **19l** in DMSO-*d6*

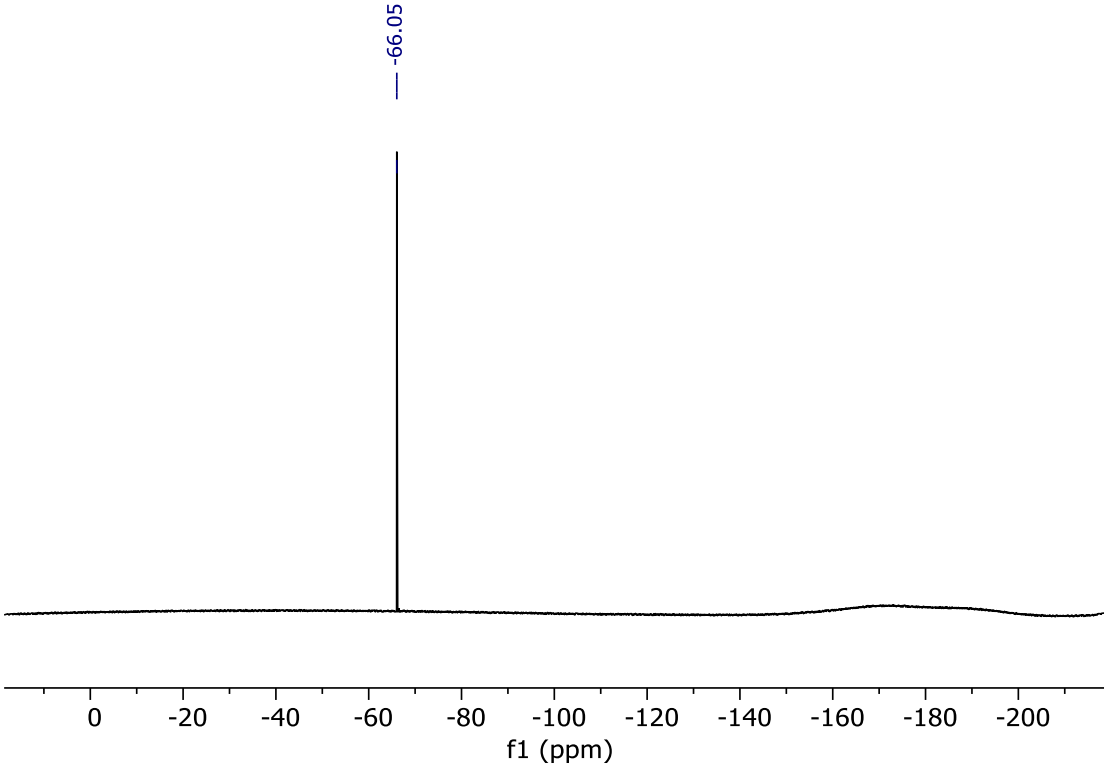


Figure 2.69 ^{19}F NMR spectra of **19l** in CD_3OD

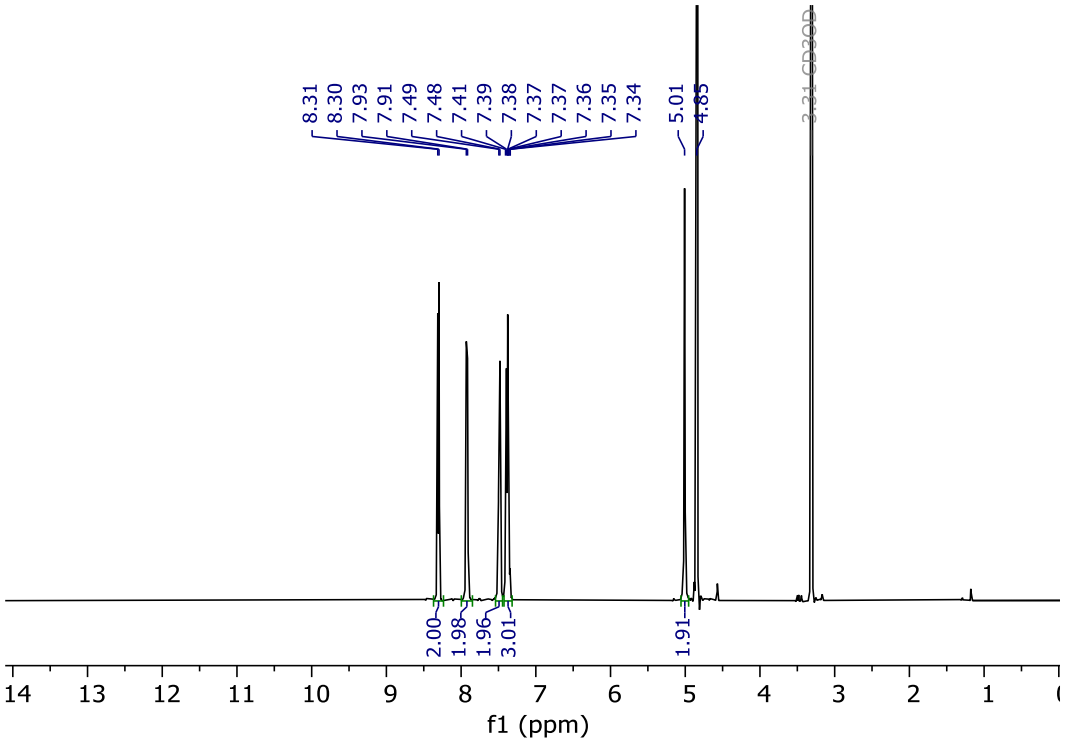


Figure 2.70 ^{1}H NMR spectra of **19m** in CD_3OD

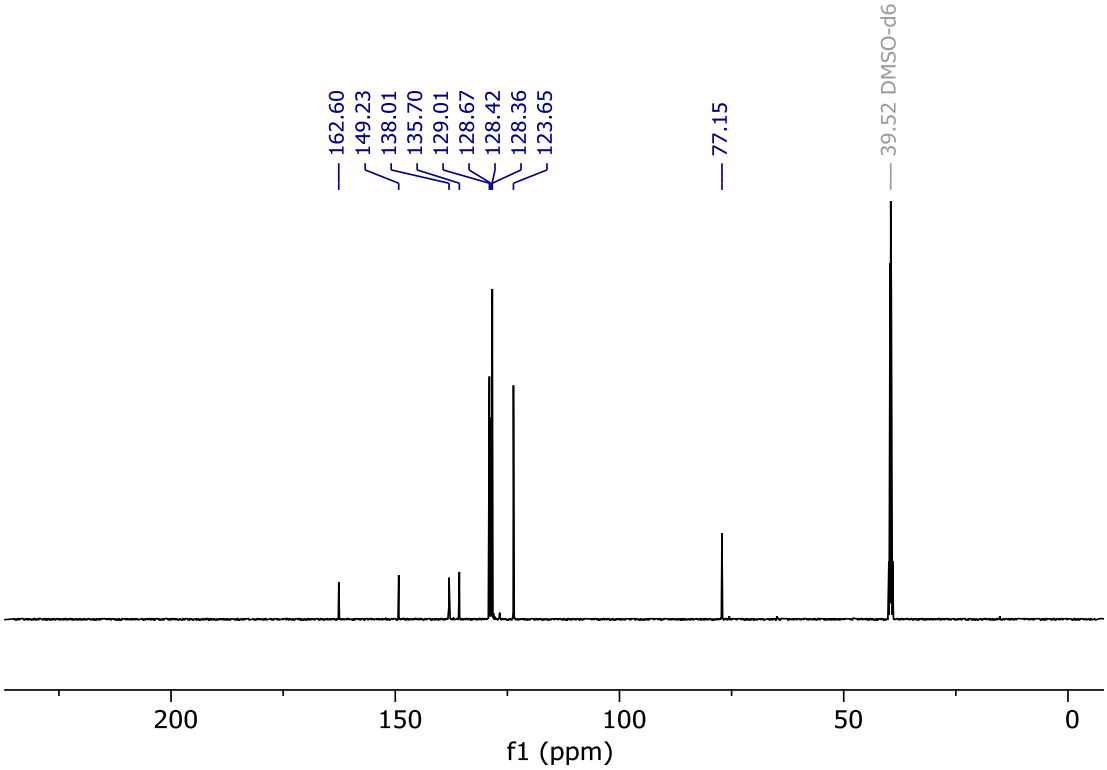


Figure 2.71 ^{13}C NMR spectra of **19m** in DMSO-*d6*

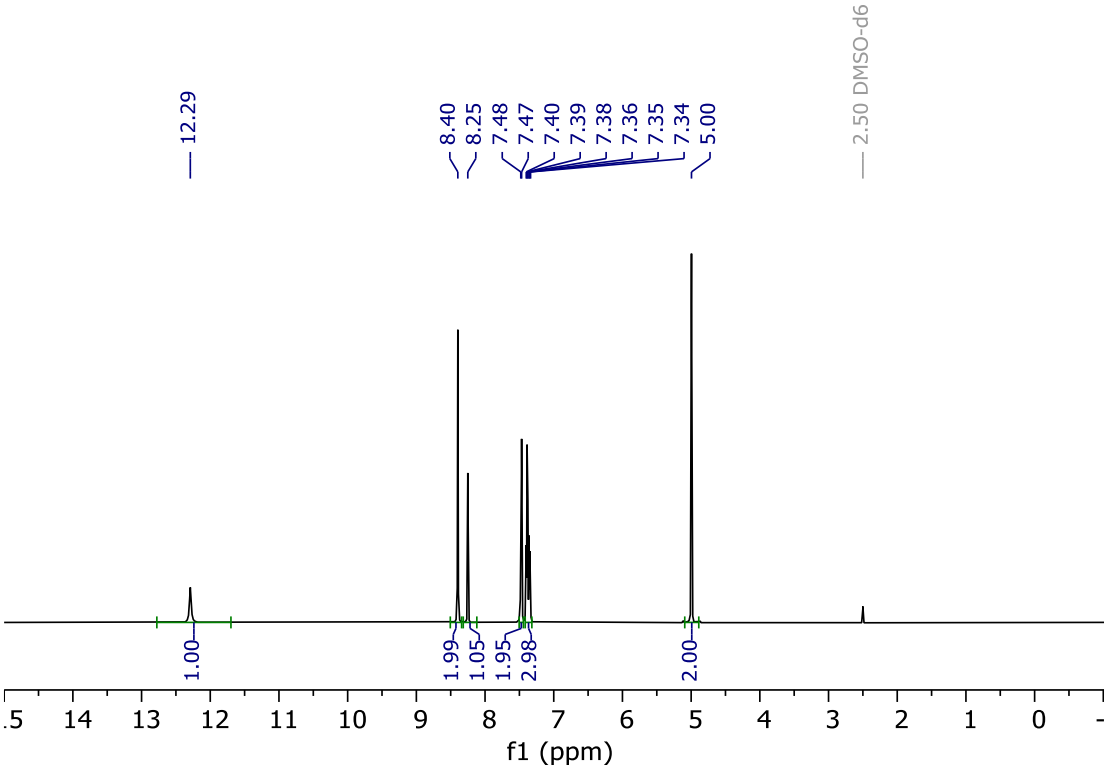


Figure 2.72 ^{1}H NMR spectra of **19n** in DMSO-*d6*

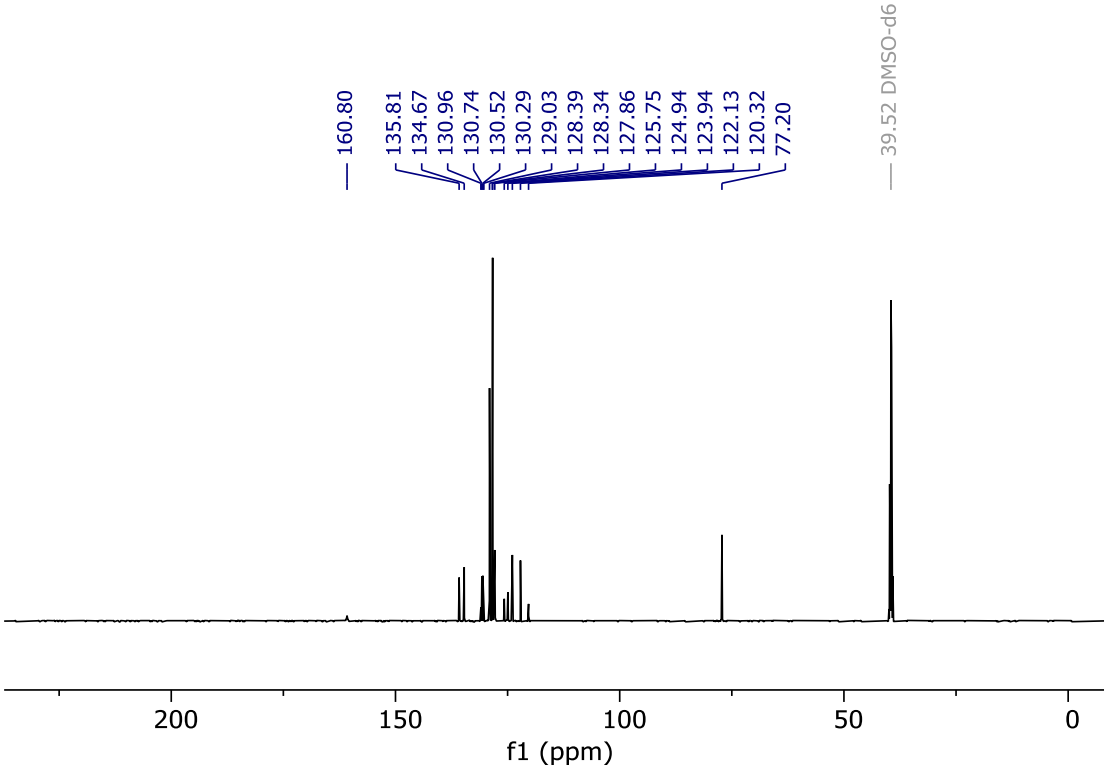


Figure 2.73 ^{13}C NMR spectra of **19n** in DMSO-*d6*

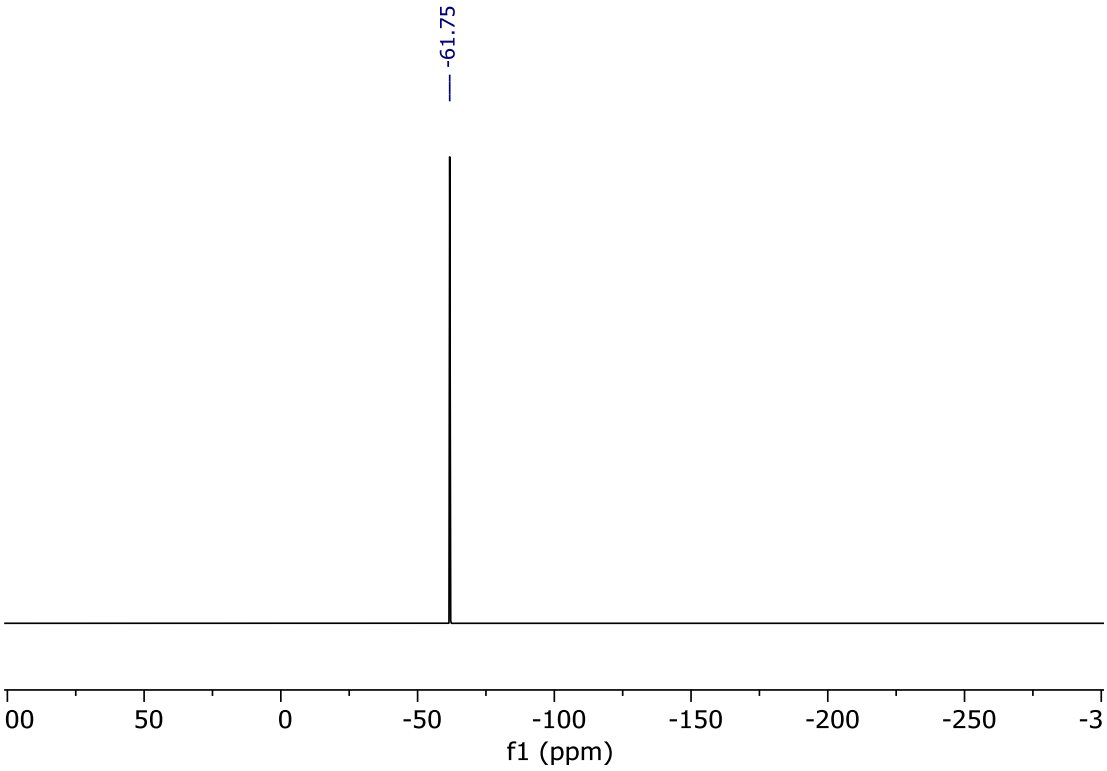


Figure 2.74 ^{19}F NMR spectra of **19n** in DMSO-*d6*

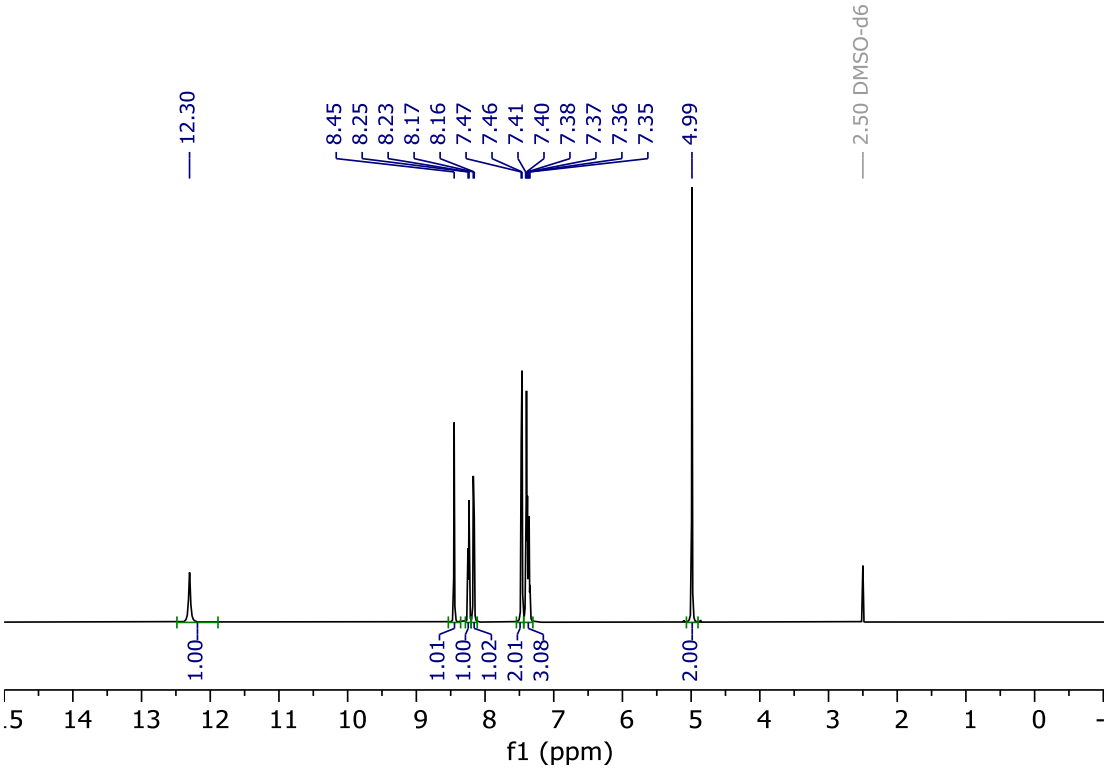


Figure 2.75 ^{1}H NMR spectra of **19o** in DMSO-*d6*

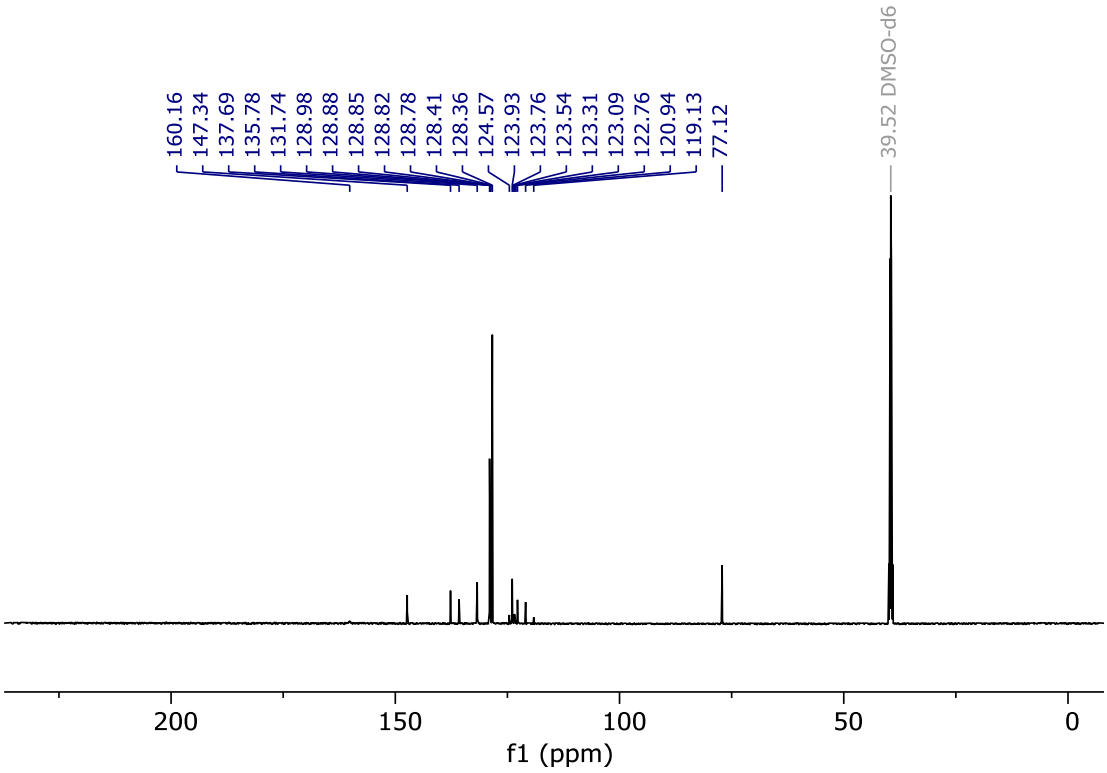


Figure 2.76 ^{13}C NMR spectra of **19o** in DMSO-*d6*

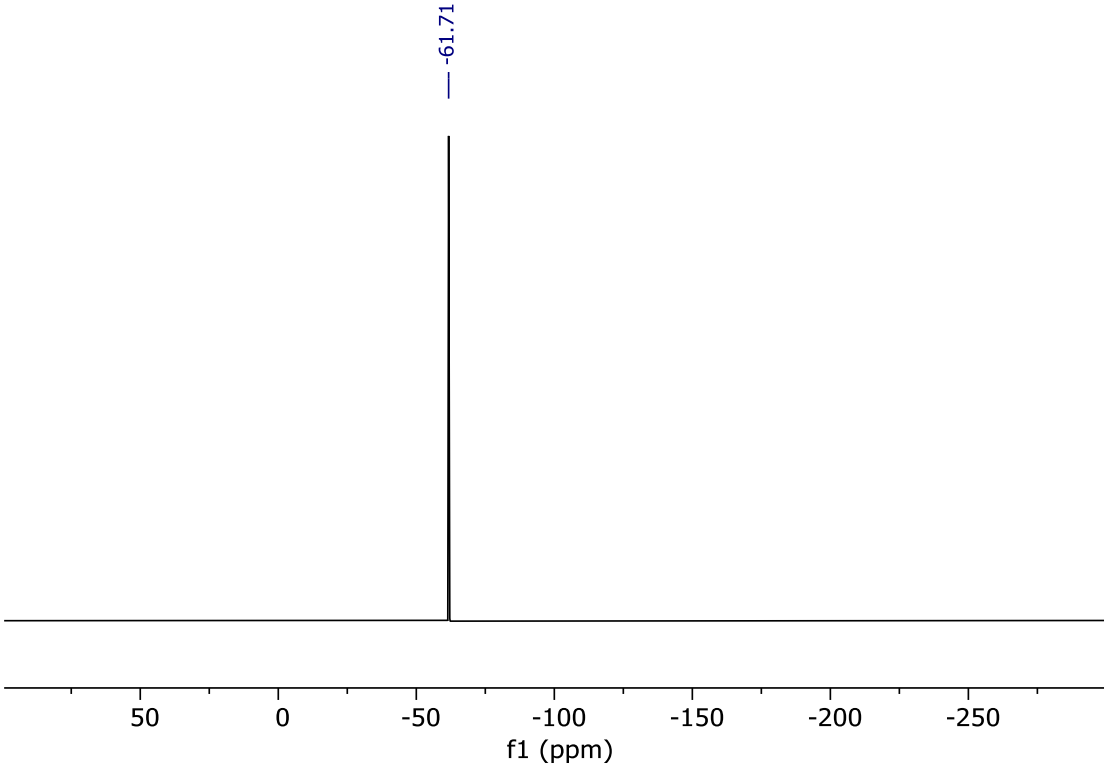


Figure 2.77 ^{19}F NMR spectra of **19o** in CD_3OD

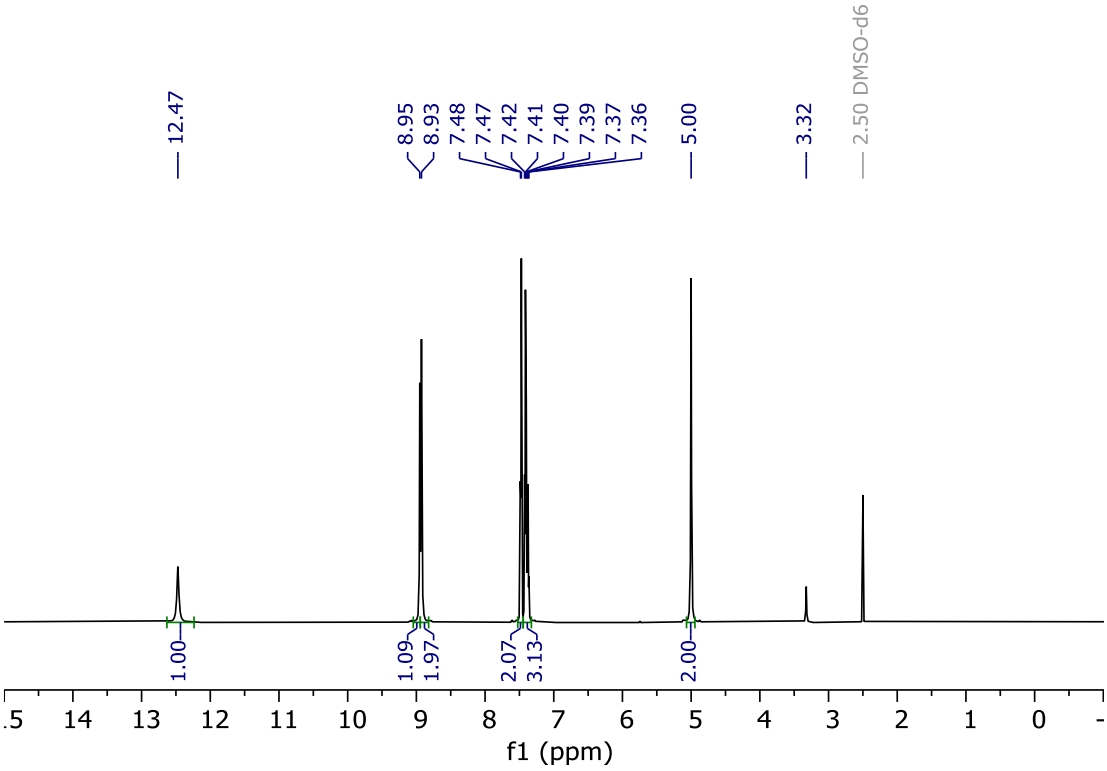


Figure 2.78 ^{1}H NMR spectra of **19p** in DMSO-*d6*

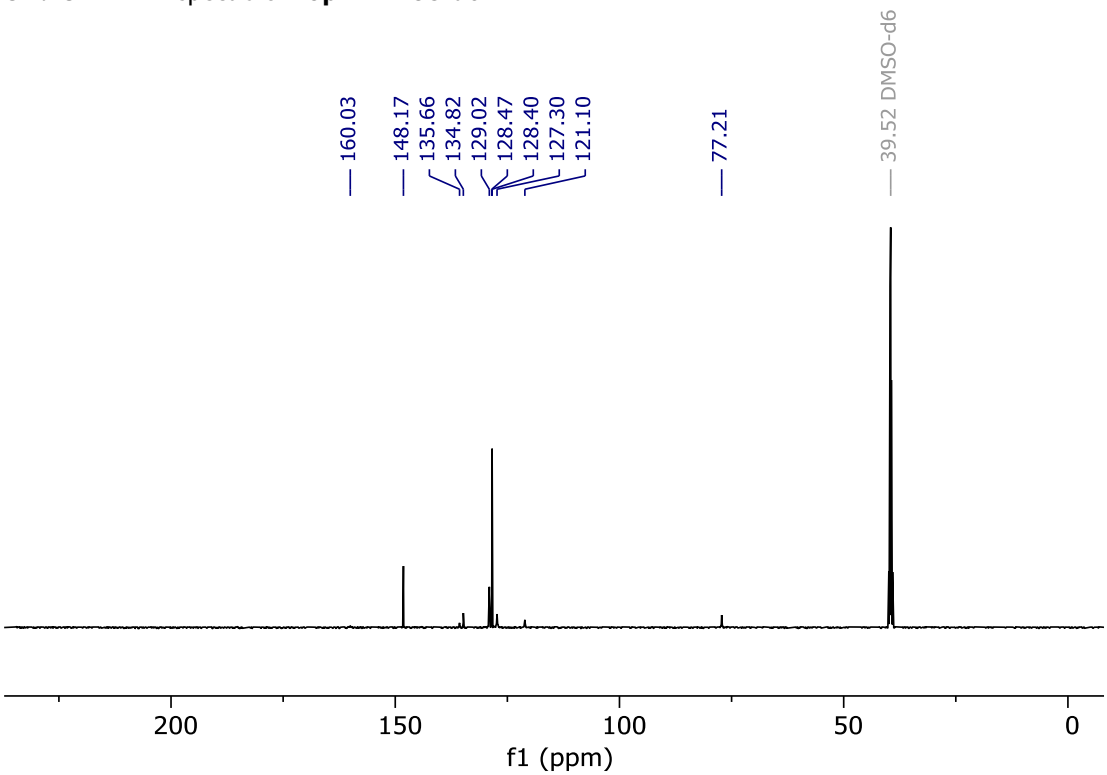


Figure 2.79 ^{13}C NMR spectra of **19p** in DMSO-*d6*

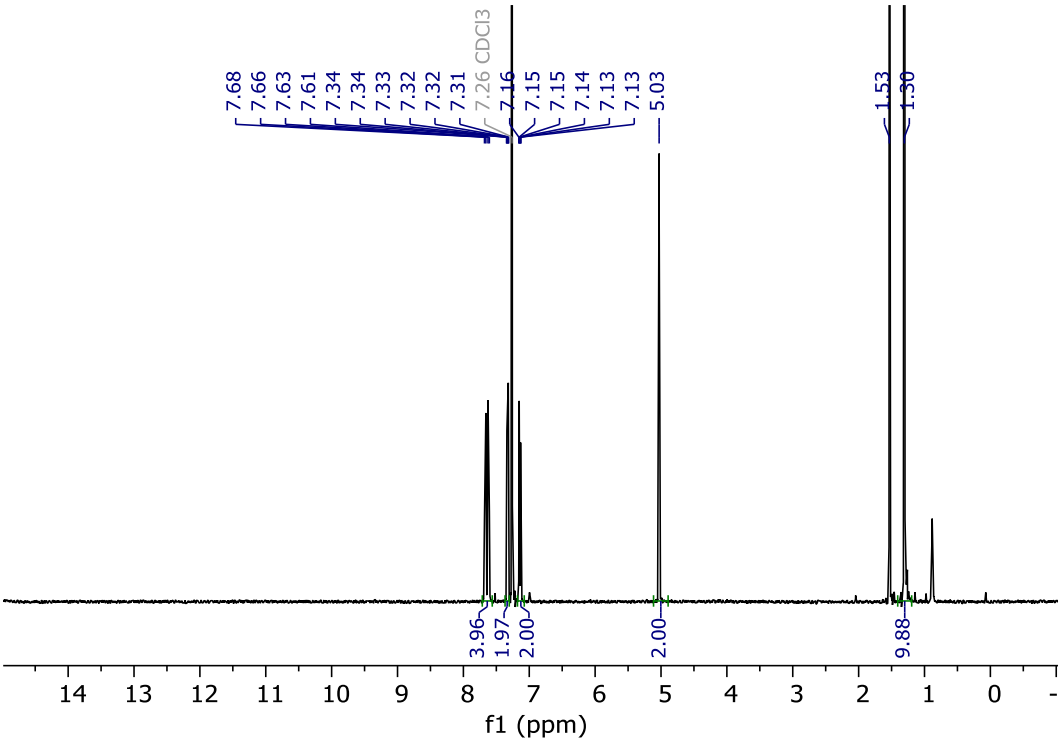


Figure 2.80 ^{1}H NMR spectra of **20d** in $CDCl_3$

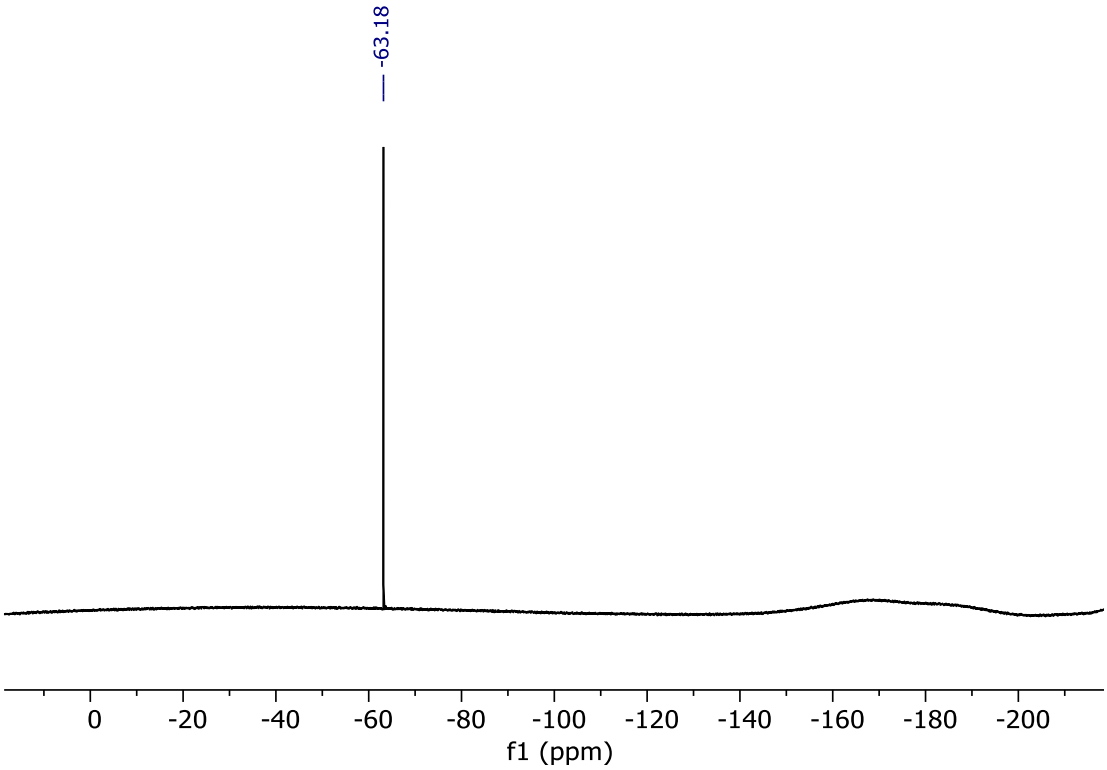


Figure 2.81 ^{19}F NMR spectra of **20d** in $CDCl_3$

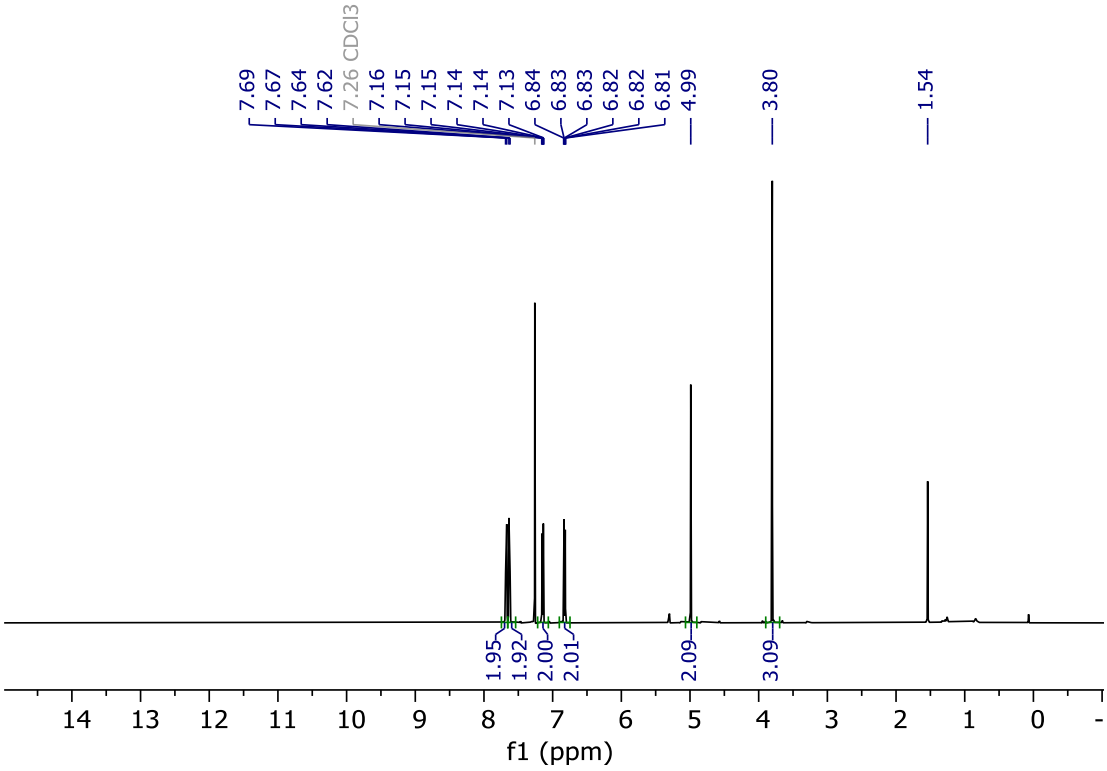


Figure 2.82 ^{1}H NMR spectra of **20e** in $CDCl_3$

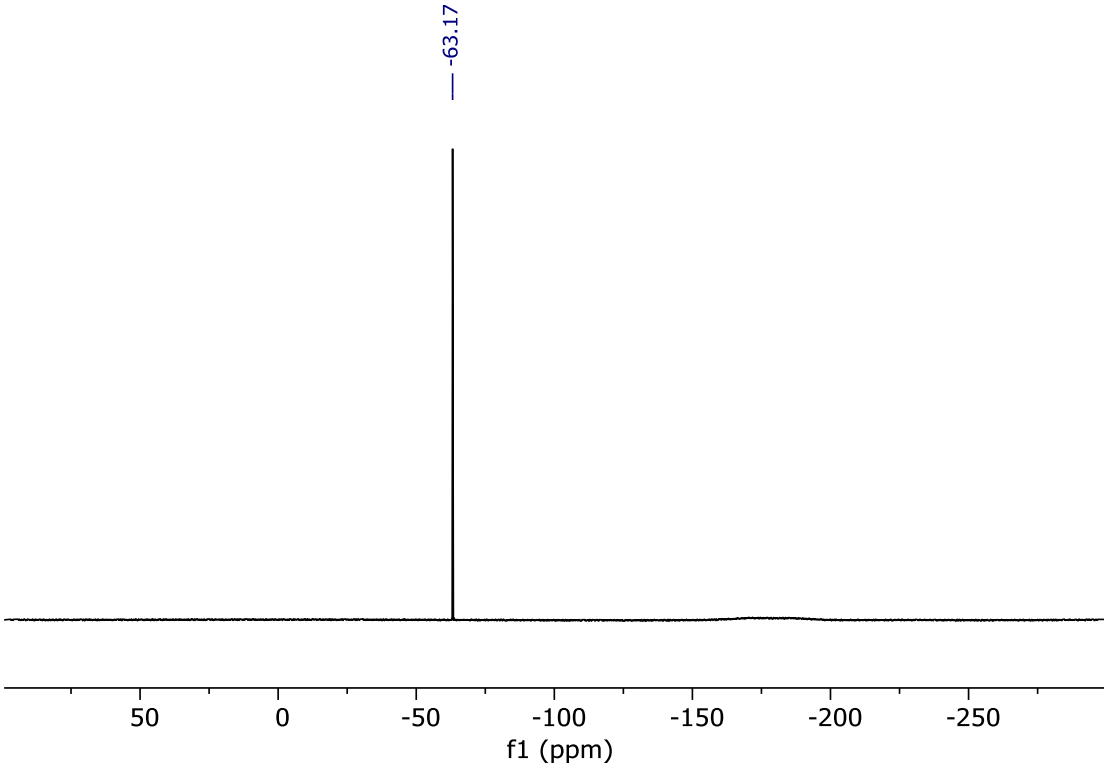


Figure 2.83 ^{19}F NMR spectra of **20e** in $CDCl_3$

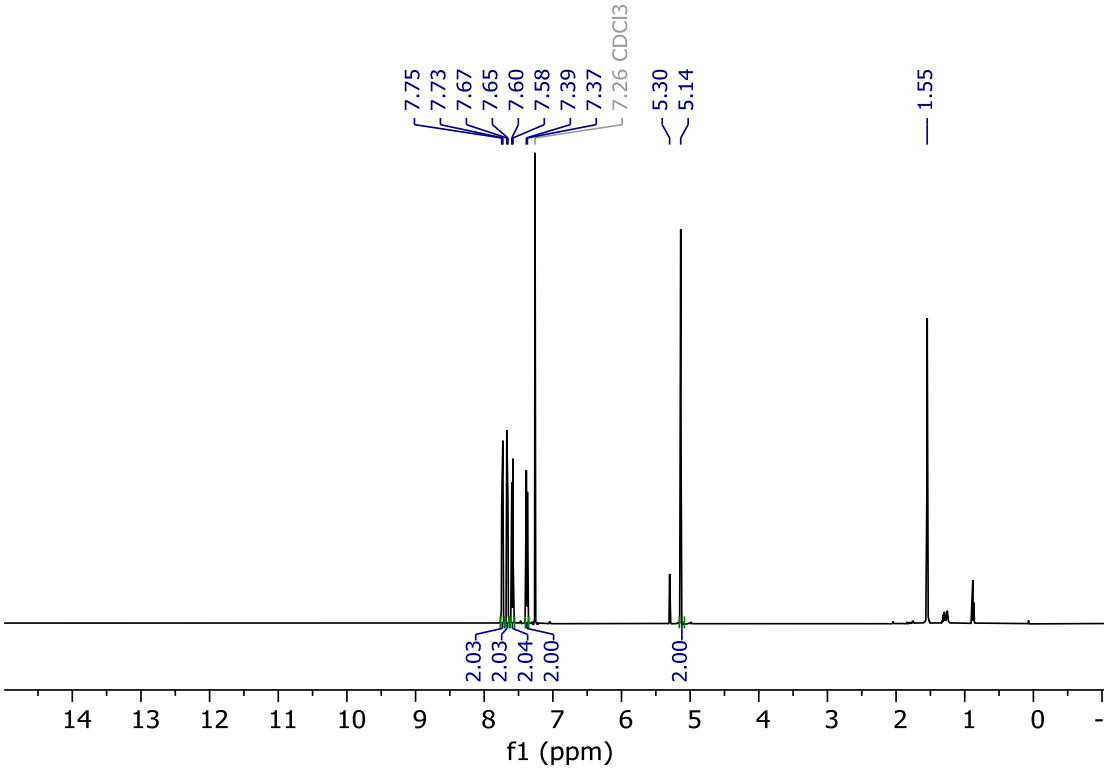


Figure 2.84 ^{1}H NMR spectra of **20f** in $CDCl_3$

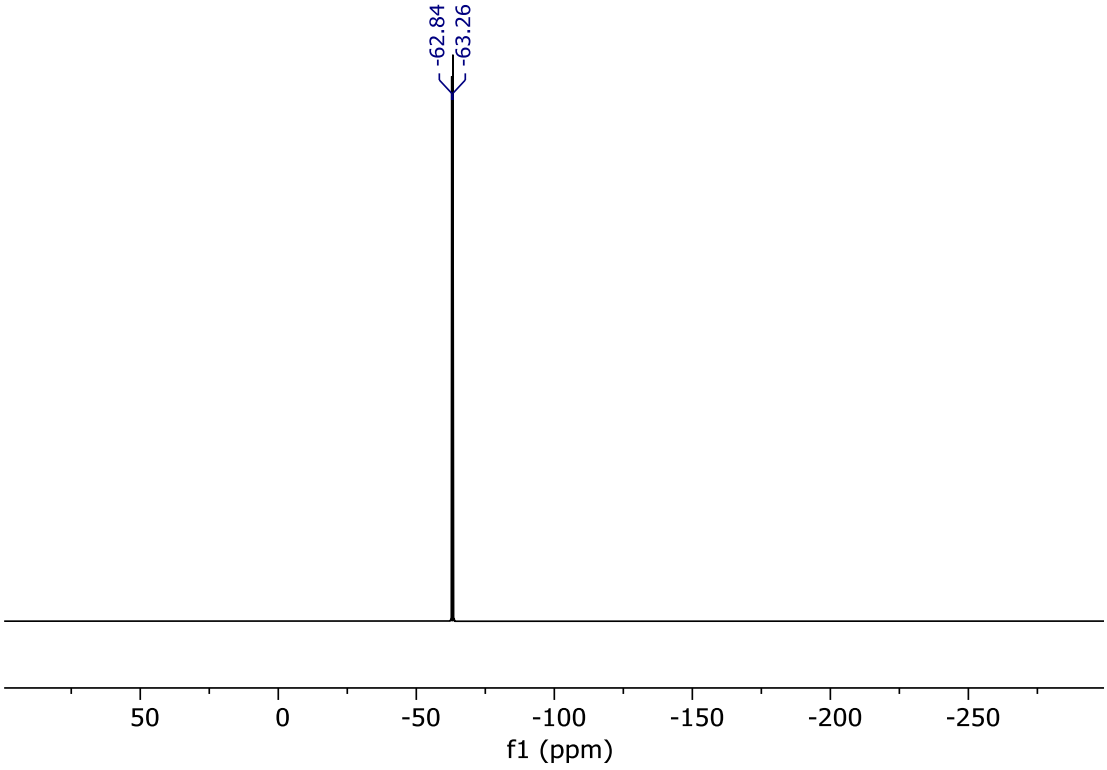


Figure 2.85 ^{19}F NMR spectra of **20f** in $CDCl_3$

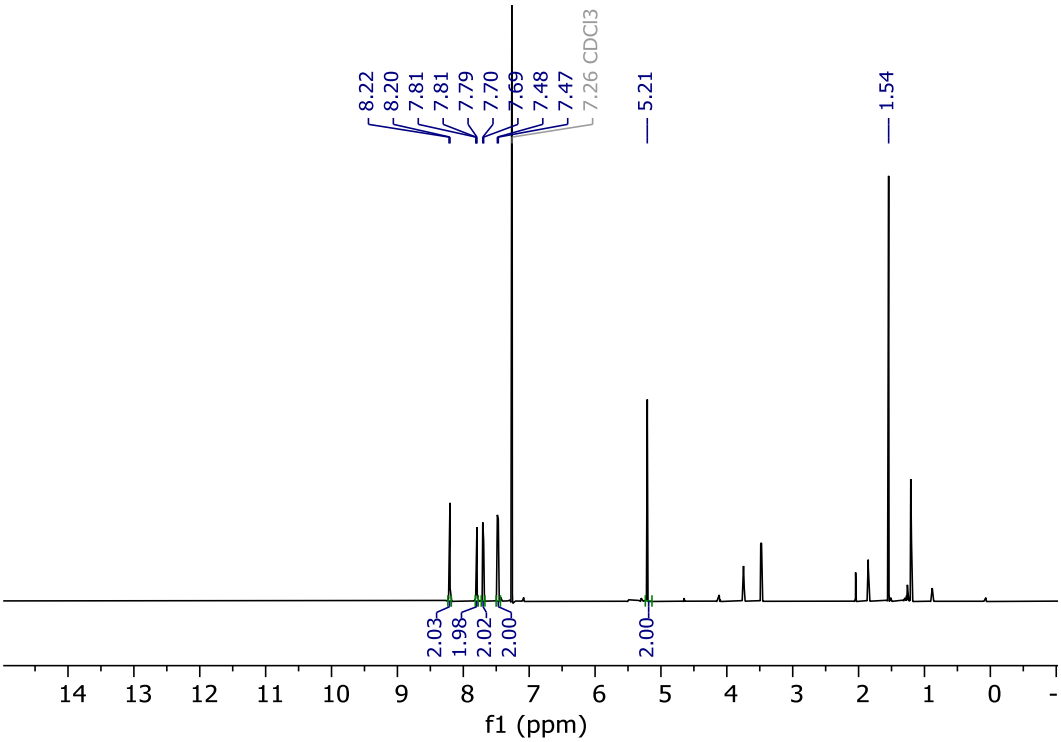


Figure 2.86 ^{1}H NMR spectra of **20g** in $CDCl_3$

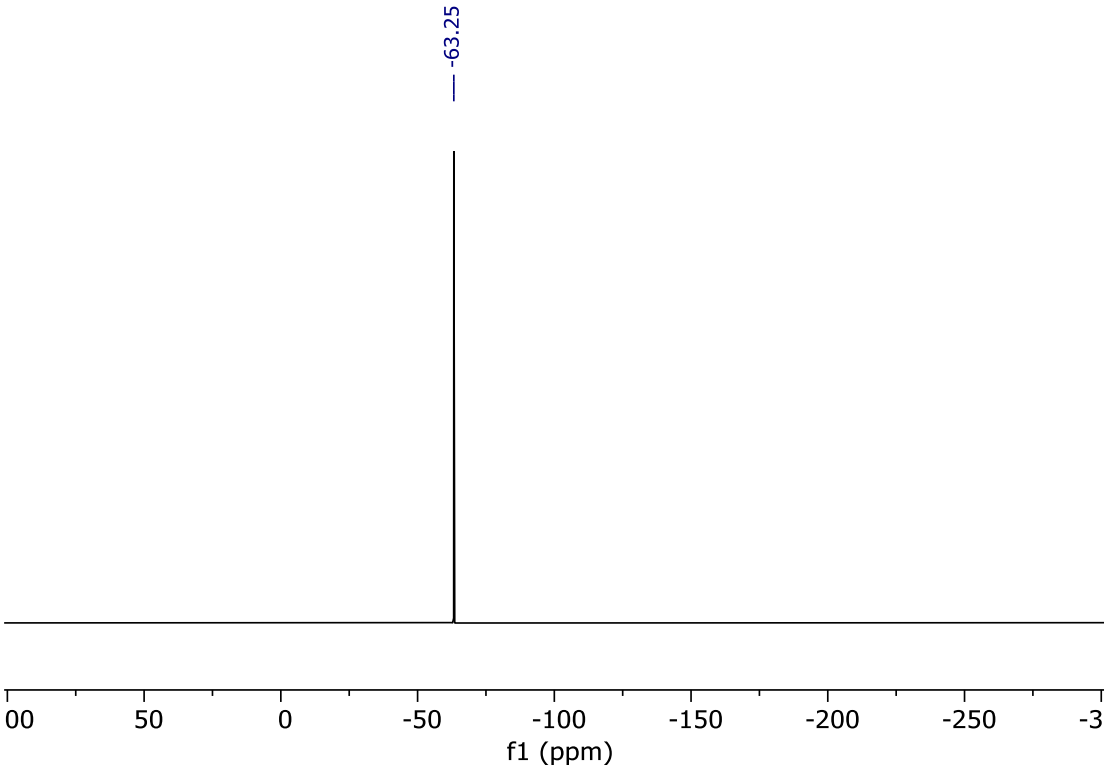


Figure 2.87 ^{19}F NMR spectra of **20g** in $CDCl_3$

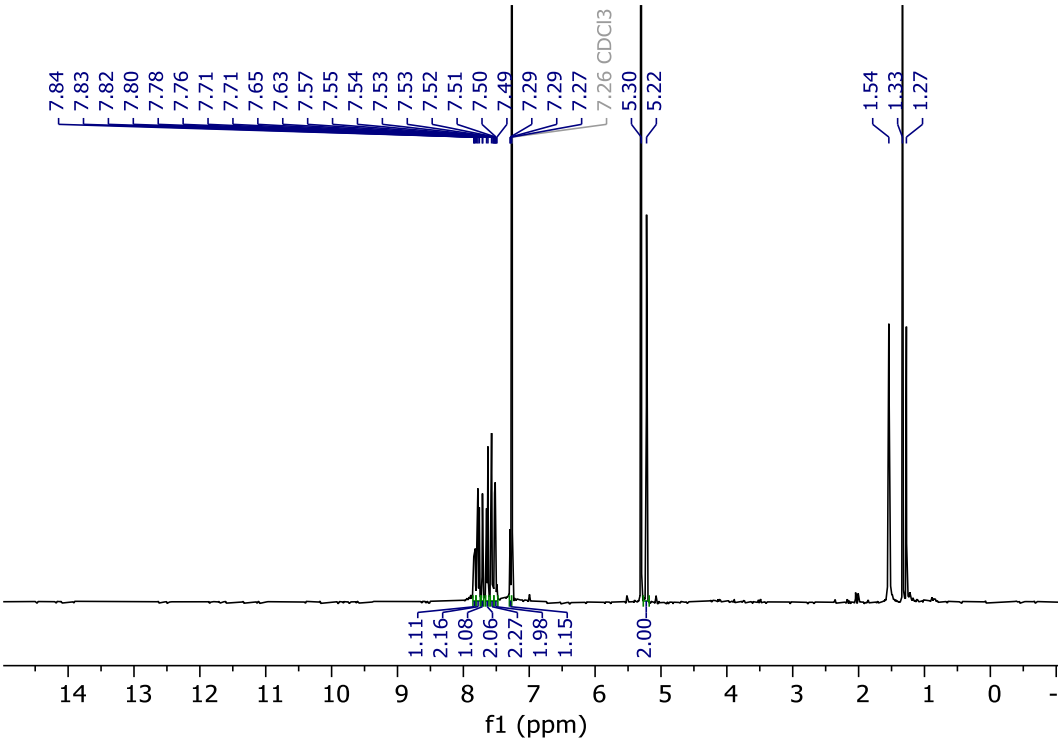


Figure 2.88 ^{1}H NMR spectra of **20h** in $CDCl_3$

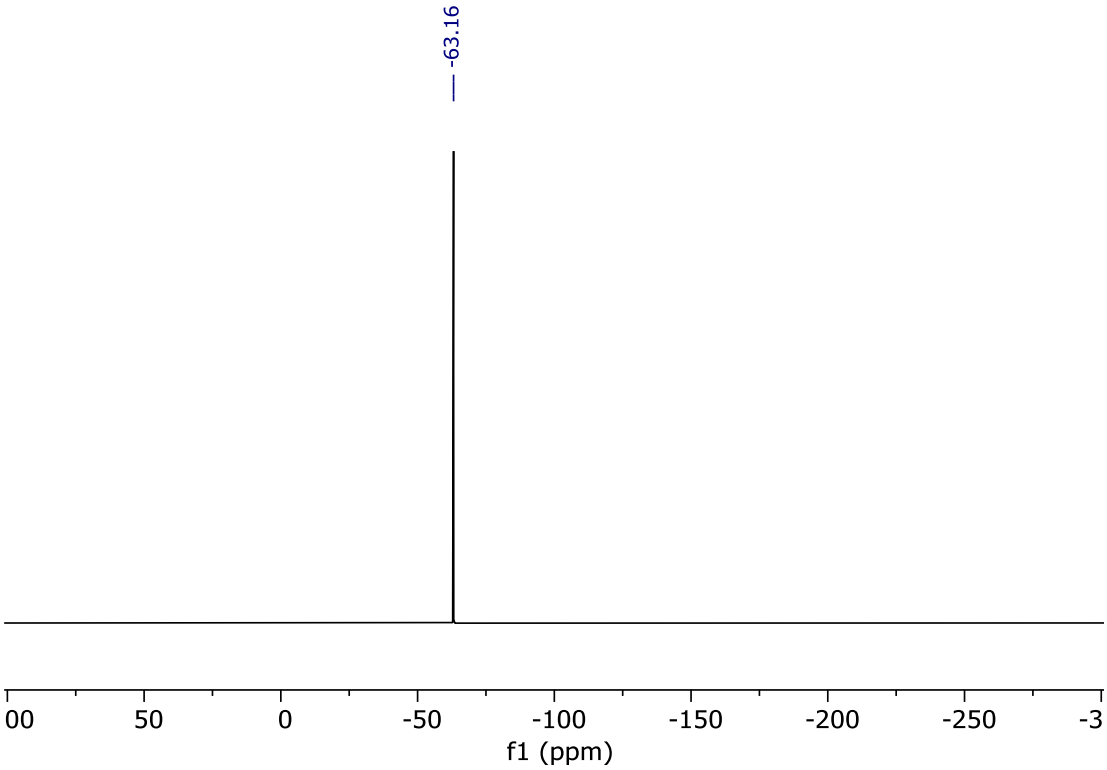


Figure 2.89 ^{19}F NMR spectra of **20h** in $CDCl_3$

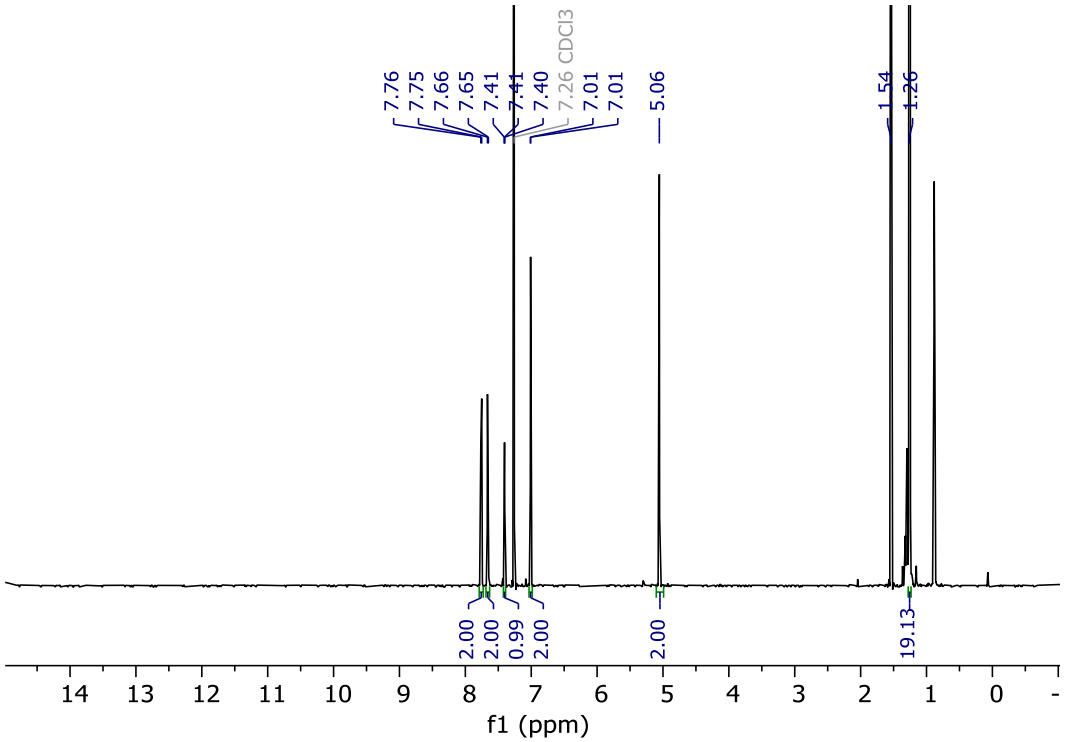


Figure 2.90 ^{1}H NMR spectra of **20i** in $CDCl_3$

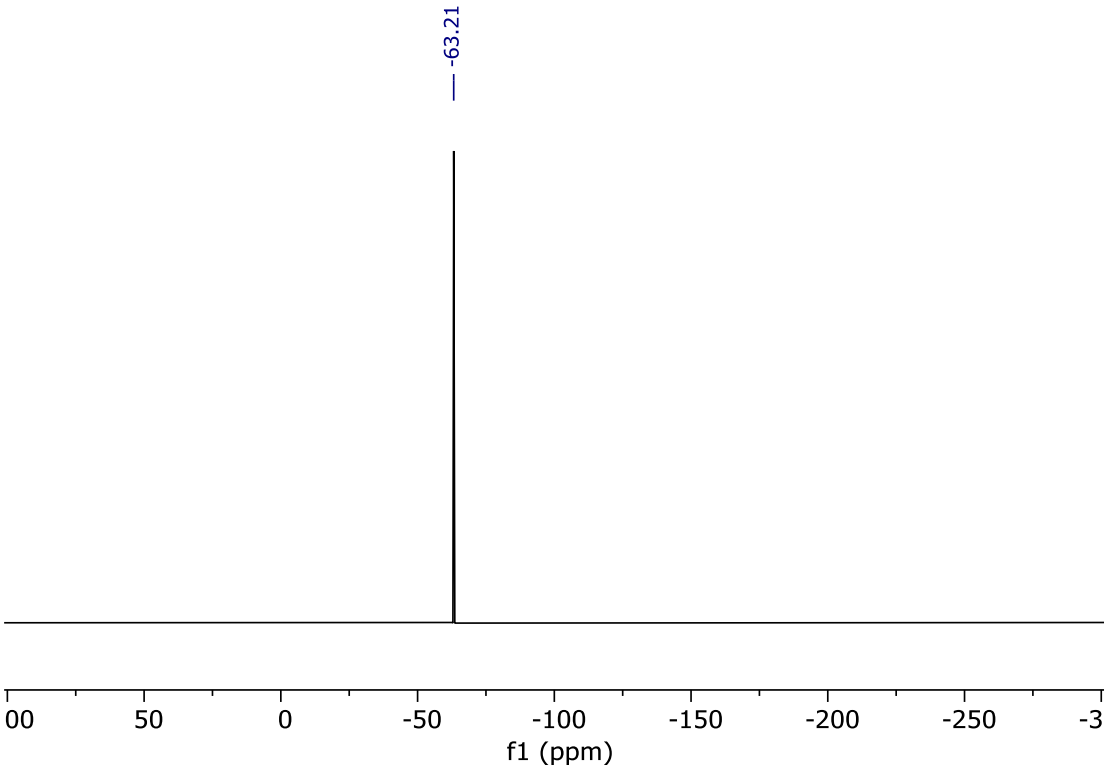


Figure 2.91 ^{19}F NMR spectra of **20i** in $CDCl_3$

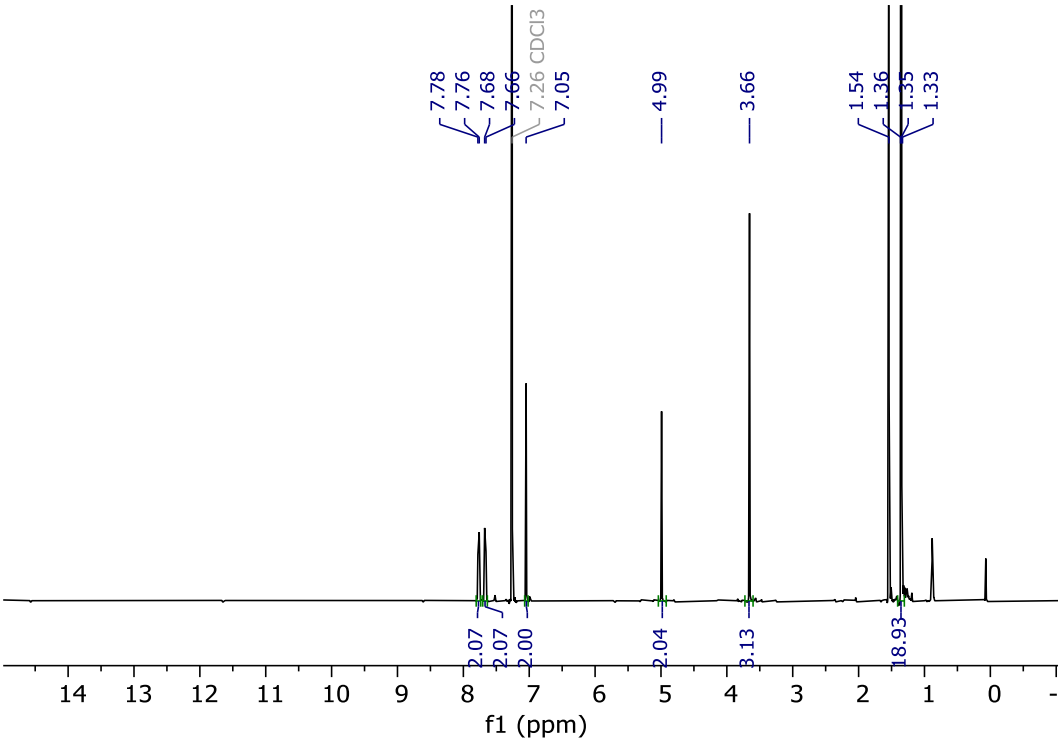


Figure 2.92 ^{1}H NMR spectra of **20j** in $CDCl_3$

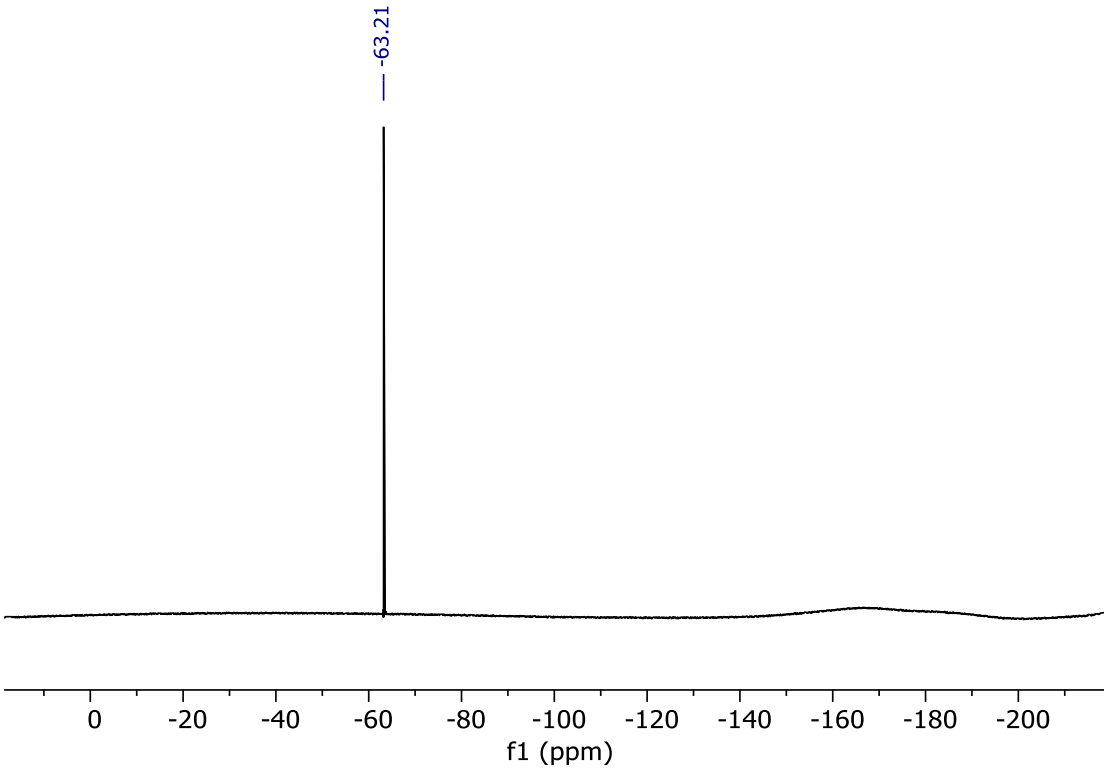


Figure 2.93 ^{19}F NMR spectra of **20j** in $CDCl_3$

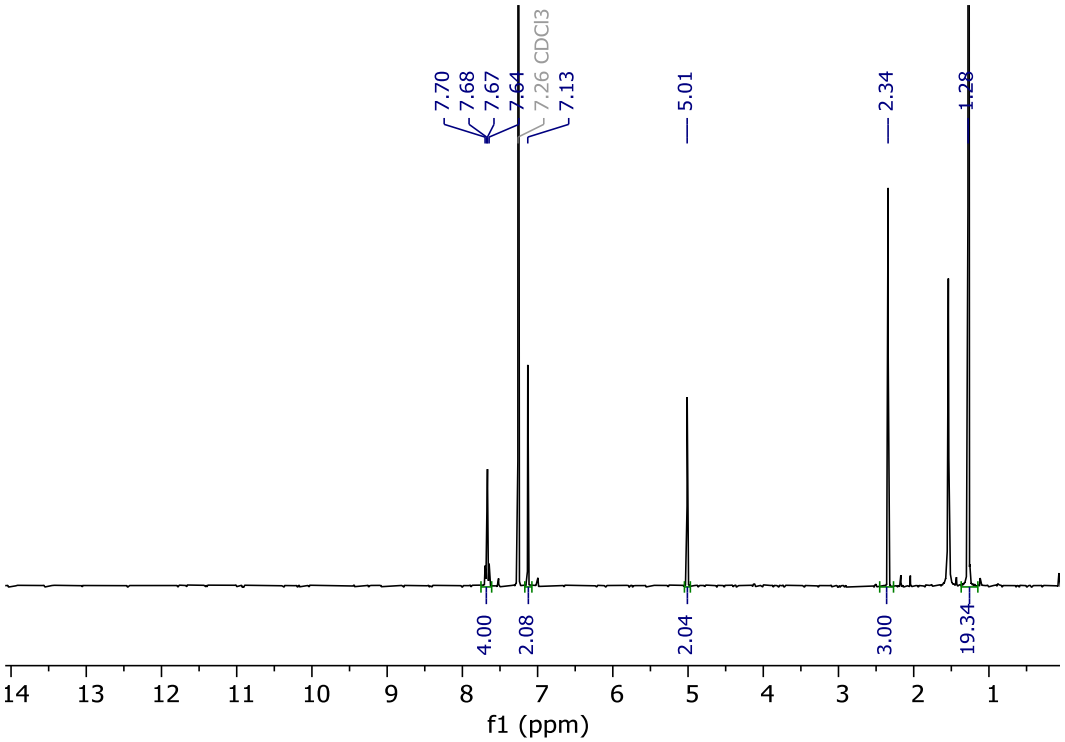


Figure 2.94 ^{1}H NMR spectra of **20k** in $CDCl_3$

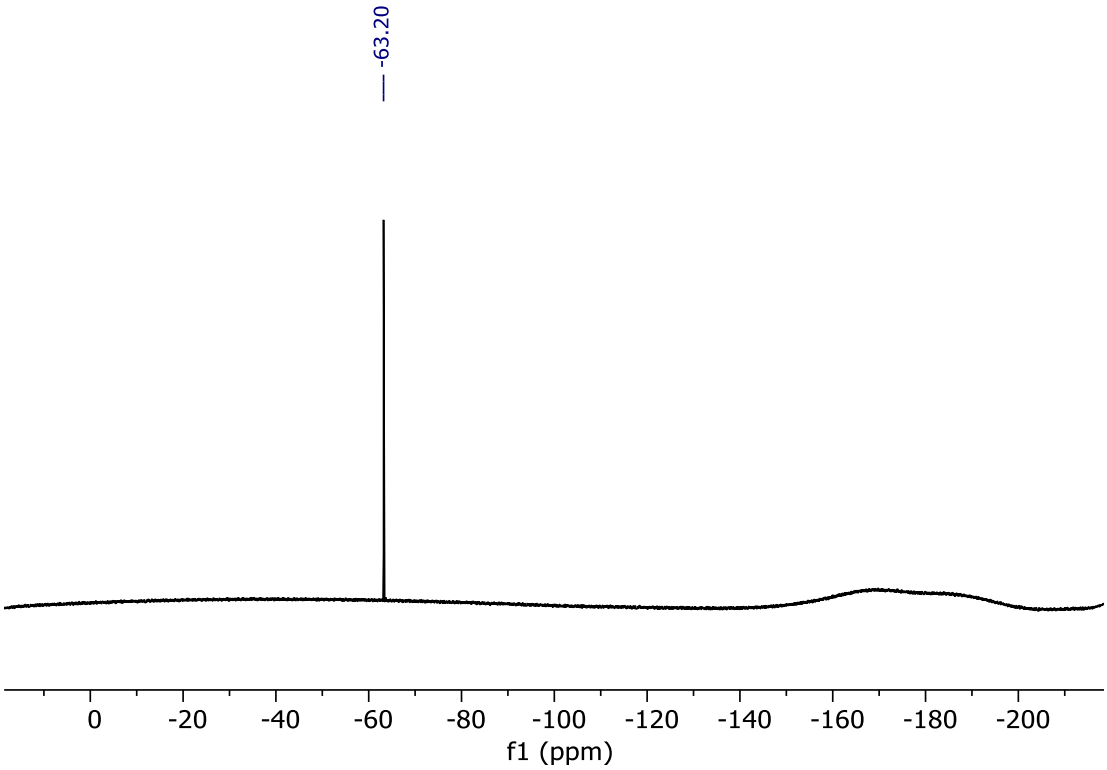


Figure 2.95 ^{19}F NMR spectra of **20k** in $CDCl_3$

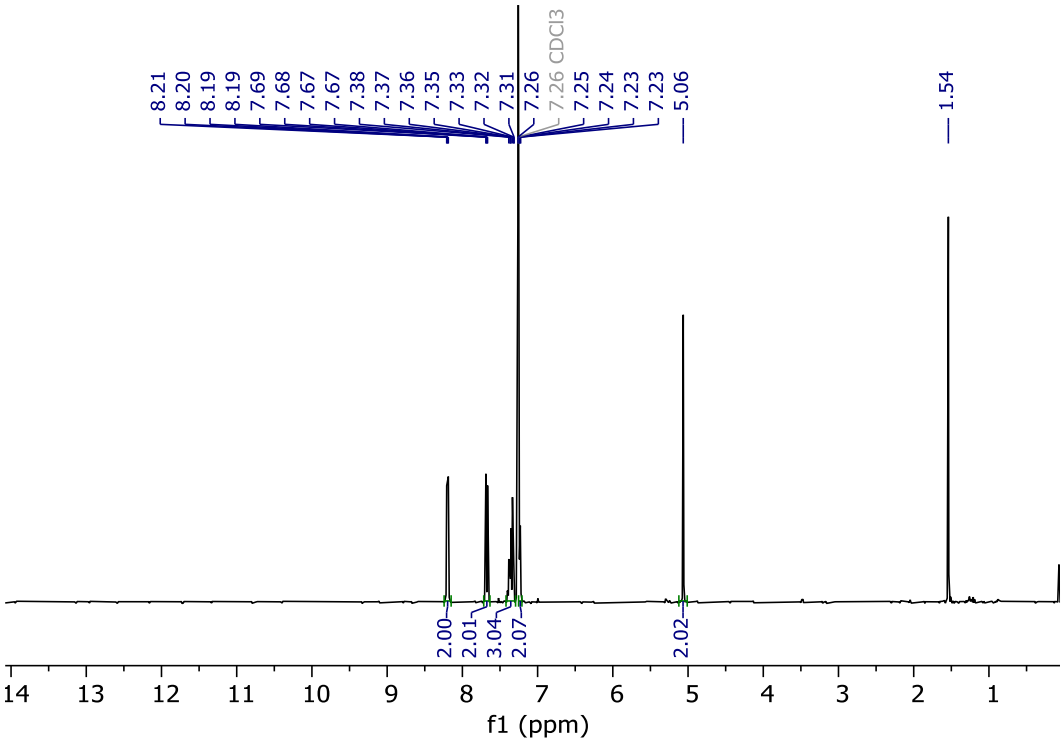


Figure 2.96 ^{1}H NMR spectra of **20m** in $CDCl_3$

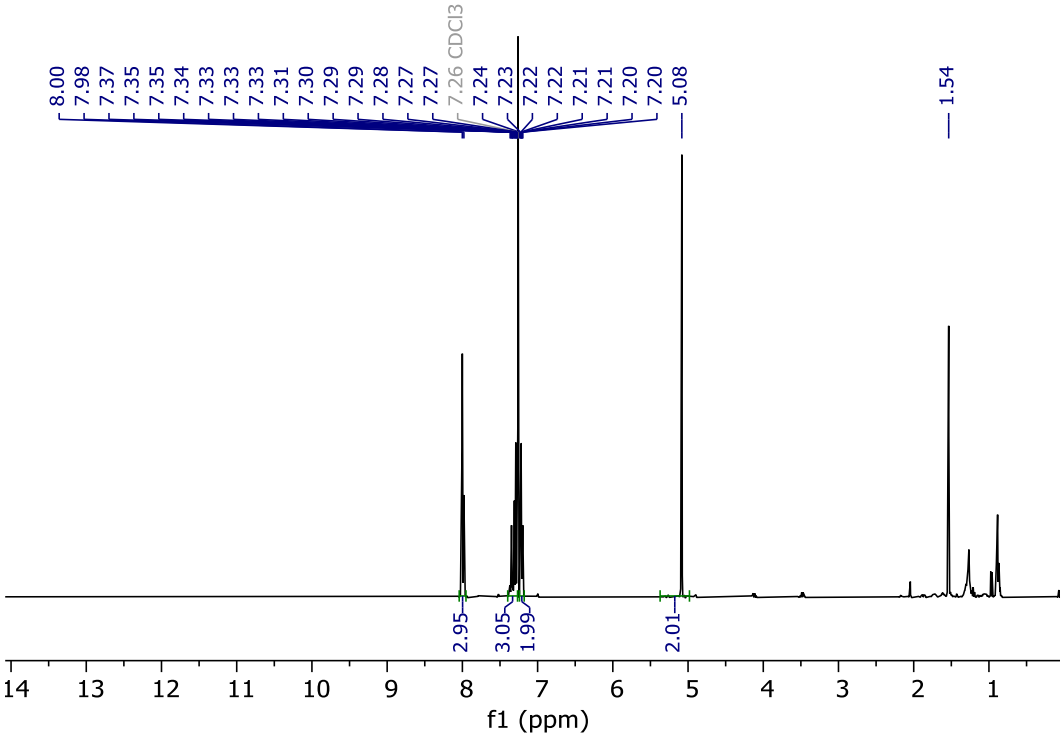


Figure 2.97 ^{1}H NMR spectra of **20n** in $CDCl_3$

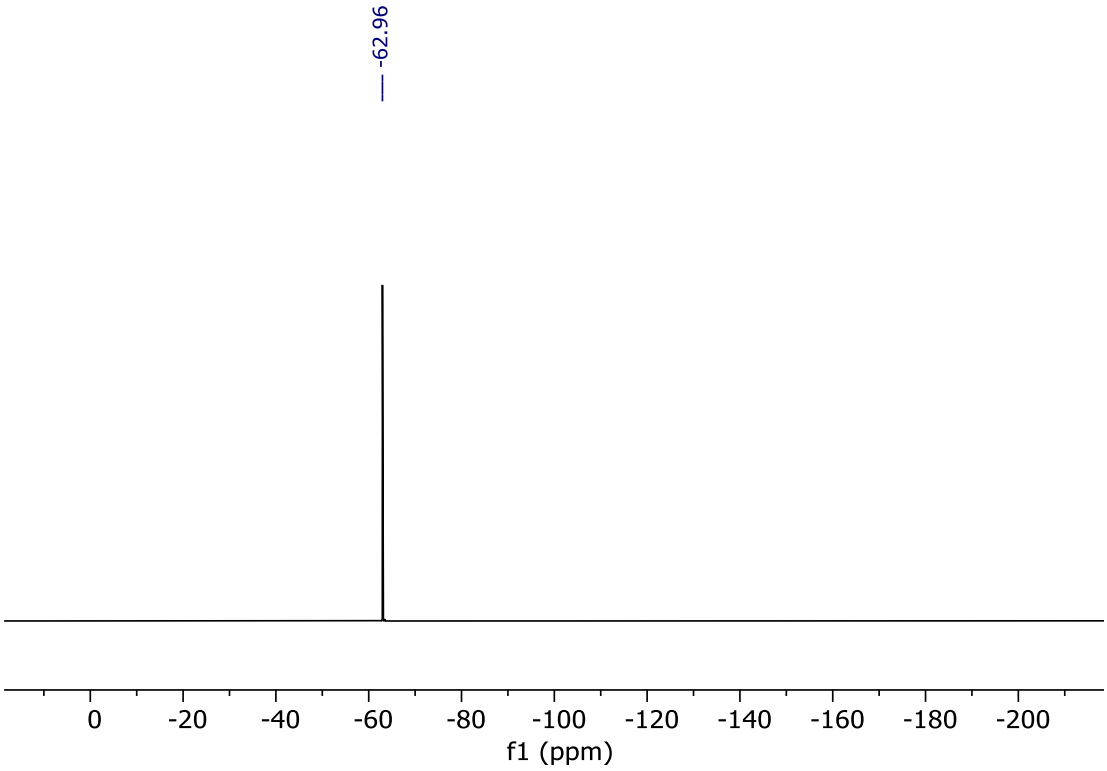


Figure 2.98 ^{19}F NMR spectra of **20n** in $CDCl_3$

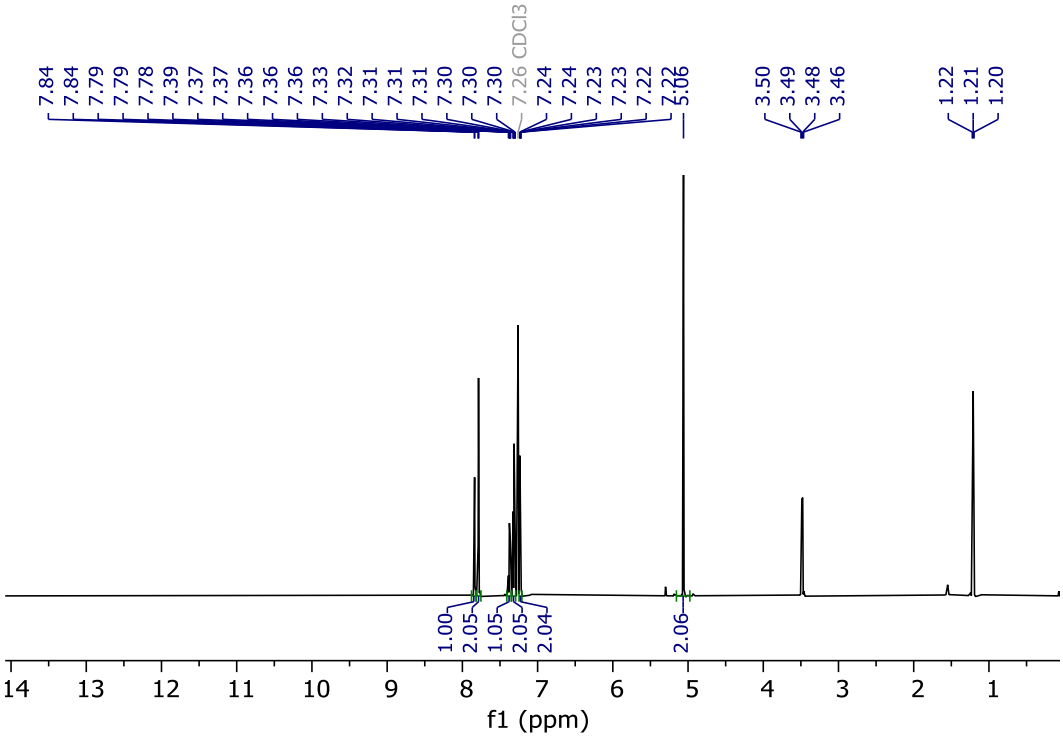


Figure 2.99 ^{1}H NMR spectra of **20o** in $CDCl_3$

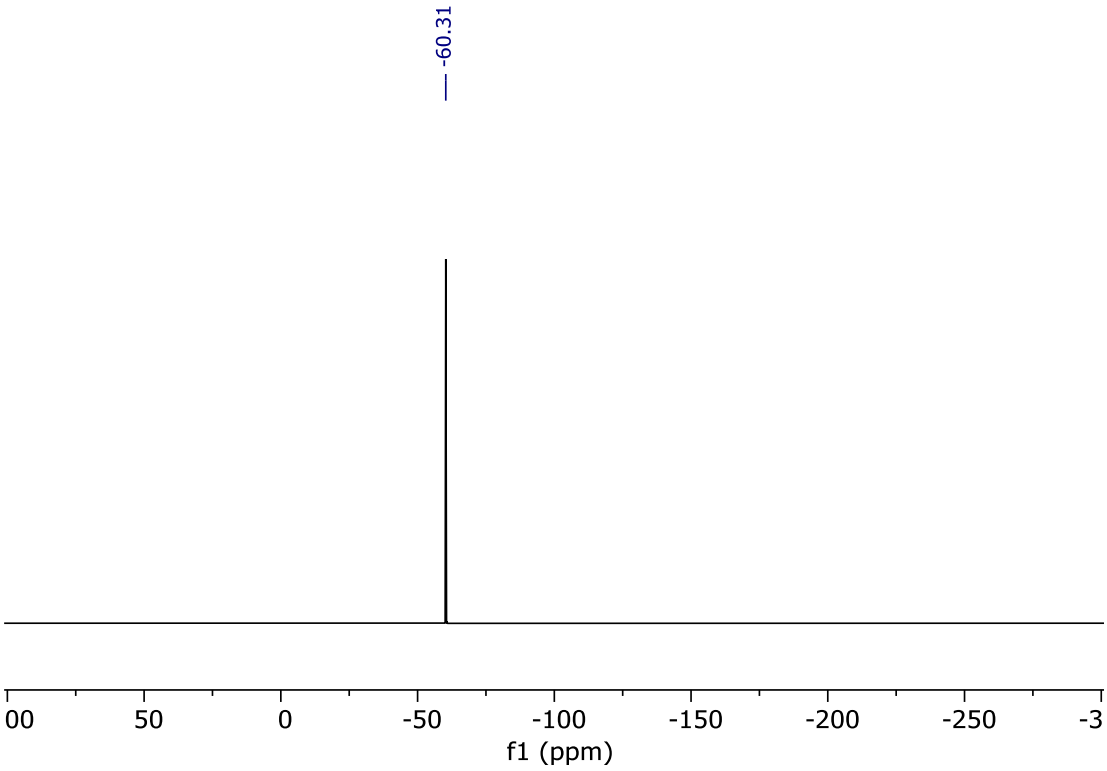


Figure 2.100 ^{19}F NMR spectra of **20o** in $CDCl_3$

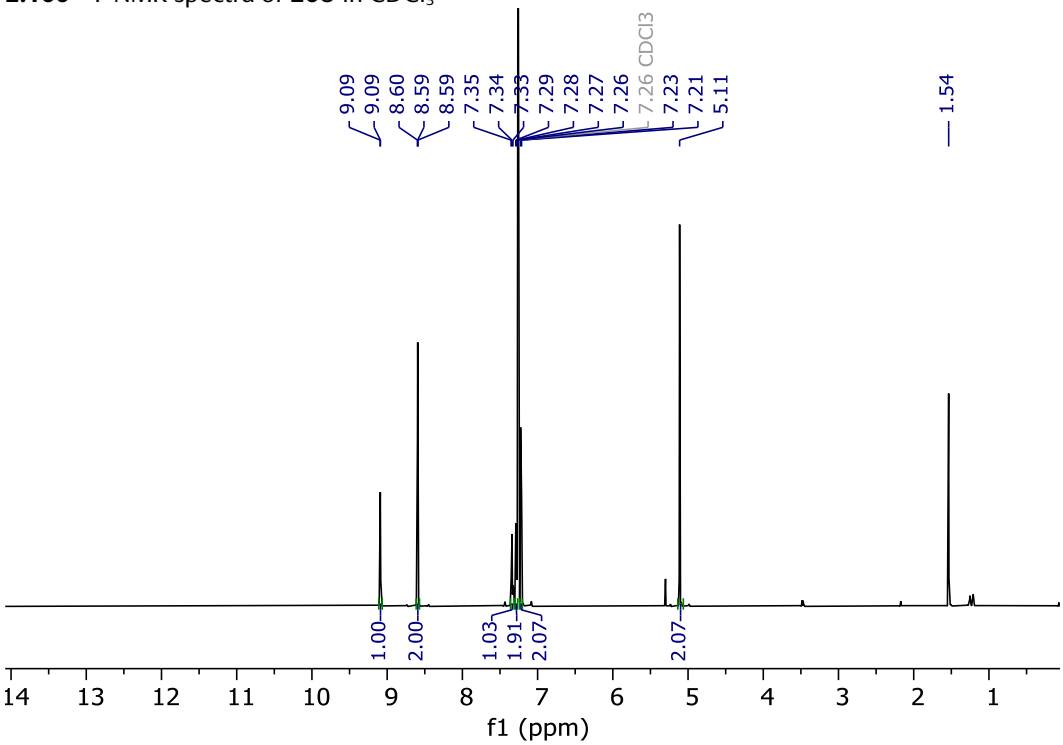


Figure 2.101 ^{1}H NMR spectra of **20p** in $CDCl_3$

2.6 Cartesian Coordinates of Select Structures

Coordinates for all computed structures are available as supplemental files in xyzfiles.zip

Table 2.6 Example computed structure of an A conformer of **1k** (1)

O	2.384644	-1.263076	-1.875227
C	1.80177	-1.472519	-0.824221
N	2.462635	-1.248579	0.385746
O	3.8556	-1.439554	0.317451
C	4.573389	-0.257843	0.240828
C	6.019734	-0.558769	-0.130384
C	6.025098	-1.023752	-1.60523
C	6.840728	0.728268	0.024686
C	6.586329	-1.669579	0.776503
O	4.084815	0.828052	0.423862
O	1.95041	-1.7175	1.568682
C	1.574705	-0.588273	2.433793
C	0.524352	0.290517	1.81811
C	-0.833185	0.080664	2.060711
C	-1.816211	0.873439	1.463639
C	-3.300999	0.699055	1.855076
C	-3.497981	-0.529122	2.76645
C	-3.7486	1.948402	2.647937
C	-4.230326	0.506406	0.631046
C	-1.370933	1.879696	0.574174
O	-2.369256	2.682375	-0.007115
C	-2.737577	2.4457	-1.296273
C	-3.827857	3.399072	-1.709469
O	-2.235186	1.600574	-2.000841
C	-0.015851	2.155055	0.326045
C	0.586999	3.246359	-0.592265
C	1.132572	2.549842	-1.859849
C	-0.37078	4.373672	-1.027799
C	1.758043	3.942671	0.146782
C	0.908483	1.31961	0.968858
C	0.352181	-1.83067	-0.748793
C	-0.523211	-1.126862	-1.578044
C	-1.875301	-1.457928	-1.610649
C	-2.345389	-2.510411	-0.827711
C	-3.794963	-2.900543	-0.84188
F	-4.328175	-2.872998	0.407558
F	-4.546106	-2.085162	-1.611181
F	-3.970524	-4.161729	-1.300632
C	-1.470336	-3.23231	-0.008592
C	-0.126196	-2.887833	0.039317
H	7.055514	-1.234846	-1.910935
H	5.621886	-0.247102	-2.262785
H	5.424085	-1.926243	-1.738737
H	6.443123	1.528303	-0.605333
H	7.877989	0.535864	-0.268259
H	6.834753	1.079829	1.061289
H	7.631994	-1.852876	0.507711
H	6.032118	-2.6042	0.662244
H	6.554728	-1.375175	1.83134
H	2.485786	-0.029519	2.66283
H	1.21855	-1.094475	3.333306
H	-1.117989	-0.718887	2.73166
H	-4.556667	-0.603349	3.034543
H	-2.931093	-0.449034	3.699457
H	-3.219168	-1.45852	2.260518
H	-3.64036	2.857042	2.050692
H	-3.153738	2.062399	3.561066
H	-4.801841	1.850601	2.937755
H	-4.533391	1.459468	0.197284
H	-5.145127	-0.011596	0.935959
H	-3.755523	-0.090391	-0.147383
H	-3.43007	4.419079	-1.727272
H	-4.649778	3.382212	-0.988455
H	-4.190558	3.129445	-2.701376
H	0.318365	2.06806	-2.409504
H	1.877906	1.788038	-1.609125
H	1.606885	3.285909	-2.52041
H	0.222687	5.17914	-1.473436
H	-0.930925	4.792285	-0.187263
H	-1.072445	4.047951	-1.796455
H	2.581111	3.263669	0.378324
H	1.414057	4.398482	1.082243
H	2.164216	4.736952	-0.488872
H	1.964714	1.453742	0.788207
H	-0.151233	-0.308734	-2.181478
H	-2.5516	-0.883684	-2.229701
H	-1.843382	-4.055821	0.591887
H	0.548878	-3.434035	0.685257

Table 2.7 Example computed structure of a B conformer of **1k** (37)

O	-3.101236	0.971608	1.712892
C	-2.429397	0.740181	0.722502
N	-2.820057	-0.321798	-0.126781
O	-4.179932	-0.658694	-0.025268
C	-5.041246	0.362721	-0.430491
C	-6.484861	-0.040439	-0.164818
C	-6.779636	-1.40402	-0.821832
C	-6.666991	-0.136948	1.366567
C	-7.405544	1.042234	-0.743538
O	-4.639982	1.398202	-0.890887
O	-2.428772	-0.315023	-1.454785
C	-1.770163	-1.580821	-1.77368
C	-0.382259	-1.656106	-1.206651
C	-0.184835	-1.999816	0.12866
C	1.08432	-1.996139	0.716348
C	1.250667	-2.442682	2.186929
C	1.750137	-1.289834	3.087112
C	-0.094055	-2.908901	2.782674
C	2.221272	-3.642506	2.268558
C	2.159688	-1.63181	-0.120096
O	3.454083	-1.631865	0.428012
C	3.943882	-0.462289	0.943276
C	5.323861	-0.688233	1.501514
O	3.334087	0.577413	0.946682
C	2.026006	-1.36719	-1.498019
C	3.228311	-1.199466	-2.455591
C	4.078616	-2.490377	-2.420438
C	2.757824	-1.002675	-3.911172
C	4.115253	0.018519	-2.109242
C	0.720388	-1.358985	-2.002331
C	-1.106752	1.397121	0.489336
C	-0.420385	1.780863	1.651686
C	0.793686	2.449599	1.568519
C	1.322365	2.762939	0.316258
C	2.598634	3.546696	0.203244
F	3.377854	3.105165	-0.812699
F	2.34368	4.855444	-0.058014
F	3.335249	3.510369	1.329428
C	0.637369	2.407036	-0.845005
C	-0.570219	1.720297	-0.76376
H	-7.826195	-1.672078	-0.64181
H	-6.14581	-2.193103	-0.409579
H	-6.622018	-1.363519	-1.905337
H	-6.024988	-0.911168	1.794087
H	-7.710739	-0.382472	1.590481
H	-6.423734	0.813892	1.851249
H	-7.200144	2.01677	-0.292305
H	-8.449285	0.778188	-0.543938
H	-7.273396	1.137372	-1.825738
H	-1.761567	-1.583128	-2.865819
H	-2.413437	-2.389863	-1.416354
H	-1.05102	-2.266358	0.716578
H	1.62935	-1.572263	4.139045
H	1.178832	-0.374443	2.907186
H	2.80424	-1.059885	2.937648
H	-0.53205	-3.735946	2.214277
H	-0.826233	-2.0957	2.834365
H	0.076642	-3.263677	3.804053
H	3.21182	-3.393646	1.885241
H	1.834224	-4.489449	1.690766
H	2.325133	-3.964272	3.311484
H	5.272505	-1.394813	2.33689
H	5.736201	0.260337	1.845181
H	5.974336	-1.129357	0.74019
H	3.484918	-3.35359	-2.741532
H	4.461788	-2.691968	-1.418143
H	4.931695	-2.392338	-3.102277
H	2.146367	-1.838847	-4.265534
H	3.636284	-0.938985	-4.560961
H	2.187114	-0.075545	-4.035783
H	4.785068	-0.179682	-1.272176
H	3.520767	0.900447	-1.863111
H	4.75113	0.258887	-2.968594
H	0.548338	-1.128019	-3.045438
H	-0.855656	1.547665	2.616619
H	1.334557	2.718733	2.467912
H	1.049482	2.660041	-1.816092
H	-1.096775	1.448626	-1.665975

Table 2.8 Example computed structure of an E conformer of **1k** (49)

O	-2.471022	2.664585	2.270118
C	-2.470392	2.091722	1.197574
N	-1.425643	2.282089	0.264254
O	-1.084734	1.175718	-0.566257
C	-0.929031	-0.048623	0.072659
C	-0.657495	-1.153015	-0.938315
C	-2.03962	-1.57973	-1.489105
C	0.246921	-0.670411	-2.084648
C	0.003014	-2.323911	-0.195852
O	-1.086207	-0.181559	1.26107
O	-0.335105	3.002994	0.668325
C	0.499085	2.39114	1.698461
C	1.602058	1.536247	1.124797
C	2.24345	1.896357	-0.056981
C	3.306781	1.150914	-0.579175
C	4.060123	1.652895	-1.833449
C	5.55907	1.832027	-1.4999
C	3.898737	0.706392	-3.043363
C	3.53182	3.03043	-2.284112
C	3.680422	0.001125	0.146907
O	4.716203	-0.800493	-0.368174
C	4.369586	-1.847381	-1.175725
C	5.608457	-2.567227	-1.639377
O	3.231434	-2.129423	-1.463662
C	3.126718	-0.353764	1.392396
C	3.707847	-1.462354	2.302055
C	5.189328	-1.134768	2.600714
C	2.969933	-1.512979	3.655538
C	3.603537	-2.878471	1.693481
C	2.055261	0.430884	1.83813
C	-3.615925	1.280325	0.688554
C	-4.032258	1.332272	-0.64621
C	-5.115852	0.566281	-1.06561
C	-5.775053	-0.259804	-0.153195
C	-6.881711	-1.159192	-0.627837
F	-7.78172	-1.413543	0.346816
F	-7.553169	-0.62813	-1.67315
F	-6.399718	-2.357099	-1.039378
C	-5.371475	-0.303293	1.184379
C	-4.300204	0.475955	1.605846
H	-2.71308	-1.889335	-0.683141
H	-1.902905	-2.426624	-2.16969
H	-2.516804	-0.765886	-2.041736
H	-0.211109	0.151213	-2.640986
H	0.422468	-1.503575	-2.77253
H	1.216738	-0.346315	-1.703635
H	0.151119	-3.155687	-0.891363
H	-0.617767	-2.663998	0.637133
H	0.981445	-2.028595	0.188756
H	-0.122473	1.840229	2.402163
H	0.910357	3.267446	2.209307
H	1.888236	2.774823	-0.576385
H	6.089859	2.218146	-2.37804
H	6.026572	0.892535	-1.201607
H	5.687054	2.552076	-0.683924
H	2.844968	0.48073	-3.231848
H	4.427295	-0.237988	-2.920407
H	4.308807	1.190203	-3.937195
H	3.611599	3.780607	-1.490765
H	2.488637	2.983906	-2.614467
H	4.130464	3.378656	-3.131957
H	6.236435	-1.885829	-2.222913
H	5.325869	-3.424903	-2.249667
H	6.197644	-2.896045	-0.777623
H	5.611377	-1.896516	3.266888
H	5.276102	-0.162896	3.099081
H	5.788428	-1.106282	1.68857
H	1.91836	-1.79731	3.539833
H	3.01546	-0.55599	4.185185
H	3.447704	-2.265318	4.29116
H	2.595079	-3.084847	1.324996
H	3.841804	-3.618985	2.46526
H	4.304099	-3.039671	0.874865
H	1.555692	0.18355	2.765038
H	-3.511193	1.970102	-1.350816
H	-5.448172	0.609323	-2.096766
H	-5.895415	-0.940009	1.888369
H	-3.973141	0.458545	2.639291

Table 2.9 Example computed structure of a C conformer of **1k** (50)

O	-2.001745	0.521291	-1.67466
C	-1.547593	1.213188	-0.778821
N	-2.387145	1.644346	0.271613
O	-3.532057	0.838761	0.390333
C	-4.704438	1.468958	-0.015967
C	-5.831925	0.443514	-0.067595
C	-7.169955	1.193351	-0.119987
C	-5.623085	-0.371328	-1.366015
C	-5.790903	-0.494688	1.153823
O	-4.756612	2.629092	-0.318273
O	-1.872243	1.963163	1.509048
C	-1.545374	0.802699	2.3534
C	-0.582643	-0.166862	1.736775
C	0.790554	-0.058661	1.949334
C	1.699279	-0.961428	1.388256
C	3.181934	-0.939952	1.831481
C	4.18848	-0.83046	0.664025
C	3.466945	0.254671	2.764845
C	3.460963	-2.236048	2.627572
C	1.157192	-1.942663	0.528143
O	2.044257	-2.875866	-0.036482
C	2.59736	-2.64311	-1.260974
C	3.448965	-3.814805	-1.669724
O	2.399793	-1.649915	-1.919529
C	-0.224634	-2.118474	0.308234
C	-0.846081	-3.243145	-0.552136
C	-0.299259	-4.63043	-0.148353
C	-2.377752	-3.303749	-0.36309
C	-0.609659	-2.970494	-2.054334
C	-1.068676	-1.205427	0.948725
C	-0.159622	1.758288	-0.781472
C	0.795382	1.009469	-1.475571
C	2.123163	1.420732	-1.503302
C	2.496313	2.593703	-0.847394
C	3.941995	2.99129	-0.781544
F	4.659114	2.499186	-1.813271
F	4.103232	4.33283	-0.774698
F	4.528633	2.527177	0.356012
C	1.540292	3.368654	-0.183368
C	0.214724	2.95337	-0.149329
H	-7.988998	0.473456	-0.219432
H	-7.202722	1.880356	-0.969219
H	-7.332797	1.775745	0.792826
H	-6.398435	-1.141715	-1.438773
H	-4.642027	-0.853401	-1.377008
H	-5.694456	0.274099	-2.247364
H	-5.858402	0.068152	2.091343
H	-4.876185	-1.092375	1.1749
H	-6.644671	-1.179193	1.108636
H	-2.486599	0.314997	2.619234
H	-1.130152	1.289141	3.237745
H	1.147237	0.742991	2.581676
H	5.171481	-0.558739	1.06287
H	3.893206	-0.06195	-0.050517
H	4.316022	-1.773047	0.131999
H	4.51325	0.2111	3.083062
H	2.850545	0.232183	3.669044
H	3.317172	1.21197	2.255445
H	4.502336	-2.246156	2.970591
H	3.293155	-3.125077	2.014812
H	2.811914	-2.29757	3.508126
H	4.095022	-4.131723	-0.846767
H	4.044376	-3.545947	-2.542331
H	2.796915	-4.658912	-1.922505
H	-0.501572	-4.828972	0.910461
H	0.774676	-4.723216	-0.306043
H	-0.801273	-5.405651	-0.738254
H	-2.657825	-3.453027	0.685537
H	-2.770023	-4.149464	-0.93675
H	-2.87096	-2.399996	-0.734108
H	-1.003442	-1.985129	-2.324753
H	-1.136655	-3.725285	-2.649797
H	0.441423	-2.997616	-2.337635
H	-2.138304	-1.284845	0.821471
H	0.506963	0.086944	-1.960313
H	2.856854	0.816682	-2.021247
H	1.833362	4.293059	0.302294
H	-0.521999	3.551789	0.369757

Table 2.10 Example computed structure of a G conformer of **1k** (63)

O	0.753644	0.567772	-3.46277
C	1.078047	0.77019	-2.310774
N	0.649945	1.909579	-1.578988
O	1.795601	2.505679	-0.953067
C	1.603179	2.792084	0.385678
C	2.940169	3.147942	1.030401
C	2.679092	3.579709	2.479345
C	3.83543	1.888209	1.001599
C	3.612265	4.290781	0.242156
O	0.52859	2.739396	0.925563
O	-0.026397	2.83319	-2.339324
C	-1.31179	3.156273	-1.720422
C	-1.985945	1.947366	-1.13106
C	-2.412753	1.965474	0.190294
C	-2.905333	0.820875	0.828167
C	-3.484893	0.921641	2.257588
C	-3.594551	2.394631	2.704226
C	-4.915071	0.336113	2.279646
C	-2.604963	0.207944	3.308682
C	-2.861516	-0.369801	0.079378
O	-3.202868	-1.574221	0.725473
C	-2.208666	-2.252092	1.36961
C	-2.757221	-3.517529	1.972947
O	-1.06323	-1.872667	1.434089
C	-2.535442	-0.42297	-1.292006
C	-2.633733	-1.704387	-2.149974
C	-4.044874	-2.322121	-2.03175
C	-2.399051	-1.391495	-3.642655
C	-1.560107	-2.740698	-1.747245
C	-2.114781	0.776354	-1.874663
C	1.807707	-0.207874	-1.456454
C	1.307607	-0.534377	-0.189268
C	1.946145	-1.507884	0.573042
C	3.097226	-2.127536	0.082183
C	3.833267	-3.109754	0.949
F	2.994163	-3.818866	1.735296
F	4.551782	-3.993888	0.221718
F	4.705698	-2.482027	1.775549
C	3.593252	-1.808358	-1.185579
C	2.933997	-0.863247	-1.964562
H	2.032464	4.461616	2.519322
H	3.629934	3.825189	2.963507
H	2.194711	2.780939	3.047865
H	4.035763	1.562777	-0.02237
H	3.3684	1.056055	1.53789
H	4.789956	2.115463	1.488188
H	3.820393	3.997787	-0.789838
H	4.559331	4.553281	0.725572
H	2.980261	5.185548	0.22647
H	-1.864763	3.595009	-2.556203
H	-1.152516	3.919684	-0.953517
H	-2.320416	2.88922	0.743772
H	-4.179102	2.993877	1.99832
H	-2.611626	2.861558	2.827437
H	-4.100619	2.433264	3.674354
H	-5.567499	0.887915	1.593601
H	-5.335193	0.422211	3.288702
H	-4.929675	-0.716023	1.990703
H	-1.549496	0.465391	3.179369
H	-2.69539	-0.877677	3.269052
H	-2.915898	0.517712	4.31302
H	-1.96023	-4.050371	2.491383
H	-3.181239	-4.151089	1.187214
H	-3.565086	-3.278491	2.672019
H	-4.804455	-1.611192	-2.376295
H	-4.285509	-2.60586	-1.006246
H	-4.1104	-3.217101	-2.661578
H	-2.547966	-2.308261	-4.222596
H	-1.380803	-1.039037	-3.834789
H	-3.10447	-0.64246	-4.018204
H	-1.74835	-3.195173	-0.774773
H	-0.565931	-2.28459	-1.717774
H	-1.543221	-3.551316	-2.48482
H	-1.810878	0.793885	-2.911669
H	0.406024	-0.06283	0.182255
H	1.52825	-1.79617	1.529731
H	4.47817	-2.308033	-1.563222
H	3.289793	-0.622738	-2.960899

Table 2.11 Example computed structure of an F conformer of **1k** (65)

O	-1.099967	-1.203222	3.549627
C	-1.037664	-1.391666	2.342276
N	-0.13772	-2.313598	1.830141
O	0.156604	-2.300817	0.455133
C	-0.44547	-3.351036	-0.242416
C	0.076223	-3.372914	-1.675337
C	-0.228777	-2.025641	-2.362412
C	1.601192	-3.607446	-1.633872
C	-0.621033	-4.518276	-2.421265
O	-1.246556	-4.090386	0.259012
O	0.941763	-2.727301	2.554961
C	1.818065	-1.637748	3.034833
C	2.007143	-0.529982	2.042448
C	1.329887	0.674302	2.214372
C	1.401362	1.709783	1.273587
C	0.749303	3.079538	1.57339
C	0.091338	3.082349	2.968207
C	1.853986	4.16103	1.576425
C	-0.35555	3.471361	0.567988
C	2.164607	1.443553	0.122621
O	2.175238	2.411028	-0.899056
C	1.230535	2.291996	-1.878066
C	1.388181	3.395773	-2.888016
O	0.402011	1.411709	-1.909211
C	2.966767	0.294144	-0.045558
C	3.999442	0.138905	-1.185954
C	4.952413	1.356624	-1.187632
C	4.875496	-1.113206	-0.974987
C	3.335881	-0.011281	-2.572756
C	2.844794	-0.69056	0.938826
C	-1.986275	-0.750458	1.376636
C	-1.56058	-0.072949	0.228738
C	-2.488821	0.573165	-0.582302
C	-3.844585	0.541286	-0.250217
C	-4.84568	1.183017	-1.168145
F	-5.971624	1.550576	-0.517245
F	-4.344789	2.288134	-1.765698
F	-5.223455	0.341705	-2.16092
C	-4.273973	-0.119685	0.90356
C	-3.343071	-0.751044	1.72219
H	0.294625	-1.193043	-1.88912
H	-1.301221	-1.805677	-2.347603
H	0.091162	-2.079852	-3.408812
H	2.105877	-2.804572	-1.091877
H	1.991934	-3.636979	-2.656694
H	1.843855	-4.559203	-1.148672
H	-1.704077	-4.367307	-2.45084
H	-0.428263	-5.481003	-1.93933
H	-0.248735	-4.562421	-3.45003
H	2.745911	-2.175796	3.24016
H	1.391651	-1.265911	3.967337
H	0.720989	0.791301	3.099794
H	-0.73976	2.371461	3.030999
H	-0.310763	4.0806	3.167794
H	0.808156	2.850363	3.762482
H	1.417131	5.137466	1.816239
H	2.347031	4.235797	0.604708
H	2.614705	3.934825	2.331749
H	-1.081143	2.665696	0.436178
H	0.040784	3.743734	-0.40995
H	-0.888884	4.349725	0.948079
H	2.372142	3.324514	-3.363237
H	1.335563	4.369885	-2.39212
H	0.605183	3.315549	-3.64179
H	4.420337	2.292121	-1.366051
H	5.706242	1.234181	-1.97395
H	5.474887	1.436838	-0.227926
H	5.642243	-1.143411	-1.755586
H	4.299752	-2.041643	-1.047824
H	5.386816	-1.096374	-0.007025
H	4.095947	-0.298551	-3.308089
H	2.882929	0.913907	-2.928025
H	2.562731	-0.784255	-2.562927
H	3.4057	-1.612196	0.854547
H	-0.513682	-0.020254	-0.030866
H	-2.142983	1.10542	-1.460951
H	-5.326287	-0.129803	1.164254
H	-3.6592	-1.249363	2.63206

Table 2.12 Example computed structure of an H conformer of **1k** (71)

O	-2.877502	2.859313	-0.364638
C	-2.802145	1.669735	-0.627949
N	-1.650473	1.15085	-1.214963
O	-0.520318	1.969401	-1.23367
C	-0.064771	2.388861	0.020775
C	1.060038	3.395911	-0.161101
C	0.533326	4.586817	-0.989658
C	1.510297	3.870957	1.226491
C	2.229201	2.70534	-0.895019
O	-0.525466	1.981756	1.053707
O	-1.388891	-0.190192	-1.308837
C	-0.865574	-0.819851	-0.09667
C	0.638896	-0.768158	-0.029259
C	1.403048	-0.945468	-1.179937
C	2.800757	-0.966405	-1.142347
C	3.611181	-1.045646	-2.456293
C	2.683291	-0.953421	-3.685063
C	4.590657	0.147301	-2.545131
C	4.38905	-2.374945	-2.582826
C	3.393839	-0.845562	0.131197
O	4.793161	-0.950962	0.222404
C	5.319831	-2.192519	0.460671
C	6.821205	-2.100851	0.535398
O	4.655388	-3.191065	0.589526
C	2.671638	-0.556993	1.305308
C	3.336102	-0.190523	2.652274
C	4.04667	-1.40111	3.297436
C	4.343651	0.964594	2.450321
C	2.286673	0.302524	3.670645
C	1.276188	-0.542208	1.186006
C	-3.941256	0.723321	-0.409996
C	-4.797326	1.041804	0.652885
C	-5.904858	0.247435	0.926246
C	-6.177598	-0.859115	0.118767
C	-7.341254	-1.754092	0.4429
F	-7.853284	-2.337527	-0.663178
F	-6.977845	-2.754618	1.280923
F	-8.343761	-1.080994	1.048513
C	-5.344702	-1.168048	-0.958569
C	-4.225491	-0.383378	-1.221166
H	0.249313	4.275478	-1.99768
H	1.318878	5.346153	-1.066766
H	-0.34088	5.041458	-0.512657
H	0.690441	4.355647	1.764553
H	2.328357	4.590358	1.116884
H	1.864257	3.03421	1.834406
H	2.598625	1.845213	-0.330084
H	3.051541	3.419445	-1.011926
H	1.927211	2.358928	-1.886564
H	-1.223074	-1.849074	-0.200248
H	-1.332465	-0.364418	0.777521
H	0.88392	-1.04462	-2.1226
H	2.013422	-1.816417	-3.763317
H	3.297182	-0.931432	-4.591216
H	2.075404	-0.042688	-3.671822
H	4.043678	1.096088	-2.546835
H	5.161759	0.085835	-3.478968
H	5.295198	0.160734	-1.712461
H	5.258447	-2.418812	-1.926901
H	4.755985	-2.485551	-3.609635
H	3.74925	-3.23209	-2.351927
H	7.21788	-1.67554	-0.391973
H	7.240103	-3.093375	0.700775
H	7.112497	-1.432367	1.352268
H	4.962633	-1.681346	2.777541
H	3.391363	-2.277333	3.319356
H	4.323741	-1.153093	4.328483
H	4.794386	1.232694	3.41293
H	3.839598	1.853748	2.056634
H	5.143572	0.694776	1.759799
H	2.802604	0.63841	4.575837
H	1.59344	-0.492724	3.965094
H	1.701216	1.144028	3.286448
H	0.663617	-0.329391	2.050665
H	-4.581802	1.917563	1.254139
H	-6.560825	0.490703	1.754549
H	-5.574319	-2.015561	-1.594786
H	-3.58321	-0.62718	-2.057061

Table 2.13 Example computed structure of a D conformer of **1k** (92)

O	2.538835	-3.163405	-2.006847
C	2.248346	-2.160537	-1.39089
N	0.885598	-1.775487	-1.22264
O	0.598043	-1.060919	-0.027519
C	0.972864	-1.699716	1.146501
C	0.461688	-0.919111	2.348263
C	-1.072771	-1.088362	2.392492
C	1.106598	-1.502089	3.612476
C	0.818047	0.57362	2.196196
O	1.610904	-2.721523	1.146906
O	0.007483	-2.835334	-1.352776
C	-1.059093	-2.472655	-2.274574
C	-1.941345	-1.386295	-1.726293
C	-1.652485	-0.053777	-1.98549
C	-2.372329	1.001851	-1.407166
C	-1.947001	2.433098	-1.816343
C	-2.901036	3.573918	-1.40639
C	-0.559127	2.722965	-1.203264
C	-1.853525	2.498536	-3.361401
C	-3.389095	0.633389	-0.510473
O	-4.103717	1.626452	0.179565
C	-3.517799	2.192871	1.274169
C	-4.4658	3.171066	1.91586
O	-2.400859	1.930288	1.65472
C	-3.784723	-0.705105	-0.280684
C	-5.009589	-1.086372	0.5807
C	-5.297793	-2.599609	0.505082
C	-4.781029	-0.758304	2.072432
C	-6.273107	-0.364075	0.059007
C	-3.023377	-1.696881	-0.902781
C	3.256329	-1.160892	-0.921701
C	4.514872	-1.652614	-0.557835
C	5.508052	-0.781443	-0.124427
C	5.250873	0.590928	-0.073855
C	6.298026	1.5315	0.453514
F	6.166475	1.721198	1.788501
F	7.548883	1.066286	0.245203
F	6.216916	2.751407	-0.123238
C	4.00535	1.091381	-0.460179
C	3.008135	0.216905	-0.880325
H	-1.465184	-0.566266	3.271097
H	-1.349632	-2.146222	2.465717
H	-1.543366	-0.657949	1.507938
H	2.196102	-1.40005	3.583952
H	0.870052	-2.563829	3.724505
H	0.732106	-0.96628	4.490757
H	0.311772	1.015401	1.336433
H	1.898608	0.714197	2.08237
H	0.492793	1.111034	3.092687
H	-1.598758	-3.414494	-2.397197
H	-0.605617	-2.1878	-3.228369
H	-0.817635	0.167863	-2.639281
H	-3.941685	3.357091	-1.660565
H	-2.602969	4.480639	-1.943761
H	-2.837409	3.810023	-0.343231
H	-0.607174	2.675325	-0.111702
H	-0.216648	3.722853	-1.495412
H	0.186338	1.996941	-1.544201
H	-1.541129	3.503231	-3.666083
H	-2.827655	2.291237	-3.818095
H	-1.130056	1.793283	-3.776884
H	-3.978598	3.648617	2.765911
H	-5.368869	2.649441	2.249415
H	-4.775015	3.925159	1.185894
H	-4.485335	-3.197159	0.931967
H	-5.471104	-2.932313	-0.523745
H	-6.202279	-2.81773	1.082005
H	-5.639837	-1.105837	2.658367
H	-4.668284	0.308405	2.262919
H	-3.886959	-1.264012	2.449061
H	-6.463279	-0.633762	-0.985991
H	-6.181894	0.72067	0.120163
H	-7.143705	-0.671245	0.650159
H	-3.259652	-2.740597	-0.740919
H	4.697213	-2.719879	-0.612164
H	6.480053	-1.162469	0.167917
H	3.81827	2.159229	-0.437654
H	2.042312	0.606029	-1.177811

Table 2.14 Example computed structure of a B conformer of **1j** (11)

C	3.858799	2.103304	2.717665
C	3.466065	0.983493	1.726879
C	4.484951	0.906207	0.568739
C	3.593995	-0.355854	2.491566
C	2.01091	1.205928	1.248602
C	0.971889	0.614369	1.979136
C	-0.365828	0.766597	1.629241
C	-1.444583	0.079806	2.410738
O	-1.795761	-1.238513	1.842176
N	-2.379565	-1.077212	0.615631
O	-3.772569	-1.253005	0.669832
C	-4.484326	-0.095119	0.391409
C	-5.949355	-0.435055	0.15356
C	-6.751915	0.872076	0.107858
C	-6.030549	-1.162075	-1.20898
C	-6.47906	-1.351265	1.274689
O	-3.974033	0.99402	0.333453
C	-1.794436	-1.514648	-0.566776
C	-0.326821	-1.805107	-0.55657
C	0.396037	-1.363818	-1.670426
C	1.755099	-1.632447	-1.779986
C	2.388534	-2.387818	-0.791166
C	3.840605	-2.744273	-0.933754
F	4.515067	-1.834353	-1.673346
F	4.46039	-2.826025	0.266699
F	4.007272	-3.943	-1.540005
C	1.66551	-2.865066	0.304393
C	0.314368	-2.559333	0.433168
O	-2.458712	-1.539671	-1.592714
C	-0.688322	1.485211	0.478728
C	0.293476	2.076693	-0.319241
C	-0.123401	2.770411	-1.636473
C	0.757204	2.307264	-2.818677
C	-1.582126	2.424858	-2.009174
C	-0.043461	4.305736	-1.496053
C	1.635695	1.991444	0.130509
O	2.596287	2.663684	-0.606087
C	3.02985	3.933484	-0.120791
H	3.810464	3.096661	2.267802
H	4.882532	1.945467	3.078338
H	3.188761	2.098603	3.584764
H	4.615598	1.850464	0.045278
H	4.183412	0.159441	-0.170522
H	5.458316	0.603635	0.971235
H	3.053223	-0.353787	3.442556
H	4.648732	-0.531402	2.726979
H	3.240142	-1.196679	1.890566
H	1.204847	0.01182	2.848229
H	-2.362517	0.669509	2.456967
H	-1.122051	-0.184776	3.419683
H	-6.693142	1.406899	1.061229
H	-7.803597	0.6465	-0.096674
H	-6.378843	1.536927	-0.675611
H	-5.439782	-2.081005	-1.204069
H	-5.657422	-0.523975	-2.016288
H	-7.075898	-1.411922	-1.420105
H	-7.538236	-1.562597	1.093655
H	-6.393013	-0.869394	2.25489
H	-5.939004	-2.300418	1.308049
H	-0.119486	-0.806073	-2.442733
H	2.320082	-1.257894	-2.625824
H	2.161519	-3.460413	1.063122
H	-0.23653	-2.904405	1.297821
H	-1.730547	1.554862	0.204812
H	1.808326	2.545164	-2.661556
H	0.417524	2.794202	-3.740388
H	0.670444	1.225249	-2.961895
H	-2.306772	2.835115	-1.299321
H	-1.748663	1.344068	-2.070888
H	-1.806483	2.855515	-2.990934
H	0.980965	4.656689	-1.370141
H	-0.633146	4.647818	-0.638068
H	-0.448501	4.783331	-2.39639
H	4.008606	3.847605	0.363049
H	2.311671	4.356514	0.588244
H	3.126337	4.601435	-0.98159

Table 2.15 Example computed structure of an E conformer of **1j** (12)

C	-0.04326	4.305646	-1.496293
C	-0.123271	2.770315	-1.636598
C	-1.582	2.424809	-2.009324
C	0.757352	2.307026	-2.818732
C	0.293528	2.076676	-0.319302
C	-0.688315	1.485271	0.478668
C	-0.36588	0.766724	1.62924
C	-1.444676	0.079976	2.410716
O	-1.79579	-1.238387	1.842217
N	-2.379579	-1.077178	0.615655
O	-3.772589	-1.252923	0.669889
C	-4.484314	-0.095066	0.391283
C	-5.949374	-0.434983	0.153589
C	-6.751888	0.872173	0.107769
C	-6.03071	-1.162197	-1.208836
C	-6.479022	-1.351008	1.274897
O	-3.973983	0.994043	0.333099
C	-1.794474	-1.514705	-0.566724
C	-0.326858	-1.805156	-0.556536
C	0.39594	-1.364043	-1.670503
C	1.755005	-1.632648	-1.780073
C	2.388506	-2.387828	-0.791149
C	3.840584	-2.744256	-0.933739
F	4.514979	-1.834435	-1.673516
F	4.460426	-2.825784	0.266699
F	4.007266	-3.943078	-1.539796
C	1.665541	-2.864916	0.304517
C	0.314395	-2.559198	0.4333
O	-2.458779	-1.539806	-1.592642
C	0.971818	0.614481	1.979192
C	2.010882	1.205957	1.248653
C	3.466016	0.983486	1.726975
C	4.484923	0.906098	0.56886
C	3.858778	2.103328	2.717713
C	3.593873	-0.355829	2.491729
C	1.63573	1.991417	0.130501
O	2.596366	2.663585	-0.606103
C	3.029971	3.933386	-0.120848
H	-0.448226	4.783192	-2.396689
H	0.981178	4.656556	-1.370352
H	-0.632974	4.647823	-0.638366
H	-1.806301	2.855405	-2.991124
H	-2.306649	2.835157	-1.299527
H	-1.748591	1.344024	-2.070963
H	0.417725	2.793898	-3.740498
H	0.670547	1.225003	-2.961853
H	1.808479	2.544893	-2.661597
H	-1.730527	1.554921	0.204701
H	-2.362624	0.669666	2.456845
H	-1.122206	-0.184532	3.419701
H	-7.803595	0.646608	-0.096646
H	-6.378854	1.536898	-0.675824
H	-6.693018	1.407126	1.06106
H	-7.07608	-1.412077	-1.419817
H	-5.439942	-2.081126	-1.203857
H	-5.657668	-0.524214	-2.016275
H	-7.538221	-1.562323	1.093981
H	-6.392874	-0.868997	2.255021
H	-5.939002	-2.300178	1.308351
H	-0.119635	-0.80645	-2.442885
H	2.319942	-1.258224	-2.625999
H	2.161596	-3.460128	1.063321
H	-0.236454	-2.904139	1.298035
H	1.204728	0.01198	2.84833
H	4.61567	1.85034	0.045396
H	4.183337	0.159354	-0.170404
H	5.458251	0.603444	0.971381
H	4.882494	1.945459	3.078421
H	3.188717	2.098705	3.584795
H	3.810504	3.096664	2.267797
H	3.053064	-0.353702	3.442697
H	4.648595	-0.531398	2.727192
H	3.24002	-1.196671	1.890752
H	4.008711	3.847488	0.363019
H	2.311792	4.356475	0.588151
H	3.126509	4.601298	-0.981673

Table 2.16 Example computed structure of a C conformer of **1j** (15)

C	0.513241	4.599931	-1.065937
C	0.698645	3.084035	-1.291984
C	0.053846	2.667982	-2.63338
C	2.21478	2.832993	-1.434141
C	0.09699	2.260517	-0.13033
C	0.94059	1.491968	0.674575
C	0.446991	0.654208	1.671748
C	1.383079	-0.213973	2.450471
O	1.622108	-1.534945	1.832687
N	2.183728	-1.478431	0.579766
O	3.40647	-0.78492	0.61182
C	4.479959	-1.532237	0.136643
C	5.72353	-0.650502	0.091773
C	6.924512	-1.530479	-0.279727
C	5.501023	0.432896	-0.987242
C	5.95055	0.013037	1.465213
O	4.38159	-2.679786	-0.200469
C	1.426189	-1.181501	-0.56852
C	0.003805	-1.632164	-0.578841
C	-0.832047	-0.998514	-1.504343
C	-2.170091	-1.359689	-1.607407
C	-2.675144	-2.371465	-0.790339
C	-4.114205	-2.788108	-0.896232
F	-4.646568	-3.04894	0.321093
F	-4.879577	-1.83448	-1.473288
F	-4.261563	-3.913084	-1.633756
C	-1.839456	-3.03006	0.116697
C	-0.504249	-2.659541	0.227729
O	1.972676	-0.699118	-1.547672
C	-0.928298	0.578772	1.871761
C	-1.839748	1.340299	1.131905
C	-3.345547	1.194247	1.464015
C	-3.745426	2.272903	2.498808
C	-4.2575	1.256229	0.2196
C	-3.642492	-0.17299	2.126017
C	-1.292988	2.214825	0.154467
O	-2.111355	3.013335	-0.625319
C	-2.610637	4.227313	-0.062268
H	-0.524306	4.910863	-1.174353
H	1.101342	5.155758	-1.80556
H	0.862919	4.893235	-0.069434
H	0.325535	1.636284	-2.88064
H	0.432227	3.309159	-3.438631
H	-1.032854	2.753499	-2.602813
H	2.776359	3.19114	-0.563272
H	2.581902	3.383969	-2.306506
H	2.438563	1.773282	-1.587874
H	2.009375	1.514162	0.51178
H	0.972287	-0.503572	3.419198
H	2.356534	0.259479	2.596961
H	6.773328	-2.0147	-1.248212
H	7.087267	-2.313848	0.466879
H	7.82648	-0.912123	-0.335305
H	5.295912	-0.018837	-1.963023
H	6.405082	1.045503	-1.074008
H	4.661571	1.083655	-0.731403
H	5.120092	0.67054	1.735628
H	6.865801	0.613496	1.428922
H	6.068933	-0.737552	2.254368
H	-0.424418	-0.216142	-2.130324
H	-2.818686	-0.851907	-2.311513
H	-2.236865	-3.821741	0.742794
H	0.136881	-3.164181	0.93814
H	-1.29205	-0.108137	2.624857
H	-3.603631	3.290202	2.132746
H	-3.146893	2.16279	3.410001
H	-4.801433	2.156674	2.770608
H	-5.301651	1.161797	0.538593
H	-4.042779	0.420984	-0.452265
H	-4.153814	2.173753	-0.353549
H	-3.224217	-0.253378	3.134134
H	-3.26693	-1.005558	1.52704
H	-4.726697	-0.29137	2.221554
H	-2.607919	4.978932	-0.855951
H	-1.982261	4.571018	0.764887
H	-3.63902	4.09831	0.287983

Table 2.17 Example computed structure of an H conformer of **1j** (34)

C	-4.705326	1.176817	2.211345
C	-3.660826	0.155692	2.717584
C	-2.65833	0.920547	3.604876
C	-4.360735	-0.884215	3.619618
C	-2.955518	-0.496027	1.507764
C	-1.568341	-0.403127	1.366009
C	-0.910986	-0.897269	0.240327
C	0.593118	-0.875753	0.165787
O	1.077202	-0.50092	-1.164924
N	1.274348	0.838264	-1.367061
O	0.10691	1.583068	-1.536681
C	-0.348994	2.247987	-0.393238
C	-1.520778	3.143058	-0.763728
C	-1.981748	3.88113	0.499622
C	-1.052813	4.154155	-1.832263
C	-2.660685	2.26345	-1.320046
O	0.146249	2.098752	0.691893
C	2.410552	1.521601	-0.944111
C	3.60028	0.696053	-0.563405
C	3.920203	-0.548424	-1.122379
C	5.084132	-1.205843	-0.734491
C	5.927064	-0.630887	0.218718
C	7.142994	-1.379692	0.688304
F	6.854196	-2.183639	1.740016
F	7.653791	-2.172001	-0.279963
F	8.126164	-0.54582	1.091849
C	5.618467	0.613041	0.773979
C	4.465378	1.277895	0.37307
O	2.433794	2.742362	-0.946848
C	-1.663464	-1.406783	-0.811199
C	-3.061627	-1.495712	-0.757444
C	-3.79025	-1.955023	-2.044997
C	-5.308118	-1.677145	-2.076798
C	-3.20704	-1.174703	-3.251121
C	-3.53841	-3.46128	-2.274163
C	-3.672658	-1.134293	0.464241
O	-5.021004	-1.379441	0.67101
C	-5.30096	-2.734747	1.026536
H	-4.224512	1.967379	1.625435
H	-5.208074	1.648954	3.063995
H	-5.459982	0.69426	1.588291
H	-1.93439	0.24895	4.079898
H	-3.207056	1.430298	4.403583
H	-2.103297	1.679677	3.044365
H	-4.688228	-0.402974	4.548718
H	-3.677502	-1.698382	3.887138
H	-5.242626	-1.308231	3.140306
H	-0.975265	0.071216	2.135698
H	1.014227	-1.878811	0.286658
H	1.033104	-0.210147	0.909311
H	-2.829754	4.528498	0.25357
H	-1.179203	4.500073	0.911213
H	-2.297106	3.178329	1.274958
H	-0.196023	4.734845	-1.475459
H	-1.871664	4.846722	-2.054659
H	-0.762123	3.649443	-2.756654
H	-3.522045	2.898151	-1.554675
H	-2.975155	1.510339	-0.59174
H	-2.350851	1.748099	-2.231943
H	3.270452	-0.998262	-1.861347
H	5.3409	-2.161427	-1.17803
H	6.281806	1.061593	1.504985
H	4.220597	2.254271	0.775116
H	-1.140512	-1.720407	-1.706574
H	-5.883703	-2.323038	-1.415124
H	-5.668219	-1.853045	-3.097086
H	-5.529533	-0.639292	-1.813387
H	-2.136066	-1.336958	-3.392379
H	-3.372824	-0.099271	-3.132213
H	-3.710253	-1.496402	-4.16956
H	-2.467434	-3.675329	-2.35667
H	-4.022249	-3.789972	-3.201587
H	-3.93607	-4.067049	-1.45334
H	-4.709545	-3.045597	1.894231
H	-5.096059	-3.419563	0.197706
H	-6.364244	-2.775223	1.273591

Table 2.18 Example computed structure of an F conformer of **1j** (44)

C	-4.451639	-1.991075	-1.920606
C	-3.622445	-0.693932	-1.77227
C	-2.873671	-0.42179	-3.094867
C	-4.610769	0.470691	-1.568622
C	-2.688033	-0.861456	-0.552384
C	-2.839616	-0.0525	0.573735
C	-2.121429	-0.286769	1.751078
C	-2.254781	0.617463	2.939658
O	-1.545984	1.914073	2.820869
N	-0.386427	1.871685	2.107266
O	-0.635709	2.172048	0.752657
C	-0.159672	3.427117	0.372854
C	-0.684845	3.763046	-1.019296
C	-2.207664	3.993414	-0.898818
C	0.01298	5.039675	-1.505721
C	-0.409037	2.597632	-1.989393
O	0.542596	4.101076	1.074536
C	0.606998	0.953526	2.422504
C	1.639751	0.64964	1.381363
C	1.322292	0.284461	0.067403
C	2.333344	-0.084431	-0.813484
C	3.662846	-0.09749	-0.386595
C	4.749574	-0.441771	-1.365671
F	5.846545	-0.937013	-0.754278
F	4.337034	-1.361772	-2.268113
F	5.146548	0.644121	-2.07085
C	3.983718	0.245215	0.928359
C	2.971014	0.606021	1.811304
O	0.671147	0.494469	3.554473
C	-1.296332	-1.402351	1.821376
C	-1.106937	-2.274365	0.737726
C	-0.255736	-3.54031	1.006355
C	1.221015	-3.140315	1.219373
C	-0.779426	-4.20297	2.307424
C	-0.333782	-4.637562	-0.075142
C	-1.739441	-1.919406	-0.470231
O	-1.474047	-2.629345	-1.628761
C	-0.255568	-2.237636	-2.262427
H	-5.142849	-1.899035	-2.767003
H	-5.043349	-2.177019	-1.017338
H	-3.804443	-2.852944	-2.096254
H	-2.321514	-1.296428	-3.435141
H	-2.180827	0.420223	-2.997234
H	-3.599245	-0.164032	-3.875013
H	-5.232603	0.334477	-0.67791
H	-5.281252	0.523784	-2.432437
H	-4.098112	1.435941	-1.48962
H	-3.529074	0.781787	0.555257
H	-1.878472	0.133849	3.842139
H	-3.285091	0.943342	3.098299
H	-2.429077	4.822345	-0.21826
H	-2.713131	3.097544	-0.528245
H	-2.616396	4.241648	-1.884176
H	-0.161679	5.871298	-0.817969
H	-0.374201	5.314362	-2.492365
H	1.094107	4.891135	-1.587372
H	0.660988	2.372695	-2.048741
H	-0.755748	2.87326	-2.991048
H	-0.936879	1.692298	-1.68097
H	0.291647	0.259786	-0.256238
H	2.088897	-0.376609	-1.828467
H	5.015233	0.21864	1.260756
H	3.20083	0.851214	2.842148
H	-0.773973	-1.589787	2.751378
H	1.813543	-4.023935	1.484166
H	1.327429	-2.406263	2.024594
H	1.655154	-2.701474	0.315897
H	-0.210476	-5.117928	2.504875
H	-1.836364	-4.473073	2.207024
H	-0.675669	-3.560144	3.18471
H	-1.368617	-4.888068	-0.322478
H	0.149975	-5.539198	0.317598
H	0.181689	-4.374154	-0.998192
H	-0.160346	-2.853423	-3.159156
H	0.607306	-2.405762	-1.611449
H	-0.28384	-1.179375	-2.547558

Table 2.19 Example computed structure of a D conformer of **1j** (51)

C	-6.104302	0.436319	1.168216
C	-5.236436	-0.676671	0.544062
C	-4.90461	-1.730007	1.622972
C	-6.132677	-1.344008	-0.531772
C	-3.936376	-0.193054	-0.145779
C	-3.292501	-1.098004	-1.004623
C	-2.208262	-0.73219	-1.791809
C	-1.464215	-1.751253	-2.605158
O	-0.389921	-2.386791	-1.846949
N	0.548711	-1.437125	-1.500963
O	0.33714	-1.02348	-0.15592
C	0.720217	-1.936878	0.812661
C	0.271224	-1.449302	2.183972
C	0.630873	0.039778	2.358863
C	-1.260955	-1.631332	2.254361
C	0.965702	-2.300063	3.255078
O	1.315087	-2.950534	0.550233
C	1.884365	-1.811198	-1.820199
C	2.942207	-0.972589	-1.176664
C	2.739903	0.36686	-0.818921
C	3.777472	1.099154	-0.250817
C	5.017257	0.493391	-0.032536
C	6.110012	1.264608	0.653497
F	6.026513	1.148443	2.001022
F	7.33805	0.829557	0.298056
F	6.048888	2.585213	0.371912
C	5.228044	-0.838224	-0.398709
C	4.194176	-1.564855	-0.979294
O	2.113708	-2.648732	-2.666097
C	-1.781754	0.596956	-1.775561
C	-2.327978	1.53622	-0.900871
C	-1.873197	3.010588	-0.953856
C	-3.096811	3.905663	-1.255277
C	-1.210226	3.47027	0.362553
C	-0.843713	3.242066	-2.077333
C	-3.35245	1.087347	-0.027356
O	-3.791986	1.967265	0.948679
C	-3.280284	1.673524	2.249664
H	-7.073698	0.003294	1.440565
H	-6.283176	1.249915	0.460206
H	-5.676767	0.865045	2.073731
H	-4.298523	-1.305485	2.429569
H	-4.349251	-2.5735	1.199575
H	-5.828179	-2.120715	2.066197
H	-6.365999	-0.636636	-1.334876
H	-7.075141	-1.664741	-0.074632
H	-5.672834	-2.22701	-0.982204
H	-3.649363	-2.120857	-1.063984
H	-1.028023	-1.314661	-3.508513
H	-2.093014	-2.601076	-2.87993
H	0.348615	0.362018	3.366904
H	0.101221	0.663195	1.634501
H	1.706167	0.207552	2.235569
H	-1.620109	-1.291691	3.232163
H	-1.539738	-2.683794	2.13646
H	-1.765052	-1.053445	1.476822
H	2.053002	-2.18348	3.207808
H	0.734071	-3.360851	3.127858
H	0.627205	-1.984754	4.247464
H	1.777887	0.835937	-0.987297
H	3.627566	2.139584	0.015442
H	6.195667	-1.29912	-0.235276
H	4.340496	-2.596738	-1.277885
H	-0.978162	0.879393	-2.44253
H	-3.85847	3.806791	-0.479921
H	-3.542748	3.635524	-2.219162
H	-2.788202	4.956749	-1.307574
H	-0.763892	4.461775	0.222273
H	-0.409828	2.783511	0.661796
H	-1.93083	3.545837	1.175698
H	-1.234745	2.958055	-3.059797
H	0.087734	2.690256	-1.904214
H	-0.592012	4.306906	-2.116079
H	-3.635503	2.470096	2.907182
H	-2.185252	1.65788	2.249412
H	-3.643619	0.709704	2.61875

Table 2.20 Example computed structure of a G conformer of **1j** (56)

C	-4.940291	0.639525	-2.27544
C	-4.024711	-0.394434	-1.570274
C	-4.983839	-1.404371	-0.905065
C	-3.180652	-1.103764	-2.652827
C	-3.089548	0.354177	-0.58944
C	-2.511684	1.549467	-1.041593
C	-1.703271	2.337048	-0.230826
C	-0.925457	3.482746	-0.812964
O	0.073769	3.01136	-1.783877
N	0.678542	1.879426	-1.288745
O	2.085206	2.098623	-1.124322
C	2.436763	2.456171	0.160994
C	3.957005	2.492935	0.287032
C	4.314902	2.973693	1.699401
C	4.490336	1.060856	0.057719
C	4.542395	3.450557	-0.771317
O	1.632235	2.677443	1.030851
C	0.48512	0.723625	-2.097777
C	1.042189	-0.514003	-1.48431
C	1.342018	-1.59662	-2.317814
C	1.79897	-2.791479	-1.771299
C	1.936852	-2.910109	-0.385917
C	2.473785	-4.181188	0.211806
F	2.23584	-5.252211	-0.575244
F	3.813771	-4.114514	0.394465
F	1.926577	-4.435596	1.421409
C	1.618389	-1.838755	0.453049
C	1.170183	-0.641023	-0.093805
O	-0.194215	0.73488	-3.103134
C	-1.527789	1.974955	1.103623
C	-2.054758	0.789932	1.62027
C	-1.899648	0.461206	3.121007
C	-1.208302	1.612969	3.877643
C	-3.300799	0.269719	3.743971
C	-1.050476	-0.805202	3.364938
C	-2.755862	-0.054123	0.721476
O	-3.124176	-1.308118	1.184069
C	-2.274394	-2.364307	0.730008
H	-5.515853	1.215833	-1.542762
H	-5.646567	0.113956	-2.927255
H	-4.386639	1.342582	-2.902321
H	-4.487156	-2.298777	-0.533188
H	-5.720942	-1.72528	-1.65024
H	-5.5237	-0.948222	-0.069722
H	-2.53631	-1.877254	-2.22322
H	-2.530863	-0.395982	-3.175919
H	-3.837187	-1.583394	-3.389025
H	-2.653041	1.852943	-2.071922
H	-0.41284	4.051297	-0.033229
H	-1.535987	4.155188	-1.421003
H	3.926066	3.979241	1.885419
H	5.403722	2.996605	1.811497
H	3.900863	2.30688	2.461045
H	4.255349	0.703344	-0.948048
H	4.061893	0.357374	0.779575
H	5.578131	1.057418	0.183612
H	4.309582	3.117314	-1.785667
H	5.631234	3.488623	-0.6597
H	4.152539	4.466242	-0.643494
H	1.207875	-1.491781	-3.388886
H	2.036249	-3.631968	-2.413552
H	1.701454	-1.949226	1.528749
H	0.883354	0.181689	0.550438
H	-0.917468	2.613483	1.725848
H	-0.178475	1.770022	3.538013
H	-1.172548	1.367286	4.944283
H	-1.753216	2.55701	3.772508
H	-3.208342	0.046644	4.813954
H	-3.837082	-0.550419	3.263535
H	-3.895788	1.184149	3.639401
H	-0.835334	-0.902845	4.435577
H	-0.091832	-0.742239	2.837329
H	-1.565766	-1.710816	3.048417
H	-2.434479	-2.584092	-0.329401
H	-2.534187	-3.245152	1.321918
H	-1.219309	-2.117481	0.88067

Table 2.21 Example computed structure of an A conformer of **1j** (63)

C	-0.754398	1.477576	-2.772154
C	-0.212579	2.62062	-1.884413
C	0.827082	3.438878	-2.677846
C	-1.379689	3.59987	-1.590955
C	0.283313	2.031179	-0.540545
C	-0.709373	1.581876	0.340175
C	-0.412042	1.090073	1.605182
C	-1.50096	0.500713	2.446186
O	-1.784565	-0.899792	2.072742
N	-2.325733	-0.942414	0.815436
O	-3.723671	-1.107245	0.891087
C	-4.427252	-0.111801	0.232531
C	-5.897219	-0.500651	0.138915
C	-6.435644	-0.869099	1.536461
C	-6.678316	0.687744	-0.437224
C	-5.998816	-1.718634	-0.807257
O	-3.912796	0.887205	-0.201465
C	-1.740581	-1.650946	-0.235428
C	-0.25972	-1.878591	-0.22732
C	0.338158	-1.937324	-1.496732
C	1.694395	-2.198648	-1.626732
C	2.467883	-2.424359	-0.483469
C	3.925975	-2.747344	-0.64148
F	4.523285	-1.922134	-1.537082
F	4.606143	-2.634798	0.520773
F	4.116131	-4.007439	-1.093495
C	1.880692	-2.389119	0.779357
C	0.521886	-2.110169	0.910346
O	-2.432245	-1.94633	-1.199064
C	0.91094	1.11395	2.048794
C	1.953789	1.546565	1.226798
C	3.378933	1.717641	1.797716
C	3.438083	1.331659	3.28866
C	4.435495	0.858319	1.072293
C	3.771993	3.208905	1.686572
C	1.620913	1.915171	-0.103828
O	2.660269	2.213968	-0.968488
C	2.967445	1.163719	-1.887919
H	0.032922	0.760593	-3.027776
H	-1.156059	1.883942	-3.708198
H	-1.557181	0.9285	-2.268985
H	0.307976	3.954578	-3.494076
H	1.607693	2.82806	-3.129722
H	1.307797	4.194371	-2.050613
H	-1.055055	4.399307	-0.915661
H	-2.247189	3.106986	-1.146861
H	-1.711625	4.059977	-2.528239
H	-1.745133	1.59083	0.030235
H	-2.440471	1.053523	2.365527
H	-1.21847	0.409595	3.49687
H	-6.345224	-0.026231	2.230689
H	-5.903221	-1.724353	1.95971
H	-7.496622	-1.128068	1.455592
H	-6.601292	1.565148	0.212395
H	-7.735389	0.417924	-0.529806
H	-6.301654	0.965698	-1.425253
H	-5.450411	-2.575871	-0.409993
H	-5.590333	-1.483553	-1.795026
H	-7.052183	-1.995338	-0.924122
H	-0.280516	-1.777018	-2.371284
H	2.15433	-2.225058	-2.608965
H	2.482269	-2.570562	1.662315
H	0.076049	-2.078599	1.892973
H	1.119549	0.783591	3.058915
H	2.749985	1.927454	3.897525
H	4.45091	1.511561	3.663602
H	3.211595	0.270787	3.44664
H	4.137725	-0.193211	1.030038
H	5.384558	0.910825	1.618874
H	4.621129	1.213878	0.06015
H	4.774701	3.364724	2.102998
H	3.069989	3.836395	2.247401
H	3.77545	3.536695	0.645168
H	3.708562	1.569031	-2.580629
H	2.081442	0.846696	-2.445411
H	3.385266	0.294376	-1.375403

Table 2.22 Example computed structure of an F conformer of **1i** (100)

O	-0.918025	-0.104018	3.541296
C	-0.990267	-0.61963	2.437177
N	-0.042756	-1.556485	2.007753
O	0.221632	-1.492507	0.60861
C	0.161714	-2.725325	-0.010673
C	0.450965	-2.604042	-1.505628
C	0.735787	-1.163199	-1.952664
C	1.665564	-3.510559	-1.793073
C	-0.793845	-3.148447	-2.238053
O	-0.107563	-3.744811	0.570703
O	1.10441	-1.744384	2.723217
C	1.92494	-0.535653	2.972329
C	2.253252	0.257161	1.742334
C	3.350931	-0.081252	0.950939
C	3.656903	0.643346	-0.207946
C	4.904043	0.281479	-1.028412
C	6.154882	0.455009	-0.139163
C	4.811001	-1.185208	-1.499293
C	5.068267	1.171818	-2.271121
C	2.806293	1.698093	-0.560372
C	1.691785	2.064242	0.209364
C	0.743339	3.179213	-0.25575
C	0.026818	3.847523	0.933314
C	1.495094	4.280493	-1.029372
C	-0.315633	2.543255	-1.185034
C	1.441429	1.335487	1.374922
C	-2.127464	-0.370577	1.500868
C	-2.688037	-1.36994	0.695409
C	-3.755708	-1.067998	-0.143411
C	-4.262912	0.233615	-0.184444
C	-5.437526	0.547819	-1.069082
F	-6.612099	0.324405	-0.434839
F	-5.441552	1.841216	-1.459721
F	-5.443347	-0.21405	-2.185273
C	-3.726705	1.226786	0.637405
C	-2.670672	0.918589	1.489066
H	-0.122894	-0.510886	-1.772085
H	0.946108	-1.159768	-3.028173
H	1.594848	-0.736825	-1.431332
H	1.879996	-3.504339	-2.867068
H	1.46563	-4.53905	-1.480563
H	2.55588	-3.154308	-1.265652
H	-1.667894	-2.514985	-2.050224
H	-1.024414	-4.166745	-1.913569
H	-0.606693	-3.156562	-3.316941
H	2.815274	-0.985316	3.415671
H	1.404546	0.065629	3.716239
H	3.977285	-0.915016	1.255796
H	6.242092	1.489509	0.210903
H	7.060927	0.20655	-0.704251
H	6.11842	-0.195594	0.740394
H	5.713367	-1.463201	-2.056258
H	3.94775	-1.328151	-2.157462
H	4.712239	-1.877869	-0.657394
H	5.966542	0.871249	-2.820944
H	5.181033	2.227856	-2.002867
H	4.214987	1.078733	-2.952146
H	3.01898	2.257075	-1.460623
H	-0.590462	4.677701	0.573365
H	0.744269	4.245492	1.659315
H	-0.63823	3.155135	1.456648
H	0.803739	5.092026	-1.281258
H	1.91713	3.914216	-1.970141
H	2.31021	4.700802	-0.429842
H	0.158619	2.08569	-2.060036
H	-1.025689	3.301813	-1.536763
H	-0.87883	1.764612	-0.660438
H	0.60962	1.59527	2.018392
H	-2.306562	-2.38333	0.739746
H	-4.191683	-1.840063	-0.767739
H	-4.128126	2.233391	0.606864
H	-2.254797	1.673702	2.14625

Table 2.23 Example computed structure of an A conformer of **1i** (11)

O	2.094283	-1.625069	1.559164
C	1.442257	-1.497149	0.534735
N	2.074364	-1.058461	-0.627872
O	3.443899	-1.379064	-0.683883
C	4.27253	-0.332367	-0.311929
C	5.691879	-0.849008	-0.113283
C	5.689974	-1.694202	1.18181
C	6.122333	-1.718441	-1.311495
C	6.631857	0.354344	0.038407
O	3.884889	0.796895	-0.15403
O	1.487824	-1.179173	-1.860092
C	1.239671	0.157165	-2.432238
C	0.266062	0.950926	-1.612618
C	-1.108501	0.88741	-1.872624
C	-2.021523	1.57863	-1.073745
C	-3.523759	1.618774	-1.391999
C	-3.944694	0.486466	-2.345247
C	-4.370865	1.500411	-0.108224
C	-3.829654	2.974279	-2.068345
C	-1.51477	2.31639	0.011047
C	-0.151418	2.38596	0.30484
C	0.410918	3.161155	1.503451
C	-0.685444	3.885821	2.299999
C	1.128156	2.171422	2.448675
C	1.426066	4.211846	1.003381
C	0.734605	1.701831	-0.537218
C	-0.045336	-1.657433	0.505047
C	-0.734832	-2.330303	-0.511812
C	-2.105437	-2.536427	-0.401496
C	-2.797728	-2.049327	0.70966
C	-4.270936	-2.316665	0.82796
F	-4.519974	-3.572829	1.265194
F	-4.875737	-1.471216	1.692615
F	-4.900498	-2.190014	-0.364774
C	-2.117539	-1.373643	1.724149
C	-0.741985	-1.19456	1.62675
H	6.700273	-2.077244	1.36182
H	4.99948	-2.537261	1.103532
H	5.390642	-1.08964	2.043796
H	5.482837	-2.597403	-1.421718
H	7.151963	-2.057672	-1.156268
H	6.091421	-1.148621	-2.246789
H	6.331416	0.985983	0.878453
H	6.633824	0.972291	-0.86516
H	7.652328	-0.000705	0.215508
H	0.853992	-0.085792	-3.424454
H	2.205634	0.65999	-2.524824
H	-1.451878	0.288696	-2.709003
H	-3.460988	0.572863	-3.323781
H	-5.02633	0.530912	-2.512255
H	-3.711529	-0.496929	-1.926896
H	-4.217278	2.346605	0.568234
H	-4.141827	0.584159	0.440582
H	-5.435411	1.481853	-0.367418
H	-4.896749	3.051573	-2.310083
H	-3.258187	3.084092	-2.996759
H	-3.566962	3.810181	-1.410872
H	-2.212879	2.856575	0.636948
H	-1.422922	3.184063	2.705423
H	-1.21477	4.621806	1.684337
H	-0.236	4.419344	3.144506
H	0.415223	1.448911	2.860923
H	1.585828	2.709977	3.287115
H	1.915293	1.612217	1.933808
H	0.94863	4.917136	0.313782
H	2.267181	3.744599	0.482339
H	1.830274	4.780267	1.849353
H	1.8004	1.722489	-0.346268
H	-0.204209	-2.691206	-1.382284
H	-2.639169	-3.066558	-1.182989
H	-2.658936	-0.994146	2.58297
H	-0.193773	-0.6962	2.417074

Table 2.24 Example computed structure of a B conformer of **1i** (31)

O	-2.927587	-1.918108	-0.750354
C	-2.183372	-1.123324	-0.205665
N	-2.527945	0.251501	-0.188851
O	-3.899352	0.489129	-0.382682
C	-4.707958	-0.019655	0.634931
C	-6.174681	0.183418	0.280718
C	-6.437824	1.671282	-0.027998
C	-6.480442	-0.680333	-0.963267
C	-7.029103	-0.274599	1.470105
O	-4.254991	-0.550378	1.614075
O	-2.048584	1.053177	0.835288
C	-1.364913	2.22562	0.28607
C	0.053224	1.925647	-0.109578
C	1.097703	2.185557	0.774939
C	2.422785	1.855581	0.45206
C	3.558777	2.192425	1.429915
C	3.585737	3.720581	1.651946
C	3.325695	1.484258	2.781862
C	4.934279	1.751806	0.901787
C	2.654358	1.248776	-0.783728
C	1.626226	0.972657	-1.700988
C	1.968868	0.36636	-3.069364
C	2.670249	1.451049	-3.916852
C	2.914876	-0.842135	-2.913238
C	0.712272	-0.110521	-3.817759
C	0.324715	1.328179	-1.347092
C	-0.799996	-1.48487	0.230726
C	-0.165701	-0.978636	1.369092
C	1.147075	-1.341688	1.65154
C	1.831586	-2.205424	0.799068
C	3.295793	-2.464288	1.001403
F	3.628324	-3.747271	0.743297
F	4.0492	-1.695465	0.169215
F	3.701864	-2.181972	2.259619
C	1.180059	-2.774479	-0.299268
C	-0.134217	-2.42086	-0.575102
H	-7.499423	1.809013	-0.259421
H	-5.850915	2.012927	-0.884227
H	-6.194313	2.303048	0.833387
H	-7.543501	-0.590823	-1.211754
H	-6.25764	-1.73504	-0.773031
H	-5.890885	-0.357304	-1.824895
H	-8.089346	-0.149762	1.226615
H	-6.808001	0.313498	2.366099
H	-6.84708	-1.327012	1.704383
H	-1.408217	2.940961	1.110543
H	-1.964579	2.598818	-0.548277
H	0.870703	2.650728	1.730667
H	2.648945	4.083122	2.087559
H	3.74195	4.247765	0.70427
H	4.400446	3.99154	2.33377
H	3.421858	0.399972	2.672417
H	2.335736	1.703179	3.195031
H	4.073655	1.813192	3.512797
H	4.968744	0.671407	0.729298
H	5.705687	1.998767	1.639235
H	5.193784	2.261356	-0.032774
H	3.668065	0.988532	-1.055889
H	3.592024	1.794627	-3.435219
H	2.017792	2.320547	-4.054273
H	2.929952	1.056258	-4.906535
H	3.149203	-1.258636	-3.899636
H	2.448604	-1.625385	-2.310672
H	3.860529	-0.574139	-2.43448
H	1.002695	-0.585787	-4.760863
H	0.040441	0.718827	-4.06276
H	0.150901	-0.843702	-3.227975
H	-0.502633	1.137328	-2.019757
H	-0.685224	-0.29119	2.019368
H	1.640118	-0.934016	2.5242
H	1.702924	-3.479208	-0.936714
H	-0.65418	-2.846425	-1.425886

Table 2.25 Example computed structure of an E conformer of **1i** (39)

O	-1.715297	-1.413265	-3.13938
C	-1.784599	-1.345095	-1.927656
N	-0.739678	-1.83223	-1.106382
O	-0.502126	-1.145123	0.12162
C	-0.461297	0.240903	0.057422
C	-0.256954	0.828404	1.446799
C	-0.082905	2.345762	1.29892
C	-1.520805	0.517672	2.280587
C	0.986221	0.207306	2.111913
O	-0.635228	0.850379	-0.968418
O	0.410217	-2.23838	-1.722051
C	1.223798	-1.186547	-2.332166
C	2.262812	-0.643762	-1.383006
C	2.57698	0.716399	-1.401117
C	3.59644	1.22988	-0.589142
C	3.996691	2.712333	-0.599024
C	5.444312	2.832487	-1.123951
C	3.081782	3.556542	-1.501694
C	3.926255	3.286276	0.832762
C	4.273759	0.335319	0.247726
C	3.963874	-1.030814	0.30903
C	4.729144	-1.936859	1.283319
C	4.518724	-1.424797	2.725164
C	4.251414	-3.396492	1.21777
C	6.23407	-1.902113	0.940377
C	2.951308	-1.507603	-0.52692
C	-3.009057	-0.915477	-1.188922
C	-3.417447	-1.525469	0.002488
C	-4.574794	-1.092898	0.642659
C	-5.319056	-0.045157	0.096369
C	-6.51471	0.481268	0.839421
F	-7.142203	-0.489028	1.539894
F	-6.157717	1.438307	1.730519
F	-7.423986	1.037467	0.010266
C	-4.923677	0.555852	-1.101976
C	-3.775645	0.112348	-1.748347
H	0.073598	2.792187	2.286254
H	-0.965217	2.804528	0.844224
H	0.781127	2.578688	0.671149
H	-2.423202	0.911701	1.801744
H	-1.42141	0.988998	3.264087
H	-1.648718	-0.558406	2.423894
H	0.889283	-0.876838	2.207501
H	1.105027	0.634779	3.113475
H	1.890125	0.421425	1.537539
H	0.580349	-0.405485	-2.733526
H	1.693902	-1.715378	-3.166885
H	2.010539	1.370571	-2.053124
H	5.759015	3.882734	-1.139873
H	5.522229	2.435739	-2.142193
H	6.147194	2.27873	-0.492997
H	3.135224	3.235439	-2.547465
H	3.392745	4.605962	-1.461395
H	2.034814	3.505978	-1.182812
H	4.213809	4.344065	0.829952
H	4.599323	2.76049	1.516923
H	2.911588	3.210722	1.237397
H	5.065915	0.716711	0.883557
H	4.873119	-0.396206	2.846141
H	5.066261	-2.054915	3.43598
H	3.457039	-1.4483	2.994344
H	3.190749	-3.486972	1.476407
H	4.821369	-4.002317	1.930438
H	4.39915	-3.827393	0.221572
H	6.408528	-2.263123	-0.079238
H	6.796358	-2.541414	1.631146
H	6.643421	-0.889437	1.01274
H	2.669356	-2.55292	-0.515822
H	-2.833654	-2.335584	0.423506
H	-4.899839	-1.567648	1.561698
H	-5.513154	1.361601	-1.524692
H	-3.453403	0.563299	-2.680068

Table 2.26 Example computed structure of an H conformer of **1i** (42)

O	-2.006526	2.630003	-1.230663
C	-2.04066	1.41641	-1.103361
N	-0.931762	0.642072	-1.436969
O	0.274961	1.312937	-1.641701
C	0.73607	2.055807	-0.549814
C	1.966626	2.849256	-0.958585
C	2.472373	3.613044	0.272108
C	3.052411	1.879729	-1.470287
C	1.558986	3.836134	-2.073973
O	0.198334	2.040779	0.525199
O	-0.800915	-0.676479	-1.090017
C	-0.352701	-0.930146	0.280223
C	1.150074	-1.001185	0.383802
C	1.889237	-1.649676	-0.602168
C	3.282671	-1.765353	-0.502605
C	4.065278	-2.467845	-1.620653
C	3.853099	-1.700706	-2.944126
C	5.574539	-2.52506	-1.334082
C	3.547709	-3.914122	-1.777169
C	3.902932	-1.217372	0.623269
C	3.187709	-0.547033	1.629815
C	3.942835	0.038979	2.831112
C	5.050271	0.995745	2.338362
C	3.01536	0.824077	3.773317
C	4.586566	-1.116141	3.628941
C	1.80192	-0.446657	1.49068
C	-3.272532	0.688314	-0.663226
C	-3.642837	-0.590337	-1.100943
C	-4.84007	-1.153184	-0.668529
C	-5.666532	-0.448999	0.209536
C	-6.92006	-1.09361	0.731921
F	-6.67634	-1.813341	1.853704
F	-7.864127	-0.181212	1.049651
F	-7.462907	-1.944171	-0.167064
C	-5.307693	0.829241	0.643201
C	-4.120849	1.398927	0.196587
H	3.369469	4.181333	0.005478
H	2.724926	2.924659	1.083336
H	1.716321	4.310049	0.644725
H	3.336113	1.158961	-0.698584
H	3.941792	2.455542	-1.749101
H	2.710342	1.324959	-2.347055
H	2.41955	4.46303	-2.331177
H	0.74284	4.487222	-1.744492
H	1.232433	3.306182	-2.972125
H	-0.812323	-1.899887	0.495297
H	-0.777508	-0.176537	0.944076
H	1.367351	-2.050257	-1.464922
H	2.79406	-1.646106	-3.215222
H	4.385876	-2.199208	-3.762542
H	4.231846	-0.676038	-2.863264
H	6.009061	-1.523178	-1.246113
H	6.085228	-3.037071	-2.156683
H	5.792148	-3.076562	-0.412699
H	3.684956	-4.478932	-0.848324
H	4.095122	-4.429121	-2.575342
H	2.483515	-3.938607	-2.031685
H	4.977582	-1.301	0.724246
H	4.624841	1.825525	1.76418
H	5.777752	0.485049	1.700003
H	5.59353	1.415921	3.19271
H	3.599543	1.24243	4.599952
H	2.240365	0.182957	4.207135
H	2.52138	1.654975	3.257547
H	5.288147	-1.687908	3.012714
H	3.820845	-1.808046	3.996842
H	5.137209	-0.723586	4.492052
H	1.21042	0.080164	2.229118
H	-3.005917	-1.140338	-1.78097
H	-5.135011	-2.135993	-1.019227
H	-5.95801	1.377444	1.315587
H	-3.836298	2.398646	0.504041

Table 2.27 Example computed structure of a G conformer of **1i** (71)

O	-0.521952	0.229591	-3.120795
C	0.13547	0.473138	-2.130338
N	0.057627	1.711288	-1.433738
O	1.382999	2.236847	-1.279456
C	1.639689	2.720987	-0.013261
C	3.12309	3.054154	0.117993
C	3.524349	4.063188	-0.978001
C	3.364231	3.65237	1.510055
C	3.927068	1.744968	-0.04776
O	0.794042	2.832473	0.838262
O	-0.763771	2.64271	-2.023688
C	-1.82579	3.014982	-1.078068
C	-2.375518	1.803394	-0.377368
C	-2.921803	0.760313	-1.136272
C	-3.231375	-0.463627	-0.547494
C	-3.685239	-1.678027	-1.367898
C	-4.998214	-2.249163	-0.794107
C	-3.912066	-1.327267	-2.847847
C	-2.573209	-2.749509	-1.294572
C	-3.034185	-0.596798	0.83912
C	-2.527204	0.436248	1.628813
C	-2.256735	0.278891	3.131407
C	-2.765497	-1.06314	3.682116
C	-0.732055	0.35588	3.373135
C	-2.957334	1.415041	3.906395
C	-2.189347	1.639848	0.990579
C	0.964659	-0.533763	-1.411287
C	1.007276	-0.554229	-0.010387
C	1.730433	-1.545304	0.644263
C	2.414319	-2.511337	-0.098351
C	3.254804	-3.535137	0.61294
F	4.510673	-3.076733	0.832189
F	2.740726	-3.857884	1.820327
F	3.372503	-4.67754	-0.097647
C	2.361542	-2.502295	-1.494855
C	1.625117	-1.520657	-2.150082
H	4.584503	4.31416	-0.866014
H	2.94565	4.989448	-0.893184
H	3.369904	3.65053	-1.978058
H	4.426583	3.890642	1.625237
H	3.078579	2.94869	2.297162
H	2.785706	4.569937	1.652592
H	4.993377	1.95942	0.079705
H	3.776196	1.305534	-1.037025
H	3.636314	1.002975	0.703131
H	-2.553063	3.504195	-1.73142
H	-1.423405	3.73885	-0.365209
H	-3.025406	0.899602	-2.204885
H	-4.888121	-2.564439	0.248357
H	-5.316358	-3.123414	-1.374163
H	-5.798519	-1.501769	-0.836607
H	-4.680995	-0.555323	-2.966352
H	-4.248232	-2.218952	-3.388432
H	-2.990927	-0.974821	-3.3225
H	-2.859459	-3.637335	-1.871268
H	-2.382661	-3.06299	-0.262837
H	-1.636853	-2.358337	-1.707262
H	-3.265959	-1.547957	1.302113
H	-2.571776	-1.116468	4.75896
H	-2.25867	-1.913776	3.213448
H	-3.844193	-1.179593	3.529096
H	-0.305506	1.28818	2.989968
H	-0.225549	-0.478091	2.873398
H	-0.510324	0.292431	4.445271
H	-2.77008	1.312406	4.981743
H	-4.040451	1.385989	3.743302
H	-2.596727	2.400946	3.597654
H	-1.720615	2.440844	1.550661
H	0.45393	0.186779	0.554078
H	1.754531	-1.576226	1.728127
H	2.884113	-3.264506	-2.061694
H	1.556552	-1.509027	-3.232518

Table 2.28 Example computed structure of a D conformer of **1i** (85)

O	-1.832768	-2.796117	-2.451632
C	-1.671485	-1.850436	-1.711732
N	-0.367553	-1.331964	-1.452646
O	-0.205996	-0.746416	-0.162882
C	-0.502566	-1.576695	0.905763
C	-0.143609	-0.879096	2.210927
C	-0.890253	0.470099	2.280853
C	-0.564619	-1.783403	3.376167
C	1.381299	-0.64049	2.230259
O	-0.986419	-2.670272	0.761857
O	0.63068	-2.258802	-1.675921
C	1.709197	-1.6489	-2.443173
C	2.497107	-0.650818	-1.639301
C	2.091608	0.685266	-1.599942
C	2.747313	1.612711	-0.786137
C	2.299745	3.076355	-0.67275
C	3.426229	3.996538	-1.189607
C	1.025867	3.357702	-1.48647
C	2.003244	3.407215	0.80634
C	3.848459	1.162901	-0.045367
C	4.290106	-0.166232	-0.068306
C	5.502427	-0.575849	0.779659
C	5.220659	-0.264997	2.26585
C	5.819997	-2.07487	0.655871
C	6.739088	0.223302	0.314156
C	3.588132	-1.069026	-0.874084
C	-2.79311	-1.039296	-1.14672
C	-2.720709	0.350091	-0.985714
C	-3.80961	1.048407	-0.473975
C	-4.969614	0.358718	-0.113298
C	-6.111055	1.105384	0.51826
F	-5.96646	1.183378	1.863433
F	-6.198348	2.374581	0.061646
F	-7.299293	0.507163	0.285966
C	-5.051808	-1.025537	-0.283861
C	-3.968283	-1.720004	-0.810669
H	-1.974482	0.329651	2.214855
H	-0.581792	1.137574	1.472167
H	-0.665749	0.956097	3.236259
H	-1.642527	-1.970356	3.362286
H	-0.308207	-1.299517	4.324285
H	-0.054484	-2.749726	3.329588
H	1.92864	-1.585224	2.144323
H	1.660804	-0.170306	3.179401
H	1.697581	0.010393	1.413168
H	1.275148	-1.200236	-3.341278
H	2.316219	-2.512137	-2.725406
H	1.23521	0.980703	-2.19402
H	3.129152	5.048694	-1.106791
H	3.648667	3.784938	-2.241315
H	4.349839	3.861416	-0.617426
H	0.189733	2.733369	-1.150263
H	1.177679	3.181218	-2.556731
H	0.732278	4.405377	-1.361304
H	1.679398	4.449974	0.904215
H	2.884755	3.270235	1.440155
H	1.20699	2.763912	1.196892
H	4.379142	1.874357	0.579092
H	4.353159	-0.829658	2.623772
H	5.019032	0.798477	2.428283
H	6.085581	-0.539812	2.880924
H	6.686047	-2.320075	1.279909
H	6.063568	-2.354676	-0.374874
H	4.98163	-2.695305	0.991437
H	6.961559	0.016558	-0.738526
H	7.616958	-0.05188	0.91054
H	6.586248	1.302236	0.419244
H	3.879583	-2.112697	-0.913656
H	-1.819514	0.88352	-1.264178
H	-3.760767	2.125421	-0.358199
H	-5.95883	-1.552944	-0.010701
H	-4.014981	-2.793303	-0.956397

Table 2.29 Example computed structure of a C conformer of **1i** (9)

O	1.791487	-0.656032	-1.578214
C	1.223572	-1.103482	-0.594793
N	1.971927	-1.438256	0.55054
O	3.22558	-0.801571	0.580104
C	4.266214	-1.60183	0.11953
C	5.555286	-0.786579	0.101841
C	5.395152	0.352728	-0.928853
C	5.81782	-0.196942	1.502856
C	6.705545	-1.71549	-0.308738
O	4.11535	-2.742736	-0.220588
O	1.414723	-1.471189	1.806064
C	1.224807	-0.144319	2.427521
C	0.353177	0.775276	1.630655
C	0.932046	1.581886	0.647736
C	0.142566	2.383128	-0.180065
C	0.738494	3.23269	-1.310624
C	0.390967	4.718058	-1.076481
C	2.267764	3.091034	-1.393103
C	0.148361	2.768244	-2.659875
C	-1.239272	2.388128	0.049624
C	-1.853318	1.616919	1.047676
C	-3.358368	1.762679	1.320378
C	-4.175079	1.774034	0.012221
C	-3.902691	0.627234	2.204962
C	-3.570602	3.106979	2.053632
C	-1.031473	0.793379	1.822821
C	-0.225896	-1.463407	-0.59031
C	-1.014495	-0.819504	-1.549675
C	-2.379565	-1.071031	-1.624804
C	-2.962724	-1.976813	-0.739096
C	-4.434971	-2.266238	-0.79622
F	-4.977054	-2.313335	0.445206
F	-5.114383	-1.328896	-1.494446
F	-4.694712	-3.459935	-1.376821
C	-2.176272	-2.652063	0.198997
C	-0.812266	-2.398543	0.274631
H	4.603213	1.046585	-0.636868
H	5.152483	-0.043127	-1.920235
H	6.336399	0.908512	-1.000804
H	5.899416	-0.987417	2.256943
H	5.021531	0.488405	1.805389
H	6.762021	0.357971	1.490178
H	6.530368	-2.145608	-1.298646
H	6.820579	-2.540334	0.400908
H	7.641335	-1.147528	-0.335564
H	2.216564	0.2802	2.599951
H	0.777022	-0.418917	3.384098
H	2.006485	1.547944	0.517744
H	0.816386	5.337526	-1.874601
H	0.796401	5.066169	-0.119879
H	-0.690873	4.885936	-1.063781
H	2.560099	2.052099	-1.577024
H	2.75779	3.435247	-0.475085
H	2.648785	3.699874	-2.220078
H	-0.945496	2.815026	-2.664864
H	0.451116	1.737742	-2.872752
H	0.516745	3.403865	-3.473627
H	-1.860909	3.027109	-0.567853
H	-4.069791	0.832281	-0.530922
H	-3.881759	2.589001	-0.656184
H	-5.237379	1.910409	0.244057
H	-4.98126	0.757931	2.343677
H	-3.445191	0.626417	3.199828
H	-3.742593	-0.354194	1.747937
H	-3.012355	3.129303	2.99615
H	-4.633197	3.256612	2.279492
H	-3.229809	3.948787	1.441074
H	-1.457288	0.15302	2.586743
H	-0.547418	-0.113921	-2.223711
H	-2.989219	-0.556876	-2.358384
H	-2.633294	-3.367113	0.874914
H	-0.210858	-2.916362	1.008945

Table 2.30 Example computed structure of an A conformer of **1f** (1)

O	-1.375639	3.430809	0.612962
C	-1.393334	2.385156	-0.005721
N	-0.338985	2.036233	-0.885814
O	-0.014039	0.65046	-0.995037
C	0.084079	-0.0574	0.196277
C	0.320349	-1.537191	-0.073678
C	0.748822	-2.201581	1.242752
C	-1.034454	-2.118066	-0.545966
C	1.392871	-1.755525	-1.156094
O	-0.086724	0.460248	1.272267
O	0.762357	2.848247	-0.903974
C	1.58965	2.84446	0.298667
C	2.664343	1.788545	0.233424
C	3.006011	1.056398	1.37425
C	4.006583	0.087998	1.321232
C	4.670275	-0.154662	0.117822
C	5.655308	-1.281656	0.021494
F	6.614522	-1.043763	-0.900025
F	6.272867	-1.523913	1.198521
F	5.04288	-2.437701	-0.34325
C	4.342597	0.578078	-1.026709
C	3.345737	1.545575	-0.965278
C	-2.56105	1.456706	-0.044018
C	-3.276917	1.261821	1.14198
C	-4.367709	0.40029	1.161838
C	-4.758213	-0.249155	-0.012814
C	-5.884387	-1.244194	0.023309
F	-6.794277	-0.946373	0.97564
F	-6.537456	-1.312788	-1.15719
F	-5.427398	-2.491546	0.292011
C	-4.067626	-0.031266	-1.206598
C	-2.964921	0.817379	-1.22131
H	0.889917	-3.274322	1.076881
H	-0.006319	-2.063816	2.020902
H	1.692679	-1.781523	1.602715
H	-1.341953	-1.683659	-1.500639
H	-1.826692	-1.934675	0.18713
H	-0.929589	-3.200292	-0.675139
H	2.369496	-1.39104	-0.82934
H	1.130472	-1.256443	-2.091734
H	1.48326	-2.829342	-1.351213
H	0.964582	2.743723	1.18397
H	2.024771	3.848141	0.287578
H	2.471664	1.228045	2.303187
H	4.262452	-0.483109	2.206972
H	4.862041	0.38564	-1.959172
H	3.074735	2.103689	-1.855204
H	-2.958979	1.776285	2.041727
H	-4.916462	0.233273	2.081826
H	-4.389815	-0.52342	-2.117364
H	-2.419322	0.985595	-2.142632

Table 2.31 Example computed structure of an F conformer of **1f** (45)

O	0.731679	-2.707494	-2.312716
C	0.859251	-2.135497	-1.24296
N	0.031847	-2.419623	-0.145552
O	-0.301584	-1.252471	0.601359
C	-0.094636	-1.395498	1.967723
C	-0.388796	-0.073668	2.67355
C	-1.723802	0.520311	2.189835
C	-0.43062	-0.335524	4.185258
C	0.762634	0.900777	2.333621
O	0.302432	-2.415452	2.464947
O	-1.040577	-3.255781	-0.296503
C	-2.00934	-2.905388	-1.351957
C	-2.633118	-1.552023	-1.177845
C	-3.714583	-1.375984	-0.306457
C	-4.269271	-0.116156	-0.112679
C	-3.735019	0.985215	-0.786908
C	-4.250193	2.359764	-0.474573
F	-4.036653	3.229886	-1.485099
F	-5.575781	2.358322	-0.211546
F	-3.636913	2.87391	0.622417
C	-2.667813	0.821609	-1.67169
C	-2.127257	-0.446585	-1.870394
C	1.96426	-1.173726	-0.959219
C	2.327785	-0.277404	-1.969656
C	3.37434	0.61572	-1.764473
C	4.07872	0.590299	-0.558326
C	5.169932	1.594094	-0.307567
F	4.685276	2.709042	0.289943
F	6.131117	1.101692	0.503727
F	5.766353	1.990174	-1.452687
C	3.742563	-0.327866	0.439307
C	2.682187	-1.206162	0.242414
H	-1.93049	1.443347	2.741313
H	-2.553681	-0.17201	2.362116
H	-1.695902	0.758361	1.126
H	-0.603926	0.608092	4.712734
H	0.509579	-0.766429	4.539452
H	-1.237809	-1.028192	4.443502
H	0.824537	1.086478	1.257966
H	1.727764	0.511139	2.67225
H	0.583001	1.854864	2.840302
H	-2.743342	-3.703815	-1.228529
H	-1.513941	-3.006463	-2.315522
H	-4.119324	-2.232268	0.225442
H	-5.106507	0.017392	0.56379
H	-2.266606	1.678632	-2.201126
H	-1.303077	-0.580358	-2.564937
H	1.786463	-0.28629	-2.909535
H	3.651399	1.321376	-2.539475
H	4.310292	-0.357667	1.36261
H	2.419108	-1.924318	1.010989

Table 2.32 Example computed structure of a D conformer of **1f** (52)

O	1.636433	3.655018	0.046582
C	1.396302	2.483214	-0.137368
N	0.055787	2.026924	-0.353785
O	-0.195774	0.702563	0.121559
C	0.109845	0.486552	1.458396
C	-0.184808	-0.958517	1.842718
C	-0.044825	-1.088237	3.365718
C	-1.601163	-1.36265	1.393324
C	0.868098	-1.843067	1.135148
O	0.59786	1.341995	2.151874
O	-0.875353	2.907225	0.167255
C	-1.974292	3.077177	-0.762775
C	-2.887581	1.879883	-0.761472
C	-3.751768	1.665887	0.31894
C	-4.529047	0.514886	0.385752
C	-4.445087	-0.435447	-0.635396
C	-5.179923	-1.736045	-0.495806
F	-4.449893	-2.636065	0.21256
F	-6.354191	-1.590911	0.156939
F	-5.446418	-2.305791	-1.691277
C	-3.605266	-0.222798	-1.729405
C	-2.831963	0.934538	-1.788831
C	2.444599	1.434721	-0.318551
C	3.582089	1.514422	0.491835
C	4.588457	0.561727	0.375012
C	4.469484	-0.457548	-0.57337
C	5.516719	-1.533049	-0.650757
F	5.637804	-2.031696	-1.90078
F	6.732939	-1.085413	-0.271485
F	5.210794	-2.575629	0.159057
C	3.351425	-0.522186	-1.407846
C	2.335558	0.418842	-1.275358
H	-0.227645	-2.126744	3.660041
H	-0.76743	-0.450155	3.88387
H	0.956892	-0.802154	3.697318
H	-1.719787	-1.285795	0.311042
H	-2.3608	-0.729728	1.861454
H	-1.794179	-2.399028	1.68883
H	0.724785	-2.88413	1.443229
H	1.886983	-1.543618	1.40262
H	0.768814	-1.787171	0.0482
H	-1.569053	3.282889	-1.757063
H	-2.478104	3.96949	-0.383284
H	-3.803288	2.399622	1.118372
H	-5.193077	0.348321	1.227028
H	-3.552111	-0.960006	-2.522911
H	-2.165528	1.095929	-2.631084
H	3.657391	2.315256	1.218757
H	5.463924	0.609957	1.012711
H	3.275946	-1.305751	-2.15346
H	1.459996	0.365634	-1.911922

Table 2.33 Example computed structure of a B conformer of **1f** (62)

O	-2.216057	0.403265	-2.032655
C	-1.688564	0.29823	-0.942867
N	-2.237775	-0.582105	0.020207
O	-3.620366	-0.781037	-0.104835
C	-4.365709	0.385565	0.080105
C	-5.838998	0.11002	-0.180815
C	-6.315322	-1.066592	0.695069
C	-6.636206	1.379291	0.147986
C	-5.988967	-0.245311	-1.67734
O	-3.853482	1.433576	0.374778
O	-1.896579	-0.395825	1.352872
C	-1.28996	-1.616184	1.870598
C	0.093214	-1.806811	1.314184
C	0.316668	-2.642722	0.217799
C	1.57965	-2.717343	-0.370625
C	2.622352	-1.945956	0.138823
C	3.986806	-1.974263	-0.486825
F	4.421813	-0.722988	-0.784256
F	4.909771	-2.508735	0.34612
F	4.017331	-2.689286	-1.631114
C	2.415168	-1.116965	1.246294
C	1.156956	-1.053912	1.828421
C	-0.36272	0.902976	-0.611104
C	-0.180488	1.753601	0.484779
C	1.066823	2.326776	0.711728
C	2.133883	2.032626	-0.140927
C	3.50898	2.544476	0.178671
F	4.187984	1.681634	0.98147
F	4.260658	2.713033	-0.928771
F	3.472113	3.726896	0.831695
C	1.949296	1.20064	-1.246279
C	0.694905	0.65308	-1.490698
H	-5.770981	-1.98542	0.463184
H	-7.381078	-1.241093	0.513562
H	-6.184906	-0.845392	1.760103
H	-7.698258	1.203848	-0.051968
H	-6.301978	2.223826	-0.46079
H	-6.523407	1.656265	1.200638
H	-5.437351	-1.155189	-1.926785
H	-5.617231	0.565108	-2.312444
H	-7.048572	-0.403704	-1.904618
H	-1.949652	-2.458066	1.644076
H	-1.277293	-1.443354	2.949141
H	-0.504289	-3.223706	-0.191228
H	1.747056	-3.35743	-1.229076
H	3.223745	-0.501079	1.621672
H	0.986455	-0.391183	2.671408
H	-1.010736	1.960047	1.1484
H	1.214752	2.993286	1.55424
H	2.782339	0.97383	-1.900015
H	0.534038	0.011999	-2.350395

Table 2.34 Example computed structure of an E conformer of **1f** (7)

O	1.375629	3.430615	-0.613024
C	1.393401	2.384984	0.005702
N	0.339104	2.03607	0.885861
O	0.014215	0.650307	0.995248
C	-0.084053	-0.05765	-0.196
C	-0.320407	-1.537394	0.074128
C	-0.748578	-2.201977	-1.2423
C	1.034243	-2.118268	0.546843
C	-1.393205	-1.755474	1.156331
O	0.086671	0.459907	-1.272046
O	-0.762264	2.848035	0.904068
C	-1.589569	2.844255	-0.298581
C	-2.664302	1.788385	-0.233377
C	-3.34591	1.545603	0.965237
C	-4.342914	0.578243	1.026598
C	-4.670525	-0.154528	-0.117923
C	-5.655793	-1.281333	-0.021772
F	-6.273532	-1.523111	-1.198811
F	-5.043583	-2.437622	0.342555
F	-6.614859	-1.043488	0.899909
C	-4.006582	0.087909	-1.321246
C	-3.005865	1.056156	-1.374191
C	2.561174	1.456605	0.043971
C	3.277155	1.261942	-1.141999
C	4.368026	0.400516	-1.161886
C	4.758493	-0.249063	0.012708
C	5.884762	-1.243994	-0.023501
F	6.537481	-1.313056	1.157162
F	5.427962	-2.491264	-0.292904
F	6.794914	-0.945671	-0.975427
C	4.067786	-0.031408	1.206462
C	2.965009	0.817147	1.221205
H	0.006787	-2.064404	-2.020268
H	-1.692296	-1.781919	-1.60261
H	-0.889799	-3.274679	-1.076282
H	0.929292	-3.200472	0.676143
H	1.341523	-1.683738	1.501532
H	1.826676	-1.935023	-0.186079
H	-1.483807	-2.829262	1.351516
H	-2.369708	-1.390853	0.829354
H	-1.130916	-1.256362	2.091986
H	-0.964496	2.743514	-1.18388
H	-2.024668	3.847945	-0.287492
H	-3.074989	2.103772	1.855155
H	-4.86253	0.385954	1.958994
H	-4.262382	-0.483252	-2.206975
H	-2.471342	1.227649	-2.303054
H	2.959245	1.776506	-2.041699
H	4.91687	0.23368	-2.081855
H	4.38994	-0.523661	2.117187
H	2.419333	0.985194	2.142511

Table 2.35 Example computed structure of a B conformer of **1g** (11)

O	-0.981517	3.370112	-0.645498
C	-1.054643	2.335735	-0.012857
N	-0.018979	1.946415	0.875704
O	0.240052	0.548325	0.998522
C	0.307632	-0.175825	-0.185198
C	0.486866	-1.659573	0.102103
C	-0.891355	-2.191871	0.562677
C	0.91114	-2.351779	-1.201507
C	1.53853	-1.894042	1.201374
O	0.16467	0.337702	-1.26727
O	1.12385	2.700923	0.878021
C	1.940767	2.63607	-0.32715
C	2.980382	1.546285	-0.240911
C	3.650214	1.300963	0.965557
C	4.637054	0.325482	1.041999
C	4.945372	-0.4043	-0.105821
N	5.976614	-1.444307	-0.031313
O	6.223286	-2.085025	-1.054053
O	6.538262	-1.621566	1.050478
C	4.295089	-0.185274	-1.317861
C	3.30763	0.794101	-1.375358
C	-2.264878	1.464866	0.033482
C	-2.989703	1.29592	-1.151139
C	-4.117918	0.483917	-1.165668
C	-4.535718	-0.141434	0.012581
C	-5.704897	-1.086136	-0.01768
F	-5.302971	-2.353254	-0.281203
F	-6.358446	-1.120463	1.163875
F	-6.601768	-0.752701	-0.970311
C	-3.835348	0.051934	1.204916
C	-2.695959	0.850645	1.214679
H	-1.200539	-1.73177	1.50468
H	-0.820632	-3.27421	0.712243
H	-1.665916	-1.998116	-0.18645
H	1.006317	-3.427759	-1.024999
H	1.876833	-1.973504	-1.550214
H	0.175153	-2.190726	-1.993283
H	1.252469	-1.418821	2.142478
H	2.51591	-1.505814	0.903163
H	1.638275	-2.97064	1.373805
H	2.417522	3.620641	-0.348049
H	1.309031	2.535071	-1.207242
H	3.382174	1.86939	1.849311
H	5.162315	0.119919	1.965728
H	4.557263	-0.778815	-2.184166
H	2.774854	0.96349	-2.305219
H	-2.649688	1.790482	-2.053959
H	-4.674324	0.3367	-2.084426
H	-4.178725	-0.420091	2.118566
H	-2.143423	0.999712	2.135149

Table 2.36 Example computed structure of an H conformer of **1g** (16)

O	2.653907	2.091736	-0.102463
C	1.873733	1.229336	-0.470895
N	2.340202	0.021971	-0.993332
O	3.720813	-0.192962	-0.932885
C	4.274785	-0.230629	0.348103
C	5.789511	-0.124328	0.254596
C	6.378473	-0.335405	1.655945
C	6.334647	-1.186135	-0.722497
C	6.124435	1.29428	-0.259917
O	3.610711	-0.320532	1.347927
O	1.593259	-1.12003	-1.089041
C	1.194901	-1.749554	0.185641
C	-0.305888	-1.82424	0.241678
C	-1.018997	-2.461677	-0.784017
C	-2.407934	-2.47977	-0.774893
C	-3.076069	-1.862882	0.282275
N	-4.542357	-1.855998	0.289352
O	-5.124138	-2.369464	-0.66723
O	-5.110541	-1.336324	1.249477
C	-2.395873	-1.243402	1.326338
C	-1.004631	-1.228871	1.296565
C	0.390944	1.395945	-0.446892
C	-0.143085	2.103737	0.637196
C	-1.519672	2.243524	0.765925
C	-2.363146	1.700125	-0.206973
C	-3.85256	1.823524	-0.040676
F	-4.519015	0.906353	-0.777592
F	-4.217935	1.649419	1.249497
F	-4.304898	3.040535	-0.416941
C	-1.832756	1.053611	-1.323593
C	-0.456395	0.892957	-1.439814
H	6.130658	-1.327723	2.045418
H	5.997999	0.409136	2.360445
H	7.468496	-0.245339	1.608573
H	5.939239	-1.045011	-1.731229
H	6.082441	-2.19883	-0.38901
H	7.425944	-1.106361	-0.764669
H	5.703456	2.060334	0.398113
H	5.728251	1.453965	-1.265601
H	7.212411	1.417169	-0.286579
H	1.614844	-1.17791	1.009913
H	1.649349	-2.744821	0.17211
H	-0.48122	-2.925929	-1.604715
H	-2.976513	-2.953808	-1.564442
H	-2.952895	-0.761549	2.118817
H	-0.45892	-0.723744	2.086709
H	0.529218	2.512521	1.383347
H	-1.940106	2.750606	1.627579
H	-2.493763	0.643526	-2.077652
H	-0.045796	0.354907	-2.28479

Table 2.37 Example computed structure of an F conformer of **1g** (44)

O	0.29459	-2.176245	-2.69793
C	0.49015	-1.81485	-1.54959
N	-0.335024	-2.229402	-0.4911
O	-0.573032	-1.190844	0.452847
C	-0.337485	-1.579151	1.767958
C	-0.541903	-0.385666	2.696516
C	-0.447273	-0.881717	4.145507
C	0.576994	0.641104	2.408344
C	-1.915562	0.260572	2.43465
O	0.008562	-2.690147	2.067554
O	-1.470311	-2.949142	-0.748179
C	-2.425614	-2.363751	-1.703795
C	-2.91607	-0.99625	-1.322599
C	-2.322982	0.144178	-1.880018
C	-2.755242	1.41696	-1.521801
C	-3.800336	1.529678	-0.607584
N	-4.261086	2.867729	-0.218438
O	-3.697903	3.839549	-0.723367
O	-5.182906	2.944493	0.594548
C	-4.421368	0.414739	-0.046812
C	-3.966747	-0.847785	-0.407575
C	1.669575	-0.999897	-1.137004
C	2.401936	-1.292836	0.020195
C	3.527132	-0.539133	0.33645
C	3.914457	0.514394	-0.495332
C	5.081451	1.378412	-0.103211
F	4.693858	2.386782	0.713695
F	6.025407	0.677143	0.561434
F	5.674121	1.946134	-1.175321
C	3.195546	0.800014	-1.658288
C	2.083026	0.031797	-1.986237
H	0.519945	-1.35301	4.340141
H	-1.22965	-1.614833	4.364397
H	-0.566337	-0.034265	4.828259
H	0.452342	1.501127	3.074599
H	0.538675	0.994904	1.374631
H	1.567527	0.211875	2.588068
H	-1.977718	0.666768	1.423822
H	-2.070505	1.078333	3.146284
H	-2.728181	-0.461542	2.565106
H	-3.231798	-3.098501	-1.667002
H	-1.967241	-2.367392	-2.690681
H	-1.520844	0.031703	-2.602493
H	-2.306598	2.309615	-1.938007
H	-5.23256	0.549289	0.65679
H	-4.431133	-1.729224	0.024134
H	2.099955	-2.115413	0.658634
H	4.106402	-0.77116	1.223258
H	3.511325	1.609817	-2.306098
H	1.52858	0.226909	-2.897784

Table 2.38 Example computed structure of a D conformer of **1g** (53)

O	-1.213617	3.604258	-0.069685
C	-1.039304	2.413782	-0.198153
N	0.279619	1.874995	-0.360019
O	0.452108	0.563689	0.174458
C	0.101259	0.421136	1.511646
C	0.343168	-1.011179	1.969025
C	0.121248	-1.076676	3.486219
C	-0.681897	-1.910957	1.241025
C	1.777256	-1.447809	1.612499
O	-0.373466	1.324889	2.149951
O	1.247666	2.722115	0.153794
C	2.352782	2.824796	-0.774458
C	3.191027	1.571833	-0.784523
C	3.067433	0.638564	-1.819644
C	3.795136	-0.54743	-1.798102
C	4.649639	-0.782224	-0.723597
N	5.412531	-2.03521	-0.684901
O	6.1579	-2.225553	0.276781
O	5.262615	-2.829225	-1.614394
C	4.800101	0.1303	0.319367
C	4.062657	1.307591	0.280244
C	-2.141595	1.420381	-0.364639
C	-3.303237	1.618416	0.389478
C	-4.36214	0.723074	0.285619
C	-4.269712	-0.358833	-0.593807
C	-5.379222	-1.371543	-0.654017
F	-5.485117	-1.932321	-1.878709
F	-5.169088	-2.382592	0.223271
F	-6.577735	-0.829676	-0.349126
C	-3.125446	-0.54278	-1.373232
C	-2.058865	0.342214	-1.253818
H	0.270874	-2.104787	3.831119
H	-0.892065	-0.763411	3.751552
H	0.825178	-0.428107	4.016687
H	-1.709081	-1.589875	1.443445
H	-0.568621	-2.940696	1.595893
H	-0.525609	-1.89848	0.159357
H	2.518447	-0.801851	2.09341
H	1.949656	-1.419579	0.534333
H	1.940084	-2.47202	1.964009
H	2.916707	3.679248	-0.392621
H	1.963515	3.060922	-1.768219
H	2.388853	0.837171	-2.643362
H	3.710013	-1.28276	-2.587685
H	5.478036	-0.09134	1.133373
H	4.15833	2.027846	1.08723
H	-3.356779	2.466171	1.063122
H	-5.257703	0.864002	0.880148
H	-3.069638	-1.374227	-2.066907
H	-1.165168	0.197251	-1.849399

Table 2.39 Example computed structure of a C conformer of **1g** (63)

O	0.399501	1.187872	1.642811
C	0.87111	0.891391	0.560767
N	0.096495	1.009507	-0.618788
O	-1.27477	1.188529	-0.341372
C	-1.64944	2.524097	-0.259868
C	-3.129651	2.60194	0.100544
C	-3.345769	1.894147	1.455746
C	-3.52261	4.08148	0.203088
C	-3.956508	1.902389	-0.998291
O	-0.884226	3.433531	-0.4338
O	0.246416	0.065762	-1.618752
C	0.053903	-1.317024	-1.182146
C	-1.352563	-1.622374	-0.746588
C	-2.378176	-1.71779	-1.696298
C	-3.688715	-1.955706	-1.300383
C	-3.95639	-2.099228	0.060618
N	-5.340349	-2.333994	0.489405
O	-6.209584	-2.392469	-0.381008
O	-5.555737	-2.455858	1.695557
C	-2.956822	-2.021357	1.026909
C	-1.650789	-1.782453	0.610905
C	2.297466	0.504253	0.362859
C	2.966648	-0.022691	1.475607
C	4.30362	-0.390275	1.379112
C	4.982451	-0.212667	0.171085
C	6.412177	-0.663474	0.043266
F	7.098182	0.083198	-0.848382
F	7.068979	-0.599076	1.22109
F	6.485769	-1.948127	-0.379638
C	4.328251	0.333812	-0.935568
C	2.986453	0.689393	-0.843891
H	-4.3966	1.990652	1.749387
H	-2.726638	2.344788	2.238289
H	-3.097756	0.832191	1.393415
H	-4.583759	4.159266	0.46151
H	-3.356943	4.601899	-0.744771
H	-2.938638	4.592228	0.974052
H	-3.689932	0.846998	-1.088813
H	-3.806699	2.38292	-1.971498
H	-5.020674	1.969098	-0.74767
H	0.775461	-1.543823	-0.391865
H	0.329378	-1.875646	-2.079244
H	-2.14946	-1.59178	-2.750169
H	-4.496594	-2.02762	-2.016923
H	-3.208651	-2.138316	2.072904
H	-0.86153	-1.695091	1.35114
H	2.426787	-0.132704	2.409451
H	4.82131	-0.802205	2.237957
H	4.869466	0.489287	-1.862037
H	2.481408	1.119221	-1.699396

Table 2.40 Example computed structure of an A conformer of **1g** (6)

O	1.778657	-1.261358	-1.826365
C	1.243085	-1.131118	-0.740723
N	1.983918	-0.643235	0.346614
O	3.358768	-0.920542	0.240926
C	4.130138	0.213259	0.032292
C	5.534793	-0.1903	-0.39437
C	5.428808	-0.676619	-1.85958
C	6.447049	1.040382	-0.304791
C	6.072495	-1.324458	0.500492
O	3.700695	1.332161	0.154644
O	1.541052	-0.841473	1.636957
C	1.3238	0.452012	2.293955
C	0.192709	1.191329	1.636756
C	-1.132414	0.867744	1.95607
C	-2.188316	1.402906	1.23025
C	-1.894513	2.289886	0.196311
N	-2.994437	2.791311	-0.631875
O	-4.098322	2.257969	-0.501532
O	-2.753203	3.701698	-1.425669
C	-0.591723	2.670748	-0.113658
C	0.455298	2.105293	0.608632
C	-0.231767	-1.286064	-0.53535
C	-1.066289	-0.650636	-1.461147
C	-2.449264	-0.744059	-1.33747
C	-2.997867	-1.514477	-0.311844
C	-4.485389	-1.544742	-0.101914
F	-5.168803	-1.226034	-1.217549
F	-4.909654	-2.762308	0.305888
F	-4.863466	-0.664325	0.861842
C	-2.16912	-2.199949	0.580079
C	-0.787778	-2.074753	0.479403
H	4.72993	-1.511754	-1.950211
H	6.417369	-0.999593	-2.203008
H	5.08391	0.129799	-2.514949
H	6.52478	1.401925	0.725727
H	6.068405	1.858727	-0.922609
H	7.450685	0.775508	-0.652818
H	5.459363	-2.225191	0.422245
H	6.106444	-1.018991	1.552029
H	7.092031	-1.572749	0.187502
H	2.257169	1.016255	2.266956
H	1.090474	0.161195	3.319984
H	-1.336636	0.155959	2.749769
H	-3.213176	1.115798	1.420903
H	-0.412683	3.364553	-0.92504
H	1.483084	2.3354	0.351442
H	-0.624746	-0.06491	-2.259585
H	-3.099011	-0.216683	-2.02601
H	-2.604547	-2.815579	1.359762
H	-0.145482	-2.578155	1.191039

Table 2.41 Example computed structure of an E conformer of **1g** (8)

O	-0.981618	3.369754	0.645494
C	-1.054724	2.335358	0.012883
N	-0.019024	1.946098	-0.875725
O	0.240171	0.548003	-0.998415
C	0.307826	-0.17604	0.185335
C	0.487379	-1.65977	-0.101865
C	-0.890652	-2.192301	-0.56274
C	1.539305	-1.89409	-1.20092
C	0.911478	-2.351874	1.201859
O	0.16468	0.33752	1.267372
O	1.123734	2.700697	-0.877995
C	1.940629	2.635994	0.327211
C	2.980403	1.546361	0.240949
C	3.650525	1.301419	-0.965438
C	4.637464	0.326043	-1.041929
C	4.945594	-0.404023	0.105762
N	5.976913	-1.443952	0.031195
O	6.538827	-1.620872	-1.050511
O	6.223373	-2.084957	1.053806
C	4.295051	-0.185353	1.317723
C	3.307489	0.79392	1.375271
C	-2.264998	1.464547	-0.033488
C	-2.69589	0.850063	-1.214619
C	-3.835399	0.051521	-1.204907
C	-4.536098	-0.141395	-0.012695
C	-5.705473	-1.085858	0.017527
F	-6.602528	-0.751976	0.969827
F	-6.358717	-1.120384	-1.164192
F	-5.303874	-2.352983	0.28151
C	-4.118476	0.484204	1.165486
C	-2.990126	1.296016	1.151008
H	-1.665429	-1.998612	0.186183
H	-0.819738	-3.274639	-0.712226
H	-1.199659	-1.732297	-1.504849
H	1.253294	-1.419017	-2.142114
H	1.639333	-2.970679	-1.373241
H	2.516542	-1.505602	-0.902583
H	1.00693	-3.427836	1.025379
H	0.175252	-2.190985	1.993448
H	1.876998	-1.973401	1.550832
H	1.308899	2.534898	1.207294
H	2.417227	3.62064	0.3481
H	3.38263	1.870054	-1.849103
H	5.162936	0.120766	-1.965602
H	4.557105	-0.779087	2.183933
H	2.774504	0.963018	2.305062
H	-2.14314	0.99882	-2.135009
H	-4.178628	-0.420695	-2.118513
H	-4.67513	0.337335	2.08415
H	-2.650257	1.79078	2.053771

Table 2.42 Example computed structure of a B conformer of **1e** (15)

O	-1.898294	-0.500492	-2.005373
C	-1.367381	-0.282825	-0.932753
N	-1.978322	0.592293	-0.009766
O	-3.375709	0.662145	-0.118599
C	-4.010264	-0.549771	0.153503
C	-5.506065	-0.423281	-0.09597
C	-6.181927	-1.734993	0.32524
C	-6.074453	0.759055	0.714736
C	-5.706426	-0.177796	-1.608474
O	-3.404188	-1.529044	0.502834
O	-1.595164	0.535964	1.318938
C	-1.057516	1.838306	1.724951
C	0.264119	2.113883	1.077353
C	1.430128	1.531228	1.580635
C	2.651143	1.658311	0.923489
C	2.713392	2.383271	-0.273537
O	3.84252	2.541397	-1.017597
C	5.056651	1.992041	-0.51559
C	1.556618	2.992408	-0.780371
C	0.347853	2.852135	-0.111143
C	0.008571	-0.759348	-0.592918
C	0.272757	-1.515696	0.55447
C	1.557822	-1.995748	0.783183
C	2.580885	-1.704333	-0.122938
C	3.987763	-2.121096	0.187117
F	4.041309	-3.267837	0.89564
F	4.731038	-2.29137	-0.926925
F	4.631825	-1.177724	0.935521
C	2.316974	-0.962395	-1.275256
C	1.025451	-0.507027	-1.517863
H	-7.258193	-1.667306	0.135724
H	-6.02997	-1.934444	1.390454
H	-5.781942	-2.583255	-0.236992
H	-5.616804	1.705866	0.417453
H	-5.910873	0.617058	1.788703
H	-7.153876	0.82762	0.542747
H	-6.778717	-0.13029	-1.826669
H	-5.269597	-0.989434	-2.199135
H	-5.24292	0.760572	-1.923018
H	-0.974948	1.728469	2.808841
H	-1.805542	2.601681	1.492638
H	1.382249	0.940654	2.491563
H	3.525305	1.160462	1.322078
H	4.992162	0.904988	-0.402023
H	5.323527	2.438698	0.450365
H	5.821301	2.238063	-1.253533
H	1.628419	3.556527	-1.704565
H	-0.548169	3.308229	-0.522603
H	-0.525588	-1.723722	1.255344
H	1.768224	-2.590744	1.665128
H	3.113246	-0.742997	-1.977528
H	0.80354	0.061884	-2.413555

Table 2.43 Example computed structure of an F conformer of **1e** (35)

O	-0.241807	-1.157333	-3.297022
C	-0.152641	-1.122382	-2.078247
N	-1.159095	-1.658598	-1.287912
O	-1.225276	-1.275565	0.06574
C	-0.843375	-2.28759	0.946188
C	-1.160978	-1.860265	2.376048
C	-0.695916	-0.414074	2.637291
C	-2.694276	-1.952301	2.548744
C	-0.456794	-2.83004	3.334681
O	-0.363453	-3.324951	0.580596
O	-2.404131	-1.886266	-1.798166
C	-3.062268	-0.68298	-2.359741
C	-2.969163	0.510816	-1.464734
C	-3.75777	0.608594	-0.306266
C	-3.597117	1.660888	0.579493
C	-2.632237	2.65243	0.326297
O	-2.53847	3.634842	1.261818
C	-1.563925	4.652558	1.065329
C	-1.852329	2.581953	-0.833045
C	-2.029608	1.511479	-1.714404
C	1.086761	-0.641846	-1.38297
C	2.306722	-1.131462	-1.863696
C	3.505953	-0.685268	-1.317639
C	3.489302	0.280247	-0.308849
C	4.776139	0.730655	0.323213
F	5.823527	0.618903	-0.522132
F	4.714798	2.020667	0.725286
F	5.075607	-0.005211	1.420288
C	2.276446	0.79803	0.150877
C	1.076326	0.334894	-0.38008
H	-0.889661	-0.161199	3.685177
H	-1.233216	0.300774	2.008959
H	0.377977	-0.303338	2.454649
H	-3.053023	-2.969443	2.35876
H	-3.20787	-1.266816	1.869427
H	-2.957712	-1.683306	3.577376
H	-0.769199	-3.861679	3.153089
H	-0.703975	-2.565927	4.368108
H	0.630336	-2.780887	3.216547
H	-4.086935	-1.039862	-2.482021
H	-2.617535	-0.493947	-3.337391
H	-4.49588	-0.160972	-0.096287
H	-4.200384	1.742793	1.477711
H	-1.648484	5.317148	1.925786
H	-1.757225	5.218254	0.145805
H	-0.551468	4.231546	1.025907
H	-1.11171	3.339764	-1.057183
H	-1.411671	1.4535	-2.606229
H	2.306074	-1.862653	-2.664505
H	4.450087	-1.075222	-1.680888
H	2.270463	1.565645	0.917171
H	0.138851	0.744942	-0.030226

Table 2.44 Example computed structure of a D conformer of **1e** (39)

O	-0.977933	3.544794	0.352554
C	-0.842236	2.37331	0.076531
N	0.450459	1.821225	-0.182048
O	0.582561	0.442453	0.168361
C	0.278601	0.138285	1.485481
C	0.522407	-1.342403	1.74764
C	-0.476869	-2.148271	0.887433
C	1.969123	-1.705649	1.357744
C	0.278711	-1.615559	3.23766
O	-0.154713	0.957764	2.255017
O	1.459408	2.556712	0.406503
C	2.561881	2.731378	-0.52878
C	3.355032	1.473524	-0.736699
C	4.30448	1.068513	0.203786
C	5.011373	-0.125454	0.058702
C	4.762649	-0.940882	-1.052659
O	5.387411	-2.126369	-1.29562
C	6.332334	-2.590394	-0.340146
C	3.814923	-0.544059	-2.008129
C	3.123591	0.648694	-1.846167
C	-1.985183	1.445187	-0.180023
C	-3.12814	1.604083	0.611001
C	-4.225662	0.770336	0.426801
C	-4.190629	-0.209539	-0.56869
C	-5.343162	-1.161718	-0.722941
F	-6.513796	-0.608823	-0.33836
F	-5.489322	-1.575992	-2.00103
F	-5.167499	-2.274297	0.030892
C	-3.064703	-0.351651	-1.382943
C	-1.960284	0.470814	-1.185013
H	-0.303242	-1.987291	-0.179553
H	-1.511933	-1.870259	1.112904
H	-0.35465	-3.215382	1.101492
H	2.693068	-1.118012	1.931004
H	2.15736	-1.526884	0.297193
H	2.14357	-2.76602	1.570891
H	0.96498	-1.036145	3.86261
H	0.436357	-2.679383	3.44339
H	-0.742849	-1.352643	3.526045
H	3.156189	3.509702	-0.043706
H	2.156721	3.118718	-1.467901
H	4.496937	1.693298	1.072451
H	5.743212	-0.407145	0.805941
H	7.177169	-1.897323	-0.242896
H	6.691738	-3.549022	-0.716436
H	5.867143	-2.734644	0.643063
H	3.641218	-1.186912	-2.864988
H	2.385228	0.944264	-2.586661
H	-3.137508	2.373766	1.374452
H	-5.106985	0.88079	1.048494
H	-3.052962	-1.101548	-2.166023
H	-1.081705	0.357418	-1.809007

Table 2.45 Example computed structure of a C conformer of **1e** (42)

O	-0.09641	0.994726	1.650015
C	-0.60247	0.809208	0.556962
N	0.140833	1.000789	-0.623885
O	1.526958	1.104527	-0.382054
C	1.956039	2.402943	-0.166878
C	3.447612	2.380077	0.156808
C	3.657665	1.54174	1.436875
C	4.215144	1.742561	-1.020001
C	3.914678	3.823882	0.381112
O	1.229504	3.359756	-0.215617
O	-0.0868	0.20262	-1.724361
C	0.025317	-1.246092	-1.466173
C	1.374214	-1.683207	-0.990766
C	2.452793	-1.779217	-1.883513
C	3.721105	-2.112706	-1.434988
C	3.941746	-2.356727	-0.069066
O	5.221682	-2.66118	0.276204
C	5.510422	-2.864588	1.654164
C	2.872922	-2.280981	0.831617
C	1.602862	-1.945457	0.360138
C	-2.050735	0.495377	0.372665
C	-2.771684	0.819226	-0.784904
C	-4.130004	0.527478	-0.858801
C	-4.770337	-0.092892	0.216583
C	-6.221134	-0.472018	0.101871
F	-6.366986	-1.706503	-0.436767
F	-6.834549	-0.494398	1.304993
F	-6.905422	0.38323	-0.688458
C	-4.059159	-0.409146	1.376626
C	-2.705004	-0.105581	1.455967
H	3.083119	1.95157	2.27424
H	4.719568	1.558202	1.707133
H	3.350095	0.504558	1.285182
H	4.061469	2.310008	-1.944819
H	3.901796	0.709826	-1.189185
H	5.287478	1.745989	-0.795377
H	3.371614	4.290647	1.207882
H	3.756323	4.434801	-0.51261
H	4.983546	3.828556	0.619595
H	-0.222462	-1.651998	-2.449636
H	-0.761927	-1.52621	-0.759816
H	2.294303	-1.576914	-2.939519
H	4.561647	-2.186931	-2.1172
H	6.580854	-3.066436	1.708159
H	4.956888	-3.721878	2.05657
H	5.275538	-1.970744	2.245149
H	3.016111	-2.471973	1.887975
H	0.784124	-1.866097	1.070021
H	-2.276407	1.30288	-1.616903
H	-4.694283	0.789647	-1.746758
H	-4.564902	-0.878473	2.212899
H	-2.139133	-0.322395	2.355011

Table 2.46 Example computed structure of an A conformer of **1e** (4)

O	-1.726796	-1.43998	-1.615016
C	-1.18486	-1.134201	-0.565637
N	-1.923814	-0.524286	0.447564
O	-3.295702	-0.831066	0.407515
C	-4.079745	0.215308	-0.053445
C	-5.488866	-0.288417	-0.339792
C	-6.022578	-1.0969	0.859892
C	-6.393458	0.920338	-0.613478
C	-5.405254	-1.191291	-1.592358
O	-3.662882	1.334198	-0.208876
O	-1.464896	-0.458576	1.738578
C	-1.244224	0.952058	2.121002
C	-0.132832	1.568047	1.332186
C	1.197555	1.377991	1.713788
C	2.253597	1.822781	0.921677
C	1.975274	2.473438	-0.287234
O	2.924557	2.91827	-1.156246
C	4.291496	2.768126	-0.787851
C	0.644494	2.69083	-0.672356
C	-0.395694	2.237524	0.127477
C	0.295183	-1.23513	-0.36155
C	1.105878	-0.781612	-1.407198
C	2.489909	-0.87232	-1.30957
C	3.064531	-1.454803	-0.178714
C	4.556692	-1.47488	-0.028082
F	5.005982	-0.351708	0.6042
F	4.985336	-2.521516	0.707746
F	5.192611	-1.521235	-1.217547
C	2.259378	-1.947866	0.850379
C	0.876305	-1.827639	0.765459
H	-5.409335	-1.979807	1.055024
H	-7.044333	-1.426539	0.643711
H	-6.049456	-0.486341	1.769232
H	-6.018715	1.511665	-1.453091
H	-6.45403	1.576102	0.260944
H	-7.40335	0.572591	-0.854389
H	-6.404475	-1.573565	-1.827455
H	-4.731703	-2.035686	-1.428248
H	-5.039961	-0.628204	-2.457307
H	-1.00696	0.862755	3.183296
H	-2.190357	1.481685	1.99418
H	1.419536	0.847553	2.636221
H	3.272272	1.623673	1.228548
H	4.559944	1.715302	-0.653884
H	4.515432	3.316548	0.135786
H	4.869264	3.191505	-1.610588
H	0.452733	3.201518	-1.610558
H	-1.424117	2.373222	-0.190358
H	0.644049	-0.343185	-2.284155
H	3.118913	-0.493774	-2.107352
H	2.713239	-2.414451	1.717707
H	0.25181	-2.183486	1.574985

Table 2.47 Example computed structure of an H conformer of **1e** (76)

O	-2.621724	-2.233847	-0.269823
C	-1.750786	-1.416531	-0.519894
N	-2.063238	-0.132348	-0.959439
O	-3.416491	0.229213	-0.928704
C	-4.018132	0.218191	0.330348
C	-5.52971	0.31392	0.176007
C	-5.895492	1.526586	-0.703916
C	-6.013649	-0.993147	-0.49153
C	-6.150896	0.460129	1.57168
O	-3.393833	0.130117	1.354629
O	-1.177242	0.90824	-0.88705
C	-0.857177	1.386995	0.481871
C	0.541555	1.909636	0.435855
C	0.82039	3.192603	-0.039014
C	2.131979	3.657308	-0.148632
C	3.192291	2.819425	0.220354
O	4.507565	3.163583	0.148449
C	4.834701	4.457398	-0.341319
C	2.926344	1.529029	0.704227
C	1.616514	1.088501	0.810303
C	-0.288259	-1.721058	-0.443119
C	0.134686	-2.523863	0.623099
C	1.485796	-2.814509	0.783852
C	2.412063	-2.326965	-0.142049
C	3.879071	-2.545104	0.095331
F	4.126397	-3.733842	0.686579
F	4.595209	-2.499574	-1.047031
F	4.389475	-1.590515	0.918026
C	1.988718	-1.568435	-1.234935
C	0.640757	-1.259078	-1.382024
H	-5.472972	1.436533	-1.707533
H	-5.536725	2.461484	-0.259198
H	-6.985262	1.590598	-0.791758
H	-5.720054	-1.866921	0.098145
H	-5.595072	-1.103185	-1.494881
H	-7.106304	-0.974749	-0.566379
H	-5.896276	-0.391801	2.207994
H	-7.240648	0.514418	1.480934
H	-5.799775	1.369709	2.068824
H	-0.963073	0.549939	1.169911
H	-1.591842	2.15406	0.738846
H	0.002176	3.844664	-0.334204
H	2.31425	4.658737	-0.519011
H	5.923514	4.518618	-0.319241
H	4.412112	5.244692	0.295302
H	4.481984	4.596164	-1.37092
H	3.756541	0.885744	0.973927
H	1.421864	0.088227	1.183847
H	-0.600506	-2.898946	1.326518
H	1.820206	-3.415615	1.622162
H	2.712372	-1.202978	-1.954176
H	0.315641	-0.642205	-2.210189

Table 2.48 Example computed structure of a B conformer of **1d** (11)

O	1.996275	-1.247824	-1.827413
C	1.470356	-1.18411	-0.729104
N	2.190068	-0.683381	0.360043
O	1.772864	-0.918463	1.648303
C	1.443599	0.355724	2.310702
C	0.275271	1.035182	1.66285
C	0.474429	1.991236	0.66032
C	-0.613035	2.554161	-0.000759
C	-1.932361	2.179464	0.299516
C	-3.099721	2.831625	-0.452915
C	-4.461502	2.256029	-0.031146
C	-3.1005	4.347858	-0.157735
C	-2.929061	2.610957	-1.971407
C	-2.118923	1.218375	1.302339
C	-1.033613	0.661636	1.976322
O	3.579491	-0.873278	0.23545
C	4.27932	0.303711	0.024663
C	5.70383	-0.017497	-0.410311
C	6.541859	1.265296	-0.329276
C	6.313533	-1.114295	0.484734
C	5.620262	-0.513699	-1.873234
O	3.788374	1.396257	0.149838
C	0.015887	-1.464001	-0.511057
C	-0.874133	-0.93144	-1.449736
C	-2.238553	-1.170223	-1.331922
C	-2.713887	-1.968267	-0.290464
C	-4.192224	-2.142655	-0.101726
F	-4.702798	-1.176718	0.71126
F	-4.870339	-2.061857	-1.266263
F	-4.49973	-3.326278	0.470136
C	-1.826412	-2.541326	0.622244
C	-0.463762	-2.282962	0.518037
H	2.33966	0.979197	2.302754
H	1.22495	0.030843	3.330319
H	1.486655	2.272635	0.388943
H	-0.425662	3.29633	-0.770967
H	-4.524266	1.177759	-0.205225
H	-5.257669	2.737016	-0.609623
H	-4.666043	2.440023	1.029345
H	-2.167503	4.822111	-0.478665
H	-3.221068	4.534271	0.915131
H	-3.927319	4.837584	-0.685776
H	-2.932675	1.543303	-2.212402
H	-1.991652	3.035742	-2.343361
H	-3.752254	3.086114	-2.517403
H	-3.115107	0.876322	1.554041
H	-1.208856	-0.090979	2.740774
H	6.60372	1.63357	0.699905
H	6.110786	2.057952	-0.946229
H	7.557565	1.060176	-0.682947
H	7.345119	-1.301564	0.168249
H	5.755349	-2.050512	0.411752
H	6.332884	-0.804414	1.535361
H	4.971871	-1.389238	-1.95787
H	6.624488	-0.778039	-2.221737
H	5.223565	0.268421	-2.528795
H	-0.490159	-0.318658	-2.25719
H	-2.932586	-0.74337	-2.046516
H	-2.200878	-3.178012	1.41616
H	0.222438	-2.705462	1.240436

Table 2.49 Example computed structure of an E conformer of **1d** (13)

O	1.996266	-1.247797	-1.827425
C	1.470343	-1.184055	-0.729123
N	2.190078	-0.683398	0.360069
O	1.772865	-0.918596	1.648312
C	1.443574	0.355542	2.310815
C	0.275264	1.03503	1.662959
C	0.474471	1.991235	0.660582
C	-0.612955	2.554179	-0.000545
C	-1.932287	2.17936	0.299537
C	-3.099617	2.831577	-0.452899
C	-3.100602	4.347737	-0.157349
C	-2.928733	2.611304	-1.971423
C	-4.461391	2.255733	-0.031448
C	-2.118901	1.218128	1.302218
C	-1.03363	0.661358	1.97624
O	3.5795	-0.873287	0.235441
C	4.27934	0.303702	0.024771
C	5.703792	-0.017522	-0.410377
C	6.541929	1.265191	-0.329155
C	6.313504	-1.114579	0.484337
C	5.619989	-0.513403	-1.873403
O	3.788433	1.396251	0.150096
C	0.015851	-1.463824	-0.511052
C	-0.874184	-0.931076	-1.449605
C	-2.238605	-1.169892	-1.331805
C	-2.713921	-1.968114	-0.290473
C	-4.192262	-2.142572	-0.101794
F	-4.499733	-3.326222	0.470025
F	-4.702938	-1.176685	0.711198
F	-4.870339	-2.061771	-1.266349
C	-1.82643	-2.541301	0.622139
C	-0.463781	-2.282926	0.517935
H	2.339613	0.979042	2.302985
H	1.224882	0.030565	3.330393
H	1.486712	2.272743	0.389372
H	-0.425546	3.296465	-0.770634
H	-3.221343	4.533875	0.915545
H	-3.927399	4.837504	-0.685389
H	-2.167608	4.822167	-0.478028
H	-3.751931	3.086461	-2.51741
H	-2.932148	1.543707	-2.212672
H	-1.991345	3.036325	-2.343158
H	-5.257523	2.736703	-0.609989
H	-4.66614	2.439532	1.029036
H	-4.52399	1.177483	-0.205702
H	-3.11509	0.876001	1.553785
H	-1.208907	-0.091375	2.740568
H	6.603857	1.633291	0.700088
H	6.110893	2.05799	-0.945951
H	7.557608	1.060061	-0.682903
H	5.755196	-2.050712	0.411243
H	6.333053	-0.804926	1.53502
H	7.345019	-1.301904	0.167652
H	6.624144	-0.777749	-2.222104
H	5.223266	0.268892	-2.528741
H	4.971519	-1.388871	-1.958128
H	-0.490228	-0.318166	-2.256971
H	-2.932646	-0.742969	-2.046349
H	-2.200869	-3.178123	1.415956
H	0.222438	-2.705551	1.240247

Table 2.50 Example computed structure of an A conformer of **1d** (1)

O	2.219688	-1.832306	-1.31126
C	1.617146	-1.399959	-0.342363
N	2.272542	-0.527062	0.537193
O	1.863783	-0.386854	1.841929
C	1.569526	1.028797	2.124597
C	0.307596	1.474195	1.452018
C	0.327886	1.936762	0.130199
C	-0.861278	2.239285	-0.525088
C	-2.109351	2.09582	0.104493
C	-3.394449	2.46057	-0.650782
C	-3.36631	3.971034	-0.972884
C	-3.479758	1.65948	-1.967684
C	-4.65953	2.159206	0.170046
C	-2.113567	1.646842	1.431031
C	-0.925062	1.3429	2.093504
O	3.675981	-0.659332	0.485161
C	4.291165	0.372125	-0.205894
C	5.750633	0.017414	-0.462986
C	6.47102	1.264364	-0.992632
C	6.419405	-0.477861	0.835013
C	5.765577	-1.103908	-1.527727
O	3.715311	1.371721	-0.5524
C	0.141984	-1.591635	-0.169663
C	-0.600914	-1.616574	-1.357921
C	-1.981274	-1.771342	-1.323232
C	-2.626387	-1.920965	-0.094197
C	-4.118517	-2.073423	-0.030194
F	-4.642037	-1.391376	1.019524
F	-4.727117	-1.613063	-1.146657
F	-4.494485	-3.363362	0.122473
C	-1.888578	-1.950251	1.089702
C	-0.508564	-1.780868	1.05558
H	2.438047	1.61522	1.817721
H	1.483955	1.036392	3.213294
H	1.278922	2.036398	-0.383642
H	-0.81387	2.594126	-1.550195
H	-3.302846	4.563789	-0.053576
H	-4.278326	4.262714	-1.507052
H	-2.508897	4.232706	-1.601459
H	-2.600651	1.814358	-2.60065
H	-4.36224	1.971917	-2.538267
H	-3.570448	0.588856	-1.766739
H	-5.546884	2.414853	-0.419103
H	-4.695493	2.748476	1.092962
H	-4.72825	1.09908	0.433606
H	-3.050305	1.518643	1.960157
H	-0.961614	0.981174	3.118625
H	6.460251	2.072341	-0.25412
H	5.997857	1.635551	-1.905515
H	7.513659	1.015511	-1.216051
H	7.472288	-0.701489	0.633072
H	5.940854	-1.38406	1.213718
H	6.380486	0.287117	1.618443
H	6.802709	-1.388355	-1.735827
H	5.30806	-0.762614	-2.461994
H	5.217366	-1.984031	-1.18384
H	-0.083777	-1.496259	-2.302703
H	-2.555142	-1.759433	-2.242411
H	-2.394541	-2.074879	2.040894
H	0.055277	-1.776338	1.977201

Table 2.51 Example computed structure of an H conformer of **1d** (51)

O	3.045912	2.067935	-0.170375
C	2.195666	1.250393	-0.485934
N	2.555933	-0.003491	-0.973133
O	1.714694	-1.077096	-1.004684
C	1.28969	-1.617969	0.309359
C	-0.204063	-1.741429	0.300468
C	-0.849343	-2.527585	-0.662406
C	-2.236619	-2.593009	-0.705883
C	-3.036697	-1.892977	0.214554
C	-4.564578	-2.004122	0.129919
C	-4.976228	-3.486577	0.262495
C	-5.271046	-1.207499	1.238941
C	-5.037742	-1.458456	-1.235171
C	-2.380292	-1.116858	1.176485
C	-0.986986	-1.039949	1.216686
O	3.918625	-0.325682	-0.922399
C	4.485113	-0.369612	0.350829
C	6.002421	-0.41108	0.233715
C	6.592232	-0.613173	1.635923
C	6.428118	-1.563635	-0.698633
C	6.461635	0.943937	-0.350729
O	3.833242	-0.359142	1.362336
C	0.72931	1.536095	-0.433971
C	0.297478	2.365799	0.609296
C	-1.051027	2.667969	0.745595
C	-1.96955	2.162651	-0.179603
C	-3.422567	2.484497	0.014897
F	-4.208754	1.963906	-0.952368
F	-3.878111	2.00431	1.202129
F	-3.64286	3.817877	0.036729
C	-1.541778	1.369481	-1.242992
C	-0.192778	1.049668	-1.3665
H	1.64799	-0.955481	1.09385
H	1.791968	-2.58553	0.405646
H	-0.259763	-3.078953	-1.390238
H	-2.706105	-3.20605	-1.469306
H	-4.646896	-3.897321	1.223406
H	-4.54469	-4.103078	-0.532394
H	-6.066858	-3.582016	0.20522
H	-6.355332	-1.329181	1.141839
H	-5.048545	-0.138912	1.176153
H	-4.984813	-1.562389	2.235389
H	-4.776393	-0.401208	-1.338478
H	-6.126635	-1.55158	-1.323684
H	-4.585614	-2.005518	-2.068877
H	-2.950419	-0.540197	1.894423
H	-0.508309	-0.405306	1.957306
H	7.685081	-0.629835	1.571616
H	6.257457	-1.558192	2.074797
H	6.295257	0.195617	2.309092
H	7.521258	-1.591267	-0.758824
H	6.029972	-1.431929	-1.707595
H	6.086021	-2.530949	-0.31427
H	6.123537	1.775908	0.274489
H	6.067092	1.093752	-1.358619
H	7.555922	0.963393	-0.394608
H	1.028064	2.755628	1.309142
H	-1.391917	3.292174	1.565186
H	-2.258709	0.983311	-1.957082
H	0.13535	0.40723	-2.173117

Table 2.52 Example computed structure of an A conformer of **1a** (10)

O	-1.564449	-0.625374	2.014703
C	-1.021364	-0.298081	0.977376
N	-1.670132	0.594707	0.093719
O	-3.071595	0.540298	0.14418
C	-3.589611	-0.698924	-0.232279
C	-5.100594	-0.70983	-0.052581
C	-5.727507	0.474144	-0.816423
C	-5.64423	-2.040794	-0.588981
C	-5.391115	-0.582166	1.459884
O	-2.888071	-1.601465	-0.608741
O	-1.234202	0.649228	-1.220976
C	-0.805789	2.009762	-1.535289
C	0.454803	2.379606	-0.807119
C	0.400696	3.118052	0.379127
C	1.566408	3.386638	1.098357
C	2.794081	2.909264	0.638934
C	2.856972	2.16818	-0.543953
C	1.693041	1.911158	-1.263648
C	0.394854	-0.640929	0.64509
C	0.739864	-1.300515	-0.540314
C	2.067645	-1.634957	-0.78107
C	3.051164	-1.294079	0.151594
C	4.495441	-1.537326	-0.175336
F	5.258691	-1.660384	0.931671
F	4.669849	-2.652727	-0.917107
F	5.020005	-0.509511	-0.896811
C	2.706109	-0.656674	1.343804
C	1.373639	-0.348517	1.598057
H	-5.502071	0.417823	-1.887072
H	-5.365685	1.432911	-0.436805
H	-6.815748	0.443425	-0.697405
H	-6.729842	-2.07281	-0.450364
H	-5.200455	-2.889433	-0.061338
H	-5.427932	-2.155978	-1.655519
H	-4.914883	-1.39264	2.021011
H	-6.472543	-0.637502	1.624422
H	-5.024861	0.368348	1.855895
H	-1.629986	2.691899	-1.307545
H	-0.65893	1.966755	-2.617095
H	-0.558816	3.4748	0.743079
H	1.514104	3.962321	2.018031
H	3.700967	3.109007	1.202736
H	3.80486	1.768688	-0.888942
H	1.738313	1.321052	-2.174714
H	-0.029406	-1.544083	-1.262046
H	2.342853	-2.151481	-1.69416
H	3.473502	-0.401133	2.0654
H	1.090058	0.143109	2.521887

Table 2.53 Example computed structure of a B conformer of **1a** (12)

O	1.564583	-0.626047	2.014309
C	1.021372	-0.298466	0.977135
N	1.670035	0.594377	0.093537
O	3.071485	0.540161	0.144063
C	3.589672	-0.699006	-0.232408
C	5.100611	-0.709753	-0.052448
C	5.39079	-0.582434	1.460114
C	5.644549	-2.040486	-0.589097
C	5.727495	0.474519	-0.81585
O	2.888283	-1.601588	-0.609033
O	1.234066	0.649101	-1.221122
C	0.805898	2.009766	-1.535222
C	-0.454661	2.379679	-0.807037
C	-0.400525	3.118478	0.378982
C	-1.566197	3.387155	1.098239
C	-2.793855	2.909488	0.639088
C	-2.856778	2.168058	-0.54358
C	-1.692893	1.910981	-1.263325
C	-0.394918	-0.641118	0.644975
C	-1.373602	-0.348793	1.598063
C	-2.706111	-0.656831	1.343867
C	-3.051291	-1.294056	0.151598
C	-4.495597	-1.537179	-0.175301
F	-5.258905	-1.65984	0.931704
F	-5.019984	-0.509489	-0.897079
F	-4.670134	-2.65275	-0.916788
C	-2.067867	-1.634856	-0.781195
C	-0.740054	-1.300502	-0.540502
H	5.024371	0.367959	1.856265
H	6.472182	-0.637729	1.624888
H	4.914487	-1.393064	2.020947
H	5.200817	-2.889331	-0.061748
H	6.730142	-2.072364	-0.450295
H	5.428463	-2.155432	-1.655702
H	5.365327	1.433123	-0.436148
H	5.502418	0.41836	-1.88658
H	6.815705	0.444026	-0.696481
H	0.659089	1.966961	-2.617045
H	1.6302	2.691726	-1.30733
H	0.558984	3.475434	0.742742
H	-1.513868	3.963115	2.017738
H	-3.700707	3.109286	1.202923
H	-3.804656	1.768381	-0.888378
H	-1.738188	1.320627	-2.174226
H	-1.089918	0.14267	2.521949
H	-3.473434	-0.401345	2.065554
H	-2.343175	-2.15124	-1.694333
H	0.02915	-1.543976	-1.262341

Table 2.54 Example computed structure of an H conformer of **1a** (17)

O	-0.131308	-2.551155	-0.289794
C	-0.417379	-1.395557	-0.558189
N	0.540112	-0.541547	-1.102688
O	1.870933	-0.960008	-1.054342
C	2.373629	-1.198747	0.229093
C	3.77169	-1.787342	0.130207
C	4.388516	-1.793962	1.535776
C	3.624007	-3.230596	-0.402894
C	4.641399	-0.949173	-0.827578
O	1.742313	-0.978227	1.228134
O	0.374205	0.815933	-1.193825
C	0.629936	1.5716	0.032613
C	2.074193	1.987858	0.153105
C	2.72228	1.946871	1.39127
C	4.047463	2.369483	1.510116
C	4.737982	2.829874	0.388009
C	4.096771	2.866893	-0.853046
C	2.771642	2.450814	-0.968918
C	-1.802341	-0.850507	-0.397103
C	-2.560542	-1.419865	0.634741
C	-3.870201	-1.00871	0.854661
C	-4.43924	-0.041202	0.023492
C	-5.835212	0.448997	0.28992
F	-6.459927	0.835215	-0.844432
F	-6.601471	-0.497781	0.873839
F	-5.833738	1.519983	1.119815
C	-3.699616	0.5114	-1.024172
C	-2.382266	0.11352	-1.232564
H	3.777103	-2.371385	2.234353
H	4.481248	-0.77529	1.924874
H	5.387002	-2.241176	1.492412
H	3.186786	-3.238557	-1.404798
H	2.986437	-3.830147	0.254668
H	4.61277	-3.699649	-0.448431
H	5.647129	-1.381776	-0.864109
H	4.724591	0.085452	-0.48278
H	4.232019	-0.942561	-1.84047
H	0.294891	0.991005	0.892695
H	-0.024217	2.439977	-0.092787
H	2.194163	1.565926	2.259942
H	4.540639	2.330713	2.477154
H	5.770868	3.153715	0.477912
H	4.630682	3.218206	-1.731354
H	2.276543	2.466471	-1.934949
H	-2.108812	-2.185759	1.254608
H	-4.451833	-1.443973	1.659505
H	-4.154626	1.245594	-1.679731
H	-1.81336	0.545049	-2.045496

Table 2.55 Example computed structure of an F conformer of **1a** (21)

O	0.533129	-2.39145	-2.276757
C	0.406659	-1.353827	-1.643223
N	1.44094	-0.430247	-1.599701
O	1.433605	0.546331	-0.587509
C	1.125933	1.825081	-1.055657
C	1.360923	2.840609	0.057927
C	2.890567	2.99571	0.217525
C	0.730914	4.173954	-0.367217
C	0.747216	2.355201	1.386056
O	0.757956	2.03764	-2.177605
O	2.71593	-0.786654	-1.936568
C	3.271022	-1.886292	-1.122699
C	3.09626	-1.669535	0.350339
C	3.899052	-0.748826	1.036322
C	3.673987	-0.482352	2.38426
C	2.640776	-1.136759	3.063479
C	1.846225	-2.066304	2.392129
C	2.075671	-2.331773	1.039995
C	-0.892779	-0.956739	-1.008135
C	-2.041424	-1.073525	-1.79936
C	-3.292819	-0.783648	-1.265273
C	-3.40216	-0.407583	0.075216
C	-4.743157	-0.040218	0.645767
F	-5.754242	-0.676306	0.015389
F	-4.830794	-0.341684	1.961011
F	-4.983585	1.288201	0.533503
C	-2.263269	-0.323801	0.879114
C	-1.009182	-0.592054	0.338415
H	3.097604	3.743805	0.990401
H	3.353199	3.332226	-0.716359
H	3.352384	2.051116	0.517047
H	-0.3521	4.076165	-0.492363
H	1.149346	4.524436	-1.31429
H	0.922826	4.929756	0.401392
H	0.883746	3.132172	2.14591
H	1.22867	1.440645	1.741543
H	-0.326512	2.167511	1.282306
H	4.319845	-1.871333	-1.425557
H	2.803896	-2.813741	-1.456082
H	4.693956	-0.233535	0.503436
H	4.300898	0.233717	2.907626
H	2.464337	-0.928	4.114691
H	1.048962	-2.584321	2.917205
H	1.454359	-3.050984	0.513121
H	-1.944737	-1.389522	-2.83223
H	-4.181064	-0.860317	-1.882171
H	-2.357013	-0.056324	1.925953
H	-0.129061	-0.534486	0.964817

Table 2.56 Example computed structure of a D conformer of **1a** (22)

O	-0.026027	-3.229304	-1.067971
C	-0.068673	-2.145266	-0.529888
N	1.123628	-1.502593	-0.071532
O	1.074048	-0.076315	-0.099877
C	0.768045	0.478236	-1.333495
C	0.809861	1.998166	-1.245903
C	-0.306903	2.451066	-0.278673
C	2.185833	2.446277	-0.713997
C	0.559797	2.569896	-2.647638
O	0.476791	-0.194474	-2.289345
O	2.245837	-1.948769	-0.74249
C	3.323163	-2.196967	0.20012
C	3.933516	-0.926847	0.72847
C	4.836758	-0.201193	-0.057185
C	5.374803	0.997838	0.407125
C	5.011638	1.48504	1.664991
C	4.111036	0.767922	2.454766
C	3.576291	-0.432957	1.986946
C	-1.33944	-1.458846	-0.146717
C	-2.422804	-1.582532	-1.023152
C	-3.633023	-0.964242	-0.728296
C	-3.768743	-0.240662	0.459191
C	-5.048417	0.492171	0.749605
F	-5.300232	0.562318	2.075693
F	-5.000051	1.767455	0.29334
F	-6.114468	-0.093964	0.163663
C	-2.700366	-0.140585	1.353468
C	-1.484636	-0.743798	1.048227
H	-0.328942	3.545506	-0.244405
H	-0.133025	2.076481	0.733277
H	-1.289445	2.099534	-0.611119
H	2.218552	3.540704	-0.678693
H	2.993724	2.102161	-1.367436
H	2.377547	2.058409	0.28852
H	1.330375	2.241258	-3.351403
H	0.575363	3.663757	-2.6024
H	-0.410977	2.251325	-3.037655
H	4.036386	-2.766492	-0.400897
H	2.940948	-2.830668	1.005251
H	5.115802	-0.579444	-1.037427
H	6.077795	1.551015	-0.209056
H	5.431742	2.4183	2.028982
H	3.827986	1.141761	3.434642
H	2.87148	-0.990527	2.598011
H	-2.298747	-2.152831	-1.936803
H	-4.469713	-1.045344	-1.412914
H	-2.819922	0.40651	2.281999
H	-0.651165	-0.66096	1.735663

Table 2.57 Example computed structure of an E conformer of **1a** (58)

O	1.080935	-2.100895	0.240745
C	0.433775	-1.184622	-0.233013
N	1.057618	-0.170232	-0.989964
O	0.479337	1.133872	-0.954542
C	0.174712	1.646128	0.299397
C	-0.423604	3.040332	0.161872
C	-1.743585	2.929544	-0.632819
C	-0.698031	3.58705	1.569465
C	0.572215	3.950846	-0.586038
O	0.345334	1.024293	1.317764
O	2.420562	-0.134339	-1.022753
C	3.07796	0.200586	0.252258
C	4.457203	-0.381192	0.183023
C	4.61559	-1.773922	0.173438
C	5.889622	-2.332643	0.110184
C	7.016505	-1.5064	0.058786
C	6.86395	-0.119865	0.065812
C	5.585989	0.439793	0.12246
C	-1.057822	-1.130231	-0.204168
C	-1.698746	-1.615986	0.940632
C	-3.086161	-1.592295	1.025571
C	-3.836723	-1.101507	-0.046228
C	-5.332548	-1.004955	0.067629
F	-5.839209	-1.935349	0.904823
F	-5.712581	0.204558	0.546726
F	-5.941014	-1.158927	-1.129
C	-3.203152	-0.643701	-1.203619
C	-1.813833	-0.654428	-1.28174
H	-1.568856	2.566528	-1.648769
H	-2.207441	3.919632	-0.693038
H	-2.447829	2.251176	-0.140312
H	-1.133766	4.58822	1.491
H	0.223576	3.654933	2.155028
H	-1.396838	2.94517	2.113093
H	0.777556	3.578124	-1.59249
H	1.521399	4.02713	-0.043982
H	0.148162	4.957087	-0.667738
H	2.494462	-0.227391	1.065184
H	3.099747	1.290353	0.351433
H	3.731165	-2.402805	0.210581
H	6.006768	-3.412642	0.103544
H	8.00985	-1.943943	0.012523
H	7.736506	0.525761	0.023031
H	5.464589	1.520195	0.121813
H	-1.098989	-1.996514	1.759641
H	-3.586023	-1.955771	1.916271
H	-3.793326	-0.28525	-2.039602
H	-1.318023	-0.299547	-2.177528

Table 2.58 Example computed structure of a C conformer of **1a** (61)

O	1.297745	-0.507411	-1.72765
C	0.77357	-0.579428	-0.629392
N	1.576009	-0.569788	0.530628
O	2.858414	-0.055773	0.278932
C	3.844279	-1.036971	0.214202
C	5.153734	-0.400566	-0.238171
C	6.284545	-1.417564	-0.034259
C	4.998616	-0.065357	-1.739792
C	5.438624	0.885068	0.562947
O	3.633526	-2.195628	0.445042
O	1.103645	-0.127235	1.747427
C	1.02203	1.338125	1.863846
C	-0.004198	1.950215	0.959333
C	0.376562	2.535156	-0.252456
C	-0.587809	3.044906	-1.123766
C	-1.939242	2.965715	-0.78898
C	-2.329254	2.381849	0.420616
C	-1.36501	1.884258	1.290576
C	-0.688174	-0.808482	-0.437298
C	-1.253379	-1.4064	0.69667
C	-2.635473	-1.509113	0.808667
C	-3.455308	-1.017221	-0.209897
C	-4.943511	-0.978378	-0.021154
F	-5.332743	0.205592	0.5232
F	-5.610803	-1.104214	-1.18873
F	-5.383483	-1.949663	0.806858
C	-2.895552	-0.470736	-1.365582
C	-1.514304	-0.378358	-1.481668
H	6.08495	-2.342853	-0.580787
H	6.404027	-1.669834	1.024284
H	7.226959	-0.99354	-0.396348
H	4.823477	-0.972938	-2.326418
H	5.918406	0.406766	-2.101924
H	4.159947	0.614683	-1.909059
H	5.489491	0.680508	1.638063
H	4.671411	1.644454	0.391855
H	6.404374	1.29682	0.251094
H	2.019892	1.746633	1.690356
H	0.764393	1.454998	2.918374
H	1.428954	2.574837	-0.520744
H	-0.283396	3.493954	-2.064484
H	-2.691313	3.350834	-1.471595
H	-3.382189	2.288407	0.668058
H	-1.664838	1.414764	2.223204
H	-0.620495	-1.769803	1.495414
H	-3.07802	-1.960793	1.689421
H	-3.536852	-0.10523	-2.159834
H	-1.059091	0.058482	-2.361955

Table 2.59 Example computed structure of a B conformer of **1h** (17)

O	-1.932392	-0.176395	-2.025991
C	-1.43379	-0.212533	-0.917149
C	-0.090696	-0.810841	-0.647688
C	0.107019	-1.806957	0.313784
C	1.368899	-2.373237	0.470697
C	2.432945	-1.929422	-0.317149
C	3.823243	-2.436305	-0.069752
F	3.833482	-3.636702	0.546818
F	4.530747	-2.558557	-1.214097
F	4.530332	-1.584962	0.725964
C	2.23363	-0.947861	-1.289972
C	0.967599	-0.403681	-1.466689
N	-2.042887	0.487218	0.147417
O	-3.42772	0.661973	0.005198
C	-4.137626	-0.539392	-0.000148
C	-5.61274	-0.272239	-0.262187
C	-5.738954	0.285979	-1.697604
C	-6.376393	-1.597258	-0.136855
C	-6.147904	0.755023	0.75597
O	-3.600002	-1.604249	0.157493
O	-1.731621	0.136756	1.450549
C	-1.177898	1.302179	2.1441
C	0.22463	1.567476	1.685762
C	0.48307	2.470999	0.677244
C	1.778984	2.586766	0.110136
C	2.830864	1.755326	0.611357
C	2.548599	0.861484	1.678286
C	1.281828	0.767568	2.195978
C	4.110191	1.818742	0.001575
C	4.342003	2.669859	-1.055928
C	3.305023	3.501459	-1.546046
C	2.053132	3.461406	-0.974056
H	-0.722126	-2.130264	0.930603
H	1.529766	-3.148293	1.211497
H	3.06438	-0.602708	-1.894736
H	0.798615	0.356639	-2.220856
H	-5.33049	-0.417728	-2.430021
H	-5.207344	1.235073	-1.80268
H	-6.797206	0.448836	-1.928367
H	-6.280148	-2.015993	0.86962
H	-6.000383	-2.338105	-0.847714
H	-7.438462	-1.426029	-0.340594
H	-6.035659	0.38975	1.782719
H	-7.214163	0.922919	0.57082
H	-5.627951	1.712429	0.670736
H	-1.223039	1.002067	3.1937
H	-1.845368	2.151371	1.976589
H	-0.32242	3.07873	0.272783
H	3.343063	0.221456	2.047532
H	1.067582	0.052845	2.985741
H	4.894626	1.162868	0.368567
H	5.322472	2.704506	-1.522089
H	3.501319	4.168589	-2.380356
H	1.252021	4.090574	-1.353584

Table 2.60 Example computed structure of an E conformer of **1h** (30)

O	1.049445	3.273279	-1.077185
C	1.134499	2.342834	-0.299595
C	2.331806	1.457951	-0.186785
C	2.816113	1.012532	1.048077
C	3.940247	0.193817	1.098371
C	4.573838	-0.186973	-0.086185
C	5.725166	-1.151688	-0.035497
F	5.292273	-2.435436	-0.080553
F	6.572018	-0.987289	-1.074585
F	6.444788	-1.02216	1.1007
C	4.103751	0.270279	-1.32066
C	2.990471	1.101355	-1.36823
N	0.14796	2.122459	0.691133
O	-0.128056	0.769373	1.049855
C	-0.272954	-0.131952	0.003441
C	-0.486279	-1.54011	0.541377
C	0.888998	-2.030164	1.054649
C	-1.514043	-1.549668	1.68737
C	-0.964391	-2.431862	-0.613658
O	-0.153666	0.190835	-1.152468
O	-0.973066	2.90334	0.655409
C	-1.886465	2.679074	-0.466354
C	-2.925019	1.636753	-0.147161
C	-3.260649	0.672237	-1.072098
C	-4.264402	-0.294125	-0.799859
C	-4.93321	-0.260934	0.465582
C	-4.569908	0.745553	1.401845
C	-3.595034	1.666774	1.106234
C	-5.920861	-1.240561	0.746019
C	-6.232797	-2.211026	-0.179903
C	-5.570858	-2.244375	-1.431392
C	-4.609846	-1.30591	-1.734306
H	2.315681	1.306797	1.963325
H	4.323889	-0.148387	2.052993
H	4.608276	-0.021586	-2.234835
H	2.610396	1.46736	-2.31526
H	0.791949	-3.066883	1.393725
H	1.240175	-1.423227	1.893262
H	1.646103	-1.996353	0.264321
H	-1.185188	-0.93476	2.528353
H	-1.642139	-2.578699	2.039765
H	-2.485925	-1.181198	1.35073
H	-0.253835	-2.418597	-1.444269
H	-1.938247	-2.103447	-0.98705
H	-1.064624	-3.461529	-0.255427
H	-1.320809	2.440119	-1.365349
H	-2.343146	3.665913	-0.587999
H	-2.738931	0.62844	-2.023998
H	-5.074108	0.769823	2.36449
H	-3.313075	2.420639	1.834523
H	-6.42578	-1.212999	1.708213
H	-6.989024	-2.956871	0.046961
H	-5.825892	-3.014785	-2.153198
H	-4.099476	-1.326489	-2.693841

Table 2.61 Example computed structure of an H conformer of **1h** (36)

O	-1.201382	2.742661	-0.009425
C	-1.360764	1.607722	-0.429668
C	-2.65442	0.868776	-0.280369
C	-3.17012	-0.035705	-1.218159
C	-4.412002	-0.626514	-1.003607
C	-5.138568	-0.326842	0.15054
C	-6.44319	-1.026051	0.413007
F	-6.255474	-2.190386	1.080043
F	-7.277907	-0.275029	1.163897
F	-7.091383	-1.332674	-0.732437
C	-4.634382	0.580309	1.085259
C	-3.402594	1.184647	0.861721
N	-0.344344	0.969929	-1.135056
O	0.924658	1.548312	-1.10132
C	1.483398	1.681111	0.175077
C	2.784995	2.4618	0.085038
C	3.50413	2.358337	1.437391
C	3.679653	1.898309	-1.036519
C	2.411046	3.931491	-0.215961
O	0.954849	1.250515	1.165179
O	-0.353634	-0.365704	-1.438444
C	0.095857	-1.2629	-0.371101
C	1.586281	-1.470461	-0.405711
C	2.332436	-1.433214	0.75155
C	3.737248	-1.633789	0.729078
C	4.382461	-1.88228	-0.524674
C	3.588204	-1.924425	-1.70289
C	2.230665	-1.723796	-1.64703
C	5.790302	-2.059141	-0.548997
C	6.528536	-1.989206	0.611356
C	5.890782	-1.740546	1.851186
C	4.52583	-1.568605	1.908149
H	-2.61129	-0.271347	-2.114192
H	-4.819261	-1.314273	-1.736376
H	-5.207225	0.819409	1.974224
H	-3.005143	1.908441	1.563902
H	2.874927	2.730654	2.250295
H	4.422314	2.953946	1.405244
H	3.77522	1.321835	1.659722
H	3.928427	0.849177	-0.855557
H	4.613491	2.469978	-1.066025
H	3.196837	1.97491	-2.013459
H	1.901991	4.020306	-1.179325
H	3.324399	4.535295	-0.245236
H	1.752334	4.336716	0.558788
H	-0.441917	-2.185688	-0.609854
H	-0.247098	-0.882014	0.591602
H	1.852328	-1.214991	1.7008
H	4.07656	-2.109191	-2.656123
H	1.636903	-1.736407	-2.55563
H	6.277129	-2.24691	-1.502557
H	7.605875	-2.123205	0.579822
H	6.484645	-1.686153	2.758872
H	4.031208	-1.377631	2.856996

Table 2.62 Example computed structure of an A conformer of **1h** (3)

O	1.930311	-1.533681	-1.528889
C	1.375075	-1.157361	-0.510436
C	-0.104759	-1.262768	-0.312471
C	-0.693079	-1.75367	0.860171
C	-2.07381	-1.896216	0.934558
C	-2.874212	-1.522987	-0.148632
C	-4.362503	-1.69595	-0.044908
F	-4.721018	-2.997336	-0.168518
F	-4.833056	-1.283856	1.157702
F	-5.031629	-1.011177	-0.995936
C	-2.294665	-1.035605	-1.319083
C	-0.910192	-0.923398	-1.404189
N	2.107773	-0.459364	0.456392
O	3.477525	-0.782797	0.452233
C	4.279601	0.228662	-0.050993
C	5.686793	-0.305088	-0.288795
C	6.609912	0.87687	-0.612628
C	6.192834	-1.054309	0.960392
C	5.611134	-1.272796	-1.492559
O	3.878536	1.342757	-0.271187
O	1.642426	-0.314959	1.742175
C	1.417633	1.111354	2.03394
C	0.30798	1.660486	1.188142
C	-1.005624	1.491624	1.573915
C	-2.075785	1.826965	0.70997
C	-1.776424	2.366609	-0.582427
C	-0.418479	2.572827	-0.939416
C	0.599236	2.224229	-0.082398
C	-2.847749	2.646678	-1.47127
C	-4.150593	2.396439	-1.104102
C	-4.445258	1.864702	0.175586
C	-3.430688	1.593638	1.063495
H	-0.07551	-2.013612	1.710215
H	-2.532619	-2.27824	1.840444
H	-2.920094	-0.731096	-2.149322
H	-0.44437	-0.553775	-2.310355
H	7.618747	0.505094	-0.819674
H	6.666151	1.577586	0.226465
H	6.254583	1.426817	-1.488039
H	7.214119	-1.405194	0.778254
H	5.566981	-1.919398	1.191824
H	6.21223	-0.396837	1.836608
H	6.608436	-1.681155	-1.688689
H	5.269843	-0.751717	-2.392973
H	4.922133	-2.097536	-1.295942
H	2.361056	1.639812	1.883053
H	1.164217	1.093446	3.09579
H	-1.235924	1.048101	2.539838
H	-0.192211	2.990749	-1.917095
H	1.636536	2.340407	-0.377177
H	-2.619082	3.053804	-2.452937
H	-4.960799	2.60301	-1.797376
H	-5.475331	1.655213	0.446172
H	-3.650826	1.165259	2.0371

Table 2.63 Example computed structure of an F conformer of **1h** (43)

O	-0.184658	-1.406348	-3.274796
C	-0.130263	-1.337773	-2.055496
C	1.104907	-0.875787	-1.340822
C	2.324354	-1.381938	-1.807057
C	3.523315	-0.942035	-1.255937
C	3.509035	0.036512	-0.259196
C	4.796248	0.484367	0.374093
F	5.846928	0.354441	-0.464844
F	4.743104	1.779112	0.760709
F	5.084626	-0.241426	1.480837
C	2.298268	0.570434	0.186253
C	1.098057	0.109602	-0.346299
N	-1.185044	-1.811685	-1.285288
O	-1.278499	-1.396105	0.056496
C	-0.950594	-2.398335	0.970766
C	-1.295797	-1.929967	2.381193
C	-0.651666	-2.901249	3.379824
C	-0.790901	-0.494464	2.62754
C	-2.835695	-1.9696	2.510109
O	-0.488909	-3.455764	0.641547
O	-2.424769	-1.984069	-1.833813
C	-2.999914	-0.758581	-2.432216
C	-2.916465	0.416984	-1.510007
C	-1.905956	1.34275	-1.661025
C	-1.701383	2.373835	-0.70685
C	-2.581245	2.457368	0.419554
C	-3.643885	1.517792	0.529139
C	-3.802277	0.5227	-0.403076
C	-2.354236	3.463531	1.393734
C	-1.29819	4.338823	1.267614
C	-0.424409	4.251788	0.156659
C	-0.624975	3.293251	-0.811457
H	2.322864	-2.118991	-2.6024
H	4.466289	-1.344864	-1.607995
H	2.290339	1.35085	0.93927
H	0.165413	0.532461	-0.003465
H	-0.91958	-2.606747	4.399791
H	0.439424	-2.889912	3.292803
H	-0.992654	-3.925959	3.210799
H	-1.283146	0.226179	1.970193
H	0.291214	-0.422525	2.477293
H	-1.007695	-0.214148	3.663931
H	-3.307077	-1.28321	1.801819
H	-3.119502	-1.670458	3.524988
H	-3.221177	-2.979007	2.331325
H	-4.027401	-1.07396	-2.624075
H	-2.484677	-0.576721	-3.37576
H	-1.226466	1.270181	-2.506639
H	-4.321331	1.592087	1.375771
H	-4.601075	-0.20606	-0.296121
H	-3.025197	3.526932	2.246441
H	-1.130034	5.100567	2.023218
H	0.406104	4.946233	0.07115
H	0.045445	3.217967	-1.663347

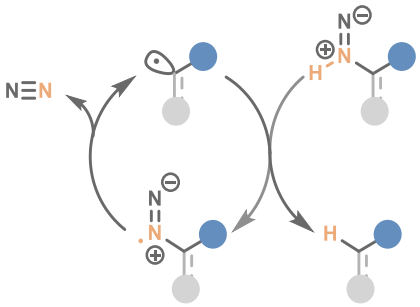
Table 2.64 Example computed structure of a G conformer of **1h** (46)

O	-0.667163	0.283343	-2.941307
C	-0.108936	0.51583	-1.890993
C	0.991285	-0.315816	-1.324401
C	1.06159	-0.599727	0.046052
C	2.077909	-1.414575	0.533081
C	3.029809	-1.937962	-0.345943
C	4.173028	-2.749486	0.197081
F	4.656865	-3.619268	-0.715606
F	5.206112	-1.956687	0.571658
F	3.812662	-3.461507	1.287419
C	2.954218	-1.669578	-1.714792
C	1.926257	-0.870127	-2.204427
N	-0.549418	1.547441	-1.012274
O	0.588107	2.317102	-0.589433
C	0.603296	2.5823	0.763037
C	1.898018	3.304336	1.128064
C	3.092209	2.390566	0.775037
C	1.985264	4.619688	0.325053
C	1.880979	3.599327	2.633615
O	-0.287054	2.268151	1.513388
O	-1.47155	2.393426	-1.587229
C	-2.661916	2.456053	-0.742808
C	-3.248802	1.095291	-0.504338
C	-3.163224	0.506833	0.738822
C	-3.664373	-0.800425	0.969312
C	-4.259244	-1.516128	-0.119223
C	-4.324777	-0.890766	-1.393869
C	-3.832386	0.377488	-1.582925
C	-4.753769	-2.826492	0.110594
C	-4.662097	-3.405393	1.356642
C	-4.070663	-2.698803	2.432441
C	-3.583491	-1.425445	2.24165
H	0.312849	-0.198042	0.719469
H	2.128024	-1.650855	1.59024
H	3.688921	-2.091416	-2.391243
H	1.842082	-0.665352	-3.266206
H	4.0235	2.891197	1.06014
H	3.127855	2.173324	-0.295376
H	3.038191	1.439313	1.314225
H	2.901556	5.151162	0.603176
H	1.134033	5.273529	0.544195
H	2.007123	4.430438	-0.751085
H	2.8041	4.117122	2.913499
H	1.810389	2.67658	3.216803
H	1.031777	4.233915	2.903455
H	-3.324553	3.09896	-1.328306
H	-2.405723	2.95006	0.196944
H	-2.680054	1.038924	1.553274
H	-4.767856	-1.437381	-2.222262
H	-3.866587	0.838026	-2.565889
H	-5.20497	-3.367435	-0.717337
H	-5.042925	-4.40958	1.519506
H	-4.003732	-3.167437	3.410079
H	-3.128639	-0.878097	3.063443

Table 2.65 Example computed structure of a C conformer of **1h** (47)

O	0.19774	0.82498	-1.667359
C	0.745562	0.810593	-0.57929
C	2.190894	0.483679	-0.398265
C	2.970814	0.984329	0.653161
C	4.321698	0.660183	0.727911
C	4.895337	-0.168128	-0.239675
C	6.337818	-0.57424	-0.112134
F	7.081071	0.383795	0.482731
F	6.469687	-1.695321	0.636913
F	6.897017	-0.836995	-1.313071
C	4.125147	-0.662105	-1.295289
C	2.778547	-0.327253	-1.378008
N	0.058327	1.223657	0.580211
O	-1.334914	1.322911	0.379131
C	-1.742071	2.568116	-0.071797
C	-3.242267	2.526085	-0.350631
C	-3.508245	1.4712	-1.447081
C	-3.99264	2.141875	0.941258
C	-3.681462	3.915761	-0.829542
O	-0.991952	3.494892	-0.225908
O	0.315718	0.614519	1.791319
C	0.172709	-0.851566	1.783642
C	-1.202519	-1.316969	1.417704
C	-1.460227	-1.797424	0.152376
C	-2.775966	-2.138843	-0.251573
C	-3.846806	-1.995271	0.688318
C	-3.549688	-1.528593	1.998032
C	-2.265873	-1.193059	2.351547
C	-5.167523	-2.308921	0.27631
C	-5.420405	-2.737421	-1.007754
C	-4.36158	-2.877235	-1.937824
C	-3.068125	-2.587843	-1.566193
H	2.526928	1.628927	1.400866
H	4.93201	1.057268	1.53129
H	4.579627	-1.293675	-2.050261
H	2.16776	-0.681852	-2.200668
H	-4.576666	1.465308	-1.689297
H	-3.222358	0.471106	-1.116575
H	-2.949325	1.703791	-2.359501
H	-5.069786	2.130142	0.741418
H	-3.803989	2.869593	1.738679
H	-3.697147	1.152058	1.29593
H	-4.756521	3.90612	-1.038132
H	-3.152685	4.204078	-1.742527
H	-3.482174	4.678168	-0.070452
H	0.436932	-1.096813	2.814939
H	0.930605	-1.268498	1.114168
H	-0.655199	-1.882345	-0.573177
H	-4.361142	-1.430083	2.714414
H	-2.05322	-0.814945	3.347732
H	-5.978684	-2.198555	0.991272
H	-6.436538	-2.968687	-1.31373
H	-4.575675	-3.212935	-2.948188
H	-2.252533	-2.687203	-2.277507

Chapter 3 : Mechanistic Investigations of Primary Amine Deletion



Note: Portions of this work have been published in an alternate format in Berger, K. J.; Driscoll, J. L.; Yuan, M.; Dherange, B. D.; Gutierrez, O.; Levin, M. D. Direct Deamination of Primary Amines *via* Isodiazene Intermediates. *J. Am. Chem. Soc.* **2021**, *143*, 17366 – 17373. https://doi.org/10.1021/jacs.1c09779

3.1 Introduction

While modern reaction development is often focused on increasing the functionality of a molecule, defunctionalization reactions can be equally important.[1] Strategic defunctionalization reactions with mild conditions offer new opportunities to refine natural products into more valuable compounds, rapidly generate novel analogues for structure-activity-relationship studies in drug development, and can enable traceless directing groups for selective transformations at otherwise "undirectable" positions.

3.1.1 Primary Amine Activation

Primary amines are ubiquitous in natural products and drug candidates (Figure **3.1**a);[2] they have also been employed as directing groups in many site-specific transformations (Figure **3.1**b),[3] making amines a desirable target for defunctionalization reactions. The deamination of primary amines to afford alkanes has previously been achieved through a variety of approaches,[4] the majority of which first require the transformation of the amine into another,

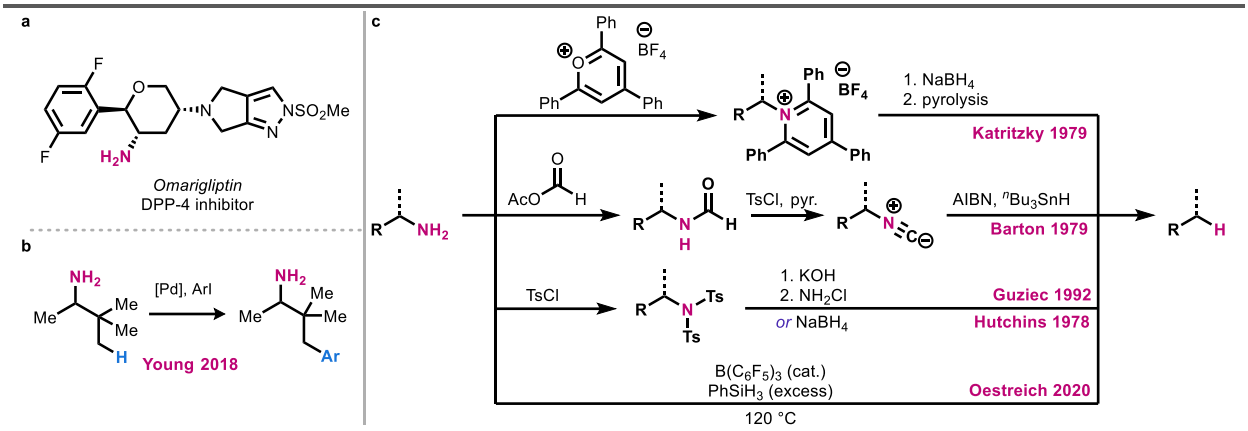


Figure 3.1 a) Examples of primary amines in pharmaceuticals and (b) directing group chemistry, c) Previous methods for primary amine reduction

more activated functional group, followed by reduction. Examples of this include Katritzky's use of pyridylation followed by treatment with $NaBH_4$ and pyrolysis[5,6] and Barton's formylation-dehydration to yield isocyanates, which generate the alkane via a radical mechanism upon treatment with tin hydride.[7] Similarly, Guziec[8] and Hutchins[9] have reported the reduction of tosylated primary amines (Figure **3.1**c). However, all of these transformations require harsh conditions and pre-functionalization of the amine.

More recently, Oestreich reported a Lewis-acid catalyzed reduction of primary amines via *in situ* silylation.[10] However, this method is limited to benzylic and α-branched primary amines and additionally is carried out at a high temperature that may be hostile towards complex functionalities. Based on our previously developed secondary-amine deletion enabled by an anomeric amide reagent (**1**),[11] we envisioned that an analogous reaction between primary amines and an anomeric amide could similarly result in the deaminated product.

3.1.2 Anomeric Amides and Secondary Amine Deletion

The secondary amine deletion reaction developed in our group is inspired by precedent from Glover and co-workers; they found that exposure of *N*-methylaniline to an *N*-acyloxy-*N*-

alkoxyamide yielded a tetrazene product, presumably resulting from dimerization of an isodiazene intermediate (**Figure 3.2**a).[12,13] Given the known rearrangement of secondary-isodiazenes to extrude dinitrogen gas and generate a carbon-carbon bond between the two alkyl substituents,[14–18] our group reasoned that anomeric amides could be exploited to "delete" nitrogen atoms from secondary amines.

In order to achieve the desired transformation, we found it necessary to replace the acetate moiety on Glover's anomeric amide with a pivalate group – to prevent carbonyl-attack by the amine at that position – and add an electron-withdrawing group on the aryl group – to increase the rate of the reaction (**Figure 3.2**b).[11] [11] This led us to anomeric amide **1**, which we found could delete nitrogen from secondary amines with at least one radical-stabilizing substituent under mild conditions (**Figure 3.2**c). We propose that the reaction proceeds via substitution of the pivalate group by the amine, followed by reductive elimination to form a

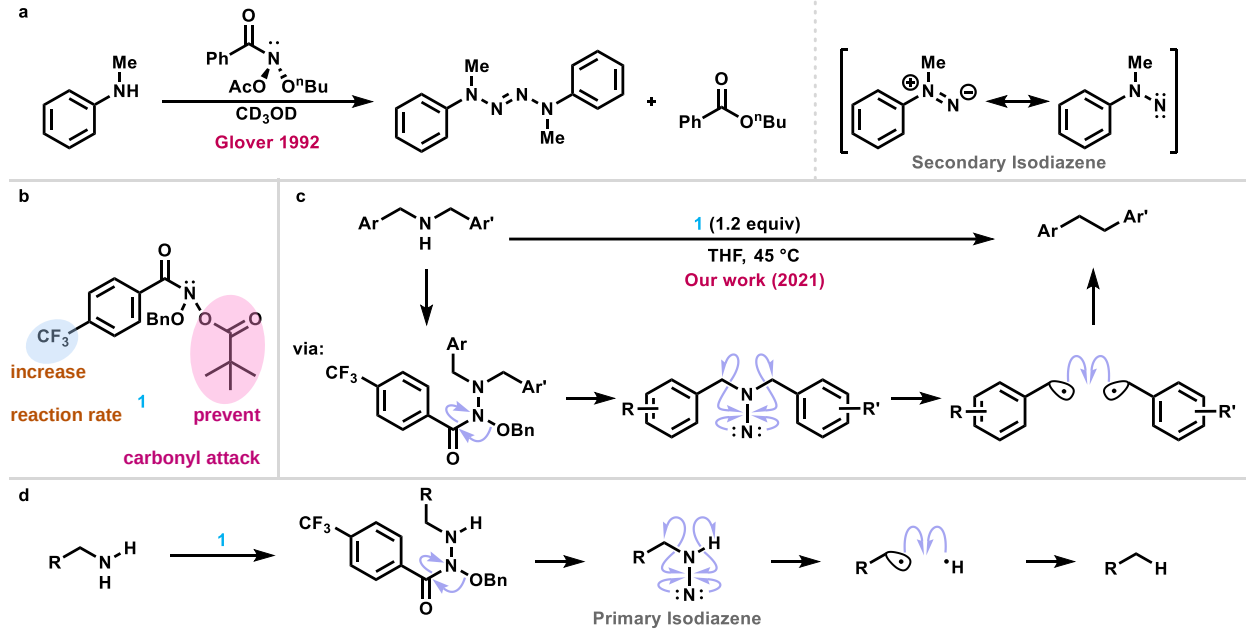


Figure 3.2 a) Precedence for isodiazene generation from secondary amines and *N*-acyloxy-*N*-alkoxyamides, **b)** Structure of anomeric amide reagent (**1**) used for secondary-amine deletion, **c)** General conditions and mechanism of secondary-amine deletion reaction, **d)** Initial mechanistic proposal for primary-amine deletion by an anomeric amide.

secondary-isodiazene intermediate. This intermediate can then lose dinitrogen to a geminate radical pair, which recombines within the solvent-cage to forge the new C-C bond. We suspected that this chemistry could also be applied to primary amines, proceeding through an analogous mechanism where after substitution of the pivalate by the amine, reductive elimination yields a primary isodiazene that can rearrange to generate dinitrogen and a radical pair that can recombine in-cage to generate the alkyl product (**Figure 3.2**d). However, while secondary isodiazenes have been isolated and thoroughly characterized,[15,16,19–25] primary isodiazenes have remained much more elusive.[26] Thus, we saw the development of a primary amine deletion by an anomeric amide reagent as an opportunity to study this reactive species.

3.2 Results and Discussion

3.2.1 Initial Discovery and Scope

Upon exposing amine **2a** to anomeric amide reagent **1** in acetonitrile, we observed that the deamination took place with remarkable ease, proceeding rapidly at room temperature with the visible formation of gas to yield butylbenzene (**3a**) in 88% yield.

I explored the scope of this reaction in collaboration with two other group members (**Figure 3.3**), and we found it to be successful with both α-primary and α-secondary amines. I also showed the reaction demonstrated functional group tolerance for amines containing nitro groups (**2b**), aromatic nitrogen-containing heterocycles (**2d**) and α-hydroxyl stereocenters (**2e**). Notably, even unprotected indoles (**2c**), which were not tolerated in our secondary amine chemistry, were found to be compatible. This tolerance was further displayed through successful application of the reaction to eight active pharmaceutical ingredients (**2k-r**), demonstrating its promise as a technique for late-stage modifications, as well as several

bioderived amines (**2s-t**). In addition to alkyl amines, anilines were also found to be compatible (**2h-k**). In studying the scope, we were shocked to find that the radical-stabilization requirements observed for the secondary amine deletion did not apply to the primary amine deletion. In particular, the deletion of unstabilized α-primary amines suggested that this transformation was behaving quite different mechanistically, likely due to a divergence in reactivity between the disubstituted isodiazene intermediate formed in the secondary amine deletion and the proposed monosubstituted isodiazene intermediate of this transformation. This prompted me to conduct in-depth mechanistic studies to better understand this divergence and fully characterize the reactivity of the monosubstituted isodiazene.

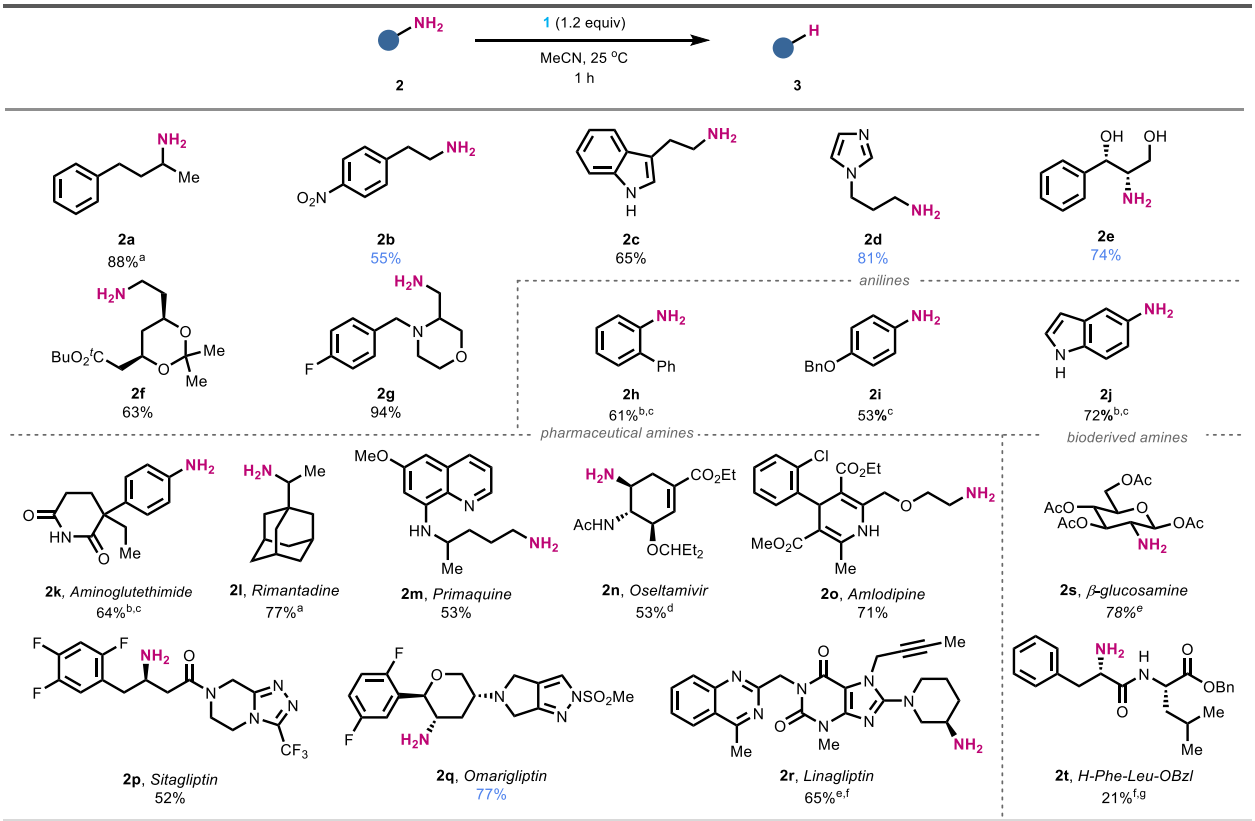


Figure 3.3 Selected reaction scope for the deletion of primary amines. Conditions: 1.2 equiv **1**, 0.08 M MeCN, 1 h. [a]NMR Yield; [b]45 °C; [c]1.5 equiv **1**, 24 h; [d]5 h; [e]16 h; [f]1:1 DMSO/MeCN; [g]3 h. Personal contributions in blue.

3.2.2 Mechanistic Investigations

3.2.2.1 Radical Clocks

I first wanted to see if the primary amine deletion was also proceeding through a radical mechanism. To probe this, I used a *trans*-(2-phenylcyclopropyl)methylamine radical clock (**2u**) (**Figure 3.4**).[27,28] After subjecting this probe to our standard conditions, I observed a strikingly different product distribution than that of the analogous secondary amine substrate used in our previous work (**4**). While we observed 19% yield of the rearranged product (**5'**) and 20% of the intact phenyl cyclopropyl deletion product (**5**) in the case of the secondary amine (**Figure 3.4**a),[11] the primary amine clock (**2u**) yielded 66% of the ring-opened product (**3u'**) with no detection of the unrearranged deletion product (**3u**) by ^{1}H NMR. These results suggested that reaction was indeed proceeding via a radical mechanism and perhaps generating cage-escaping free radicals rather than the in-cage recombination observed for secondary amines. However, given the volatility of the products produced and longer radical lifetime observed, I synthesized a second, diphenylhexene based clock substrate[29] (**2v**), with a higher molecular weight and

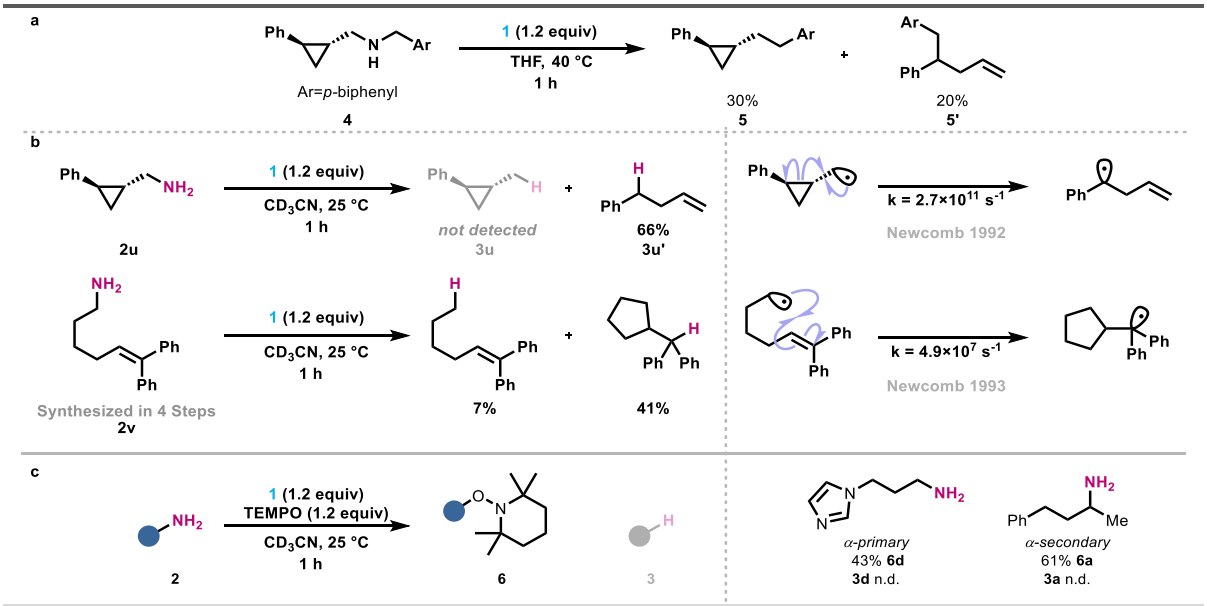


Figure 3.4 a) Secondary amine radical clock results, **b)** Evidence for free-radical intermediates via radical clock experiments and (**c**) observed TEMPO adducts.

slower rate of rearrangement, in order to better understand the characteristics of the radical species. Amine (**2v**) was synthesized in 4 steps from 6-bromohexanoic acid.[30] Upon subjection to the standard reaction conditions in deuterated solvent, 41% yield of the rearranged product (**3v'**) and 7% yield of the non-cyclized product (**3v**) were observed. These results suggest a radical lifetime allowing for cage-escape ($k \sim 10^{10}\ s^{-1}$).[31–34]

3.2.2.2 TEMPO Trapping

To validate the presence of a free-radical intermediate, I performed TEMPO trapping experiments.[35–37] The addition of excess TEMPO to the reaction with amine substrates **2d** and **2a** yields the TEMPO adducts (**6d** and **6a**) in 43% yield and 61% yield respectively, with no formation of the alkyl products (**3d** and **3a**) (**Figure 3.4**c). Interestingly, in the case of secondary amines, we found that TEMPO suppresses intermolecular products, but did not trap the majority of radicals. Thus, the increased TEMPO trapping observed with primary amine substrates further supports the generation of cage-escaping non-stabilized free radical species.

3.2.2.3 Deuterium Labelling

To determine the source of H-atoms in the product, I conducted deuterium labelling studies. Full replacement of the amine protons with deuterium was achieved with a two-step procedure involving silylation of the amine followed by deprotective deuteration to afford **2d-*N*-D_2**, confirmed by disappearance of the -NH_2 peak by ^{1}H NMR. Deletion under standard conditions of **2d-*N*-D_2** led to an average of 63 ± 9% deuterium incorporation observed by H^1 NMR spectroscopy; due to a large degree of variability, this was assessed as an average across 20 trials. Concentration, equivalencies of the anomeric amide compared to the amine, and order of addition were found to have little effect on the extent of deuterium incorporation, while

keeping the deuterated amine neat and operating in the glovebox proved to be imperative to achieving consistent results. Additionally, the deletion of protio-amine in MeCN-d_3 showed no deuterium incorporation, ruling out interference from the acetonitrile. I eventually discovered that adding 4% D_2O to the solvent mixture in the deletion of **2d-D$_2$** led to complete deuterium incorporation. Shockingly, the inclusion of 4% D_2O in the solvent system for the deletion of **2d-H$_2$** also showed significant deuterium incorporation (73 ± 7%). Based on these results, the variability was ultimately traced to adventitious water present in the acetonitrile.

While developing a method for the deuteration of amines, I found the equilibrium for proton-deuterium exchange between amines and deuterated-methanol to strongly favor proteo-amine over deutero-amine. This made us hesitant to attribute this sensitivity to proton-exchange alone. However, given that direct HAT from water to a radical intermediate would not be energetically feasible due to the high bond-dissociation energy, we wondered if an anionic intermediate, possibly resulting from electron transfer to the alkyl radical, could be responsible for this sensitivity. To investigate this, I synthesized anion probe **2w** and subjected it to our standard conditions.[38] Upon completion of the reaction, nearly full conversion to the non-rearranged product (**3w**) was observed (98%), with no detectable amount of the ester-migration product (**3w'**). This evidence argues against the presence of a carbanionic intermediate,[39–41] suggesting that the sensitivity is indeed due to proton exchange between water and the amino group on **2d**

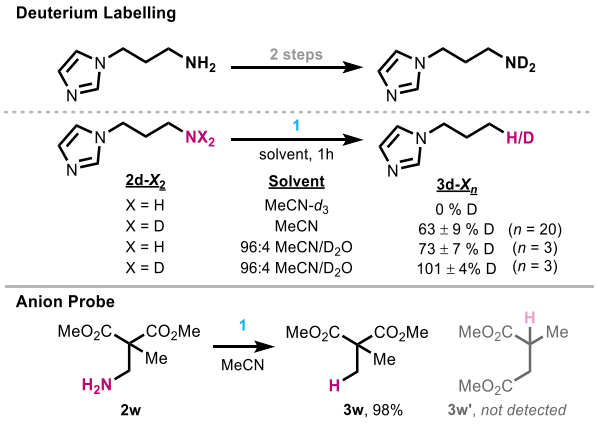


Figure 3.5 a) Deuterium labelling studies suggest that HAT occurs from the N-H bond, **b)** Anion clock experiment discounts competitive anionic mechanism.

(or an intermediate containing an N-H bond) and the H-atom source was ultimately traced to the original amino group on the substrate.

3.2.2.4 N-Centered Radical Clock and Mechanistic Proposal

Given the cage-escaping nature of the alkyl-radical intermediates detected in the radical-clock and TEMPO trapping experiments, the H-atom donor is not necessarily limited to the geminate hydro-diazenyl radical (**C**) presumed to form in the generation of the alkyl radical (**D**). Because the alkyl radical generated can come in contact with various intermediates in the reaction, HAT could feasibly occur from a hydro-diazenyl radical (**C**), an isodiazene (**B**), or an alkoxy hydrazine (**A**) intermediate (**Figure 3.6**a). To distinguish between these three pathways experimentally, I used phenyl cyclopropyl amine **2x** to detect an intermediate with an *N*-centered radical.[27] Upon subjection to the standard conditions, amine **2x** yields 74% of the unrearranged cyclopropane product (**3x**) by ^{1}H NMR, and no evidence for the aldehyde, imine, or alkene products that could result from rearrangement of an *N*-centered radical intermediate (**Figure 3.6**e).

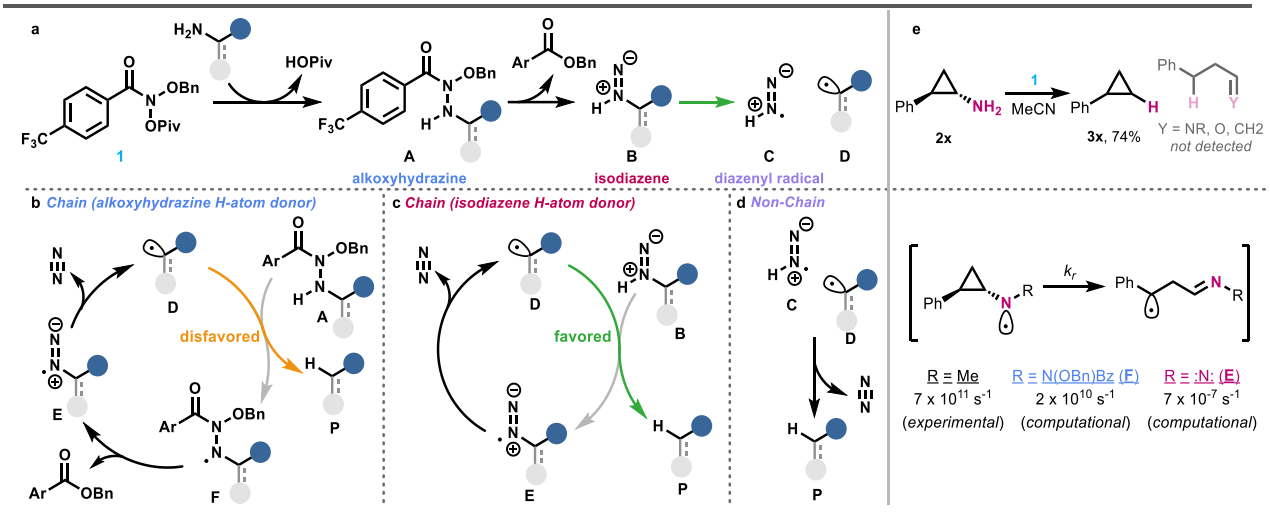


Figure 3.6 a) Mechanism for initiation, and mechanistic proposals for HAT from alkoxyhydrazine (part **b**), isodiazene (part **c**), and diazenyl radical (part **d**), **e)** N-centered radical clock experiment and computational values for rate constants Results discount mechanism where alkoxyhydrazine intermediate acts as an H-atom donor.

Using computations, we sought to verify that this result could inform on the presence or absence of an *N*-centered radical. Our collaborators (Mingbin Yuan and Prof. Osvaldo Gutierrez) determined the rate of rearrangement for an alkoxy hydrazine radical (**F**) and a diazenyl radical (**E**) to be 2×10^{10} s^{-1} and 7×10^{-7} s^{-1} respectively, benchmarked to the known rate of the methyl analog (correctly predicting the known rate at the DLPNO-CCSD(T)/def2-TZVPP-SMD(MeCN)//B3LYP/def2-TZVP-SMD(THF) level of theory). Based on these results, we reasoned the rearrangement would likely occur in the generation of radical **F**, but would not rearrange from radical **E**. Therefore, these results argue against HAT from the alkoxyhydrazine intermediate (**A**).

Additional computations at this same level of theory predicted the relative energy barriers for each of the possible mechanisms. These computations predicted HAT from the isodiazene (**Figure 3.6**c) to be the most energetically feasible pathway, as the activation energies for HAT from **A** (**Figure 3.6**b, orange arrow) and initiation to generate **C** (**Figure 3.6**a, orange arrow) are notably greater than HAT from **B** (approximately 12 and 16 kcal/mol respectively). This along with our experimental evidence of free-radical intermediates and lack of evidence for formation of radical **F** suggest a dominant mechanism whereby amine displacement of the pivalate on **1** leads to the formation of an alkoxyhydrazine intermediate (**A**). This can undergo reductive elimination to give a mono-substituted isodiazene intermediate (**B**), which cleaves homolytically to form a hydro-diazenyl radical (**C**) and alkyl radical (**D**). The alkyl radical species then undergoes HAT from isodiazene (**B**) to form an alkyl-diazenyl radical (**E**), which loses dinitrogen gas to regenerate the alkyl radical chain-carrier.

3.3 Conclusions

In summary, we found that the anomeric amide reagent developed by our group for nitrogen-deletion from secondary amines could be utilized to deaminate primary amines. The reaction with primary amines proceeds at an exceptional rate at room temperature with remarkable functional group tolerance. Mechanistic studies consisting of radical clocks, TEMPO trapping, deuterium labeling, an anion probe, and a nitrogen-centered radical clock suggest that the reaction proceeds via a radical chain process whereby a novel primary isodiazene intermediate undergoes an HAT with an alkyl radical chain carrier to generate a diazenyl radical. This rapidly rearranges to release dinitrogen gas, enabling the formation of free-radical species, even in the absence of radical stabilizing groups.

3.4 Experimental

3.4.1 General Procedures

Unless noted otherwise, all reactions were performed in oven-dried or flame-dried glassware under an atmosphere of dry N_2. THF, Et_2O, DCM, Toluene, MeCN, Et_3N, and Pentane were dried by passing these previously degassed solvents through a PPT Solvent Purificatiton System, and all other solvents were dried over molecular sieves (4A) and degassed prior to use or purchased anhydrous and sealed under N_2 (e.g. VWR Dri-solv or equivalent). Reaction temperatures were reported as the temperatures of the bather surrounding the flasks or vials. Sensitive reagents and solvents were transferred under nitrogen into a nitrogen-filled glovebox with standard techniques. Unless otherwise noted, all reagents were used as received. Analytical thin-layer chromatography (TLC) was carried out using 0.2 mm commercial silica gel plates (silica gel 60, F254) and visualized by UV irradiation or staining as indicated. Low

resolution mass spectra were recorded on either an Agilent 6530 LC Q-TOF mass spectrometer using electrospray ionization with fragmentation voltage set at 115 V or an Agilent SQ GC-MMS with a 7890B GC using an Agilent HP-5MS column with a temperature gradient of 50 to 200 °C over 15 minutes and a 5977A single quad MS using electron ionization. High resolution mass spectra were recorded on either an Agilent 6224 TOF High Resolution Accurate MS with electrospray ionization or an Agilent 7200B QTOF High Resolution Accurate Mass GCMS using an Agilent HP-5MS column with a temperature gradient of 50 to 200 °C over 15 minutes and electron ionization. All mass spectra were processed with an Agilent MassHunter Operating System. Nuclear magnetic resonance spectra (1H NMR, 13C NMR and 19F NMR) were recorded with Bruker spectrometers operating at 400 or 500 MHz for 1H. Chemical shifts are reported in parts per million (ppm, δ), downfield from tetramethylsilane (TMS, δ=0.00 ppm) and are referenced to residual solvent ($CDCl_3$, δ=7.26 ppm (^1H) and 77.160 ppm (^{13}C)). Coupling constants were reported in Hertz (Hz). Data for 1H NMR spectra were reported as follows: chemical shift (ppm, s = singlet, d = doublet, t = triplet, q = quartet, quin = quintet, dd = doublet of doublets, td = triplet of doublets, ddd = doublet of doublet of doublets, m = multiplet, coupling constant (Hz), and integration). N-(benzyloxy)-N-(pivaloyloxy)-4-(trifluoromethyl)benzamide) (**1**) was prepared according to the previously reported procedure.[11] 6,6-diphenylhex-5-en-1-amine (**2v**) was synthesized according to the literature procedure[50] from ethyl 6-bromohexanoate. Unless otherwise specified, all amines were purchased from the appropriate suppliers and used without further purification. Characterization data for substrate scope conducted by Dr. Kathleen Berger and Dr. Balu

Dherange can be found in the supporting information for *J. Am. Chem. Soc.* **2021**, *143,* 17366 – 17373.

General procedures of preparative scale primary amine deletion

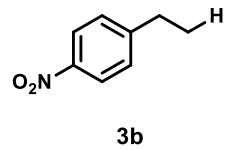
General procedure A for deamination of primary aliphatic amines

To a round bottom flask equipped with a stir bar under a nitrogen atmosphere was added the anomeric amide reagent (1.2 equiv.) and anhydrous acetonitrile. Under a nitrogen atmosphere, the primary amine (1 equiv.) was dissolved anhydrous acetonitrile, and the solution of amine was added dropwise over 10 minutes to the flask containing the anomeric amide reagent. For select reactions, the reverse addition was performed as noted below. The total volume of solvent is such that the concentration of anomeric amide in the reaction is 0.1 M. The reaction was stirred at room temperature for 1 hour. The reaction was quenched with saturated aqueous $NaHCO_3$ solution and extracted to DCM. The combined organic layers were washed with brine and dried with sodium sulphate. The volatiles were removed *in vacuo* and the crude product purified by silica gel chromatography.

General procedure B for deamination of anilines

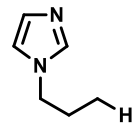
To a 2-dram screw cap vial equipped with a stir bar and PTFE/white silicone septum was added aniline (1 equiv). The anomeric amide (1.5 equiv) and dry CH_3CN was added to a second vial under nitrogen atmosphere and this solution was then transferred to the first vial containing aniline and stirred at 45 °C for 24 hours. The total volume of solvent is such that the concentration of anomeric amide in the reaction is 0.1 M. The reaction was quenched with saturated aqueous $NaHCO_3$ solution and extracted with EtOAc. The combined organic layers were washed with brine and dried with sodium sulphate. The volatiles were removed *in vacuo* and the crude product purified by silica gel chromatography.

3.4.2 Characterization Data



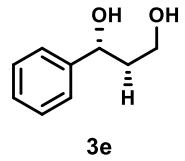
3b

1-ethyl-4-nitrobenzene (3b): Synthesized according to general procedure A from 2-(4-nitrophenyl)ethan-1-amine (2b) (47.5 mg, 0.286 mmol). The title compound was obtained in 55% yield (23.7 mg) after purification by silica gel chromatography. Rf = 0.67 (6:4 hexanes/EtOAc). ^{1}H NMR (400 MHz, $CDCl_3$) δ 8.14 (d, J = 8.7 Hz, 2H), 7.34 (d, J = 8.8 Hz, 2H), 2.76 (q, J = 7.6 Hz, 2H), 1.28 (t, J = 7.6 Hz, 3H). Spectroscopic data are in agreement with those in the literature.[42]



3d

1-propyl-1H-imidazole (3d): Synthesized according to general procedure A from 3-(1H-imidazol-1-yl)propan-1-amine (2d) (146.9 mg, 1.17 mmol). The title compound was obtained in 81% yield (105.03 mg) after purification by silica gel chromatography. Rf = 0.56 (6:4 hexanes/EtOAc). ^{1}H NMR (400 MHz, CD_3CN): δ7.43 (s, 1H), 6.99 (d, J = 1.2 Hz, 1H), 6.90 (d, J = 1.1 Hz, 1H), 3.89 (t, J = 7.1 Hz, 2H), 1.74 (h, J = 7.3 Hz, 2H), 0.85 (t, J = 7.4 Hz, 3H). Spectroscopic data are in agreement with those in the literature.[43]



3e

(R)-1-phenylpropane-1,3-diol (3e): Synthesized according to general procedure A from (1S,2S)-2-amino-1-phenyl-1,3-diol (2e) (35.4 mg, 0.212 mmol), by slow addition of the anomeric amide reagent solution to the solution of (1S,2S)-2-amino-1-phenyl-1,3-diol. The title compound was obtained in 74% yield (24.0 mg) with full stereo-retention after purification by silica gel chromatography. Rf = 0.17 (6:4 hexanes/EtOAc). ^{1}H NMR (400 MHz, 1:1 MeOD/$CDCl_3$) δ 7 7.35 – 7.26 (m, 4H), 7.24 – 7.17 (m, 1H), 4.81 (dd, J = 8.4, 4.8 Hz, 1H), 3.75 – 3.60 (m, 2H), 2.01 – 1.83 (m, 2H). Spectroscopic data are in agreement with those in the literature.[44]

A racemic sample of 1-phenylpropane-1,3-diol was synthesized according to the literature procedure from ethyl benzoyl acetate.15 Both the enantiopure and racemic diol samples were then converted to 2,2-dimethyl-4-phenyl-1,3-dioxane by treatment with camphorsulfonic acid (10 mol%) in 2,2-dimethoxypropane (50 μL/mg) for 20 h at room temperature. The enantiomeric excess of the chiral sample was then determined to be 99 using a chiral Agilent 6850 Network GC System with an Agilent J&W cycloSil-B GC 30 m, 0.25 mm, 0.25 μm, 7 inch cage column.

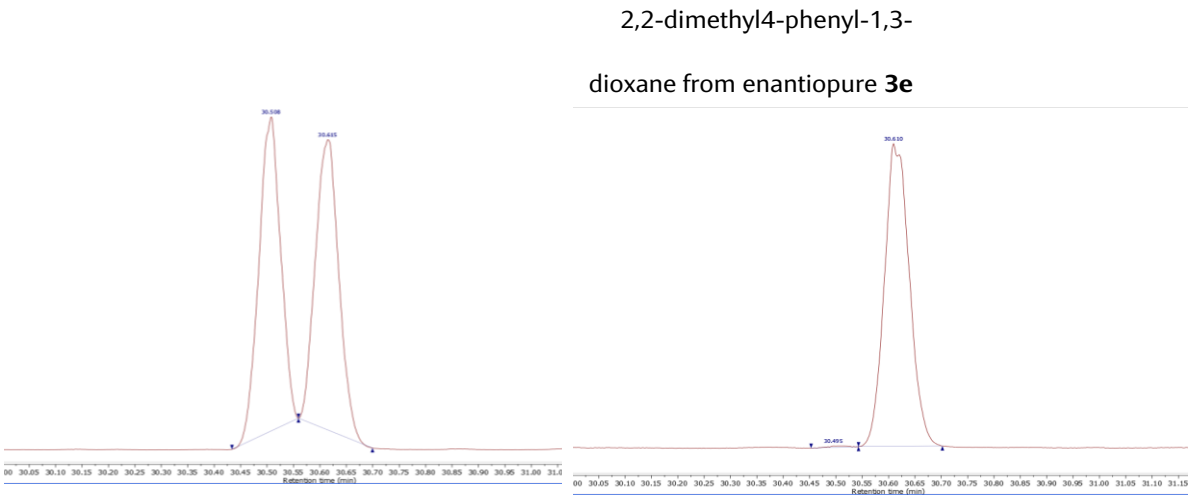
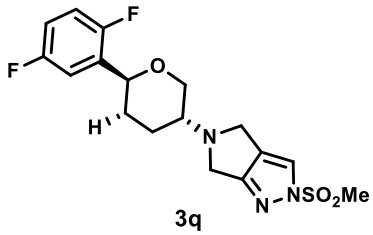


Figure 3.7 Chiral GC traces of 2,2-dimethyl4-phenyl-1,3-dioxane from racemic **3e** (left) vs **3e** from deamination of enantiopure **2e**



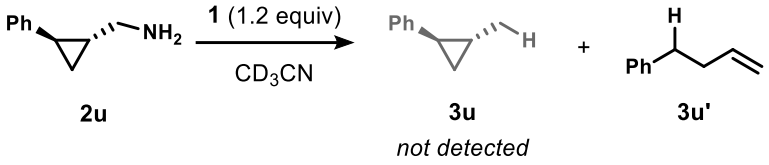
3q

5-((3R,6S)-6-(2,5-difluorophenyl)tetrahydro-2H-pyran-3-yl)-2-(methylsulfonyl)-2,4,5,6-tetrahydropyrrolo[3,4-c]pyrazole (3q): Synthesized according to general procedure A from omarigliptin (**2q**) (50 mg, 0.125 mmol). The title compound was obtained in 77% (37 mg, 0.096 mmol) yield after purification by silica gel

chromatography. Rf = 0.20 (1:1 hexanes: EtOAc). ^{1}H NMR (400 MHz, $CDCl_3$): δ 7.69 (s, 1H), 7.22 – 7.16 (m, 1H), 7.00 – 6.87 (m, 2H), 4.59 (d, J = 10.6 Hz, 1H), 4.32 (dq, J = 10.7 Hz, 2.4 Hz, 1H), 3.92 – 3.82 (m, 4H), 3.48 (t, J = 11.4 Hz, 1H), 3.27 (s, 3H), 2.91 – 2.82 (m, 1H), 2.28 – 2.20 (m, 1H), 2.10 – 2.02 (m, 1H), 1.70 (qd, J = 12.0 Hz, 3.7 Hz, 1H), 1.59 (qd, J = 13.8 Hz, 3.7 Hz, 1H). ^{19}F NMR (376 MHz, $CDCl_3$): δ -118.5 (d, J = 17.8 Hz), -125.6 (d, J = 18.5 Hz). ^{13}C (101 MHz, $CDCl_3$): δ 164.2, 159.0 (dd, 1 JC-F = 242 Hz, 4 JC-F = 1 Hz), 155.2 (dd, 1 JC-F = 242 Hz, 4 JC-F = 1 Hz), 131.4 (dd, 2 JC-F = 16 Hz, 3 JC-F = 8 Hz), 124.4, 123.5, 116.2 (dd, 2 JC-F = 12 Hz, 3 JC-F = 8 Hz), 115.0 (dd, 2 JC-F = 13 Hz, 3 JC-F = 9 Hz), 113.7 (dd, 2 JC-F = 13 Hz, 3 JC-F = 5 Hz), 73.2, 71.7, 59.3, 48.7, 48.2, 41.5, 31.7, 29.4. HRMS (ESI) calculated 392.1072, found 392.1089.

3.4.3 Mechanistic Experiments

3.4.3.1 Radical Clocks



Scheme 3.1 Reaction of radical clock **2u** with **1**

To a 1-dram screw cap vial equipped with a stir bar and PTFE/white silicone septum was added ((1R,2R)-2-phenylcyclopropyl)methanamine (**2u**) (6.9 mg, 46.9 µmol, 1 equiv) and dry CD_3CN (0.4 mL) under nitrogen. The anomeric amide (20.4 mg, 1.3 equiv) and dry CD_3CN (0.4 mL) was added to a second vial and this solution was then transferred to the first vial under nitrogen and stirred at room temperature for 1 hour. Then, 1,3,5-trimethoxybenzene (1.4 mg) was added to the crude reaction mixture as internal standard. 65.7% yield of **3u'** was obtained via ^{1}H NMR.

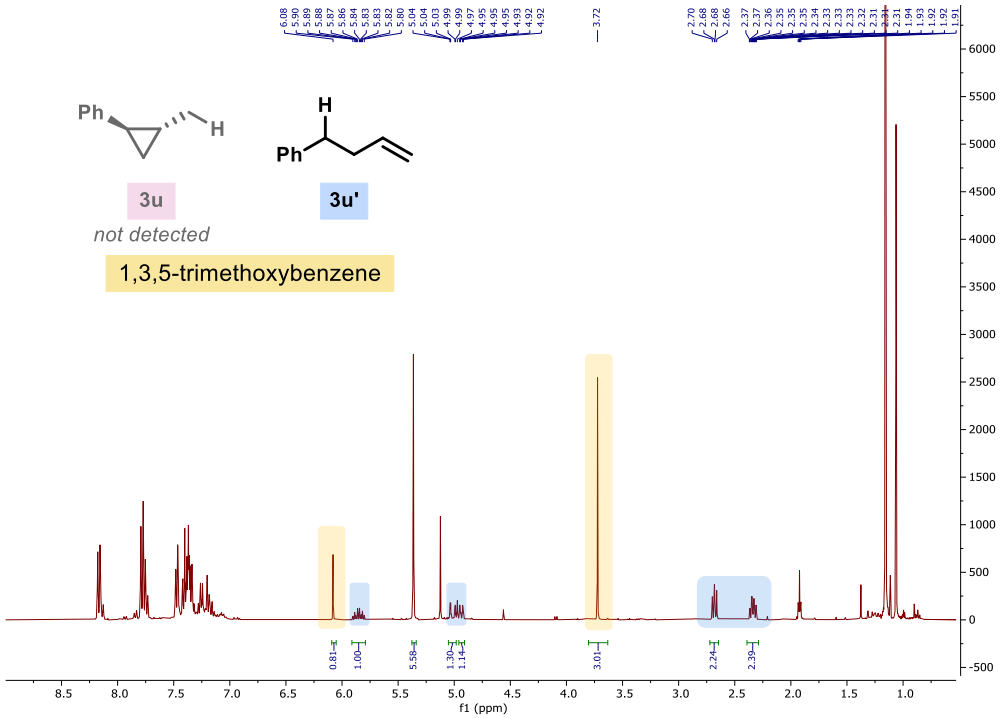
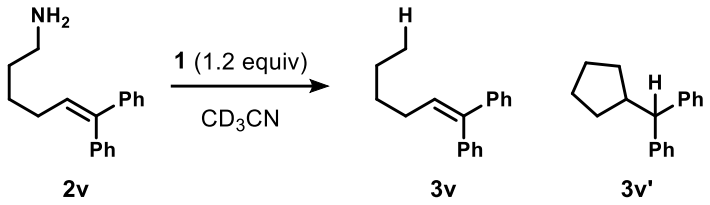


Figure 3.8 ^{1}H NMR of the crude reaction of **2u** with **1**, 1,3,5-trimethoxybenzene added as internal standard in CD_3CN



Scheme 3.2 Reaction of radical clock **2v** with **1**

To a 1-dram screw cap vial equipped with a stir bar and PTFE/white silicone septum was added 6,6-diphenylhex-5-en-1-amine (**2v**) (10.2 mg, 39.8 µmol, 1 equiv) and dry CD_3CN (0.4 mL) under nitrogen. The anomeric amide (20.4 mg, 1.3 equiv) and dry CD_3CN (0.4 mL) was added to a second vial and this solution was then transferred to the first vial under nitrogen and stirred at room temperature for 1 hour. Then, 1,3,5-trimethoxybenzene (2.2 mg) was added to the crude reaction mixture as internal standard. 41% yield of **3v** and 7% yield of **3v'** were obtained via ^{1}H NMR.[45,46]

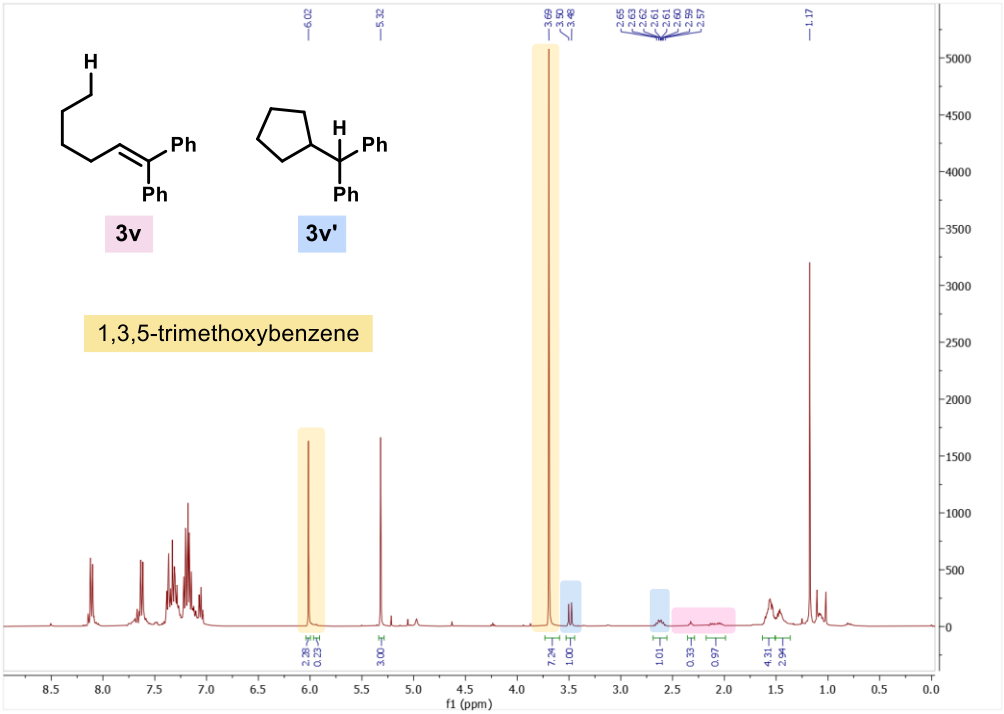
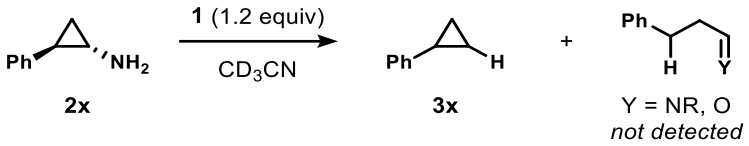


Figure 3.9 ^{1}H NMR of the crude reaction of **2v** with **1**, 1,3,5-trimethoxybenzene added as internal standard in $CDCl_3$



Scheme 3.3 Reaction of nitrogen-centered radical clock **2x** with **1**

To a 2-dram screw cap vial equipped with a stir bar and PTFE/white silicone septum was added trans-2-phenylcyclopropylamine (**2x**) (45.9 mg, 345 µmol, 1 equiv) and dry CD_3CN (1.7 mL) under nitrogen. The anomeric amide (164 mg, 1.2 equiv) and dry CD_3CN (1.7 mL) was added to a second vial and cooled to 0 °C. The amine solution was added to the anomeric amide solution over 7 minutes and the reaction was stirred for one hour at 0 °C. Then, 1,3,5-trimethoxybenzene (1.4 mg) was added to a 0.6 mL aliquot of the crude reaction (measured to be 2.8 mL total at end of reaction) as internal standard. 74% yield of **3x** was obtained via ^{1}H NMR.[47]

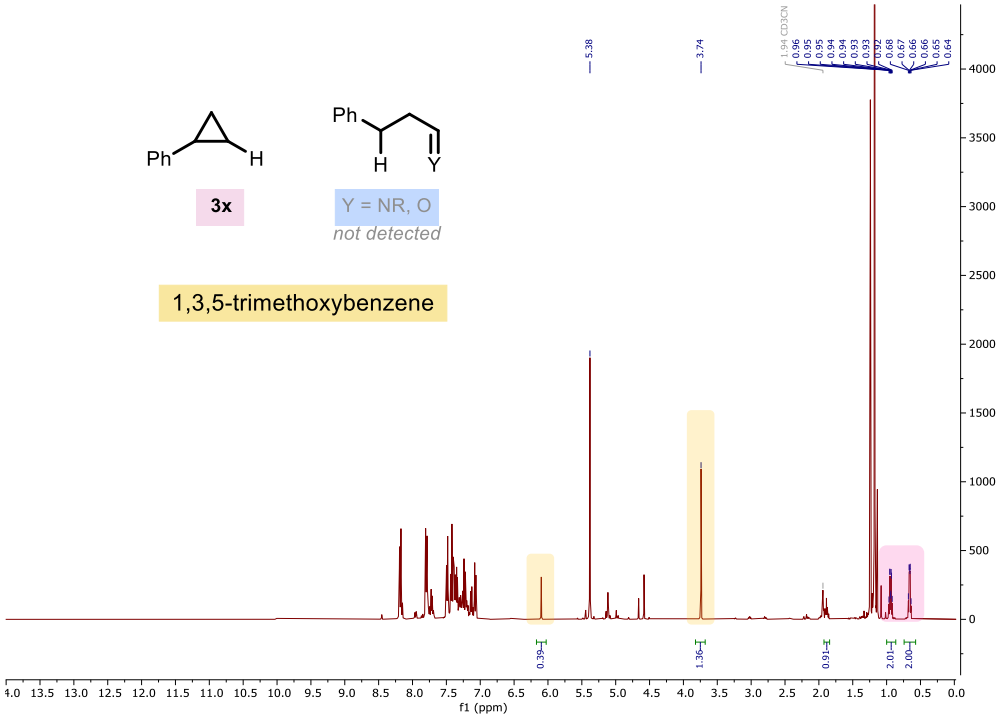


Figure 3.10 ^{1}H NMR of the crude reaction of **2x** with **1**, 1,3,5-trimethoxybenzene added as internal standard in CD_3CN

3.4.3.2 TEMPO Trap

Radical Trapping of 2a and 2c

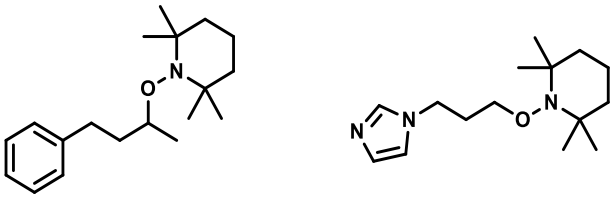


Figure 3.11 products from the trapping of radicals generated from amines **2a** and **2c**

To a 0.5-dram vial was added 100 µL **2c** or **2d** solution in CD_3CN (0.4 M) followed by 100 µL TEMPO radical solution in CD_3CN (0.48 M) then 200 µL **1** solution in CD_3CN (0.24 M in **1**), added slowly under nitrogen. After 1 hour, 1,3,5-trimethoxybenzene was added as an internal standard to determine the yield by ^1H NMR. Spectroscopic data for **8a** is in agreement with the literature.[48]

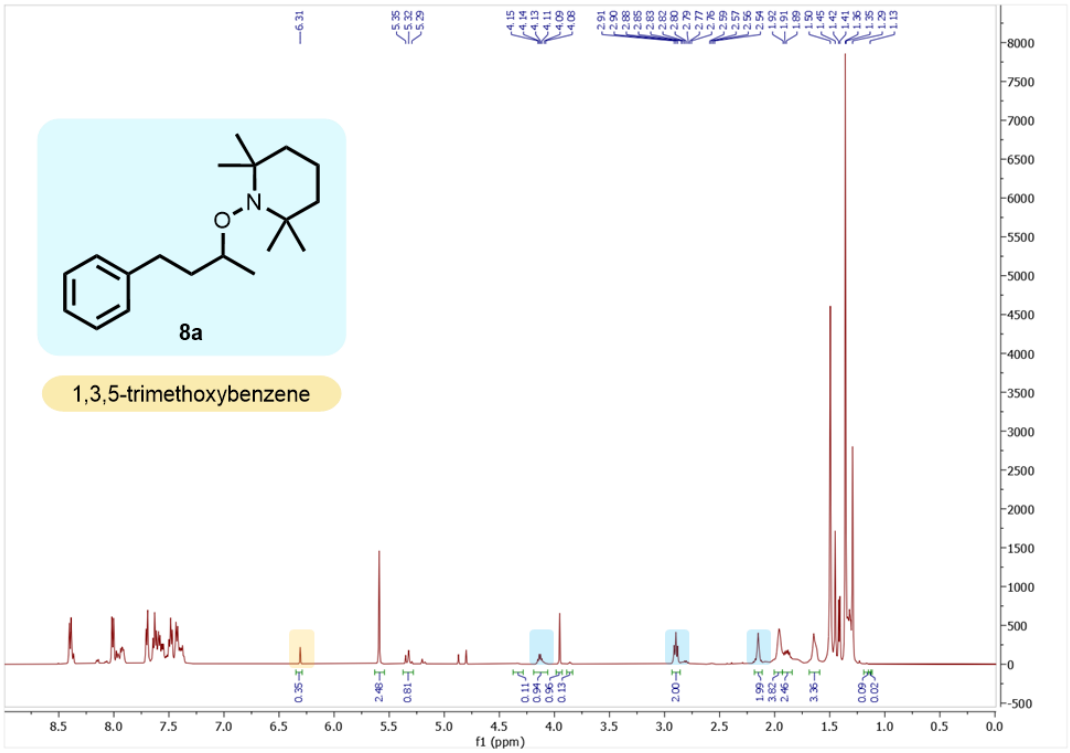


Figure 3.12 ^1H NMR of the crude reaction of **2a** and **1** with 1.2 equiv of TEMPO in CD_3CN

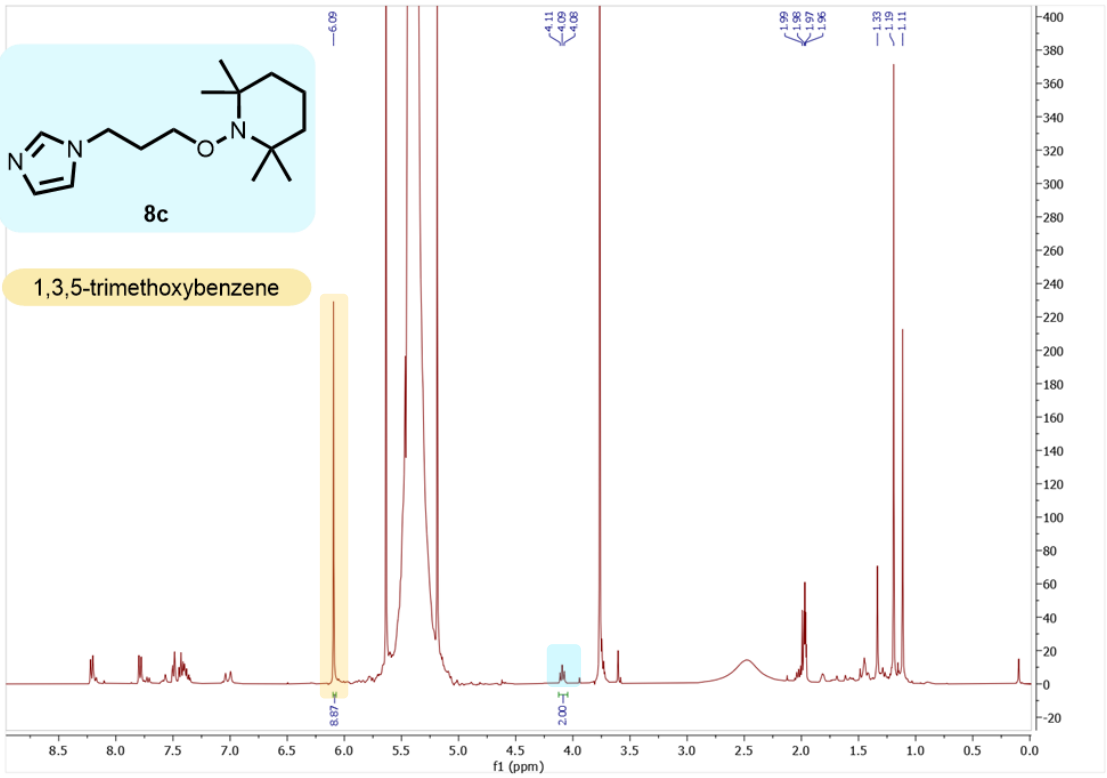


Figure 3.13 ^{1}H NMR of the crude reaction of **2c** and **1** with 1.2 equiv of TEMPO in CD_3CN

1-(3-(1H-imidazol-1-yl)propoxy)-2,2,6,6-tetramethylpiperidine (8c): 1H NMR (400 MHz, $CDCl_3$) δ 7.47 (s, 1H), 7.02 (s, 1H), 6.90 (s, 1H), 4.07 – 3.98 (m, 2H), 3.72 (t, J = 6.0 Hz, 2H), 2.02 – 1.94 (m, 2H), 1.57 – 1.44 (m, 1H), 1.39 (m, 4H), 1.32 – 1.24 (m, 1H), 1.07 (s, 6H), 1.06 (s, 6H). **13C NMR (101 MHz, $CDCl_3$)** δ 137.11, 129.34, 118.78, 77.48, 77.16, 76.84, 72.87, 59.73, 44.36, 39.56, 33.08, 30.56, 20.09, 17.05.

3.4.3.3 Deuterium Labelling

Procedure for the deuteration of amine **2d**

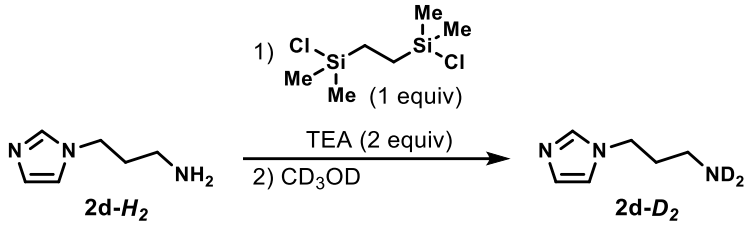


Figure 3.14 products from the trapping of radicals generated from amines **2a** and **2c**

1-(3-aminopropyl) imidazole (53.5 mg, 427 μmol) was added to a vial and purged with nitrogen. The amine was dissolved in dichloromethane (640 μL), triethylamine (120 μL, 2 equiv) was added, and the mixture was cooled to 0 °C. To a separate vial,1,2-Bis(chlorodimethylsilyl)ethane (92 mg, 1 equiv) was added and purged with nitrogen. The silane was dissolved in dichloromethane (850 μL) and the solution was added dropwise to the reaction. The reaction stirred for 2 hours at room temperature then diethyl ether was added and the mixture was filtered. The filtrate was concentrated *in vacuo* then dissolved in CD_3OD (~3 mL) and stirred overnight in a capped vial at 40 °C. The methanol was removed *in vacuo* and the deuterated amine was stored under nitrogen and used without further purification. The deuterated amine was freshly prepared for all experiments and was found to undergo rapid proton exchange if exposed to air or stored in a stock solution.

Deuterium Labelling Studies

General Procedure: To a 0.5-dram vial was added 100 μL **2c-D$_2$** solution in acetonitrile (0.2 M) followed by 100 μL **1** solution in acetonitrile (0.24 M in **1**), added slowly under nitrogen. After 1 hour, CD_3CN was added (400 μL) and the deuterium incorporation was assessed by NMR. After multipoint baseline correction, the deuterium content was assessed by integration against

the methylene indicated. In reactions where D_2O was added as a co-solvent, the amine solution was prepared in 8% D_2O in acetonitrile by volume (same total volume as above), and the procedure was otherwise identical.

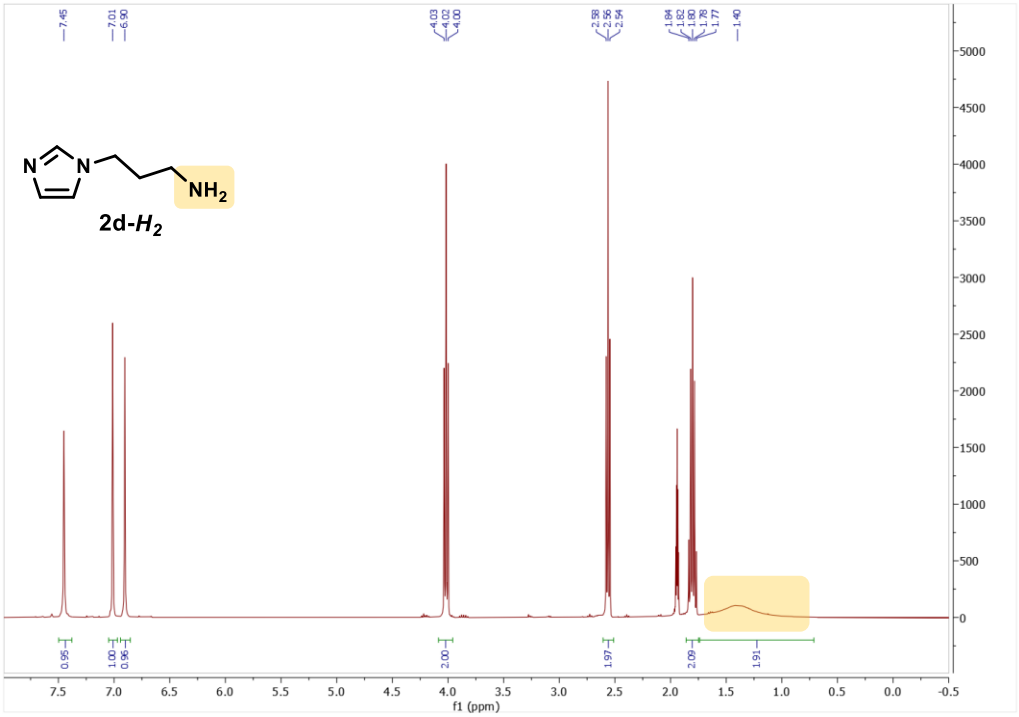


Figure 3.15 ^{1}H NMR of **2d**-*H*$_2$ in CD_3CN, NH_2 peak highlighted in gold

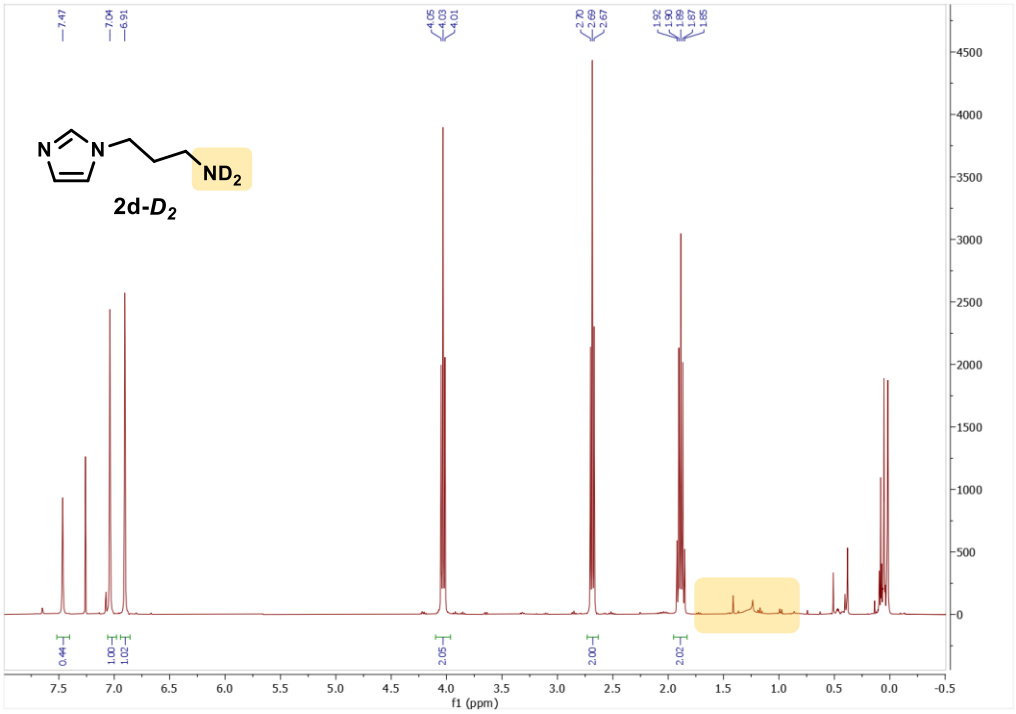


Figure 3.16 ^{1}H NMR of **2d**-D_2 in CD_3CN, disappearance of NH_2 peak highlighted in gold

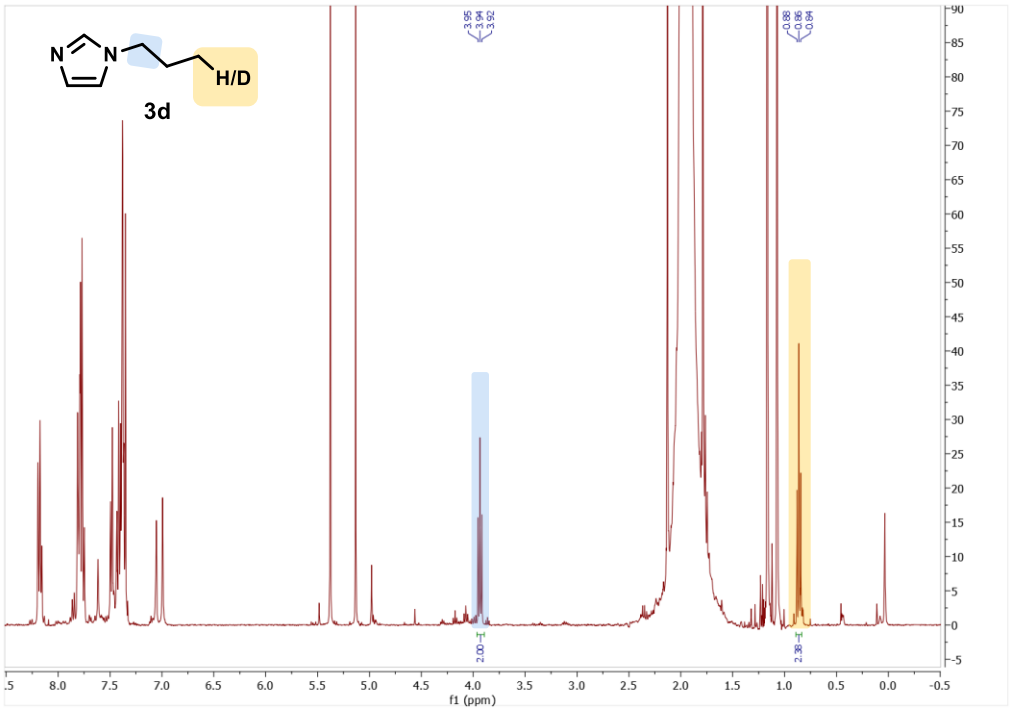
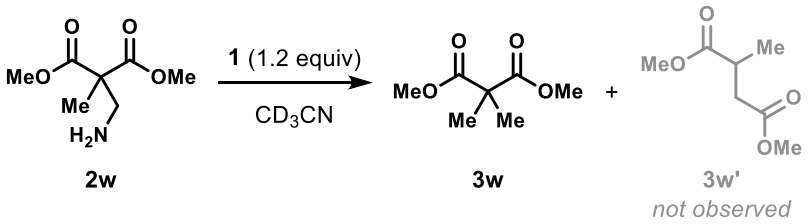


Figure 3.17 ^{1}H NMR after the deamination of **2d**-D_2 in CD_3CN, peaks used for assessing deuterium incorporation highlighted

3.4.3.4 Anion Probe



Scheme 3.4 Reaction of anion probe **2w** with **1**

Dimethyl 2-(aminomethyl)-2-methylmalonate (**2w**) was synthesized according to the literature procedure[38] from dimethyl methyl malonate. To a 1-dram screw cap vial equipped with a stir bar and PTFE/white silicone septum was added Dimethyl 2-(aminomethyl)-2-methylmalonate (**2w**) (12.7 mg, 72.7 μmol, 1 equiv) and dry CD_3CN (0.5 mL) under nitrogen. The anomeric amide (34.5 mg, 1.2 equiv) and dry CD_3CN (0.5 mL) was added to a second vial and this solution was then transferred to the first vial under nitrogen and stirred at room temperature for 1 hour. Then, 1,3,5-trimethoxybenzene (1.1 mg) was added to the crude reaction mixture as internal standard. 98% yield of **3w** was obtained via ^{1}H NMR.[49]

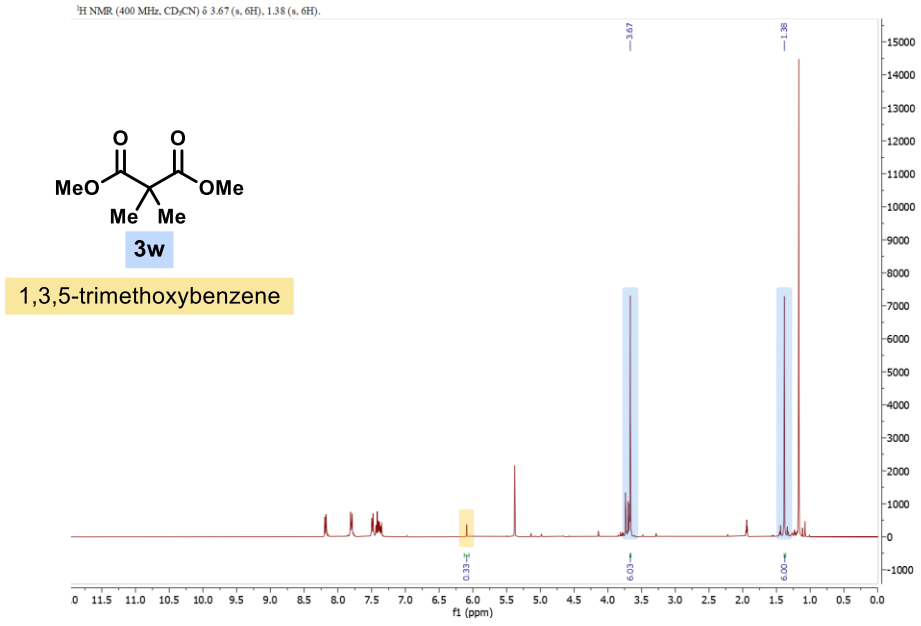


Figure 3.18 ^{1}H NMR of the crude reaction of **3w** and **1** with 1,3,5-trimethoxybenzene as an internal standard in CD_3CN

3.4.4 NMR Spectra

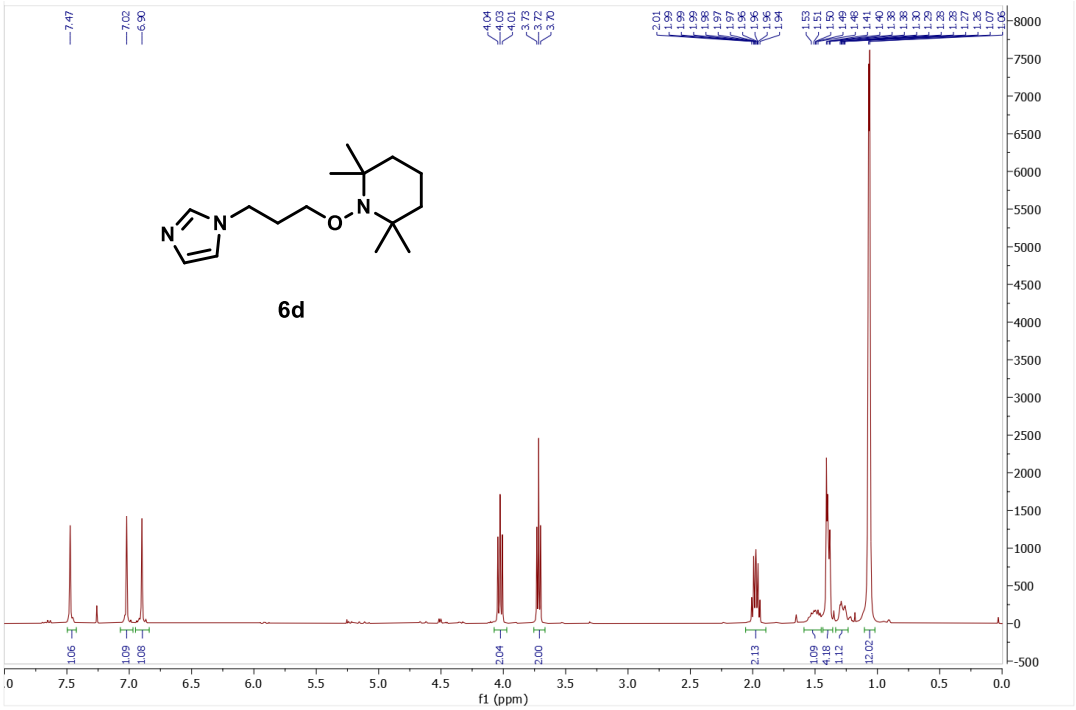


Figure 3.19^{1}H NMR of **6d** in $CDCl_3$

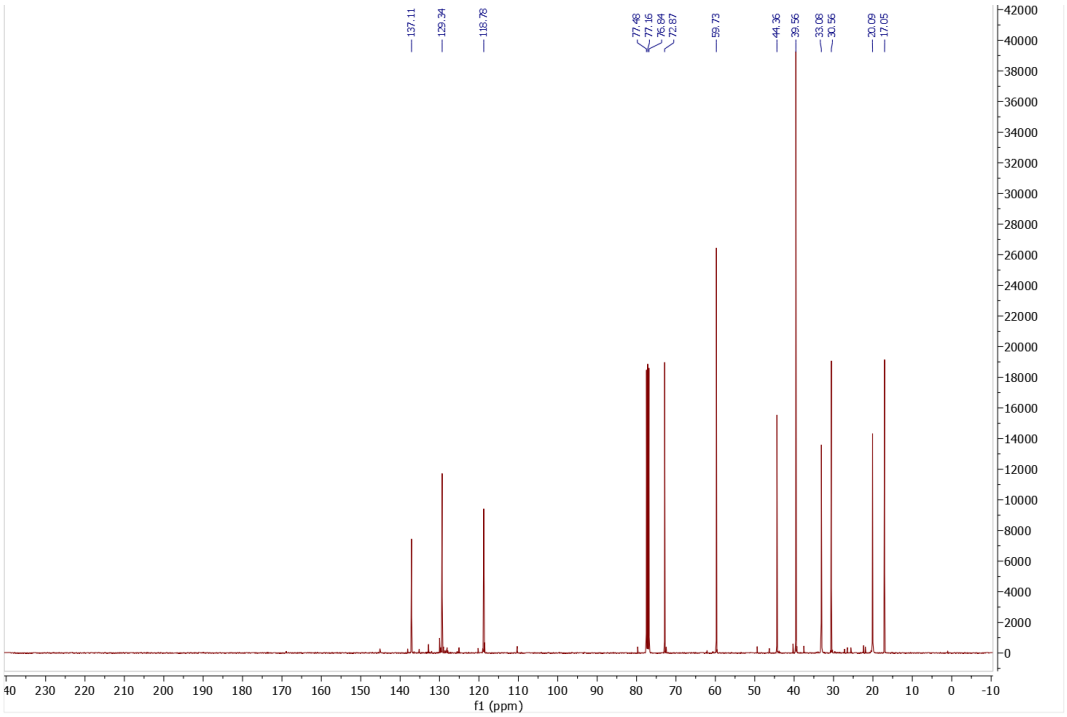


Figure 3.20^{13}C NMR of **6d** in $CDCl_3$

3.5 References

(1) Shieh, P.; Hill, M. R.; Zhang, W.; Kristufek, S. L.; Johnson, J. A. Clip Chemistry: Diverse (Bio)(Macro)Molecular and Material Function through Breaking Covalent Bonds. *Chem. Rev.* **2021**, *121* (12), 7059.

(2) McGrath, N. A.; Brichacek, M.; Njardarson, J. T. A Graphical Journey of Innovative Organic Architectures That Have Improved Our Lives. *J. Chem. Educ.* **2010**, *87* (12), 1348.

(3) Kapoor, M.; Liu, D.; Young, M. C. Carbon Dioxide-Mediated C(Sp3)–H Arylation of Amine Substrates. *J. Am. Chem. Soc.* **2018**, *140* (22), 6818–6822. https://doi.org/10.1021/jacs.8b05061.

(4) Berger, K. J.; Levin, M. D. Reframing Primary Alkyl Amines as Aliphatic Building Blocks. *Org. Biomol. Chem.* **2021**, *19* (1), 11–36. https://doi.org/10.1039/D0OB01807D.

(5) Katritzky, A. R.; Horvath, K.; Plau, B. Reductive Deamination of Alkyl and Aryl Primary Amines via 1,4-Dihydropyridines and a Note on the Mechanism of Reductive Deamination of Benzylamine via a 1,2-Dihydropyridine. *J. Chem. Soc., Chem. Commun.* **1979**, *6*, 300.

(6) Katritzky, A. R.; Horvath, K.; Plau, B. Reductive Deamination of Primary Amines. *J. Chem. Soc., Perkin Trans. 1* **1980**, *0*, 2554.

(7) Barton, D. H. R.; Bringman, G.; Lamotte, G.; Hay Motherwell, R. S.; Motherwell, W. B. Radical Deamination Reactions of Relevance to Aminoglycoside Chemistry. *Tetrahedron Lett.* **1979**, *20* (24), 2291.

(8) Guziec, F. S.; Wei, D. Convenient Halodeamination and Hydrodeamination of Primary Amines. *J. Org. Chem.* **1992**, *57* (Copyright (C) 2021 American Chemical Society (ACS). All Rights Reserved.), 3772–3776. https://doi.org/10.1021/jo00040a010.

(9) Hutchins, R. O.; Cistone, F.; Goldsmith, B.; Heuman, P. Reductive Deamination of Primary Amines. Sodium Borohydride Reduction of N,N-Disulfonimides in Hexamethylphosphoramide. *J. Org. Chem.* **1975**, *40* (13), 2018.

(10) Fang, H.; Oestreich, M. Reductive Deamination with Hydrosilanes Catalyzed by B(C6F5)3. *Angew. Chem., Int. Ed.* **2020**, *59* (28), 11394.

(11) Kennedy, S. H.; Dherange, B. D.; Berger, K. J.; Levin, M. D. Skeletal Editing through Direct Nitrogen Deletion of Secondary Amines. *Nature (London, U. K.)* **2021**, *593* (7858), 223–227. https://doi.org/10.1038/s41586-021-03448-9.

(12) Campbell, J. J.; Glover, S. A. Bimolecular Reactions of Mutagenic N-Acetoxy-N-Alkoxybenzamides and N-Methylaniline. *J. Chem. Soc., Perkin Trans. 2* **1992**, No. 10, 1661–1663. https://doi.org/10.1039/P29920001661.

(13) Glover, S. A. Anomeric Amides — Structure, Properties and Reactivity. *Tetrahedron* **1998**, *54* (26), 7229. https://doi.org/10.1016/S0040-4020(98)00197-5.

(14) Lemal, D. M.; Rave, T. W. Diazenes from Angeli's Salt. *J. Am. Chem. Soc.* **1965**, *87* (2), 393. https://doi.org/10.1021/ja01080a052.

(15) Hinsberg, W. D.; Dervan, P. B. Kinetics of the Thermal Decomposition of a 1,1-Dialkyldiazene, N-(2,2,6,6-Tetramethylpiperidyl)Nitrene. *J. Am. Chem. Soc.* **1979**, *101* (20), 6142.

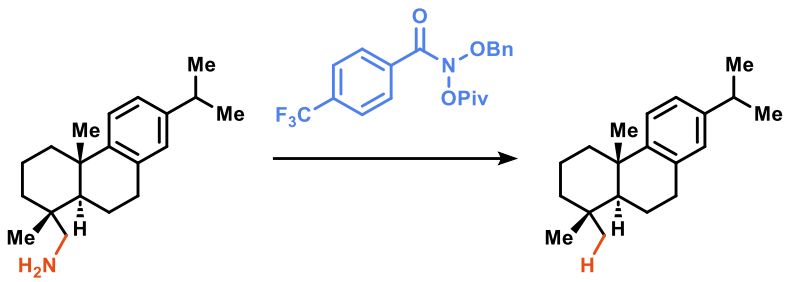
(16) Hinsberg, W. D.; Schultz, P. G.; Dervan, P. B. Direct Studies of 1,1-Diazenes. Syntheses, Infrared and Electronic Spectra, and Kinetics of the Thermal Decomposition of N-(2,2,6,6-

Tetramethylpiperidyl)Nitrene and N-(2,2,5,5-Tetramethylpyrrolidyl)Nitrene. *J. Am. Chem. Soc.* **1982**, *104* (3), 766.
(17) Zou, X.; Zou, J.; Yang, L.; Li, G.; Lu, H. Thermal Rearrangement of Sulfamoyl Azides: Reactivity and Mechanistic Study. *J. Org. Chem.* **2017**, *82* (9), 4677. https://doi.org/10.1021/acs.joc.7b00308.
(18) Qin, H.; Cai, W.; Wang, S.; Guo, T.; Li, G.; Lu, H. N-Atom Deletion in Nitrogen Heterocycles. *Angewandte Chemie International Edition* **2021**, *60* (38), 20678–20683. https://doi.org/10.1002/anie.202107356.
(19) Hinsberg, W. D.; Dervan, P. B. Synthesis and Direct Spectroscopic Observation of a 1,1-Dialkyldiazene. Infrared and Electronic Spectrum of N-(2,2,6,6-Tetramethylpiperidyl)Nitrene. *J. Am. Chem. Soc.* **1978**, *100* (5), 1608. https://doi.org/10.1021/ja00473a051.
(20) Dervan, P. B.; Uyehara, T. Stereochemical Tests of Cyclic 1,1-Dialkyldiazene Fragmentation Reactions. Thermal Decomposition of N-(Cis-(and Trans-)2,3-(and 2,5-)Dimethylpyrrolidine)Nitrenes. *J. Am. Chem. Soc.* **1979**, *101* (8), 2076.
(21) Schultz, P. G.; Dervan, P. B. Synthesis and Direct Spectroscopic Observation of N-(2,2,5,5-Tetramethylpyrrolidinyl)Nitrene. Comparison of Five- and Six-Membered Cyclic 1,1-Dialkyldiazenes. *J. Am. Chem. Soc.* **1980**, *102* (2), 878.
(22) Schultz, P. G.; Dervan, P. B. Photochemistry of a 1,1-Diazene, N-(2,2,5,5-Tetramethylpyrrolidinyl)Nitrene. *J. Am. Chem. Soc.* **1981**, *103* (6), 1563.
(23) Dervan, P. B.; Squillacote, M. E.; Lahti, P. M.; Sylwester, A. P.; Roberts, J. D. Nitrogen-15 NMR Spectrum of a 1,1-Diazene. N-(2,2,6,6-Tetramethylpiperidyl)Nitrene. *J. Am. Chem. Soc.* **1981**, *103* (5), 1120.
(24) Schultz, P. G.; Dervan, P. B. Photochemistry of 1,1-Diazenes. Direct and Sensitized Photolyses of N-(2,2,5,5-Tetramethylpyrrolidyl)Nitrene, Dl-N-(2,5-Diethyl-2,5-Dimethylpyrrolidyl)Nitrene, and N-(2,2,6,6-Tetramethylpiperidyl)Nitrene. *J. Am. Chem. Soc.* **1982**, *104* (24), 6660.
(25) McIntyre, D. K.; Dervan, P. B. 1,1-Di-Tert-Butyldiazene. *J. Am. Chem. Soc.* **1982**, *104* (23), 6466.
(26) Pasto, D. J.; Chipman, D. M. Theoretical Study of the Reactions of Ethene with Diimide Species. *J. Am. Chem. Soc.* **1979**, *101* (9), 2290.
(27) Newcomb, M. Radical Kinetics and Clocks. In *Encyclopedia of Radicals in Chemistry, Biology and Materials*; John Wiley & Sons, Ltd, 2012. https://doi.org/10.1002/9781119953678.rad007.
(28) Newcomb, M.; Johnson, C. C.; Manek, M. B.; Varick, T. R. Picosecond Radical Kinetics. Ring Openings of Phenyl-Substituted Cyclopropylcarbinyl Radicals. *J. Am. Chem. Soc.* **1992**, *114* (27), 10915–10921. https://doi.org/10.1021/ja00053a031.
(29) Ha, C.; Horner, J. H.; Newcomb, M.; Varick, T. R.; Arnold, B. R.; Lusztyk, J. Kinetic Studies of the Cyclization of the 6,6-Diphenyl-5-Hexenyl Radical. A Test of the Accuracy of Rate Constants for Reactions of Hydrogen Transfer Agents. *J. Org. Chem.* **1993**, *58* (5), 1194–1198. https://doi.org/10.1021/jo00057a036.
(30) Rodes Solanes, R.; Garcia Dominguez, N.; Lopez Ortega, B.; Alvarez de Mon Soto, M.; De La Hera Martinez, A.; Munoz Munoz, A.; Ledo Gomez, F. Diphenylalkenylamine Derivatives

and Their Preparation and Use for the Treatment of Inflammatory Diseases and Cancer, May 31, 2012.
(31) Herk, L.; Feld, M.; Szwarc, M. Studies of "Cage" Reactions. *J. Am. Chem. Soc.* **1961**, *83* (14), 2998. https://doi.org/10.1021/ja01475a005.
(32) Braden, D. A.; Parrack, E. E.; Tyler, D. R. Solvent Cage Effects. I. Effect of Radical Mass and Size on Radical Cage Pair Recombination Efficiency. II. Is Geminate Recombination of Polar Radicals Sensitive to Solvent Polarity? *Coord. Chem. Rev.* **2001**, *211* (1), 279.
(33) Barry, J. T.; Berg, D. J.; Tyler, D. R. Radical Cage Effects: Comparison of Solvent Bulk Viscosity and Microviscosity in Predicting the Recombination Efficiencies of Radical Cage Pairs. *J. Am. Chem. Soc.* **2016**, *138* (30), 9389.
(34) Barry, J. T.; Berg, D. J.; Tyler, D. R. Radical Cage Effects: The Prediction of Radical Cage Pair Recombination Efficiencies Using Microviscosity Across a Range of Solvent Types. *J. Am. Chem. Soc.* **2017**, *139* (41), 14399.
(35) Myers, A. G.; Movassaghi, M.; Zheng, B. Single-Step Process for the Reductive Deoxygenation of Unhindered Alcohols. *J. Am. Chem. Soc.* **1997**, *119* (36), 8572.
(36) Myers, A. G.; Finney, N. S. Direct Observation and Retro-Ene Reaction of a Propargylic Diazene. Stereochemical Assignment of Monoalkyl Diazenes. *J. Am. Chem. Soc.* **1990**, *112* (26), 9641.
(37) Myers, A. G.; Movassaghi, M.; Zheng, B. Mechanistic Studies of the Free-Radical Fragmentation of Monoalkyl Diazenes. *Tetrahedron Lett.* **1997**, *38* (37), 6569.
(38) Mizar, P.; Laverny, A.; El-Sherbini, M.; Farid, U.; Brown, M.; Malmedy, F.; Wirth, T. Enantioselective Diamination with Novel Chiral Hypervalent Iodine Catalysts. *Chemistry – A European Journal* **2014**, *20* (32), 9910–9913. https://doi.org/10.1002/chem.201403891.
(39) Tou, J. S.; Schleppnik, A. A. Novel 1,2-Ester Transposition Reactions. *J. Org. Chem.* **1983**, *48* (5), 753.
(40) Andrieux, C. P.; Gallardo, I.; Saveant, J. M. Outer-Sphere Electron-Transfer Reduction of Alkyl Halides. A Source of Alkyl Radicals or of Carbanions? Reduction of Alkyl Radicals. *J. Am. Chem. Soc.* **1989**, *111* (5), 1620.
(41) Wuttig, A.; Derrick, J. S.; Loipersberger, M.; Snider, A.; Head-Gordon, M.; Chang, C. J.; Toste, F. D. Controlled Single-Electron Transfer via Metal–Ligand Cooperativity Drives Divergent Nickel-Electrocatalyzed Radical Pathways. *J. Am. Chem. Soc.* **2021**, *143* (18), 6990.
(42) Cummings, S. P.; Le, T.-N.; Fernandez, G. E.; Quiambao, L. G.; Stokes, B. J. Tetrahydroxydiboron-Mediated Palladium-Catalyzed Transfer Hydrogenation and Deuteriation of Alkenes and Alkynes Using Water as the Stoichiometric H or D Atom Donor. *J. Am. Chem. Soc.* **2016**, *138* (19), 6107–6110. https://doi.org/10.1021/jacs.6b02132.
(43) Arai, T.; Morita, Y.; UDAGAWA, S.; Iseki, K.; Izumimoto, N. Cyclic Amine Derivative and Pharmaceutical Use Thereof. US10173999B2, January 8, 2019. https://patents.google.com/patent/US10173999B2/en?oq=WO2016%2f136944. (accessed 2025-03-25).
(44) Merkley, N.; Warkentin, J. Thermolysis of a Spiro-Fused Oxadiazoline: The Carbonyl Ylide–cyclic Carbene–diradical Sequence. *Can. J. Chem.* **2002**, *80* (9), 1187–1195. https://doi.org/10.1139/v02-126.

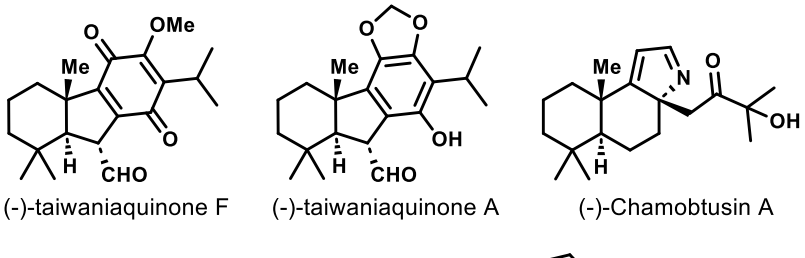
(45) Benati, L.; Leardini, R.; Minozzi, M.; Nanni, D.; Scialpi, R.; Spagnolo, P.; Strazzari, S.; Zanardi, G. A Novel Tin-Free Procedure for Alkyl Radical Reactions. *Angewandte Chemie International Edition* **2004**, *43* (27), 3598–3601. https://doi.org/10.1002/anie.200454245.
(46) Levin, V. V.; Dilman, A. D. Alkene Homologation via Visible Light Promoted Hydrophosphination Using Triphenylphosphonium Triflate. *Chem. Commun.* **2021**, *57* (6), 749–752. https://doi.org/10.1039/D0CC07025D.
(47) Ye, Y.; Ma, G.; Yao, K.; Gong, H. Zn-Mediated Hydrodeoxygenation of Tertiary Alkyl Oxalates. *Synlett* **2021**, *32*, 1625–1628. https://doi.org/10.1055/a-1328-0352.
(48) Liu, X.-G.; Dong, C.-S.; Li, F.; Zhang, B. Manganese-Mediated Direct Functionalization of Hantzsch Esters with Alkyl Iodides via an Aromatization–Dearomatization Strategy. *Org. Lett.* **2021**, *23* (10), 4002–4007. https://doi.org/10.1021/acs.orglett.1c01210.
(49) Boyle, P. H.; Cocker, W.; Gordon, R. L.; Shannon, P. V. R. The Chemistry of Terpenes. Part XIII. Synthesis of (+)-3β,7,7-Trimethyl-Anti,Cis,Anti-Tricyclo[4,1,0,02,4]Heptane and (±)-Trans-3-(1-Hydroxyethyl)-6,6-Dimethylbicyclo[3,1,0]Hexane, Deamination Products of the Cis-Caran-4-Amines. *J. Chem. Soc. C* **1971**, No. 0, 2127–2136. https://doi.org/10.1039/J39710002127.
(50) Solanes, R. R.; DOMÍNGUEZ, N. G.; ORTEGA, B. L.; Soto, M. Á. de M.; Martínez, A. de la H.; Muñoz, A. M.; Gómez, F. L. Diphenyl-Amine Derivatives: Uses, Process of Synthesis and Pharmaceutical Compositions. WO2012069442A1, May 31, 2012. https://patents.google.com/patent/WO2012069442A1/en?oq=WO2012069442 (accessed 2025-03-24).

Chapter 4 : Gram Scale Application of Nitrogen Deletion to Synthesize Abietatriene

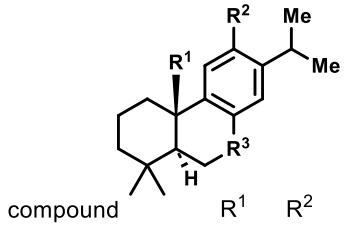


4.1 Introduction

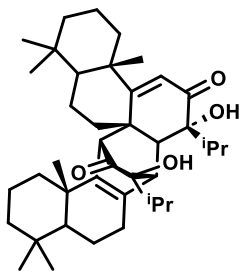
To exemplify the utility of our primary-amine deletion reaction, we wanted to develop a procedure demonstrating its ability to transform naturally abundant amines into value-added products. As such, I decided to scale the deamination of leelamine (**1**) using our anomeric amide reagent (**2**) to generate abietatriene (**3**), a naturally occurring diterpene that has been synthesized as an intermediate *en route* to a variety of terpenoid natural products and their synthetic analogs (Figure 4.1).[1–10]



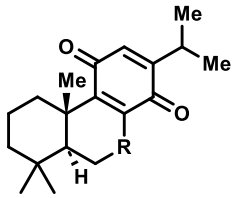
compound	X	Y
d-Kaurene	R	S
d-Phyllocladene	S	R



compound	R^1	R^2	R^3
(+)-pisiferic acid	COOH	OH	CH_2
(+)-ferruginol	Me	OH	CH_2
(±)-Sugiol	Me	OH	CO
(±)-abieta-8,11,13-trien-7β-ol	Me	OH	(R)-CHOH



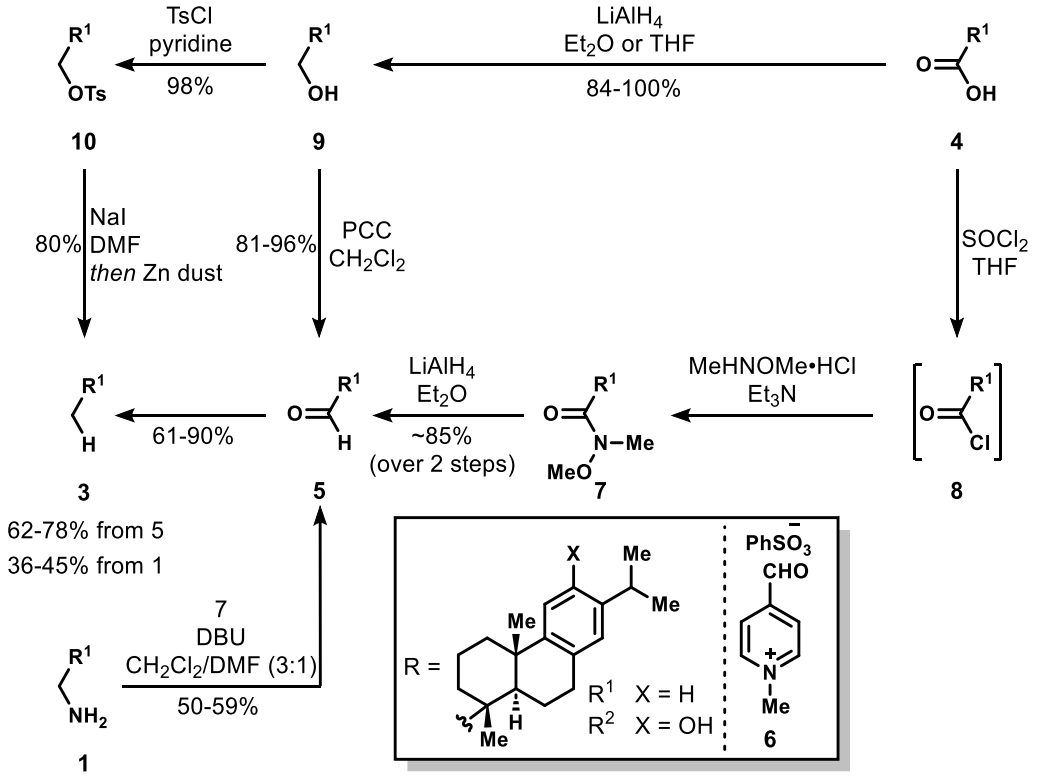
(+)-maytenone



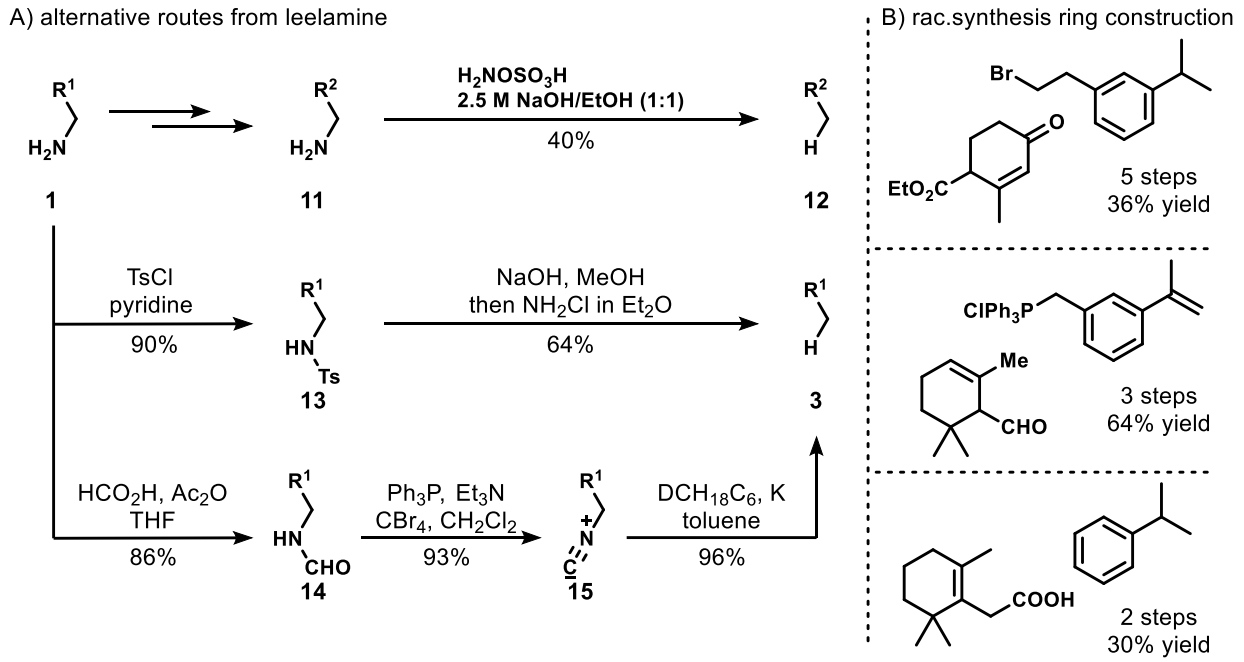
compound	R
12-deoxyroyleanone	CH_2
cryptoquinone	CO
11,14-dihydroxyabieta-8,11,13-trien-7-one	CO

Figure 4.1 Compounds synthesized from abietatriene

Due to its limited commercial availability, abietatriene is typically synthesized from leelamine (**1**) or dehydroabietic acid (**4**). Prior to the development of our deamination reaction, the most popular route to achieve this has involved transforming the amine or carboxylic acid respectively into an aldehyde (**5**), followed by a Wolff-Kishner type reduction (Scheme 4.1).[1–4,11] From leelamine (**1**), the aldehyde intermediate can be accessed using pyridinium **6**,[3,4] based on a biomimetic transformation developed by Rapoport.[12] From dehydroabietic acid, aldehyde 6 has been synthesized by conversion to Weinreb amide **7** (via acyl chloride **8**) followed by hydride reduction.[2] Alternatively, the carboxylic acid can be fully reduced to an alcohol (**9**) followed by pyridinium chlorochromate oxidation.[1,11] Alcohol **9** can also be tosylated (**10**) then reduced using sodium iodide and zinc dust.[5,6] A more direct method employing hydroxylamine-*O*-sulfonic acid (HOSA) for the direct reduction of the amine has been used to achieve



Scheme 4.1 A) synthetic routes to 3 proceeding through an aldehyde or alcohol intermediate



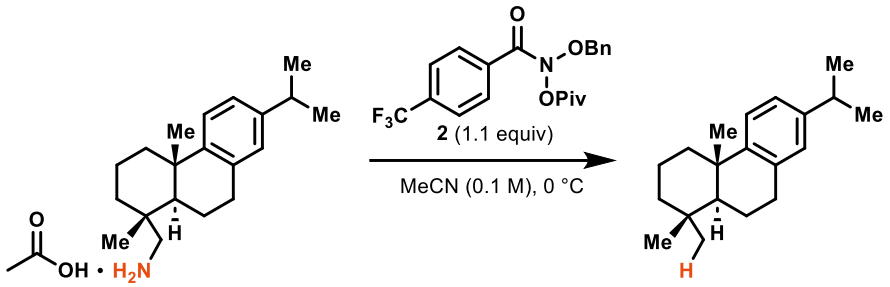
Scheme 4.2, A) alternative synthetic routes to 3 from leelamine, B) fragment pairs for the synthesis of 3 via ring construction strategies

moderate yield on a phenolic derivative (**11** and **12**) (Scheme 4.2A).[3,8] Other synthetic strategies from leelamine have included reduction of the tosylated amine (**13**) using base followed by ethereal chloramine[13] and formylation to **14** followed by dehydration to generate an isonitrile (**15**), which can be reduced using potassium (Scheme 4.2A).[7] In addition to these reduction strategies, *de novo* construction of the B ring has also been demonstrated from various combinations of cyclohexene-based and aromatic fragments (Scheme 4.2B).[9,10,14]

4.2 Optimization of Reaction Conditions

4.2.1 Experimental Results

Several factors were considered in optimizing the large-scale deamination of **1**. Regarding safety, the reaction generates a stoichiometric amount of nitrogen gas and primary amines in particular react very rapidly with anomeric amide **2**. As such, on larger scales the rate of the reaction must be carefully controlled to minimize risk of runaway. Additionally, some



leelamine acetate **16**
1 mmol
350 mg

abietatriene **3**
72% isolated yield
196 mg

Scheme 4.3 reaction of *leelamine acetate* with anomeric amide

very sterically unhindered primary amines demonstrated improved yields and reduced byproducts at 0 °C, suggesting a problematic exotherm. Given this observation, I also wanted to ensure that we were able to have careful control over the temperature of the reaction to mitigate this. Finally, our published work-up procedure relied on the diluting the acetonitrile reaction solvent with dichloromethane to enable extraction, which would not be very practical on a large-scale.

To address the first two concerns, I decided to test the reaction of leelamine acetate (**16**) with the anomeric amide reagent (**2**) at 0 °C, as the reduced solubility of the acetate salt in acetonitrile compared to the free amine and lower reaction temperature could slow down the reaction and enable better control over the rate of gas evolution. This change also improves the efficiency of the procedure, as commercially available technical grade leelamine is purified through precipitation and crystallization of acetate salt **16**. The acetate salt was found to react very well with **2** at 0 °C, and after the consumption of most of the starting materials, the reaction could be safely warmed to room temperature to react any remaining starting material.

To improve the efficiency of the workup procedure, I tested the partitioning of product **3** between hexanes and acetonitrile and found that it had a strong preference for the hexanes

layer, with no detectable amount in the acetonitrile layer by TLC after 3 extractions. As such, a workup procedure where product **3** was directly extracted from the reaction mixture using hexanes was implemented, eliminating the need to dilute the acetonitrile with a less polar solvent or evaporate the solvent prior to extraction.

Upon scaling the procedure to 5 mmol of amine **18**, an insoluble byproduct observed to form during the reaction was causing the separatory funnel to clog due to the increased amount generated on a larger scale. The byproduct was identified as N-benzyloxyamide **17**, which forms from the reduction of **2**. This was remedied by the addition of two equivalents of triethylamine at the end of the reaction, which solubilizes the compound in acetonitrile, enabling efficient extraction. This also neutralizes the pivalic acid formed as a stoichiometric byproduct in the reaction and the acetic acid from the amine salt to ensure that all of the amine is consumed in the reaction.

The last issue that I observed in scaling this reaction was the presence of very non-polar impurities that eluted closely with the desired product and interfered with our ability to crystallize **3**. Separation could be achieved by normal-phase chromatography, but required substantial amounts of silica, so the reduction or elimination of these byproducts was highly desirable. I was able to trace the impurities back to the technical grade leelamine used, which

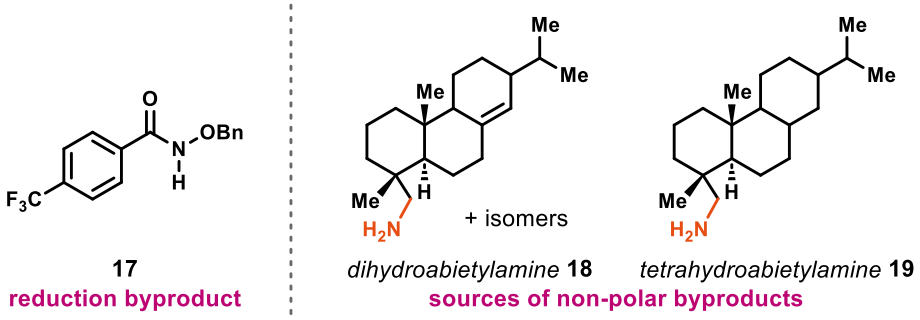
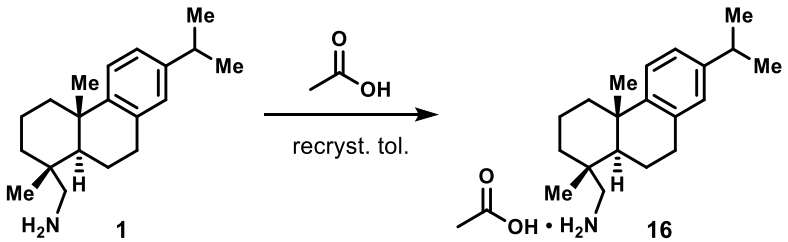


Figure 4.2 Byproducts identified during scale-up

typically consists of >90% high molecular weight amines, such as di- and tetra-hydroabietylamine (**18** and **19**).[15,16] These can similarly be deaminated by the anomeric amide (**2**), resulting in a mixture of hydrocarbons with nearly identical properties. To reduce the presence of these impurities as much as possible, I optimized the recrystallization of leelamine acetate, as the amine salts were expected to be easier to purge than their deaminated counterparts. Taking inspiration from a patent on the purification of leelamine for the recovery of penicillin,[15] I chose to recrystallize the acetate salt in toluene, which is reported to dissolve the undesired amine salts better than the methanol that was previously being used.[17,18] Additionally, the acid was added to a heated solution of amine **1** to prevent the salt from crashing out prematurely, potentially entrapping impurities. Increasing the volume of toluene was also found to increase the purity of **16** without significant impact on the yield. This increase in the purity of **16** reduced the impurities observed after deamination, enabling more efficient chromatography conditions to isolate **3**.

Table 4.1 Optimization for the crystallization of 16



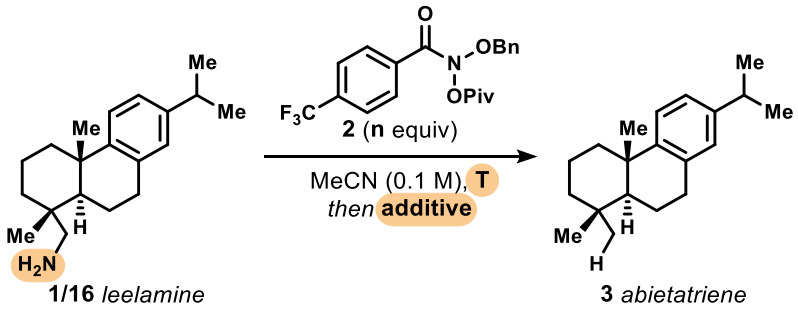
20 g

V_1 toluene	T_1	V_2 toluene	T_2	yield	purity
45 mL	RT (21 °C)	45 mL	RT (21 °C)	53%	93%
60 mL	49 °C	60 mL	49 °C	56%	95%
125 mL	35 °C	75 mL	49 °C	52%	97%

4.2.2 Conclusions: Summary of Procedural Modifications

This reaction demonstrates the use of anomeric amide reagent **4** to enable the direct deamination of leelamine (dehydroabietylamine) (**1**) to access abietatriene in a single step in good yield. This method is also applicable to the direct deamination of many other primary amines as described in the discussion for the synthesis of **4**[19] Deviations from the published standard conditions for this transformation[17] for the large scale synthesis of **3** include the use of the acetate salt (**2**) rather than the free amine (**1**), lowering of the addition temperature to 0 °C, the addition of triethylamine, and direct extraction into hexanes from the reaction solvent (Table 4.2). The reaction of **1** with primary amines was observed to be very rapid on small scale, with visible gas evolution. The use of the acetate salt and lower addition temperature enable better control over the rate at which nitrogen gas is generated throughout the reaction. Additionally, the conversion of **1** to an acid salt is necessary for its purification from the commercially supplied technical grade material, so the direct deamination of the acetate salt increases the efficiency of this route by eliminating the need to free-base the amine. Due to the reduced solubility of the acetate salt in acetonitrile and the acidification of the solution over the course of the reaction from the generation of 1 equivalent of pivalic acid, triethylamine was

Table 4.2 published general conditions for primary amine deletion[17] vs. these conditions



procedure	amine	n	T	additive	extraction solvents
general	free amine **1**	1.2	23 °C	--	CH_2Cl_2/$NaHCO_3$ (sat.)
leelamine	acetate salt **16**	1.1	0 - 23 °C	Et_3N	hexanes/MeCN

added to ensure complete consumption of the amine and removal of acidic byproducts during extraction. Product isolation is further simplified by extracting directly into hexanes from the crude reaction mixture, which was found to efficiently extract the product and remove polar byproducts while eliminating the need to evaporate the acetonitrile. Overall, these changes enabled the transformation of leelamine acetate (**16**) to abietatriene (**3**) in a single step in 80% yield on a 15 mmol scale (3.2 g abietatriene isolated).

4.3 Experimental

4.3.1 Optimized Procedure

A. *Leelamine acetate (**16**)*. (Note 2) In air, 60% (+)-dehydroabietylamine (**1**, leelamine) (20.78 g, approx. 44 mmol, 1.0 equiv) (Note 3) (Figure 4.3A) was added to a 250 mL Erlenmeyer flask followed by toluene (115 mL) (Note 4) to form a yellow solution (Figure 4.3B). A 4 cm cylindrical stir bar was added and the solution was heated to an internal temperature of 64 °C (Note 5) while stirring (Note 6). Glacial acetic acid (4.4 mL, 77 mmol, 1.75 equiv) (Notes 7 and 8) in toluene (10 mL) was added to a 30 mL separatory funnel positioned above the flask (Figure 4.3C) and this solution was added dropwise over 4 min (Notes 9, 10, and 11).

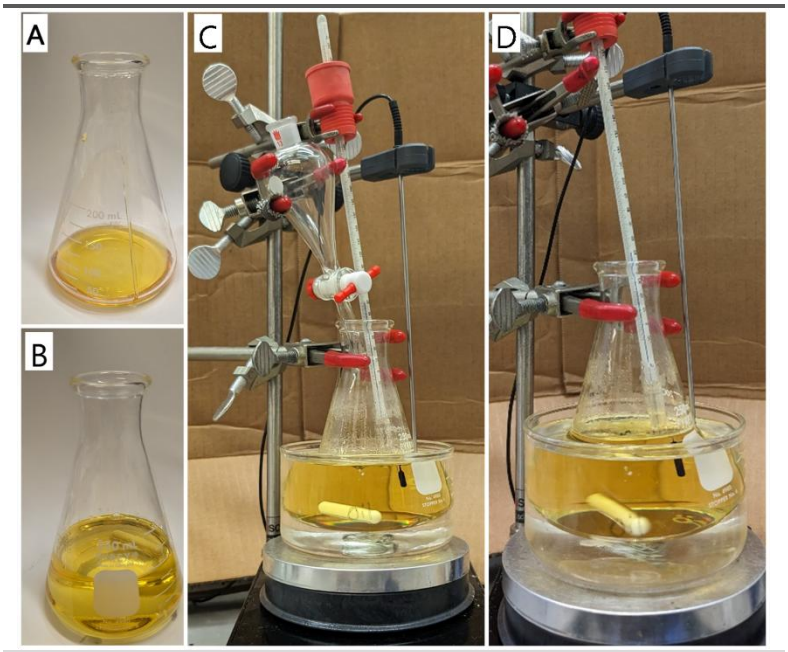


Figure 4.3 A) leelamine, B) leelamine dissolved in toluene, C) reaction setup, D) reaction after acetic acid addition, photos taken by author

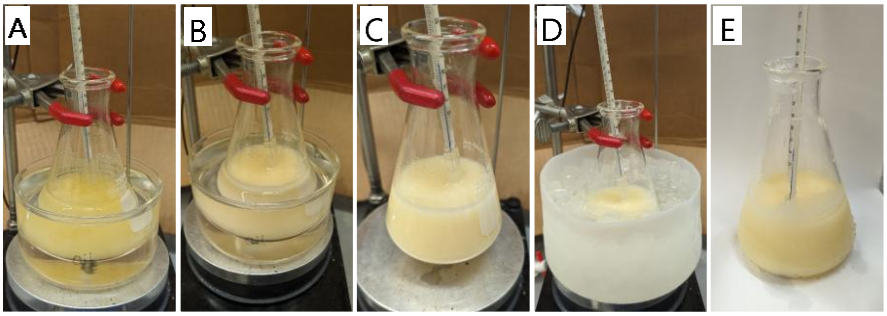


Figure 4.4 Slurry throughout procedure: A) initial slurry formation, B) after 30 min at 35 °C, C) at 26 °C, D) cooling in ice water bath, E) final slurry (5 °C), photos taken by author

Throughout the addition the solution remained clear and yellow (Figure 4.3D).

After addition, the solution was slowly cooled to 35 °C (Note 12), and a slurry began to form (Figure 4.4A). This temperature was held for 30 min to achieve slow crystallization, during which a thick slurry formed (Note 13) (Figure 4.4B). The heating source was then turned off and the solution was left in the oil bath to cool slowly. Once an internal temperature below 30 °C was achieved (Note 14) (Figure 4.4C), the flask was transferred to an ice water bath for 15 min (Note 15) (Figure 4.4D).

The slurry was vacuum-filtered using a 150 mL glass fritted Büchner funnel (Note 16) attached to a 250 mL side-arm filter flask using a rubber filter adaptor (Note 17) (Figure 4.5A-

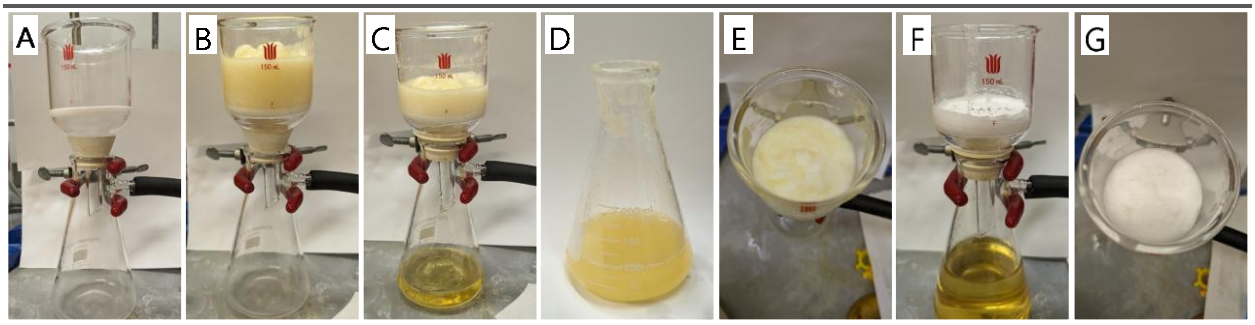


Figure 4.5 First filtration: A) vacuum filtration setup, B) slurry in funnel, C) filtered slurry and mother liquor, D) mother liquor with material remaining in reaction flask, E) filter cake immediately before washes, F, G) filter cake after washes, photos taken by author

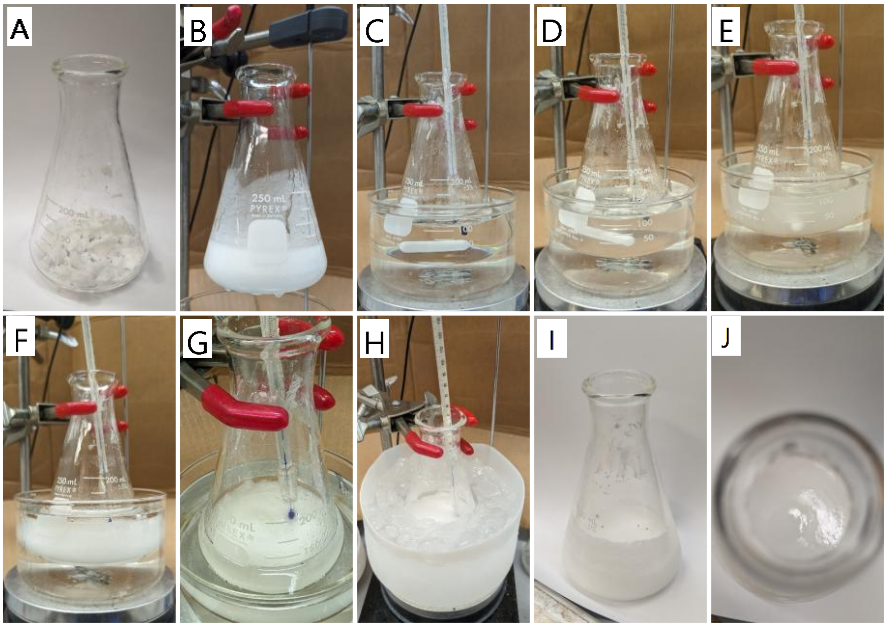


Figure 4.6 Recrystallization: A) filtered solids in flask, B) suspension in toluene, C) solution at 65 °C, D) start of crystallization (49 °C), E, F) slurry progression at 49 °C, G) at 30 °C, H) cooling in ice water bath, I, J) final slurry (5 °C), photos taken by author

B). Once the top of the cake showed no visible liquid (Figure 4.5E), it was rinsed with cold toluene (40 mL x 2) (Note 18) then filtered until dry, affording a white solid (Figure 4.5-G).

The solids were transferred to a 125 mL Erlenmeyer flask (Figure 4.6A). Toluene (75 mL) and a 4 cm cylindrical stir bar were added, and the resulting white suspension (Figure 4.6B) was heated to 65 °C to form a clear, colorless solution (Note 5) (Figure 4.6C). Once the solids were fully dissolved, the solution was slowly cooled to 49 °C (Note 12), and a slurry began to form (Note 19) (Figure 4.6D). This temperature was held for 30 min while the slurry thickened (Figure 4.6E-F) before allowing the bath and solution to cool to room temperature (Notes 14 and 20). Once the internal temperature reached 30 °C (Figure 4.6G), the flask was placed in an ice water bath for 15 min (Note 15) (Figure 4.6H).

The slurry was vacuum-filtered using a 150 mL glass fritted Büchner funnel (Note 16) attached to a 250 mL side-arm filter flask using a rubber filter adaptor (Note 17) (Figure 4.7A).

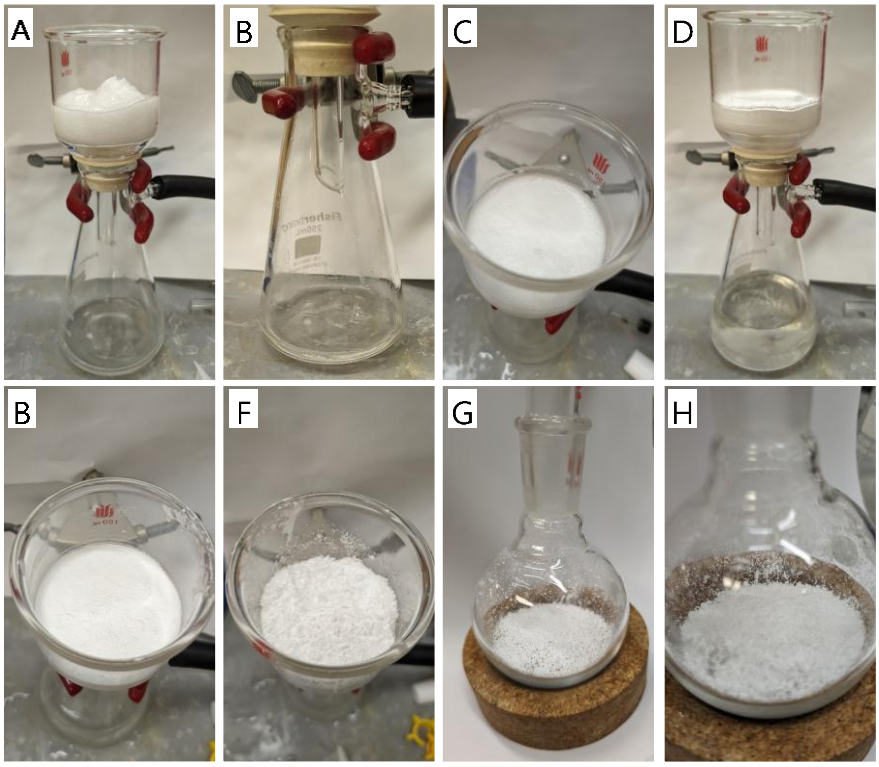


Figure 4.7 Second filtration: A) slurry in funnel, B) mother liquor, C) filter cake immediately before rinses, D, E) dried filter cake, F) solids broken up, G, H) dried solids, photos taken by author

Once no liquid was visible on top of the cake (Figure 4.7C), it was rinsed with cold toluene (40 mL x 2) followed by pentane (30 mL) (Note 21) to afford a white solid (Figure 4.7D-E). When the filter was no longer cold to the touch, the cake was broken up by scraping with a plastic spatula to form chalky white solids (Figure 4.7F). Once dry, the solids were transferred to a 250 mL round bottom flask and dried under vacuum overnight (Note 22) to afford **16** as a chalky white solid (6.58 g, 19 mmol, 44%) (Notes 23 and 24) (Figure 4.7G-H).

B. *Abietatriene (**3**).* An oven-dried, 500 mL, three-neck (24/40 joints), round-bottomed flask was equipped with: a 2.5 in. egg-shaped stir bar, an oven-dried 125 mL addition funnel with a greased PTFE stopcock and rubber stopper, a modified rubber stopper with a low-temperature thermometer, and a glass gas adapter apparatus (Note 25) connected to a Schlenk line. The system was cooled under vacuum then purged with nitrogen gas (Figure 4.8A).

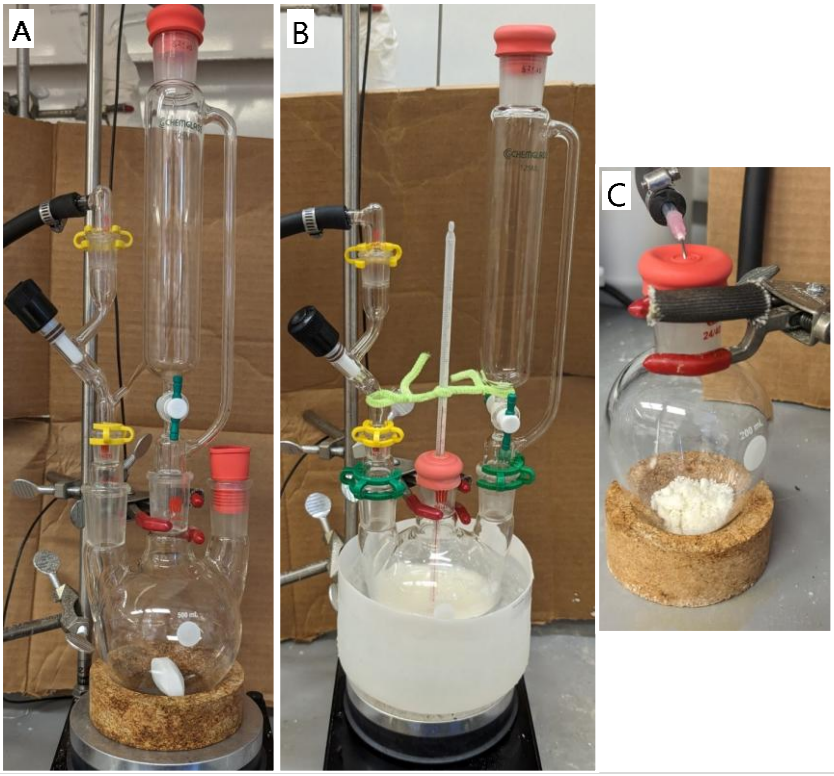


Figure 4.8 A) reaction setup, B) leelamine acetate in MeCN, C) 4 in flask, photos taken by author

Under air, Leelamine acetate (5.18 g, 15 mmol, 1.0 equiv) was added to the flask by temporarily removing the gas adapters. After replacing the adapters, the flask was evacuated (Note 26) and purged with nitrogen gas in triplicate and left under a positive nitrogen atmosphere. Through the addition funnel, dry, degassed acetonitrile (100 mL) (Note 27) was added and the flask was placed in an ice-water bath to form a white suspension equilibrated to 3 °C (Figure 4.8B) (Note 28).

N-(Benzyloxy)-N-(pivaloyloxy)-4-(trifluoromethyl)benzamide (6.52 g, 16.5 mmol, 1.1 equiv) (Note 29) was placed into an oven-dried 200 mL heart-shaped flask (24/40 joint), and the flask was sealed with a rubber stopper (Figure 4.8C). The flask was connected to a Schlenk line through rubber tubing fitted with a modified syringe and needle, then evacuated and purged with inert gas in triplicate, ending with the flask under a positive pressure of inert gas.

Dry, degassed acetonitrile (40 mL) (Note 27) was added to the flask, and once the solid was fully dissolved, the solution was transferred to the closed addition funnel via syringe. The heart-shaped flask was then rinsed with acetonitrile (5 mL) which was added to the addition funnel. An additional 5 mL of acetonitrile was then added to the heart-shaped flask (used to rinse funnel after addition is complete).

The solution in the addition funnel was added to the white suspension dropwise at a rate of 2 drop/second (ca. 18 min). Steady gas evolution was observed during the addition, and the rate of addition was controlled to minimize effervescence and to ensure that the internal temperature did not increase above 5 °C. After the addition was complete, the contents of the heart-shaped flask were slowly rinsed down the sides of the open addition funnel. The reaction was left to stir at 3 °C for 3 h, until most of the solid was dissolved and the solution had a slight

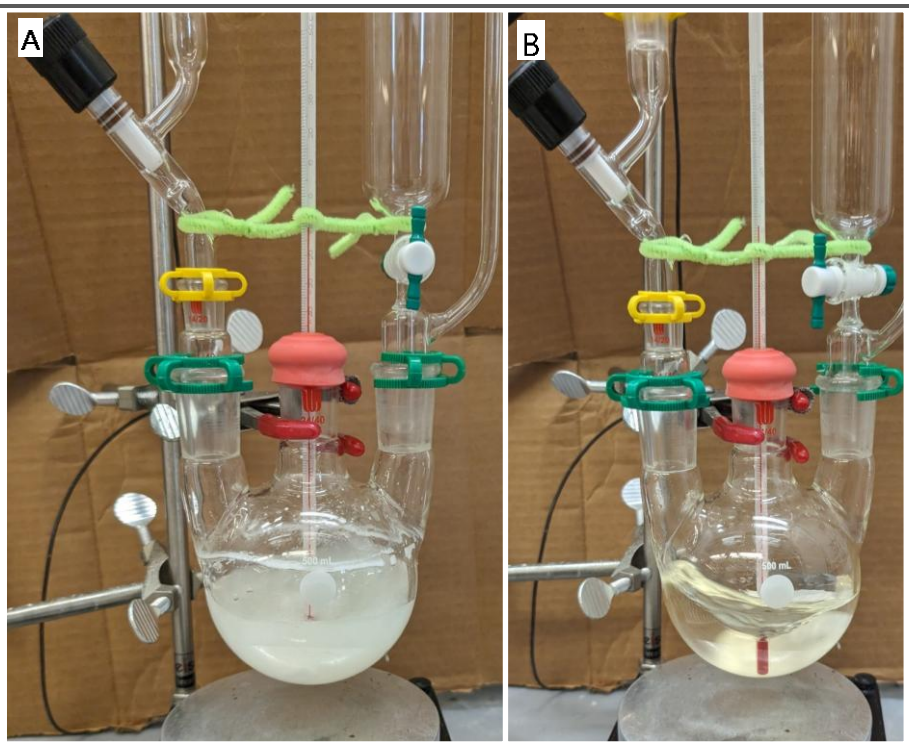


Figure 4.9 A) reaction immediately after removing ice water bath, B) reaction after 1 hour at room temperature, photos taken by author

translucent appearance (Figure 4.9A). At this point, the ice-water bath was removed, allowing the reaction to reach room temperature (23 °C) (Note 30).

After 1 hour of stirring at room temperature the reaction was nearly transparent (Figure 4.9B) and triethylamine (4.2 mL, 30 mmol, 2 equiv) (Notes 31 and 32) was added via the attached addition funnel over 1 min, during which a slight exotherm was observed (25 °C). The reaction was stirred for another 30 min until full consumption of **1** was observed by TLC (Note 33).

After the reaction was determined to be complete, the thermometer and stir bar were removed, rinsing each with a small amount of hexanes (~ 2 mL each). The vacuum adapter and addition funnel were removed, and grease was removed from the joints using a Kimwipe with hexanes (Note 34). The solution was transferred to a 500 mL separatory funnel, and the reaction flask was rinsed with hexanes (100 mL divided into 3 portions), which was subsequently transferred to the funnel and vigorously shaken (Figure 4.10A).

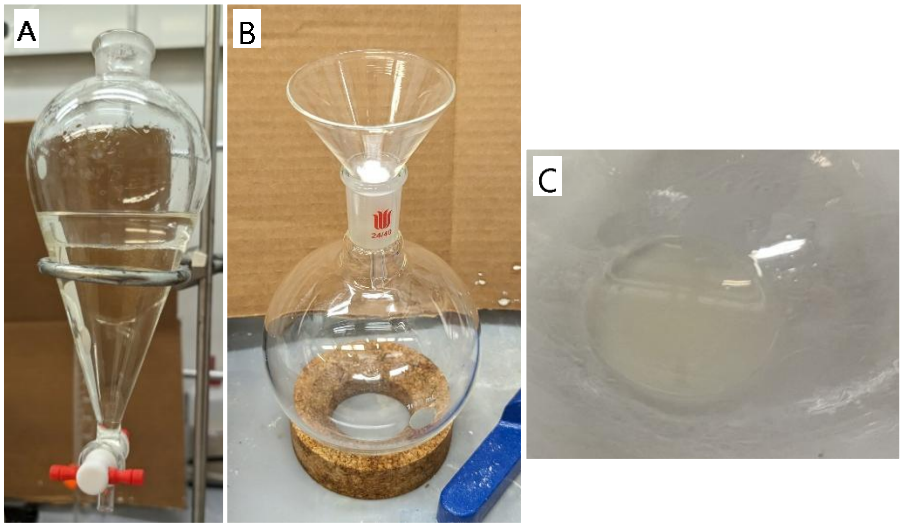


Figure 4.10 A) liquid-liquid extraction, B) funnel with cotton plug in round bottom flask, C) crude reaction oil, photos taken by author

After separating the hexanes and acetonitrile layers, the acetonitrile layer was extracted with hexanes (100 mL x 2). The combined hexanes layers were then washed sequentially with deionized water (100 mL) and brine (50 mL) followed by filtration through a 70 mm glass funnel with a loose-fitting cotton plug (Figure 4.10B) and anhydrous sodium sulphate (20 g) (Notes 35 and 36) into a 1 L round-bottom flask. The funnel was rinsed with additional hexanes (10 mL x 3) and removed from the flask. Hexanes was then removed via rotary evaporation (Note 37) to afford a pale-yellow oil (Figure 4.10C).

The crude residue was diluted with hexanes (3 mL) (Note 34) and charged on a column (2.25 x 8 in) of 235 g silica gel (Note 38), rinsing the flask with additional hexanes (up to 3 mL) to transfer all of the material. The material was then eluted with 1 L of hexanes collected in 50 mL fractions. Based on TLC analysis (Notes 39, 40, and 41) fractions 11-17 were combined and concentrated by rotary evaporation (Note 37), then placed under high-vacuum (Note 22) to afford abietatriene as a clear oil in 80% yield (Notes 42 and 43) (Figure 4.11A. Upon storage at -22 °C overnight the oil crystallized to a white solid (Figure 4.11B-C).

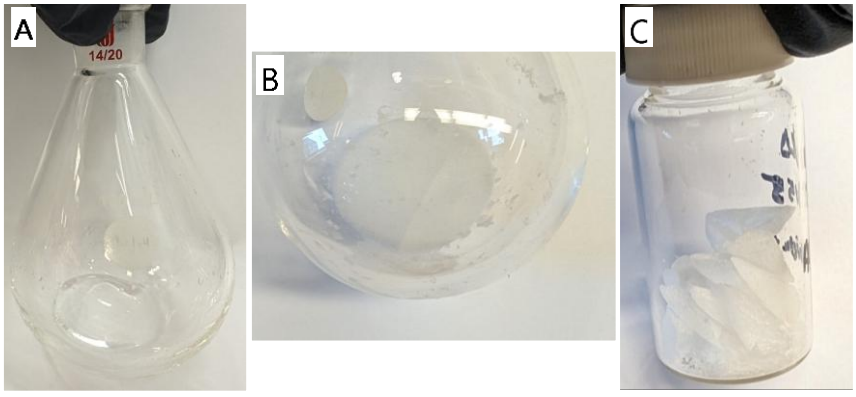


Figure 4.11 Purified product: A) oil, B, C) crystallized, photos taken by author

4.3.2 Procedure Notes and Characterization Data

1. Prior to performing each reaction, a thorough hazard analysis and risk assessment should be carried out with regard to each chemical substance and experimental operation on the scale planned and in the context of the laboratory where the procedures will be carried out. Guidelines for carrying out risk assessments and for analyzing the hazards associated with chemicals can be found in references such as Chapter 4 of "Prudent Practices in the Laboratory" (The National Academies Press, Washington, D.C., 2011; the full text can be accessed free of charge at https://www.nap.edu/catalog/12654/prudent-practices-in-the-laboratory-handling-and-management-of-chemical. See also "Identifying and Evaluating Hazards in Research Laboratories" (American Chemical Society, 2015) which is available via the associated website "Hazard Assessment in Research Laboratories" at https://www.acs.org/content/acs/en/about/governance/committees/chemicalsafety/hazard-assessment.html. In the case of this procedure, the risk assessment should include (but not necessarily be limited to) an evaluation of the potential hazards associated with leelamine, acetic acid, N-(benzyloxy)-N-(pivaloyloxy)-4-(trifluoromethyl)benzamide, triethylamine, toluene, pentane, acetonitrile, hexanes, and brine. Special caution should be taken with the storage and handling of **4**, as a DSC has shown that it decomposes when heated.[17] Additionally, Ames testing has demonstrated that some anomeric amide derivatives are mutagenic.[20–24] The mutagenicity of **4** was recently examined using Ames II testing. Compound **4** exhibits mutagenicity lower than other members of the anomeric amide reagent class and on par with other commonly handled laboratory reagents such

as benzyl chloride.[25] Nonetheless, appropriate ventilation and personal protective equipment should be employed when handling **4**. Additionally, due to the generation of N_2 gas in step b of this procedure, careful attention at the start of the addition of **4** to the reaction and while warming the is essential to prevent rapid gas generation.

2. Adapted from the procedure of Lee C. Cheney.[26]
3. (+)-dehydroabietylamine (60%) was purchased from Sigma Aldrich and used as received.
4. Toluene (certified ACS, 99.5%) was purchased from Fisher and used as received.
5. The authors set the bath temperature to 66 °C to achieve this internal temperature.
6. A stir rate of 180 rpm was used.
7. Glacial acetic acid (HPLC grade, Supelco) was purchased from Millipore Sigma and used as received.
8. Technical grade leelamine contains mostly high molecular weight primary amines.[16] Assuming these amines have a molecular weight similar to leelamine, 1.75 equiv acetic acid relative to leelamine equates to 1.05 equiv relative to the total amount of primary amine compounds.
9. The solution was added at a rate of 2-3 drops/second.
10. After the completion of the acetic acid addition the pH of the solution was checked using a universal pH indicator strip wet with DI water to ensure that the solution was acidic. If the solution is not acidic after this addition, acetic acid should be added dropwise until the pH is below 7.
11. The solution reached maximum internal temperature of 67 °C during acid addition.

12. The solution was cooled by lowering the set temperature of the oil bath to 37 °C. An internal temperature of 37 °C was reached 45 min after the set temperature was changed.
13. The stir rate was increased to 600 rpm (until top of slurry is incorporated)
14. The solution reached an internal temperature of 30 °C after 15 min.
15. Internal temperature of 5 °C
16. The funnel used was a Synthware 150 mL Buchner funnel with a fine porosity glass frit.
17. After the initial filtration, the mother liquor was used to rinse the original flask and passed through the filter to transfer as much of the solids as possible (Figure 4.5D).
18. Toluene was cooled in an ice water bath for at least 10 min prior to use.
19. The stir rate was increased to 400 rpm (until top of slurry is incorporated).
20. The stir rate was increased to 500 rpm.
21. Pentane (certified, 98%) was purchased from Fisher and used as received.
22. The product was dried at room temperature (21 °C) under high vacuum, reaching a pressure of 40 mTorr.
23. The purity of **1** was determined to be 97% through quantitative NMR using 1,3,5-trimethoxy benzene (99.8%, Acros, used as received) as an internal standard.
24. Product **1** is characterized as follows: ^{1}H NMR (400 MHz, MeOD) δ 7.15 (d, *J* = 8.2 Hz, 1H), 6.95 (dd, *J* = 8.1, 2.1 Hz, 1H), 6.86 (d, *J* = 2.0 Hz, 1H), 2.95 – 2.73 (m, 5H), 2.40 – 2.32 (m, 1H), 1.89 (s, 3H), 1.90 – 1.68 (m, 4H), 1.61 – 1.52 (m, 1H), 1.49 – 1.30 (m, 3H), 1.23 (s, 3H), 1.20 (s, 3H), 1.18 (s, 3H), 1.07 (s, 3H). ^{13}C NMR (151 MHz, MeOD) δ 179.94, 147.99, 147.05, 135.47, 127.68, 125.10, 124.92, 52.02, 47.36, 39.29, 38.61, 37.03,

36.38, 34.84, 30.62, 25.53, 24.49, 24.47, 23.96, 19.98, 19.38, 18.26. mp: 150 °C. IR (diamond ATR, neat) 2927, 1527, 1394, 1333, 649, 470 cm^{-1}. HRA-MS (MM: ESI-APCI) *m/z* calculated for $[M+H]^+$ ($C20H32N^+$): 286.26, found: 286.26.

25. To connect the flask to a Schlenk line, the authors used the following adaptors in the following order from the flask neck: 14/20 to 24/40, 14/20 vacuum adapter with Teflon valve plug, and hose to 14/20.
26. A pressure under 1000 mTorr was achieved before purging with N_2
27. Acetonitrile (HPLC grade, Fisher) was degassed under argon and dried by passing through a PPT Solvent Purification System.
28. A stir rate of 200 rpm was used.
29. N-(Benzyloxy)-N-(pivaloyloxy)-4-(trifluoromethyl)benzamide (90% purity) was prepared following an Organic Synthesis procedure.[19]
30. The reaction should be visually monitored for 3 minutes after removal of the ice water bath. Mild gas evolution is typical during this stage, but if vigorous gas evolution is observed the reaction should be placed in the ice water bath to stir for another 30 min.
31. Triethylamine (reagent grade, Fisher) was degassed under argon and dried by passing through a PPT Solvent Purification System.
32. 2 equivalents of triethylamine are used to neutralize the acetic acid released by 1 and the pivalic acid generated from N-(Benzyloxy)-N-(pivaloyloxy)-4-(trifluoromethyl)benzamide in the reaction.

33. Reaction progress was monitored by TLC using 20%vol ethyl acetate in hexanes. The plate should be visualized using UV light and ninhydrin stain to detect the disappearance of dehydroabietylamine (baseline spot).

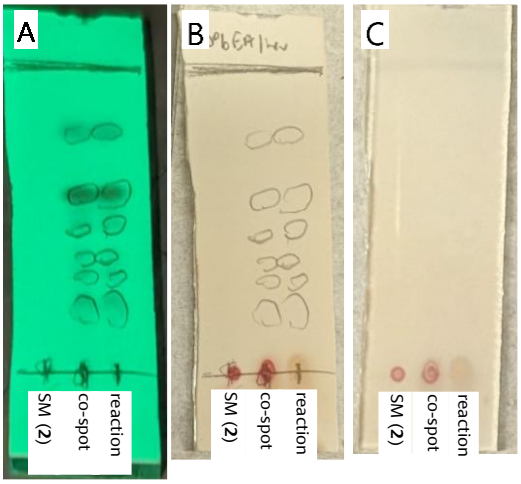


Figure 4.12 TLC of completed reaction (20% EA/hexanes) A) under UV(active spots circled w/ pencil), B) ninhydrin stain, C) back of stained plate (inverted for consistency**)** , photos taken by author

34. Hexanes (certified ACS, 98.5 %) was purchased from Fisher and used as received.

35. Sodium sulfate, anhydrous (99.5%) was purchased from Oakwood Chemical and used as received.

36. If the cotton plug is too compact the filtration will be extremely sluggish. To ensure efficient filtration, a small piece of cotton should be wet with hexanes and gently placed in the bottom of the funnel before adding the sodium sulfate. Alternatively, vacuum filtration can be employed.

37. A rotary evaporator was used with a bath temperature of 30 °C and vacuum at 300 - 75 mmHg.

38. SiliaFlash F60 (particle size 40-63 µm) was purchased from SiliCycle and used as received.

39. Column fractions were analyzed by TLC using hexanes. The plate should be visualized by UV and *p*-Anisaldehyde (PAA) stain to detect closely eluting UV-inactive byproducts.
40. Fractions 11-17 were collected to obtain the desired product. Fractions 10, 18, and 19 were excluded in the to ensure high product purity due to the detection of byproducts.

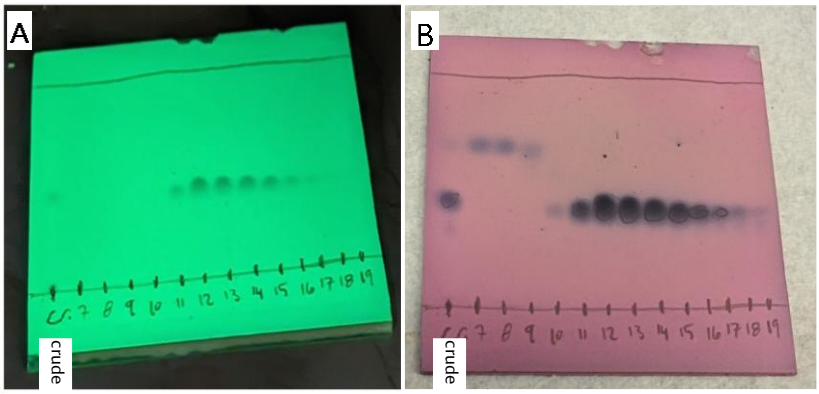


Figure 4.13 TLC of column fractions A) under UV, B) with PAA stain, photos taken by author

41. In some trials it was found that when product concentration was high in mixed fractions, the inclusion of early mixed fractions (Figure 4.14, fractions 14 and 15) was found to have minimal effect on the purity with improved yield. (Fractions 16-22: 55% yield, 100% purity; Fractions 14-22: 77% yield, 99.5% purity).

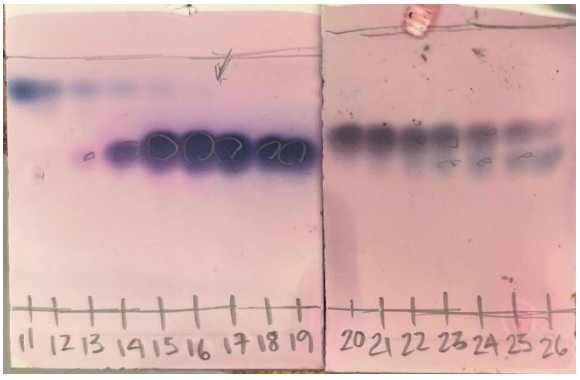


Figure 4.14 TLC of column fractions from replicate reaction with PAA stain, photos taken by author

42. The purity of **3** was determined to be 99% through quantitative NMR using 1,3,5-trimethoxy benzene (99.8%, Acros, used as received) as an internal standard.

43. ^{1}H NMR (600 MHz, $CDCl_3$) δ 7.24 (d, *J* = 8.1 Hz, 1H), 7.05 (dd, *J* = 8.2, 2.1 Hz, 1H), 6.96 (dd, *J* = 2090.6, 2.0 Hz, 1H), 2.99 (ddd, *J* = 17.2, 7.0, 1.9 Hz, 1H), 2.96 – 2.84 (m, 2H), 2.34 (dq, *J* = 12.0, 2.0 Hz, 1H), 1.94 (ddt, *J* = 13.3, 7.5, 2.1 Hz, 1H), 1.87 – 1.71 (m, 2H), 1.66 (dp, *J* = 14.0, 3.6 Hz, 1H), 1.54 (dtd, *J* = 13.2, 3.3, 1.6 Hz, 1H), 1.47 (td, *J* = 13.1, 3.8 Hz, 1H), 1.42 (dd, *J* = 12.5, 2.3 Hz, 1H), 1.31 – 1.26 (m, 7H), 1.25 (s, 3H), 1.01 (s, 3H), 1.00 (s, 3H). ^{13}C NMR (151 MHz, $CDCl_3$) δ 147.76, 145.52, 135.06, 126.96, 124.42, 123.93, 50.58, 41.90, 39.02, 37.67, 33.60, 33.59, 33.49, 30.66, 25.05, 24.17, 24.15, 21.78, 19.50, 19.28. mp: 54 °C. IR (diamond ATR, neat) 2931, 1497, 1455, 1373, 824, 630, 483 cm^{-1}. HRA-MS (MM: ESI-APCI) *m/z* calculated for $[M]^-$ ($C_{20}H_{30}^-$): 270.23, found: 270.25.

4.3.3 Byproduct Identification

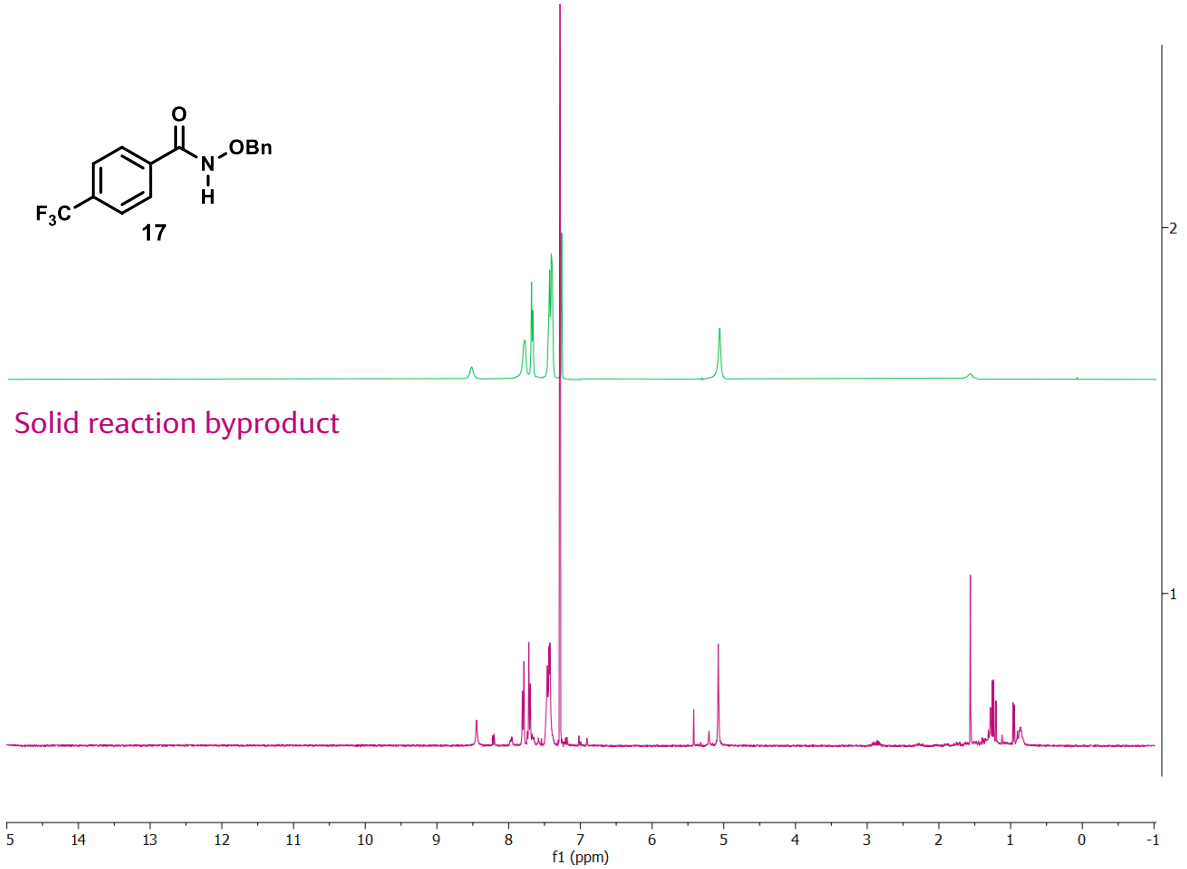


Figure 4.15 Comparison of byproduct spectra with N-(benzyloxy)-4-(trifluoromethyl)benzamide

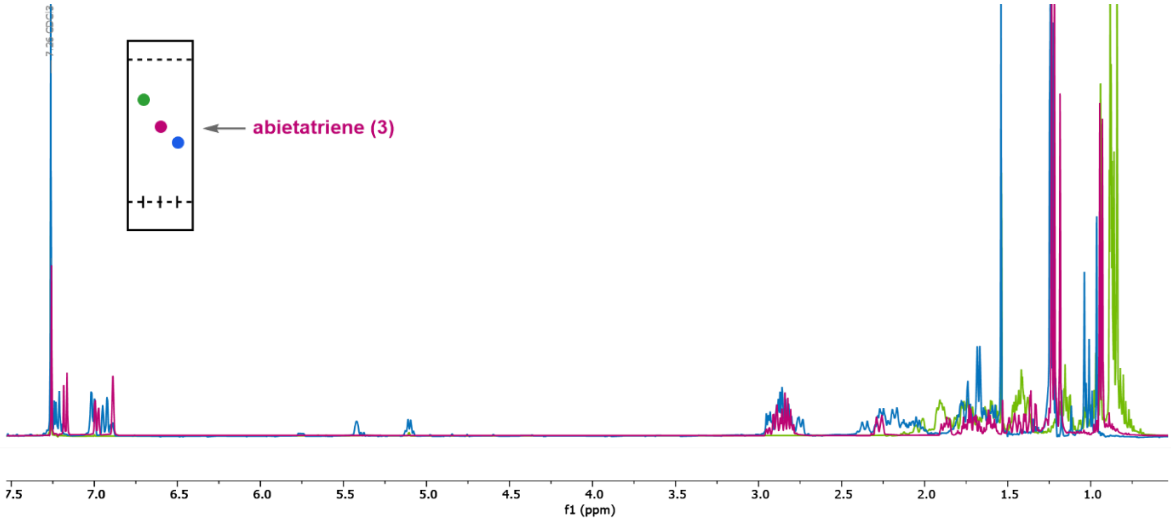


Figure 4.16 Overlayed ^{1}H NMR spectra of non-polar byproducts with product **3**

4.3.4 NMR Spectra

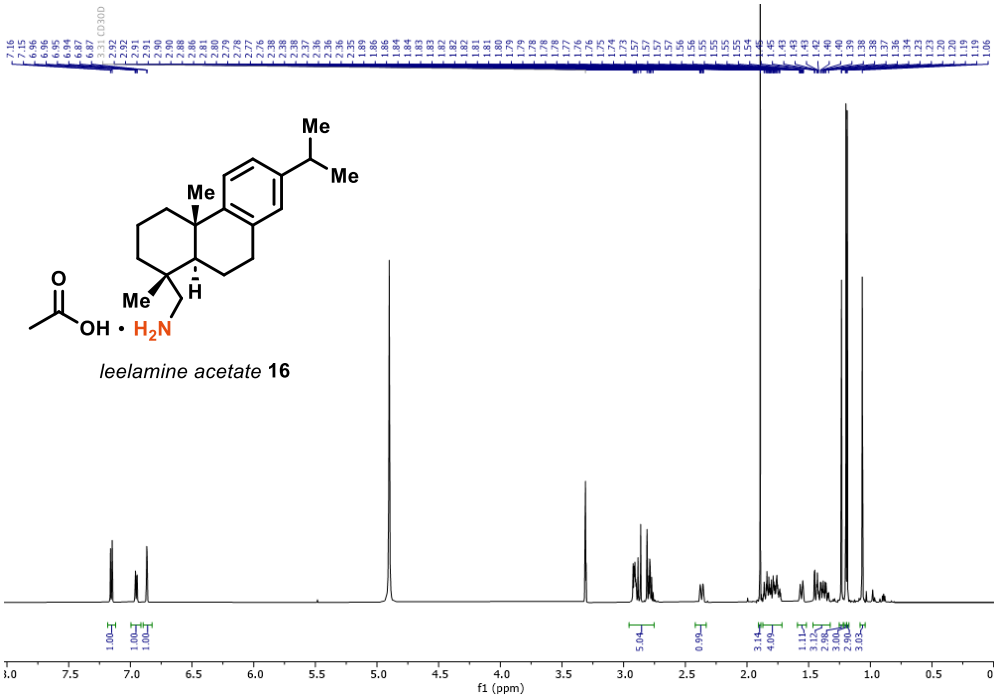


Figure 4.17 ^{1}H NMR spectra of **16** in $CDCl_3$

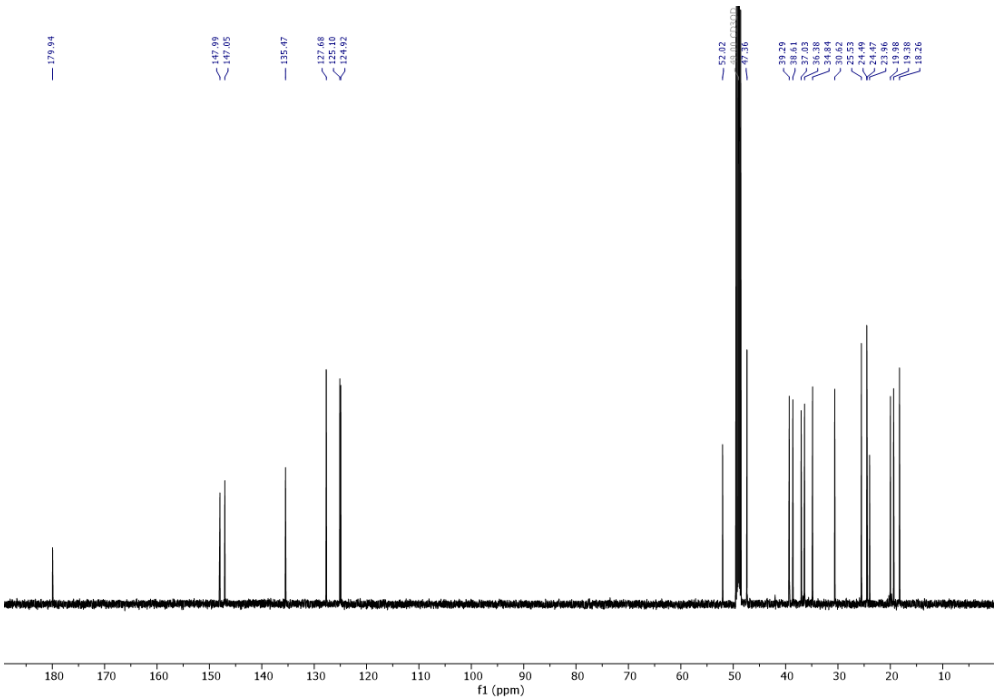
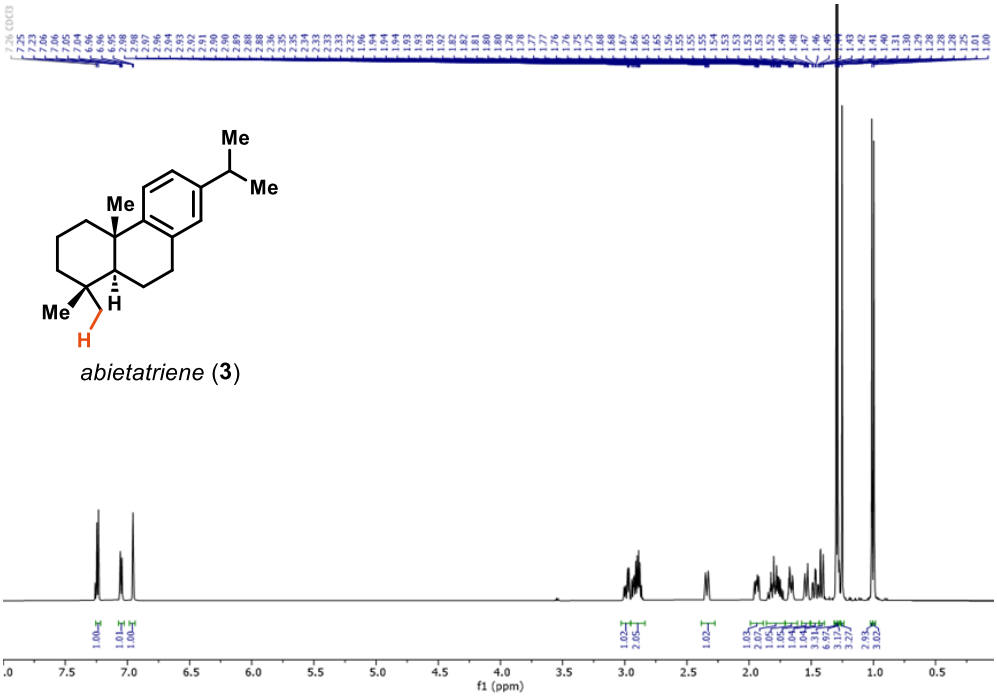


Figure 4.18 ^{13}C NMR spectra of **16** in $CDCl_3$



abietatriene (**3**)

Figure 4.19 ^{1}H NMR spectra of 3 in $CDCl_3$

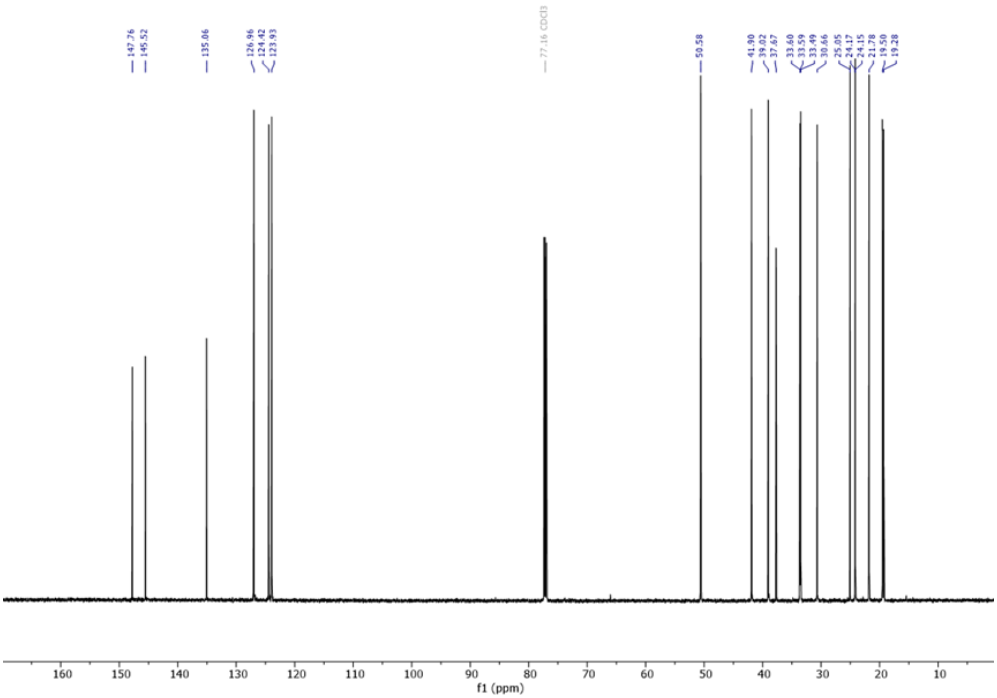


Figure 4.20 ^{13}C NMR spectra of 3 in $CDCl_3$

4.4 References

(1) Tahara, A.; Shimagaki, M.; Ohara, S.; Tanaka, T.; Nakata, T. Diterpenoids. XXXVI. Synthesis of d-Kaurene and d-Phyllocladene from l-Abietic Acid. *Chemical & Pharmaceutical Bulletin* **1975**, *23* (10), 2329–2338. https://doi.org/10.1248/cpb.23.2329.

(2) Matsushita, Y.; Iwakiri, Y.; Yoshida, S.; Sugamoto, K.; Matsui, T. Synthesis of 12-Deoxyroyleanone, Cryptoquinone, 11,14-Dihydroxy-8,11,13-Abietatrien-7-One, and Related Derivatives from Dehydroabietic Acid. *Tetrahedron Letters* **2005**, *46* (21), 3629–3632. https://doi.org/10.1016/j.tetlet.2005.03.170.

(3) González, M. A.; Pérez-Guaita, D. Short Syntheses of (+)-Ferruginol from (+)-Dehydroabietylamine. *Tetrahedron* **2012**, *68* (47), 9612–9615. https://doi.org/10.1016/j.tet.2012.09.055.

(4) Peixoto, P. A.; El Assal, M.; Chataigner, I.; Castet, F.; Cornu, A.; Coffinier, R.; Bosset, C.; Deffieux, D.; Pouységu, L.; Quideau, S. Bispericyclic Diels–Alder Dimerization of Ortho-Quinols in Natural Product (Bio)Synthesis: Bioinspired Chemical 6-Step Synthesis of (+)-Maytenone. *Angewandte Chemie International Edition* **2021**, *60* (27), 14967–14974. https://doi.org/10.1002/anie.202103410.

(5) Geiwiz, J.; Haslinger, E. Stereoselective Partial Synthesis of (+)-Pisiferic Acid. *Helvetica Chimica Acta* **1995**, *78* (4), 818–832. https://doi.org/10.1002/hlca.19950780404.

(6) Thommen, C.; Jana, C. K.; Neuburger, M.; Gademann, K. Syntheses of Taiwaniaquinone F and Taiwaniaquinol A via an Unusual Remote C–H Functionalization. *Org. Lett.* **2013**, *15* (6), 1390–1393. https://doi.org/10.1021/ol4003652.

(7) Mori, N.; Kuzuya, K.; Watanabe, H. Synthesis of (–)-Chamobtusin A from (+)-Dehydroabietylamine. *J. Org. Chem.* **2016**, *81* (23), 11866–11870. https://doi.org/10.1021/acs.joc.6b02328.

(8) Nishino, K.; Someya, K.; Tsukano, C.; Ishikawa, T.; Nagao, M. Synthesis of 8β-Hydroxy-9(11),13-Abietadien-12-One from (+)-Dehydroabietylamine and Its AhR Ligand Activity. *Results in Chemistry* **2023**, *5*, 100912. https://doi.org/10.1016/j.rechem.2023.100912.

(9) Banik, B. K.; Ghatak, U. R. An Expeditious Total Synthesis of (±)-Sempervirol, (±)-Sugiol and (±)-Xanthopherol Methyl Ether by Acid-Catalyzed Cyclialkylation Route. *Synthetic Communications* **1989**, *19* (7–8), 1351–1367. https://doi.org/10.1080/00397918908054545.

(10) Zhang, C.-L.; Bie, P.-Y.; Peng, X.-J.; Pan, X.-F. Total Synthesis of (±)-Abieta-8,11,13-Trien-7β-Ol. *Journal of the Chinese Chemical Society* **2003**, *50* (3A), 429–432. https://doi.org/10.1002/jccs.200300066.

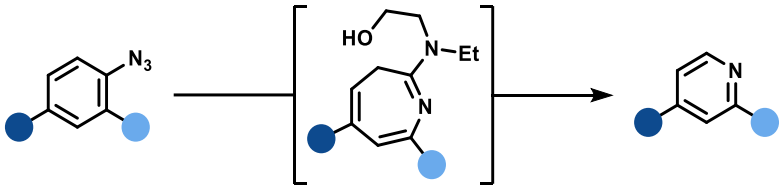
(11) Li, W.-S.; McChesney, J. D. Preparation of Potential Anti-Inflammatory Agents from Dehydroabietic Acid. *Journal of Pharmaceutical Sciences* **1992**, *81* (7), 646–651. https://doi.org/10.1002/jps.2600810711.

(12) Buckley, T. F.; Rapoport, H. Mild and Simple Biomimetic Conversion of Amines to Carbonyl Compounds. *J. Am. Chem. Soc.* **1982**, *104* (16), 4446–4450. https://doi.org/10.1021/ja00380a019.

(13) Guziec, F. S.; Wei, D. Convenient Halodeamination and Hydrodeamination of Primary Amines. *J. Org. Chem.* **1992**, *57* (Copyright (C) 2021 American Chemical Society (ACS). All Rights Reserved.), 3772–3776. https://doi.org/10.1021/jo00040a010.

(14) Bhar, S. S.; Ramana, M. M. V. Novel Domino Reactions for Diterpene Synthesis. *J. Org. Chem.* **2004**, *69* (25), 8935–8937. https://doi.org/10.1021/jo049616n.
(15) Cheney, L. C. Purification of Dehydroabietylamine. US2787637A, April 2, 1957.
(16) *(+)-Dehydroabietylamine technical grade, 60 1446-61-3*. http://www.sigmaaldrich.com/ (accessed 2024-06-12).
(17) Berger, K. J.; Driscoll, J. L.; Yuan, M.; Dherange, B. D.; Gutierrez, O.; Levin, M. D. Direct Deamination of Primary Amines via Isodiazene Intermediates. *J. Am. Chem. Soc.* **2021**, *143* (42), 17366–17373. https://doi.org/10.1021/jacs.1c09779.
(18) Laaksonen, T.; Heikkinen, S.; Wähälä, K. Synthesis and Applications of Secondary Amine Derivatives of (+)-Dehydroabietylamine in Chiral Molecular Recognition. *Org. Biomol. Chem.* **2015**, *13* (42), 10548–10555. https://doi.org/10.1039/C5OB01667C.
(19) Berger, K. J.; Dherange, B. D.; Morales, M.; Driscoll, J. L.; Tarhan, A. K.; Levin, M. D. N-(Benzyloxy)-N-(Pivaloyloxy)-4-(Trifluoromethyl)-Benzamide. *Org. Synth.* **2023**, *100*, 113–135. https://doi.org/10.15227/orgsyn.100.0113.
(20) Andrews, L. E.; Bonin, A. M.; Fransson, L. E.; Gillson, A.-M. E.; Glover, S. A. The Role of Steric Effects in the Direct Mutagenicity of N-Acyloxy-N-Alkoxyamides. *Mutation Research/Genetic Toxicology and Environmental Mutagenesis* **2006**, *605* (1), 51–62. https://doi.org/10.1016/j.mrgentox.2006.02.003.
(21) Glover, S. A.; Schumacher, R. R.; Bonin, A. M.; Fransson, L. E. Steric Effects on the Direct Mutagenicity of N-Acyloxy-N-Alkoxyamides—Probes for Drug–DNA Interactions. *Mutation Research/Genetic Toxicology and Environmental Mutagenesis* **2011**, *722* (1), 32–38. https://doi.org/10.1016/j.mrgentox.2011.02.007.
(22) Glover, S. A.; Schumacher, R. R. Mutagenicity of N-Acyloxy-N-Alkoxyamides as an Indicator of DNA Intercalation: The Role of Fluorene and Fluorenone Substituents as DNA Intercalators. *Mutation Research/Genetic Toxicology and Environmental Mutagenesis* **2021**, *863–864*, 503299. https://doi.org/10.1016/j.mrgentox.2020.503299.
(23) Campbell, J. J.; Glover, S. A. Bimolecular Reactions of Mutagenic N-Acetoxy-N-Alkoxybenzamides and N-Methylaniline. *J. Chem. Soc., Perkin Trans. 2* **1992**, No. 10, 1661–1663. https://doi.org/10.1039/P29920001661.
(24) Glover, S. A. Mutagenicity of N-Acyloxy-N-Alkoxyamides – QSAR Determination of Factors Controlling Activity. *Aust. J. Chem.* **2023**, *76* (1), 1–24.
(25) Dherange, B. D.; Yuan, M.; Kelly, C. B.; Reiher, C. A.; Grosanu, C.; Berger, K. J.; Gutierrez, O.; Levin, M. D. Direct Deaminative Functionalization. *J. Am. Chem. Soc.* **2023**, *145* (1), 17–24. https://doi.org/10.1021/jacs.2c11453.
(26) Cheney, L. C. Purification of Dehydroabietylamine, April 2, 1957.

Appendix 1 : Carbon Deletion as Heterocyclic Carbenes for Ring Contractions



Note: Portions of this work have been published in an alternate format in Pearson, T. J.; Shimazumi, R.; Driscoll, J. L.; Dherange, B. D., Park, D.; Levin, M. D. Aromatic nitrogen scanning by ipso-selective nitrene internalization. *Science.* **2023**, *381*, 1474 – 1479. https://doi.org/10.1126/science.adj5331

A1.1 The Untold Story of Ketone Condensation-Decarbonylation

My journey with this project began with the idea of using a di-nucleophilic species to "pinch" off a carbon-atom as a heterocyclic carbene within the context of decarbonylation. I proposed that after condensing a diamine, onto a cyclic ketone, a radical or anionic mechanism could enable ejection of a heterocyclic carbene species and ring contraction to form a new carbon-carbon bond (Figure A1.1) driven by the stabilization of the carbene by the heteroatoms and aromaticity in the leaving group, as well as a release of strain from the spirocyclic species.

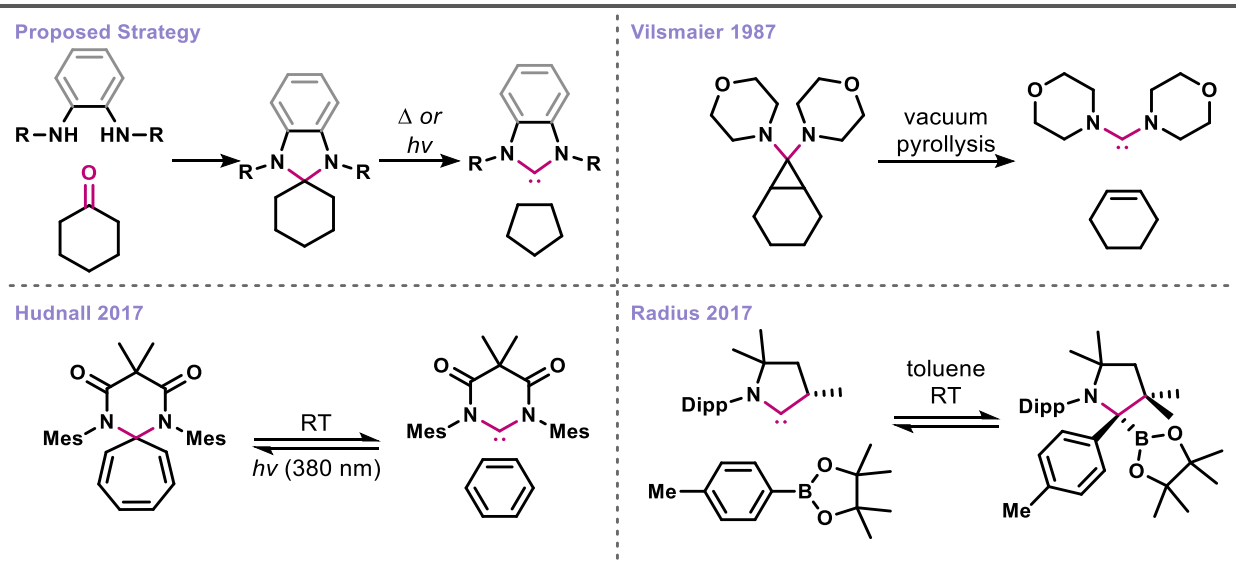
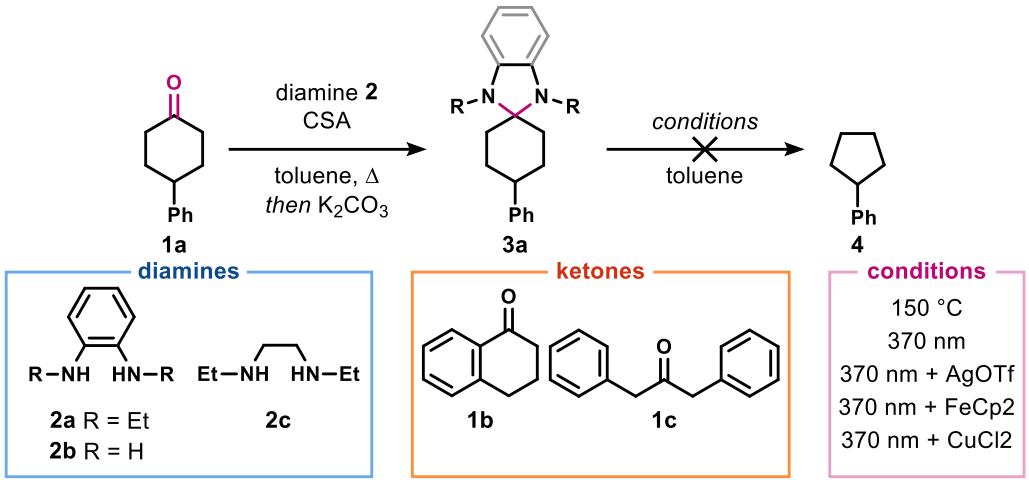


Figure A1.1 Proposed carbon deletion strategy and literature precedent examples



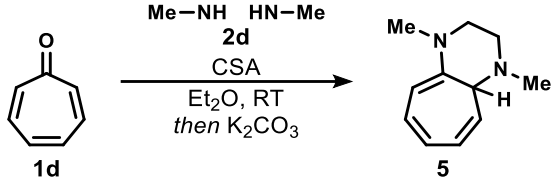
Scheme A1.1 attempted spirocyclization and carbon extrusion conditions

While this was admittedly aspirational and idealistic, it was not entirely unprecedented. Inspiration for this work came from Vilsmaier's report on the extrusion of a nitrogen-stabilized carbene from a spirocyclic alkyl species,[1] and the reversible carbene insertion-extrusion processes that have been demonstrated in aromatic[2] rings and aryl-boronate esters[3] by Hudnall and Radius respectively. (Figure A1.1)

In practice, I found that while a variety of diamines could be condensed onto 4-phenylcyclohexanone (**1a**), the spirocyclic species (**3a**) lacked the driving force to undergo carbon-extrusion and ring contraction and **4** was not observed under any of the conditions screened. I explored β-tetralone (**1b**) and dibenzyl ketone (**1c**) as alternative cyclic and acyclic model substrates that could better stabilize carbon-extrusion intermediates, but these did not form the desired spirocyclic intermediates with the diamines screened (Table A1.1).

I then turned my attention to tropone, which based on the example from Hudnall,[2] should be capable of heterocyclic-carbene extrusion from a spirocyclic species. I attempted to condense a variety of diamines onto tropone, but in most cases the starting materials were not reactive towards each other. Ethylene diamine (**2d**) was the exception to this, but rather than

the desired spirocycle, the [6,7]-fused ring (**5**) was tentatively assigned as the major product (Scheme A1.2), closely aligning with a report on the analogous thiol system from Cavazza and Morganti.[4] Based on this, it seemed unlikely that any dinucleophilic species would form the desired spirocyclic species in appreciable amounts from tropone.



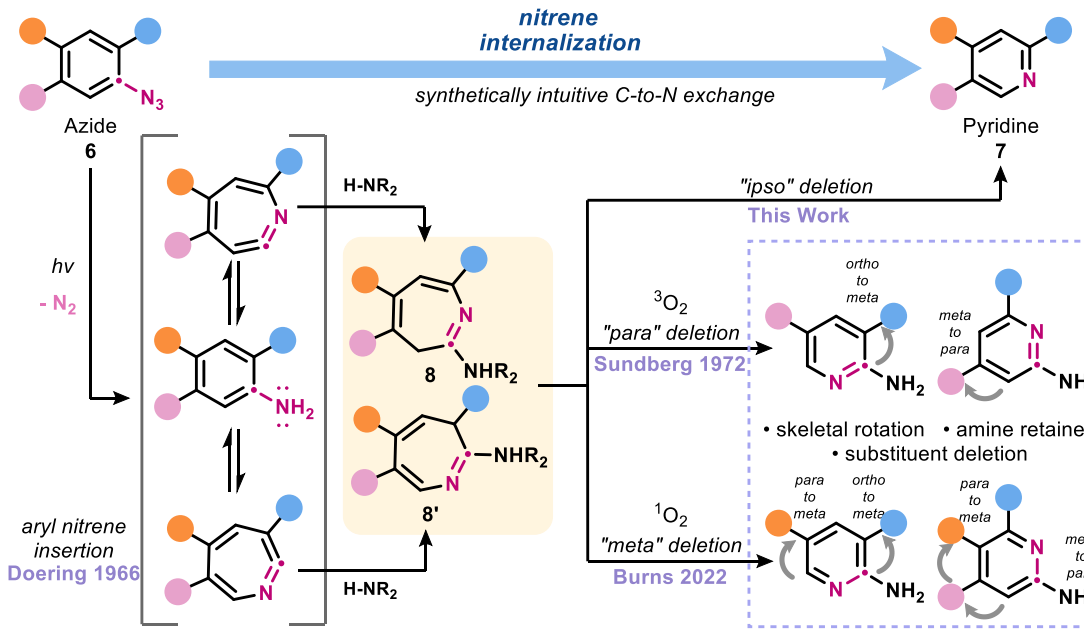
Scheme A1.2 condensation of DMEDA (2d) onto tropone

A1.2 Ipso-Selective Nitrene Internalization

A1.2.1 *Background*

While the previous results were disappointing, I was hopeful that this carbon deletion strategy could be viable in the right chemical system. Concurrent with my initial studies using ketones and diamines, another group member, Dr. Tyler Pearson, was working on a strategy to transform aryl azides (**6**) into pyridines (**7**) via 2-amino-3*H*-azepine intermediates (**8**). These azepines are known to form from the photolysis of aryl azides in the presence of protic nucleophiles.[5–7] Extrusion of the carbon atom *para* to the azide by photolyzing under air has been reported by Sundberg,[8] and more recently, Burns demonstrated removal of the *meta*-carbon atom, empowered by singlet O_2 generation (Scheme A1.3).[9]

Within our lab, Tyler was specifically working on strategies to enable deletion of the *ipso*-carbon, which would afford a direct carbon to nitrogen atom-swap, preventing rearrangement of the ring substituents. Tyler and I discussed the idea of tethering a second nucleophile to the amine, enabling the formation of a spirocycle and deletion of the *ipso* carbon. Unlike tropone, the azepine intermediates are not aromatic, so it was possible that they would not suffer from the same selectivity problems observed but would provide a similar

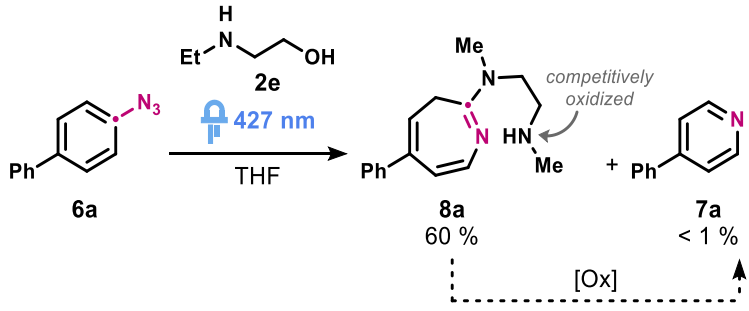


Scheme A1.3 Carbon-nitrogen atom swap strategy and literature precedent of related transformations
*figure adapted from *Science*. **2023**, *381*, 1474 – 1479.

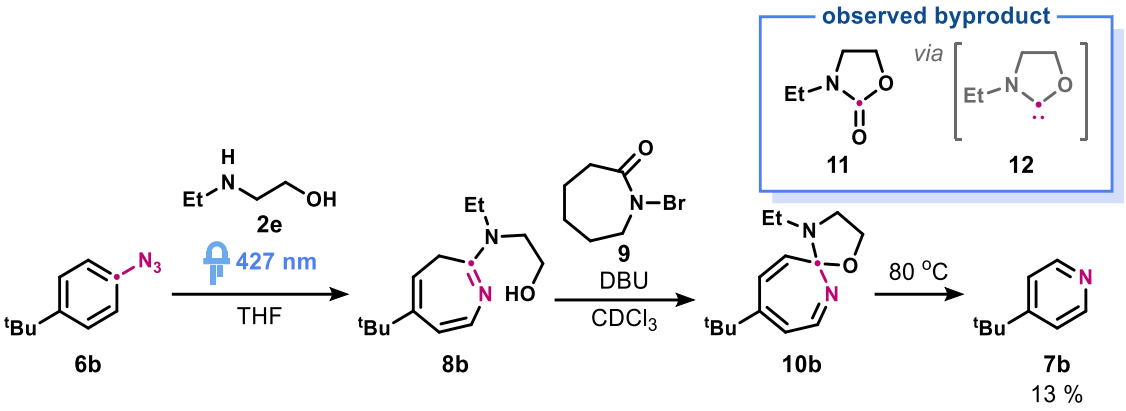
aromatic driving force for ejection of the heterocyclic carbene. If this strategy worked as envisioned, it would also remove the *ipso* carbon specifically, preventing the migration of any other ring substituents and providing a direct carbon to nitrogen atom replacement.

A1.2.2 *Reaction Development*

Tyler initially attempted this reaction using N,N'-dimethyl ethylenediamine as the bidentate nucleophile, and excitingly detected trace amounts of the pyridine product (**7a**), along with 60% of azepine **8a** (Scheme A1.4). Intermediate **8a** could be potentially converted to pyridine **7a** through oxidation, but due to the oxidative liability of the free secondary amine, DMEDA was replaced with 2-ethylamino ethanol as the bidentate nucleophile. After photolysis of aryl azide **6b**, Tyler found that N-bromo



Scheme A1.4 initial hit for pyridine formation through *ipso*-C deletion



Scheme A1.5 nitrene insertion and decarbonylation of **6b** using **2e** and observed reaction intermediates

caprolactam (**9**) was capable of converting **8b** to spirocyclic azepine **10b**, which formed pyridine **7b** upon heating. Oxazolidinone **11** was also observed as a byproduct in this transformation, presumably forming from carbene **12**, and providing support for the proposed mechanism (Scheme A1.5).

The yield of this process was improved by adding the oxidant at elevated temperatures, rapidly converting the oxidatively sensitive azepines to the less reactive pyridine product. As part of a collaborative effort to explore the scope of the reaction, I found that 4-trityl phenyl azide (**6d**) worked well under the optimized conditions, and isolated pyridine **7d** in 53% yield. Interestingly, the dihydrofuran fused azide **6q** resulted in the formation of bromopyridine **7q-Br**, rather than the desired pyridine. The azepine of this derivative (**8q**) seemed to be more prone to overoxidation, as the brominated azepine could also be isolated with one equivalent of oxidant. As such, it seems that the selectivity of the oxidation step is imperative to productive carbon-extrusion and avoiding unwanted bromopyridine products (Table A1.1).

This work represents the first *ipso*-carbon nitrogen atom swap, enabling the precise modification of a single-atom within an aryl ring. This is enabled by the dearomative nature of the nitrene insertion to form the azepine, and the unique spirocyclization of the bidentate nucleophile to selectively remove the *ipso*-carbon.

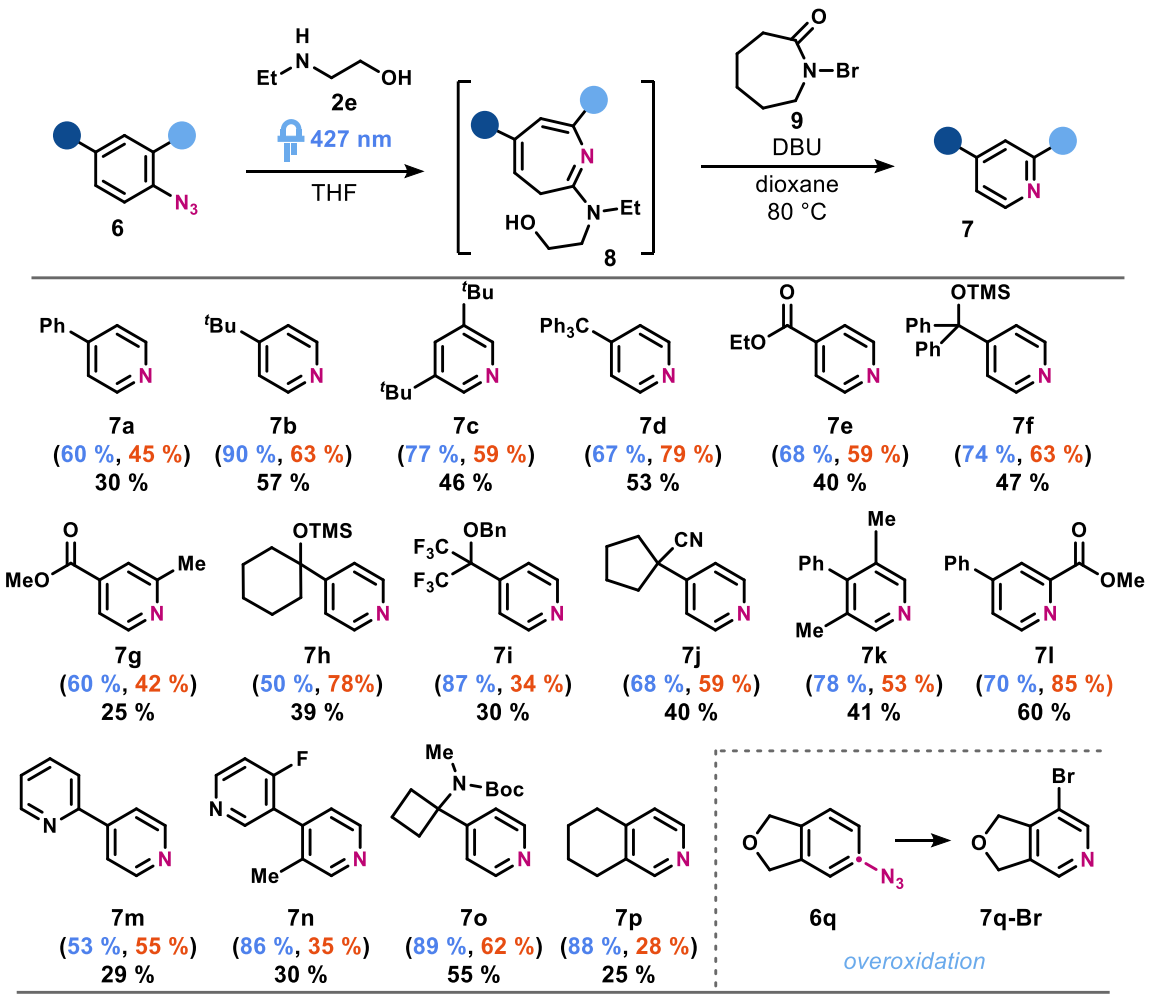


Table A1.1 (A) Scope of the reaction. Standard conditions: (i) 0.3 mmol aryl azide, 0.3 mmol ethylaminoethanol, 3 ml MeCN, and 427-nm light-emitting diode (LED); (ii) 0.3 mmol DBU, 3 ml dioxane heated to 80°C, and 0.6 mmol N-bromocaprolactam added dropwise at 80°C. Isolated yield of pyridine from aryl azide (black). Proton NMR (1H NMR) yield of photolysis (blue) and interpolated yield of pyridine based on azepine yield (orange), shown in parentheses. Asterisk indicates NMR yield. (B) Demonstration that nonsymmetric substrates form only one pyridine isomer. *figure adapted from *Science*. **2023**, *381*, 1474 – 1479.

A1.3 References

(1) Vilsmaier, E.; Kristen, G.; Tetzlaff, C. Thermal Cycloelimination of Bis(Dialkylamino)Cyclopropanes to Amidines and Cycloalkenes. *J. Org. Chem.* **1988**, *53* (8), 1806–1808. https://doi.org/10.1021/jo00243a040.

(2) Perera, T. A.; Reinheimer, E. W.; Hudnall, T. W. Photochemically Switching Diamidocarbene Spin States Leads to Reversible Büchner Ring Expansions. *J. Am. Chem. Soc.* **2017**, *139* (41), 14807–14814. https://doi.org/10.1021/jacs.7b09264.

(3) Eichhorn, A. F.; Fuchs, S.; Flock, M.; Marder, T. B.; Radius, U. Reversible Oxidative Addition at Carbon. *Angewandte Chemie International Edition* **2017**, *56* (34), 10209–10213. https://doi.org/10.1002/anie.201701679.

(4) Cavazza, M.; Morganti, G. A Facile 1,2-Annelation of Cycloheptatrienone with Dithiols. Failure of a Dithioketalization. *Tetrahedron Letters* **1978**, *19* (24), 2137–2138. https://doi.org/10.1016/S0040-4039(01)94771-9.

(5) Doering, W. von E.; Odum, R. A. Ring Enlargement in the Photolysis of Phenyl Azide. *Tetrahedron* **1966**, *22* (1), 81–93. https://doi.org/10.1016/0040-4020(66)80104-7.

(6) Gritsan, N. P.; Platz, M. S. Kinetics, Spectroscopy, and Computational Chemistry of Arylnitrenes. *Chem. Rev.* **2006**, *106* (9), 3844–3867. https://doi.org/10.1021/cr040055+.

(7) Borden, W. T.; Gritsan, N. P.; Hadad, C. M.; Karney, W. L.; Kemnitz, C. R.; Platz, M. S. The Interplay of Theory and Experiment in the Study of Phenylnitrene. *Acc. Chem. Res.* **2000**, *33* (11), 765–771. https://doi.org/10.1021/ar990030a.

(8) Sundberg, R. J.; Suter, S. R.; Brenner, M. Photolysis of 0-Substituted Aryl Azides in Diethylamine. Formation and Autoxidation of 2-Diethylamino-1H-Azepine Intermediates. *J. Am. Chem. Soc.* **1972**, *94* (2), 513–520. https://doi.org/10.1021/ja00757a032.

(9) Patel, S. C.; Burns, N. Z. Conversion of Aryl Azides to Aminopyridines. *J. Am. Chem. Soc.* **2022**, *144* (39), 17797–17802. https://doi.org/10.1021/jacs.2c08464.